UAB
Universitat Autònoma de Barcelona

CIRCULATING CELL-DERIVED EXTRACELLULAR VESICLES AND EPIGENETIC SMALL NON-CODING RIBONUCLEIC ACIDS IN CHRONIC HEART FAILURE

ALBA VILELLA FIGUEROLA

Universitat Autònoma de Barcelona

TESI DOCTORAL

CIRCULATING CELL-DERIVED EXTRACELLULAR VESICLES AND EPIGENETIC SMALL NON-CODING RIBONUCLEIC ACIDS IN CHRONIC HEART FAILURE

ALBA VILELLA FIGUEROLA

Dirigida per:

Prof. LINA BADIMON MAESTRO

Dra. TERESA PADRÓ CAPMANY

Departament de Bioquímica i Biologia Molecular
Facultat de Medicina
Universitat Autònoma de Barcelona
Gener 2023

HOSPITAL DE LA SANTA CREU I SANT PAU
UNIVERSITAT AUTÒNOMA DE BARCELONA

Institut santpau Investigació Biomèdica | Barcelona

ICCC Programa ICCC

CIRCULATING CELL-DERIVED EXTRACELLULAR VESICLES AND EPIGENETIC SMALL NON-CODING RIBONUCLEIC ACIDS IN CHRONIC HEART FAILURE

Memòria presentada per

ALBA VILELLA FIGUEROLA

per optar al grau de Doctora en Bioquímica, Biologia Molecular i Biomedicina per la Universitat Autònoma de Barcelona

Doctoranda

Alba Vilella Figuerola

Directora	**Co-directora**	**Tutor**
Prof. Lina Badimon Maestro	**Dra. Teresa Padró Capmany**	**Dr. Francisco Blanco Vaca**

Cerdanyola del Vallès, Gener 2023

Cover designed by Cristina Creus Roselló
PhD Thesis, 2023, Alba Vilella Figuerola
Universitat Autònoma de Barcelona

The bird, the pin, the song, the berries, the watch, the cracker,
the dress that burst into flames.
I am the Mockingjay.
The one that survived despite the Capitol's plans. The symbol of the rebellion.

Katniss Everdeen,
Mockingjay, **Suzanne Collins (2010)**

Als meus pares,
a l'Anna i a l'Àngels.
Sense vosaltres, tot això no hauria estat possible.

AGRAÏMENTS

Aquesta tesi ha estat possible gràcies a l'ajuda, la influència i a les aportacions de moltes persones.

En primer lloc, vull agrair a la Prof. Badimon, i la Dra. Padró l'oportunitat de poder participar en els seus projectes, cosa que ha permès la realització d'aquesta tesi doctoral. Aquests últims anys al vostre costat han estat tota una experiència i tot un aprenentatge, no sols a nivell científic i laboral, sinó també a nivell personal.

També vull donar les gràcies a la Gemma i al Javi, per obrir-me pas al món de la citometria de flux i ensenyar-me tot el que en sabeu, així com també donar-me les primeres eines estadístiques. No em puc oblidar del Rafael, qui m'ha ensenyat com fer PCRs i m'ha obert les portes al món de la bioinformàtica. Tampoc em puc deixar a la Montse, qui m'ha donat un cop de mà quan ha fet falta.

Vull fer especial esment a tots aquells que, com jo, estan realitzant la tesi al laboratori. Hem viscut moltes estones i experiències junts, tant bones com dolentes, que han fet que aquests anys fossin menys durs. Tant les llargues hores treballant, com les cerveses i els sopars després de la feina no haguessin estat iguals sense vosaltres. Elisa, *my partner in crime*! des que vas acabar no ha estat igual. Trobo molt a faltar les llargues estones asseguda al teu costat, mentre parlàvem de l'últim episodi de Crims o de qualsevol altre misteri que haguéssim descobert. També tenir una companya de gimnàs o una bona crítica d'escriptura i de llenguatge. Ah! I també vull donar-te les gràcies organitzar totes les quedades després de la feina i tots els amics invisibles. Moltes gràcies per estar al meu costat tots aquests anys! Vicky! *Cómo te voy a echar de menos! Gracias por estar a mi lado estos años y darme siempre todo tu apoyo. Siempre he sido bienvenida a tu mesa a buscar consejo y consuelo! Ánimo que ya queda poco!* Alex! Que serien sense tu els esmorzars i els dinars? Les llargues converses filosòfiques han estat una font d'inspiració constant! Gràcies també pels teus consells i la companyia. No em puc oblidar de vosaltres Aureli, Natàlia, Soumaya, Leonie, Sebastià, Hue, Anna i Noelia; heu estat un pilar molt important durant aquests anys i heu fet que totes les estones siguin molt millors. Alguns de vosaltres ja heu marxat, d'altres seguiu al peu del canó. Ànims, que ja queda poc! Tot i que sembla que això no acaba d'arribar, tot arriba i més ràpid de l'esperat.

També estic molt agraïda a tots els altres companys del centre amb els que potser no he tingut tant contacte, però a qui sempre he pogut recórrer per resoldre dubtes. Moltes gràcies Maria, Gemma V., Gemma A., Maisa, Rosa A., Rosa S., Esther, Olaya, Mònica, Sònia, Nerea, Mari, Pablo i Sergi pel vostre suport. Moltes gràcies a tots aquells que d'alguna forma han fet possible la realització d'aquest treball, però que inadvertiblement no he mencionat.

També estic molt agraïda al personal de l'hospital, que ha col·laborat des de la part clínica en aquest projecte. Vull fer especial esment a la Dra. Mirabet, que ha estat un referent i amb qui he pogut contactar sempre que ha fet falta. Moltes gràcies pel teu suport!

No em puc oblidar dels meus amics, qui han estat una font constant de suport al llarg d'aquests anys. Especialment a *mis chicas Darling, quienes han vivido experiencias parecidas y saben de primera mano cómo es la ciencia y un doctorado. Muchas gracias Bea, Lily y Noe, por estar ahí cuando más ha hecho falta, por los viajes, las (vídeo)llamadas a deshoras y unos amigos invisibles que nunca llegaban debido al colapso de correos durante la pandemia. Lamento que estéis tan lejos, aunque ¡ya queda menos para volver a organizar una quedada! ¿Dónde nos vemos la próxima vez?*

Tampoc em puc deixar a la Raquel, al Dani o al Joan Carles. Gràcies per estar sempre aquí i ser un suport constant. Per donar consell quan ha fet falta i per totes les tardes i vespres que hem passat plegats. Tampoc em puc oblidar de la Marina, el Jon o la Clara. Heu estat una font constant de suport durant tots aquests anys i heu fet que tot fos més fàcil. Vull agrair també a la Cris, la Eva i l'Aleix totes les estones que hem viscut al llarg d'aquests anys, en especialment a la Cris, per dissenyar-me la portada de la tesi.

Per últim, però per mi els més importants, vull fer menció a la meva família. En especial als meus pares. Papa, Mama, sense vosaltres res d'això no seria possible. No us podré agrair mai prou el vostre suport incondicional que ha fet possible que ara sigui on sóc. Anna i Àngels, sempre heu estat, sou i sereu una part molt important de la meva vida. Moltes gràcies per aguantar-me aquests últims mesos fent taules, buscant cites i traduint tot el que ha fet falta, som un equip impressionant. A més a més, gràcies per totes les estones viscudes i per saber que sereu aquí passi el que passi. Tiet, Fina, Pilar, Dolors i Jordi, gràcies pel vostre suport incondicional i per saber que sempre puc comptar amb vosaltres. Padrí, Padrina, gràcies per ser al nostre costat i ser un referent durant tots aquest temps. M'hagués agradat moltíssim que haguéssiu pogut veure el fruit de l'esforç d'aquests últims anys.

INDEX

LIST OF FIGURES

LIST OF TABLES

LISTS OF ABBREVIATIONS

A

ab: antibody
ABB: annexin binding buffer
ACC/AHA: American College of Cardiology/American Heart Association
ADHF: acute decompensated heart failure
ADP: adenosine diphosphate
AGO: argonaute family (AGO2)
ALIX: programmed cell death 6-interacting protein
ARF1/6: ADP ribosylation factor 1/6
ARRDC1: arrestin domain-containing protein 1
ATP: adenosine triphosphate
AUC: area under the curve
AV: annexin V

B

BMI: body mass index
BNP: Brain/B-type natriuretic peptide
BSA: bovine-serum albumin

C

CAD: coronary artery disease
CCR4: carbon catabolite repressor protein 4
cDNA: complementary DNA
cEV: circulating extracellular vesicle
CHD: coronary heart disease
CHF: chronic heart failure
CM: cardiomyocyte
cMyBP-C: myosin-binding protein C
COPD: chronic obstructive pulmonary disease
CRP: C-reactive protein
Cryo-TEM: cryogenic transmission electron microscopy
CTL: control
CV: cardiovascular
CVE: cardiovascular event

D

DAMP: danger-associated molecular pattern
DCM: dilated cardiomyopathy
DCP1/2: mRNA-decapping enzyme subunit
ddPCR: droplet-digital PCR
DGCR8: DiGeorge syndrome critical region 8
DM: diabetes mellitus
DNA: desoxyribonucleic acid
dsDNA: double-strand DNA

E

ECM: extracellular matrix

EC: endothelial cell
ED: endothelial dysfunction
eEV: endothelial-derived extracellular vesicle
eGFR: estimated glomerular filtration rate
EGFR: epidermal growth factor receptor
eIF4A-I/II: eukaryotic initiation factor 4A-I/II
eiF4E: eukaryotic initiation factor 4E
eIF4F: eukaryotic initiation factor 4F
eiF4G: eukaryotic initiation factor 4G
ELISA: enzyme-linked immunosorbent assay
eNOS: endothelial nitric oxide synthase
erEV: erythrocyte-derived extracellular vesicle
ERK: extracellular signal-regulated kinase (MAPK)
ESCRT: endosomal sorting complexes required for transport
EV: extracellular vesicle

F

FcγRIII: receptor Fcγ III
FDR: false discovery rate
***FEVE**: fracció d'ejecció del ventricle esquerre*
***FEVI**: fracción de eyección del ventrículo izquierdo*
FITC: fluorescein isothiocyanate
FL1/2/3: fluorescence channel 1/2/3
FSC: forward scatter

G

GDF-15: growth/differentiation factor 15
GW182: Glycine-Tryptophan protein of 182KDa

H

HCM: hypertrophic cardiomyopathy
HDL: high density lipoproteins
HF: heart failure
HFmrEF: heart failure with mildly reduced ejection fraction
HFpEF: heart failure with preserved ejection fraction
HFrEF: heart failure with reduced ejection fraction
hnRPA2B1: heterogeneous nuclear ribonucleoproteins A2/B1
HOMA-IR: homeostasis model assessment of insulin resistance
HS: healthy subjects
hsCRP: high-sensitivity CRP
HTN: hypertension
HTx: heart transplantation
HVD: heart valve disease

I

***IC**: insuficiència/insuficiencia cardíaca*
***ICC**: insuficiència/insuficiencia cardíaca crònica/crónica*
IL: interleukin
ITGB1: β1-integrin

J

JAK-STAT: janus kinases (JAKs), signal transducer and activator of transcription proteins (STATs)

K

KEGG: Kyoto encyclopaedia of genes and genomes

L

LCA: leukocyte common antigen
LDL: low-density lipoprotein
LEV: leukocyte-derived EV
lncRNA: long non-coding RNA
LPS: lipopolysaccharide
LV: left ventricle
LVAD: LV assist device
LVEDd: LV end-diastolic diameter
LVEDv: LV end-diastolic volume
LVEF: left ventricular ejection fraction
LVESVI: LV end-systolic volume index

M

m^{7}G-pre-miRNA: 7-methylguanosine-capped pre-miRNA
MAC-1: macrophage antigen 1
MAPK: mitogen-activated protein kinase (ERK)
MHC-I: major histocompatibility complex I
MHC-β: β-myosin heavy chain
MI: myocardial infarction
min: minute
miRISC: miRNA-induced silencing complex
miRNA: microRNA
MLC: myosin light chain
MLCK: myosin light chain kinase
MØ: macrophage
Mo: monocyte
mRNA: messenger RNA
MV: extracellular microvesicle
MVB: multivesicular body

N

NADP/NADPH: nicotinamide adenine dinucleotide phosphate oxidised/reduced
NCAM1: neural cell adhesion molecule-1
NFκB: Nuclear factor κ-light-chain-enhancer of activated B cells
NK: natural killer
NO: nitric oxide
NOT: negative on TATA
NSTEMI: non-ST elevation myocardial infarction
NT-proBNP: N-terminal pro-hormone of brain natriuretic peptide
NYHA: New York Heart Association

P

PABPC: cytoplasmatic polyadenylate-binding protein

PAD: peripheral artery disease
PAN2/3: poly(A)-nuclease-deadenylation complex subunit
PAI-1: plasminogen activator inhibitor 1
PBMC: peripheral blood mononuclear cell
PBS: phosphate buffered saline
PCR: polymerase chain reaction
PDI: protein disulphide isomerase
PDL: phospholipase D
PE: phycoerythrin
PECAM1: platelet-endothelial cell adhesion molecule 1
pEV: platelet-derived extracellular vesicle
PFP: platelet-free plasma
PHTN: pulmonary hypertension
PI3K-AKT: phosphatidylinositol 3-kinase and Akt (protein kinase B)
PPI: protein-protein interaction
PS: phosphatidylserine
PSGL1: P-selectin glycoprotein ligand 1

Q

qRT-PCR: quantitative real-time polymerase chain reaction

R

RAN-GTPase: RAS-related nuclear protein-guanosine-5’-triphosphate-ase
RBGD: repository-based gene database
RhoA: Ras homolog family member A
RIPA: radioimmunoprecipitation assay
RNA: ribonucleic acid
ROC: receiver operating characteristic
ROCK: Rho-associated protein kinase

S

SDS: sodium dodecyl sulphate
SDS-PAGE: sodium dodecyl sulphate-polyacrylamide electrophoretic gel
SEM: scanning electron microscopy
sFAS: soluble FAS
shRNA: short-hairpin RNA
SMC: smooth muscle cell
SSC: side scatter
sST2: soluble suppressor of tumorigenicity-2
STEMI: ST-elevation myocardial infarction
SUA: serum uric acid
SYNCRIP: synaptotagmin-binding, cytoplasmic RNA-interacting protein

T

T2DM: type 2 diabetes mellitus
TBS: TRIS-buffered saline
TEM: transmission electron microscopy
TF: tissue factor
TFPI: tissue factor pathway inhibitor

TGF-β: transforming growth factor β
TIA: transient ischaemic attack
TL: T-lymphocyte
TNFα: tumour necrotic factor α
TNRC6A: trinucleotide repeat-containing gene 6 A
tPA: tissue plasminogen activator
TRIS: tris(hydroxymethyl)aminomethane
TRP: transient receptor potential (channel)
TSH: thyroid stimulating hormone

U

uPA: urokinase-type plasminogen activator (urokinase)
uPAR: urokinase-type plasminogen activator receptor

V

VO_2: oxygen uptake
vWF: von Willebrand factor

X

XRN1: 5'-3'-exoribonuclease

XPO1/5: exportin 1/5

OTHER

3'-UTR: 3'-untranslated region
5'-UTR: 5'-untranslated region

PUBLISHED ARTICLES

Thesis in Article Compendium Format:

ARTICLE 1

New Factors in Heart Failure Pathophysiology: Immunity cells release of extracellular vesicles

Alba Vilella-Figuerola, *Teresa Padró*, *Eulàlia Roig*, *Sònia Mirabet**, *Lina Badimon**
*Contributed equally to this work.

Published: Frontiers in Cardiovascular Medicine

Front. Cardiovasc. Med. 2022, 9, 939625, doi:10.3389/fcvm.2022.939625

Impact Factor (2021): 5.846

ARTICLE 2

Systems Biology in Chronic Heart Failure – Identification of Potential miRNA Regulators

Alba Vilella-Figuerola, *Alex Gallinat, Rafael Escate, Sònia Mirabet, Teresa Padró*, Lina Badimon**
*Contributed equally to this work.

Published: International Journal of Molecular Sciences

Int. J. Mol. Sci. 2022, 23 (23), 15226, doi.org/10.3390/ijms232315226

Impact factor (2021): 6.208

RESUM

Introducció: La insuficiència cardíaca (IC) és una entitat complexa d'alt impacte clínic i fisiopatologia poc coneguda. És una patologia difícil de reconèixer i de diagnosticar, caracteritzada per una alteració cardíaca d'etiologia variable. Les vesícules extracel·lulars (EVs per les seves sigles en anglès) són vesícules (0.1–1μm) alliberades en resposta a l'estrès o l'activació cel·lular que tenen antígens derivats de les seves cèl·lules parentals. Són les transportadores principals d'ARN al plasma, incloent els microARNs (miRNAs per les seves sigles en anglès) que estan implicats en la regulació epigenètica. En aquesta tesi hipotetitzem que ambdós, les EVs i els miRNAs, estan desregulats i potencialment relacionats amb la fisiopatologia de la IC crònica (ICC).

Objectius: Identificar i caracteritzar les signatures circulants diferencials de les EVs i els miRNAs, i relacionar-les amb funcions moleculars i processos biològics implicats en el desenvolupament i la progressió de la ICC.

Mètodes: Les EVs i els miRNAs circulants es van aïllar del plasma dels individus amb i sense ICC (aparellats per sexe i edat) inclosos en aquest estudi. Les EVs circulants es van analitzar mitjançant citometria de flux, usant anticossos monoclonals específics i annexina V (marcador de fosfatidilserina). Els seus nivells es van relacionar amb la presència i gravetat de la ICC, i la seva etiologia. Els miRNAs es van identificar i quantificar mitjançant qRT-PCR i els seus nivells es van associar amb la gravetat, pronòstic, etiologia, i la classificació de la ICC segons la fracció d'ejecció del ventricle esquerre (FEVE). L'anàlisi *in silico*, usant xarxes d'interacció proteica i enriquiment de vies, es va utilitzar per identificar mecanismes relacionats amb el desenvolupament de la ICC. El poder discriminador de les EVs, els miRNAs i les seves combinacions amb altres biomarcadors, es va investigar mitjançant corbes ROC (per les seves sigles en anglès).

Resultats: Els pacients amb ICC, en comparació amb subjectes sense ICC, tenien nivells incrementats de EVs circulants derivades de cèl·lules immunes. Les EVs provenien de cèl·lules d'immunitat innata i adaptativa (monòcits i neutròfils, limfòcits-T i cèl·lules *natural killer*, respectivament). Les EVs derivades de limfòcits-T i neutròfils activats, i de limfòcits-T no activats, correlacionaven amb la gravetat de la ICC (classificació NYHA). A més, els pacients amb ICC isquèmica presentaven els nivells més alts de EVs derivades de limfòcits-T i neutròfils. L'anàlisi ROC va mostrar que la combinació d'EVs de leucòcits/neutròfils discriminava millor que el biomarcador NT-proBNP la gravetat de la malaltia en aquests pacients.

També es va identificar i validar un patró plasmàtic diferencial de 8 miRNAs (*let-7a-5p*, *miR-30b-5p*, *miR-107*, *miR-125a-5p*, *miR-139-5p*, *miR-150-5p*, *miR-335-5p* i *miR-342-3p*) amb expressió reduïda en pacients amb ICC, comparats amb individus sense ICC. Usant anàlisis *in silico* i aproximacions de biologia de sistemes, vam evidenciar que els gens diana de 7 d'aquests miRNAs, organitzats en grups, participaven en mecanismes moleculars i vies de senyalització relacionades amb la ICC, incloent el cicle i la senescència cel·lular, i les vies de senyalització de Ras, citocines, PI3K-AKT i TGF-β. Addicionalment, aquests grups discriminaven pacients segons la seva FEVE (preservada i reduïda) i la seva etiologia de base.

Conclusió: Els resultats d'aquesta tesi mostren un patró diferencial d'EVs i miRNAs en el plasma de pacients amb ICC, així com també una activació significativa de cèl·lules immunes, reflectida en l'alt alliberament d'EVs positives per antígens específics. Les cèl·lules immunes (innates i adaptatives), mediant l'alliberament d'EVs i la seva càrrega (incloent miRNAs) podrien promoure la progressió de la malaltia, així com també l'afectació d'òrgans allunyats del cor (ronyons, etc.). De forma concordant, els patrons alterats de miRNAs circulants en ICC podrien contribuir, mitjançant la regulació paracrina, al deteriorament clínic d'aquests pacients.

RESUMEN

Introducción: La insuficiencia cardíaca (IC) es una entidad compleja, de alto impacto clínico y fisiopatología poco conocida. Es una patología difícil de identificar y diagnosticar, caracterizada por una alteración cardíaca de etiología variable. Las vesículas extracelulares (EVs por sus siglas en inglés) son vesículas (0.1–1µm) liberadas en respuesta al estrés o activación celular que tienen antígenos derivados de sus células parentales. Son las transportadoras principales de ARN en plasma, incluyendo los microARNs (miRNAs por sus siglas en inglés), que están implicados en la regulación epigenética. En esta tesis hipotetizamos que ambos, las EVs y los miRNAs, están desregulados y potencialmente relacionados con la fisiopatología de la IC crónica (ICC).

Objetivos: Identificar y caracterizar las signaturas circulantes diferenciales de las EVs y los miRNAs, y relacionarlas con funciones moleculares y procesos biológicos implicados en el desarrollo y la progresión de la ICC.

Métodos: Las EVs y los miRNAs circulantes se aislaron del plasma de los individuos con y sin ICC (apareados por sexo y edad) incluidos en este estudio. Las EVs circulantes se analizaron mediante citometría de flujo, usando anticuerpos monoclonales específicos y anexina V (marcador de fosfatidilserina). Sus niveles se relacionaron con la presencia y gravedad de la ICC y su etiología. Los miRNAs se identificaron y cuantificaron mediante qRT-PCR y sus niveles se asociaron con la gravedad, pronóstico, etiología, y la clasificación de la ICC según la fracción de eyección del ventrículo izquierdo (FEVI). El análisis *in silico*, mediante el uso de redes de interacción proteica y enriquecimiento de vías, se usó para identificar mecanismos relacionados con el desarrollo de la ICC. El poder discriminativo de las EVs, los miRNAs y sus combinaciones con otros biomarcadores, se investigó mediante curvas ROC (por sus siglas en inglés).

Resultados: Los pacientes con ICC, comparados con sujetos sin ICC, tenían niveles incrementados de EVs circulantes derivadas de células inmunes. Las EVs provenían de células de inmunidad innata y adaptativa (monocitos y neutrófilos, y linfocitos-T y células *natural killer*, respectivamente). Las EVs derivadas de linfocitos-T y neutrófilos activados, y de linfocitos-T no activados, correlacionaban con la gravedad de la ICC (clasificación NYHA). Además, los pacientes con ICC isquémica presentaban los niveles más altos de EVs de linfocitos-T y neutrófilos. El análisis ROC reveló que la combinación de EVs de leucocitos/neutrófilos discriminaba mejor que el biomarcador NT-proBNP la gravedad de la enfermedad en estos pacientes.

También se identificó y validó un patrón plasmático diferencial de 8 miRNAs (*let-7a-5p*, *miR-30b-5p*, *miR-107*, *miR-125a-5p*, *miR-139-5p*, *miR-150-5p*, *miR-335-5p* y *miR-342-3p*), con expresión disminuida en pacientes con ICC en oposición a sujetos sin ICC. Usando un análisis *in silico* y aproximaciones de biología de sistemas, evidenciamos que los genes diana de 7 de dichos miRNAs organizados en grupos, participaban en mecanismos moleculares y vías de señalización relacionadas con la ICC, incluyendo el ciclo y la senescencia celular, y las vías de señalización de Ras, citoquinas, PI3K-AKT y TGF-β. Adicionalmente, estos grupos podían discriminar pacientes según su FEVI (preservada y reducida) y su etiología de base.

Conclusión: Los resultados de esta tesis muestran un patrón diferencial de EVs y miRNAs en el plasma de pacientes con ICC. Los resultados muestran una activación significativa de células inmunes, reflejada por la alta liberación de EVs positivas por antígenos específicos. Las células inmunes (innatas y adaptativas), mediante la liberación de EVs y su carga (incluyendo miRNAs) podrían promover la progresión de la enfermedad, así como la afectación de órganos alejados del corazón (riñones, etc.). De forma concordante, los patrones alterados de miRNAs circulantes en ICC podrían contribuir, mediante regulación paracrina, al deterioro clínico de estos pacientes.

ABSTRACT

Introduction: Heart failure (HF) is a complex entity with a high clinical impact and poorly understood pathophysiology. Characterised by cardiac function impairment and variable underlying aetiology, HF is difficult to be recognised and diagnosed. Circulating extracellular vesicles (EVs) are small vesicles (0.1–1µm) shed after cellular stress or activation that present parental-cell antigens on their surface. EVs are the main carriers of RNA in plasma, including coding and non-coding RNAs such as microRNAs (miRNAs), which are involved in epigenetic regulation. In this thesis, we hypothesise that both EVs and miRNAs are deregulated in chronic HF (CHF) and are potentially involved in its pathophysiology.

Objectives: This thesis aimed to identify and characterise differential signatures of circulating EVs and miRNAs in plasma, in association with molecular functions and biological processes related to CHF development and progression.

Methods: CHF patients and individuals without CHF (matched by sex and age) were included in the study. Circulating EVs and miRNAs were isolated from plasma samples. Circulating EVs were analysed by flow cytometry using specific monoclonal antibodies and annexin V (phosphatidylserine marker) and their levels related to the presence and severity of CHF and its underlying aetiology. MicroRNAs were analysed using a non-targeted approach (qRT-PCR) for their identification and quantification in CHF and non-CHF patients. miRNA levels in plasma were associated with CHF severity, underlying aetiology, left ventricular ejection fraction (LVEF) classification and prognosis. *In silico* analysis of miRNAs' target genes was pursued to identify pathways related to disease development using protein-protein interaction networks and pathway enrichment analysis. The value of circulating EVs and miRNAs to discriminate patients according to disease severity and underlying aetiology was investigated by receiver operating curve (ROC). Combined probabilities of circulating EVs or miRNAs with other used biomarkers were also investigated.

Results: CHF patients had increased levels of circulating EVs shed by immune cells in comparison to non-CHF. Immune-cell-derived EVs in CHF patients' plasma were mostly derived from innate and adaptative immune cells (monocytes and neutrophils, T-lymphocytes and natural killer cells, respectively), and carried activation leukocyte markers. Interestingly, EVs from activated T-lymphocytes and neutrophils, as well as EVs from non-activated T-lymphocytes, correlated with disease severity (NYHA classification). Additionally, CHF patients with ischaemic aetiology had the highest levels of EVs shed by T-lymphocytes and neutrophils. ROC curve analysis revealed that the combination of EVs derived from leukocytes/neutrophils discriminated disease severity better than the used biomarker NT-proBNP in these patients.

Regarding the circulating miRNAs, we identified and validated a differential pattern of 8 miRNAs (*let-7a-5p*, *miR-30b-5p*, *miR-107*, *miR-125a-5p*, *miR-139-5p*, *miR-150-5p*, *miR-335-5p* and *miR-342-3p*) downregulated in the systemic circulation of CHF patients. Furthermore, by using *in silico* analysis and systems biology approaches to identify their target genes and predict protein-protein interactions, we evidenced that target genes from 7 of these miRNAs, when organised in clusters, participated in molecular mechanisms and signalling pathways related to CHF, including cell cycle, cellular senescence and Ras, chemokine, PI3K-AKT and TGF-β signalling. Moreover, they could discriminate CHF patients according to their LVEF (preserved and reduced) and to their background aetiology.

Conclusion: The results of this thesis show a differential pattern of EVs and miRNAs in the plasma of CHF patients. The results suggest a significant activation of the immune cells as shown by the high release of EVs positive for specific epitopes. Activated innate and adaptive immune cells, through the release of EVs and their carried messengers including miRNAs might promote disease progression and affectation of distant organs related to the heart (e.g., kidney). In agreement, altered patterns of circulating miRNAs in CHF might contribute through paracrine regulation to the clinical deterioration of these patients.

'This must be a simply enormous wardrobe!' thought Lucy, going still further in and pushing the soft folds of the coats aside to make room for her. Then she noticed that there was something crunching under her feet. 'I wonder is that's more moth balls?' she thought, stooping down to feel it with her hands. But instead of feeling the hard, smooth wood of the floor of the wardrobe, she felt something soft and powdery and extremely cold. 'This is very queer,' she said, and went on a step or two further.
The Lion, the Witch, and the Wardrobe, **C. S. Lewis (1950)**

Introduction

1. HEART FAILURE

Heart failure (HF) is a complex disease where the heart is unable to provide a correct cardiac output. Thus, it is incapable to meet and maintain the body's metabolic requirements and to accommodate an appropriate venous return[1,2]. It results from structural and functional cardiac alterations and is usually the final stage of these disorders[3].

1.1. Epidemiology, incidence and prevalence

Recent reports suggest that an estimated 64.3 million people are living with HF worldwide, which in developed countries accounts for 1–3% of the general adult population[4–7]. This prevalence is steadily augmenting, mainly due to the general ageing of the population and improved survival to ischaemic events[8]. The incidence of HF in Europe and the United States of America is 1–9/1,000 individuals-year, with an increasing tendency. Nevertheless, these numbers vary depending on the population studied and the inclusion criteria used[6,7]. With matching trends, the incidence in Spain was 2.78/1,000 individuals-year (>18 years old) in 2019, and these values have held for the last 3 years[9]. Further, as HF incidence increases with age, in Spain, the prevalence of HF in octogenarians is 9%[9]. Similarly, a 2017 study realised in Catalonia, detected, apart from the increasing prevalence of HF due to age, a prevalence of 8.8% in people over 74 years[10], mimicking values observed overall Spain[9].

1.2. Classification for chronic and acute heart failure

The classification of HF is complex and has been changing over time. At the moment, the most used classification is that considering disease onset/course; hence HF patients are divided depending on their symptomatology. Patients presenting stable HF symptomatology are classified as having chronic HF (CHF), while those presenting sudden HF symptomatology are defined as having acute HF[8]. This thesis focuses on CHF patients.

1.2.1. Acute heart failure

As mentioned above, CHF refers to HF with stable symptomatology (see below), whereas acute HF can be defined as new onset HF (*de novo* HF) or as worsening of HF symptoms (acute decompensated HF [ADHF]) that requires urgent care and may result in an unscheduled hospitalisation[3,8,11]. Although the nomenclature of this disease state may induce the belief that acute HF is a sudden onset of symptoms, many patients may present a more subacute course, with a gradual worsening of symptomatology that ultimately reaches a level of severity sufficient to seek unscheduled medical care[3,8,11]. Thus, the majority of acute HF hospitalisations are related to ADHF rather than to *de novo* HF[11].

1.2.2. Chronic heart failure

The main classification system used to stratify CHF uses left ventricular ejection fraction (LVEF) values. LVEF is defined as the volume of blood the heart is capable of propelling into the systemic circulation during each cardiac cycle. The use of LVEF values to classify CHF is related to the original clinical trials in this disease, where substantial drug-related improvement of patients presenting LVEF values below 40% was observed. However, the fact that some CHF patients can present with LVEF values above this cut-off and the high variability in LVEF measurements needs to be considered. Nevertheless, although there is controversy and a lack of consensus on the optimal LVEF cut-off to define each group, the latest guidelines of the European Society of Cardiology divide CHF into three categories[3]:

- **Heart failure with reduced ejection fraction (HFrEF)**: This category includes CHF patients presenting LVEF values ≤40%[3].
- **Heart failure with preserved ejection fraction (HFpEF)**: This category comprises CHF patients with LVEF values ≥50%, and presenting, besides HF symptomatology, structural and/or functional cardiac abnormalities and/or increased values of natriuretic peptides[3].
- **Heart failure with mildly reduced ejection fraction (HFmrEF)**: CHF patients with LVEF values between 41% and 49% are included in this category. Additionally, diagnosis can consider elevated natriuretic peptides and the presence of structural heart disease, but these criteria are not mandatory if LVEF measurement is accurate[3]. However, as this thesis focuses on HFpEF and HFrEF, this group will be not explored in depth.

Apart from the general classification considering LVEF, CHF can be classified according to the severity of the disease symptomatology. Two main classification systems exist, namely the New York Heart Association (NYHA) and the American College of Cardiology/American Heart Association (ACA/AHA) classifications. Albeit both systems consider disease symptomatology, there are slight differences between them. NYHA considers cardiac functionality and disease severity, while ACA/AHA considers disease progression[1,3]. Both systems are outlined in **Table 1**.

The work of this thesis includes CHF patients with HFpEF and HFrEF. Their severity has been classified using the NYHA system.

1.3. Signs and symptoms

Signs and symptoms of CHF patients result from the aforementioned inadequate cardiac output and the lack of an efficient venous return. Hence, CHF patients suffer from dyspnoea, cough and wheezing due to the increased pressure in the pulmonary capillary bed that occurs due to the ineffective forward flow from the left ventricle (LV). In addition, they also present ascites and oedemas in the lower limbs as a consequence of the inability of the right ventricle to accommodate a correct venous return[1,12]. Noteworthy, HF is associated with women and with age, with prevalence increasing in older populations[13,14].

Table 1: Heart failure classifications according to disease severity.

NEW YORK HEART ASSOCIATION CLASSIFICATION[1,3]	
NYHA Class I	No limitation of physical activity. Ordinary physical activity does not cause breathlessness, fatigue or palpitations.
NYHA Class II	Slight limitation of physical activity. Comfortable at rest, but ordinary physical activity results in breathlessness, fatigue or palpitations.
NYHA Class III	Marked limitation of physical activity. Comfortable at rest, but less than ordinary physical activity results in breathlessness, fatigue or palpitations.
NYHA Class IV	Unable to carry on any physical activity without discomfort. Symptoms can be present at rest. If any physical activity is undertaken, discomfort is increased.
AMERICAN COLLEGE OF CARDIOLOGY/AMERICAN HEART ASSOCIATION CLASSIFICATION[15]	
A: High risk for developing HF	At high risk for HF but without structural heart disease or HF symptoms.
B: Asymptomatic HF	Structural heart disease but without signs or HF symptoms.
C: Symptomatic HF	Structural heart disease with prior or current HF symptoms.
D: Refractory end-stage HF	Refractory HF requiring specialised interventions.

HF: heart failure; **LVEF**: left ventricular ejection fraction; **NYHA**: New York Heart Association

Symptoms are often non-specific and do not, therefore, help discriminate between HF and other health problems. Signs and symptoms of CHF are mainly due to fluid retention and may resolve quickly with diuretic therapy. Signs, such as elevated jugular venous pressure and displacement of the apical impulse, can be more specific but are harder to detect. As symptomatology is non-specific, biomarkers are used to assist in CHF diagnosis and stratification. Established biomarkers[16] utilised in clinical practice are listed in **Table 2**. Nevertheless, the search and study of new biomarkers is still ongoing[16,17] and it is possible that new ones will be unravelled in the future. This thesis addresses cellular and molecular components (extracellular vesicles and microRNAs) that are associated with CHF and that can become new diagnostic, prognostic and stratification biomarkers in the future.

1.4. Risk factors and aetiology

Risk factors of HF include hypertension, pulmonary hypertension, diabetes mellitus, obesity, chronic lung disease, hypercholesterolaemia, chronic kidney disease, atrial fibrillation, anaemia, ischaemic heart disease and familial history of CHF[8,13], among others. Risk factors distribution can vary between HFpEF and HFrEF, as shown in **Table 3**. Of note, comorbidities are associated with HFpEF, with 50% of patients presenting at least five or more major comorbidities[14,18]. This is, on average, one more comorbidity than those observed in HFrEF[14].

Table 2: Established biomarkers for chronic heart failure diagnosis, prognosis and risk stratification.

BIOMARKER	RELEASE STIMULI	UTILITY	REFERENCES
BNP **NT-proBNP**	Myocardial stretch	- Increased in CHF plasma. - Independent predictor of mortality and hospital admissions for CHF. - Associated with disease severity.	16,17,19
sST2	Mechanical stretch Cardiac fibrosis	- Increased in CHF serum. - Independent predictor of mortality and HTx. - CVE predictor and CHF hospital readmissions.	16,17,19
Troponin T and I	Myocardial damage	- Increased in CHF serum. - Associated with all-cause mortality. - Associated with hospital readmission.	16,17,19
Galectin-3	Cardiac fibrosis Cardiac remodelling	- Increased in CHF plasma. - Increased in hypertrophic hearts. - Independent predictor of mortality.	16,17,19

BNP: brain/B-type natriuretic peptide; **CHF**: chronic heart failure; **CVE**: cardiovascular event; **HTx**: heart transplantation; **NT-proBNP**: N-terminal pro-hormone of the brain natriuretic peptide; **sST2**: soluble suppressor of tumorigenesis 2

Table 3: Heart failure risk factors, according to left ventricular ejection fraction classification.

RISK FACTOR	HFpEF	HFrEF	REFERENCES
Age	++	+	13,14,20
Sex	Female	Male	13,20
Hypertension	++	+	13,14
Pulmonary hypertension	+		13
Hyperlipidaemia	+	+	13
Diabetes mellitus	+	+	13
Obesity	++	+	13,14,20
Atrial fibrillation	+		13,14
Anaemia	+		13,14
Chronic obstructive pulmonary disease	+		13
Chronic kidney disease	+	+	13
Coronary artery disease **Ischaemic disease**	+	++	13,14

HFpEF: heart failure with preserved ejection fraction; **HFrEF**: heart failure with reduced ejection fraction

Aetiology for CHF is variable, and is related to and affected by its risk factors, such as hypertension and ischaemic heart disease. Many cardiac conditions, hereditary defects and systemic diseases can result in HF, but the main causes include ischaemic heart disease, hypertensive heart disease and heart valve disease (**Figure 1**)[21]. These aetiologies can be divided into ischaemic and non-ischaemic, with the former group comprised of ischaemic/atherosclerotic CHF and the latter comprised of genetic, hypertensive or valve disease.

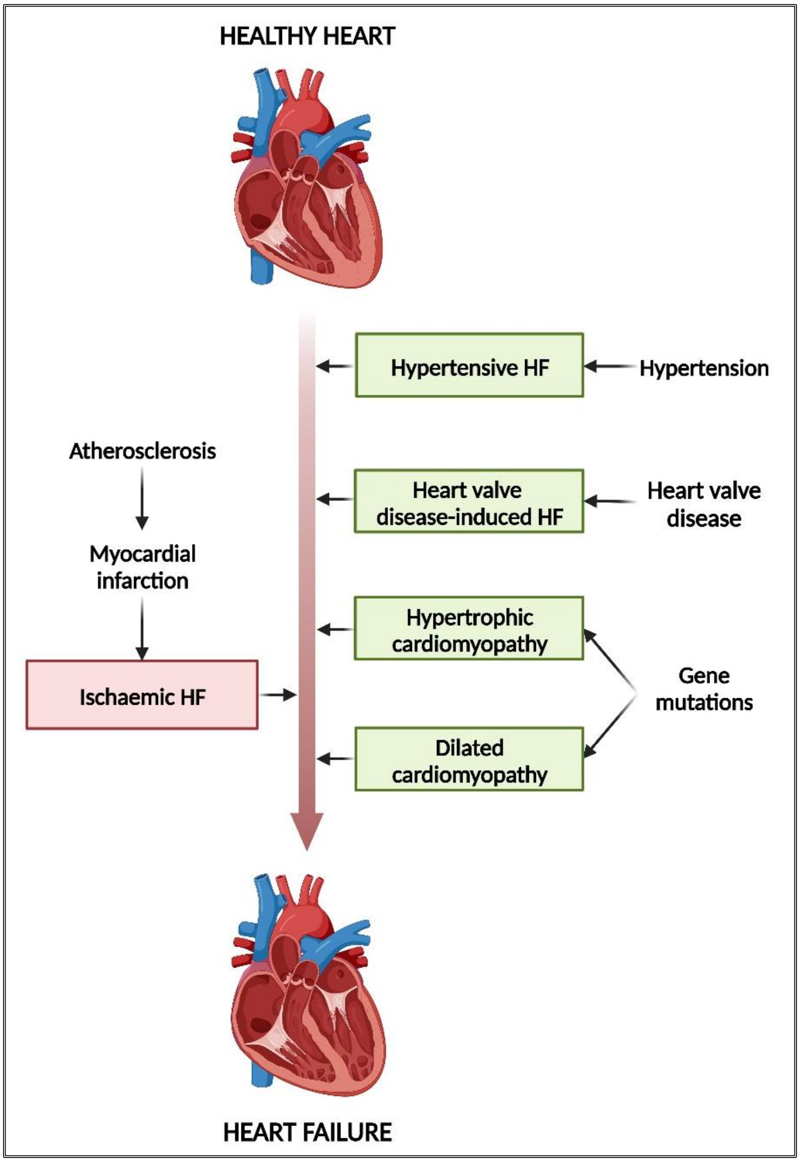

Figure 1: Aetiologies related to heart failure development.
Green boxes indicate a non-ischaemic underlying aetiology, while red boxes indicate an ischaemic underlying aetiology. **HF**: heart failure.

1.4.1. Ischaemic heart failure

Atherosclerotic ischaemic heart disease is one of the most important causes of CHF, accounting for 40% of HF cases worldwide. In the United States of America and Europe estimates are much higher, being around 60%[7].

Acute or chronic cardiac ischaemia can induce changes in the heart that can lead to CHF through cardiac remodelling. Both conditions produce a reduction of oxygen availability to cardiac cells, which ultimately induces cell death.

Pathophysiologically, myocardial ischaemia is the result of atherosclerosis or microvascular dysfunction[22]. On the one hand, in an atherosclerosis-related acute event, such as a myocardial infarction (MI), ischaemia is normally associated with the rupture of an atherosclerotic plaque and its thrombotic complications. In contrast, in atherosclerosis-related chronic ischaemia, such as stable angina pectoris, there is a reduction of blood flow due to the narrowing of the blood vessels calibre by atherosclerotic plaques, inducing insufficient perfusion of the heart[23]. On the other hand, ischaemia induced by coronary microvascular dysfunction is a consequence of the structural and functional impairment of the coronary microvasculature (vessels <500µm diameter). In normal conditions, the regulation of blood flow distribution in the myocardium occurs through the modulation of the peripheral vascular resistance in the coronary microvasculature. That is the regulation of the vasodilation and vasoconstriction of the microvessels to modulate the volume of blood flow. When this modulation is impaired, the amount of blood reserve in the coronary arteries decreases and ischaemia can occur[22]. This type of ischaemia is typically observed in HFpEF, while atherosclerosis-related ischaemia is normally observed in HFrEF[24,25].

Nevertheless, as mentioned previously, ischaemia in the coronary arteries prevents the delivery of oxygen to cardiomyocytes (CMs), provoking a metabolic shift in these cells. Specifically, CM metabolism becomes more anaerobic, producing instability of the cell membrane and ultimately cell death[26,27]. Ischaemia-induced necrosis causes the simultaneous death of millions of cells (CMs and non-CMs), which in turn, activates the immune system and initiates the influx of immune cells (neutrophils and macrophages, among others) into the infarcted area. Both neutrophils and macrophages have a role in extracellular matrix (ECM) destruction, which also contributes to the expansion of the infarcted area. When the inflammatory response downregulates, fibroblasts repopulate the infarcted area and synthesise new ECM, forming a fibrotic scar. These processes can lead to changes in cardiac geometry and architecture (adverse ventricular remodelling) and the establishment of HF[26–28].

1.4.2. Non-ischaemic heart failure

The most common causes of non-ischaemic HF are heart valve disease and hypertension[21]. Nevertheless, other causes can also produce CHF, such as dilated and hypertrophic cardiomyopathy.

HYPERTENSIVE HEART FAILURE

Hypertension (HTN) is the most common risk factor for HF. In fact, in the Framingham Heart Study cohort, the percentage of HTN in new HF diagnoses was 91%[29]. Indeed, HTN is the second leading cause of HF[30].

Induction of HF by HTN occurs through the development of chronic pressure overload, which conduces to LV hypertrophy. Progressive concentric hypertrophy and cardiac fibrosis result in diastolic dysfunction, which over time can evolve into HFpEF. Additionally, in response to pressure and volume overload, eccentric hypertrophy occurs, inducing HFrEF[31].

At the molecular level, chronic pressure overload produces ECM alterations and CM hypertrophy (increased number of sarcomeres, enhanced protein synthesis), ultimately augmenting LV mass. Later on, sarcomeres in CMs become disorganised, impairing relaxation and increasing stiffness. Moreover, enhanced collagen turnover induces cardiac fibrosis[32]. All these changes in the LV, along with cardiac remodelling, facilitate the development of diastolic dysfunction and clinical HF[31,33].

HEART VALVE DISEASE-RELATED HEART FAILURE

Globally, the majority of HF due to heart valve disease (HVD) is secondary to rheumatic disease, especially in developing countries. In America and Europe, the incidence is considerably lower, as rheumatic heart disease is practically non-existent and most HVD cases have a degenerative nature, thus are due to valve dysfunction[7,21].

Pathophysiologically, HVD derives in HF after a prolonged time during which compensatory mechanisms occur in response to valve malfunction, which causes volume overload. Regurgitant valves induce LV enlargement through ECM remodelling and CM's growth and fibre reorganisation. The synthesis of new sarcomeres in CMs contributes to LV eccentric hypertrophy. Up to this point, a correction of the valvular problem can reverse this compensatory mechanism. However, as volume overload becomes chronic due to valve malfunction, LV dilation progresses. In parallel, there is an increase in diastolic pressure and the development of diastolic dysfunction. Once this maladaptive structural and functional remodelling has taken place, the lesion becomes irreversible and can progress to HF[34,35].

HYPERTROPHIC CARDIOMYOPATHY-RELATED HEART FAILURE

Hypertrophic cardiomyopathy (HCM) is a dominant monogenetic disease with a high incidence (1:500 individuals of the general population)[36,37]. Mutations have been identified in at least 11 genes, affecting those coding for contractile proteins of the sarcomere or the Z-disc. The most frequent mutations, accounting for 70% of cases, have been found in the genes *MYH7* and *MYBPC3*, coding for the proteins MHC-β and cMyBP-C, respectively[36]. Mutations in other genes, such as those involved in Ca^{2+} signalling have also been documented[37].

Phenotypically, HCM patients undergo cardiac remodelling, with thickening (hypertrophying) of the LV[36] that can transition to LV dilation[37]. They also present cardiac fibrosis and develop diastolic dysfunction[37,38]. Worsening of the condition leads to a HF phenotype[36].

DILATED CARDIOMYOPATHY-RELATED HEART FAILURE

With a prevalence of 1:2,500 individuals[39], dilated cardiomyopathy (DCM) is another cause of non-ischaemic HF. As HCM, DCM can have a genetic basis, comprising 30–40% of the cases. More than 100 genes have been found to have a role in DCM, encoding proteins related to the sarcomere, the sarcolemma, the cytoskeleton, the nucleus and the nuclear lamina, and the Z-disc[39].

Phenotypically, DCM patients present ventricular dilation and systolic dysfunction (HFrEF). The mechanisms underlying this cardiomyopathy are variable depending on the aetiologic background. In genetic DCM, alterations in the heart structure are due to mutations affecting either structural- or pathway signalling-related proteins. This induces defective force generation and transmission, and altered muscle contraction. In both, genetic and non-genetic DCM, increased volume overload, myocardial remodelling, abnormal Ca^{2+} cycling, myocardial energy deficit or excessive neurohumoral stimulation can have a role in ventricle dilation and the induction of HF[39]. DCM can also be the result of autoimmunity triggered by infections or tissue injury. Autoantibodies against CM-proteins have been found to be involved in DCM development[40].

1.5. Pathophysiology

The pathophysiology of CHF is complex and variable. Several mechanisms have been related to CHF development, most of them related to cardiac remodelling.

Cardiac remodelling is defined as the molecular and interstitial modifications, resulting from cardiac injury, that clinically manifest changes in heart size, shape, and function[41,42]. Initial insult can be variable and includes ischaemic disease (MI), pressure overload (aortic stenosis, HTN, HVD), inflammation (myocarditis) or volume overload (valvular regurgitation, HVD)[41]. Cardiac remodelling is a complex process that finalises with the development of cardiac dysfunction, which at the same time, is the leading cause of ventricular dysfunction and ultimately CHF[42]. Although the mechanisms underlying cardiac remodelling are not fully understood, factors potentially involved in this process are described below (**Figure 2**). Indeed, endothelial dysfunction, inflammation, cardiac fibrosis, cardiac hypertrophy and dilation, among others, are involved in cardiac remodelling.

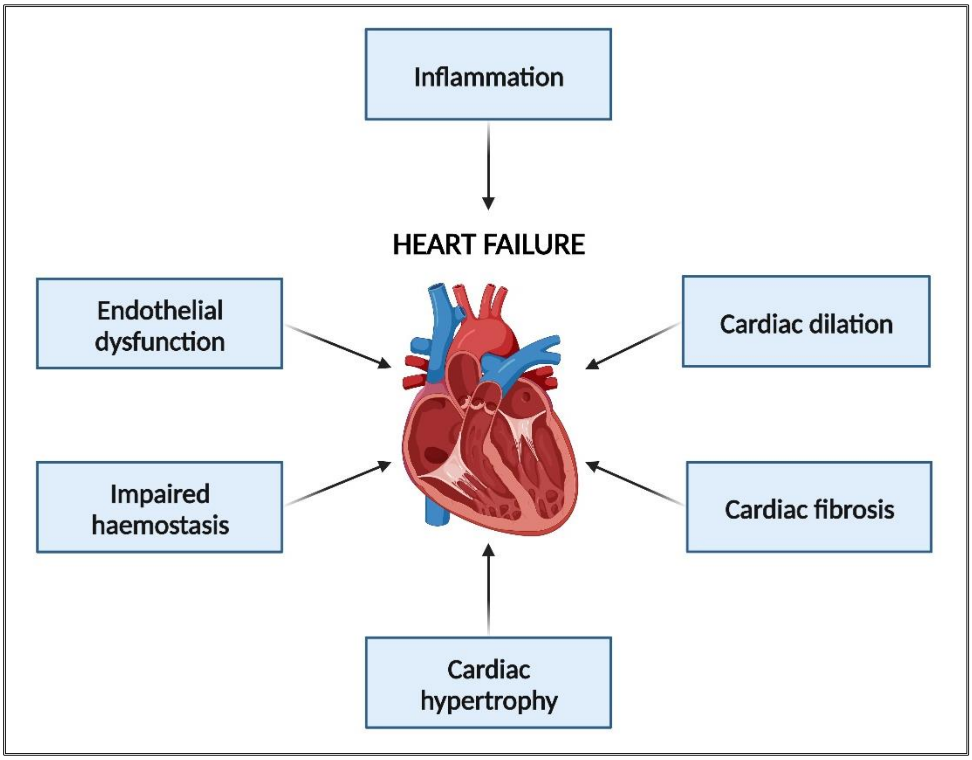

Figure 2: Mechanisms related to chronic heart failure development.

1.5.1. Endothelial dysfunction

The endothelium is a cellular mono-layer lining the inner surface of blood vessels. It is a structural barrier between the circulating blood and the vessel wall that regulates cell adhesion and aggregation, molecular permeability and blood flow. Additionally, it has anti-inflammatory properties, protects against oxidative stress, is crucial for haemostasis and fibrinolysis regulation and modulates vascular tone[43,44].

The endothelium regulates vascular function through the release of vasoconstrictor and vasodilator substances. Vasodilation of the endothelium is mainly mediated by the synthesis and release of nitric oxide (NO) by endothelial cells (ECs) after receptor- and flow-mediated stimuli. The production of NO induces the relaxation of smooth muscle cells (SMCs) and thus vasodilation. Further, NO inhibits platelet aggregation and induces the endothelium's anti-inflammatory effects[43,45,46]. In that regard, the endothelium expresses molecules that prevent coagulation and thrombosis, preventing platelet activation and adhesion[46].

Endothelial dysfunction (ED) relates to the deleterious alterations caused by an imbalance between endothelium-derived vasodilatory and vasoconstrictive actions. Therefore, ED is defined by a reduction of flow- or agonist-mediated vasodilation. Given that ED is characterised by a decreased bioavailability of NO, it is accompanied by a reduction of anticoagulant properties (decreased expression of anticoagulant molecules) and an increase of inflammation (increased expression of adhesion molecules and increased release of cytokines and chemokines)[43,45,46].

Independently of their LVEF[44] or underlying aetiology[47], CHF patients have altered endothelial-dependent vasodilation. Several studies have demonstrated that vasodilation is reduced in CHF compared to healthy subjects in both coronary and non-coronary vascular beds[47,48]. In CHF ED is mediated by oxidative stress, as there is an impairment in the balance between the formation of reactive oxygen species (superoxide radicals and other oxidative species) and their inactivation through endogenous antioxidant systems[43,44]. This increases reactive oxygen species production and the direct inactivation of NO[43,45]. Reduced bioavailability of NO, which can also be mediated by inflammation[49], is related to a decreased vasodilation, reduced sensitivity to myofilament Ca^{2+} sensitivity (affected contractility), endothelial nitric oxide synthase (eNOS) uncoupling (production of eNOS-derived superoxide instead of NO synthesis) and impaired protein kinase G signalling (involved in the suppression of cardiac hypertrophy and collagen turnover, which, in turn, is involved in cardiac fibrosis)[43,45,50].

1.5.2. Metabolic changes

The heart is the most energy-consuming organ of the whole body. It synthesises adenosine triphosphate (ATP) from different molecules (fatty acids, glucose, lactate, ketones, pyruvate and amino acids) mainly by mitochondrial oxidative phosphorylation[51,52]. Cardiac metabolism is also the most oxygen-consuming, which implies that oxygen deprivation has catastrophic consequences for cardiac function. For this reason, defective cardiac metabolism is related to several cardiac diseases[51].

An energy deficit is characteristic of CHF[51,53]. This is due to mitochondrial dysfunction, which, apart from being related to altered metabolism, is associated with impaired Ca^{2+} homeostasis, deregulation of apoptosis and enhanced reactive oxygen species production, all hallmarks of CHF[51,53].

In the normal heart, 90–95% of the consumed energy is produced by mitochondrial oxidative phosphorylation, while the remaining 5–10% is obtained through glycolysis. Between 40–60% of the ATP synthesised by mitochondrial oxidative phosphorylation is derived from fatty acid oxidation, while the remaining is derived from pyruvate, branched-chain amino acid and ketone oxidation[51,52]. Fatty acid oxidation produces the greatest ATP yield of all substrates, albeit having the highest oxygen requirements[53].

By contrast, in CHF there is a metabolic shift from fatty acid oxidation to glycolysis, where fatty acid oxidation is downregulated and glycolysis is upregulated[51–53]. However, the energy produced through this glycolytic increase does not compensate for the energy deficit[51], as ATP generated through this pathway is not enough to compensate for that obtained through mitochondrial oxidative phosphorylation[53]. Changes in other metabolic pathways also occur in the failing heart. In that sense, enhanced oxidation of ketone bodies and the accumulation of branched-chain amino acids due to its impaired oxidation have also been observed[51–53]. Most of these changes have been related to the development of LV hypertrophy[53], although the exact mechanisms behind this are poorly understood.

1.5.3. Immune system and inflammation

Inflammation is a complex process that can be, in broad terms, divided into innate and adaptive immune responses. Both immune responses are activated after a detrimental stimulus. The innate immune response provides a global and non-specific defence against tissue injury (pathogenic [e.g., bacteria, virus] or environmental [e.g., ischaemia, pressure overload]), while the adaptive immune response provides a more specific cellular-based response[54].

In the heart, short-term activation of the immune system is beneficial and provides a physiological adaptation to stress[54]. However, deregulation of this response (chronic inflammation) is detrimental and leads to myocardial damage, specifically LV dysfunction, cardiac fibrosis and cardiac remodelling, and hence to HF[54,55] (**Figure 3**).

Inflammation is an important characteristic of CHF, as most patients present a chronic and unresolving inflammatory state[56]. Further, this inflammation is independent of the underlying aetiology or LVEF. Both ischaemic and non-ischaemic CHF present a persistent low-grade inflammation[57,58], as do both CHF types, HFpEF and HFrEF[49]. Indeed, inflammation markers, such as C-reactive protein or tumour necrotic factor α (TNFα) are increased in CHF patients[54,55,59].

Although inflammation has been detected in ischaemic and non-ischaemic CHF[57,58], the effect of inflammation in the former has been broadly studied and is better characterised.

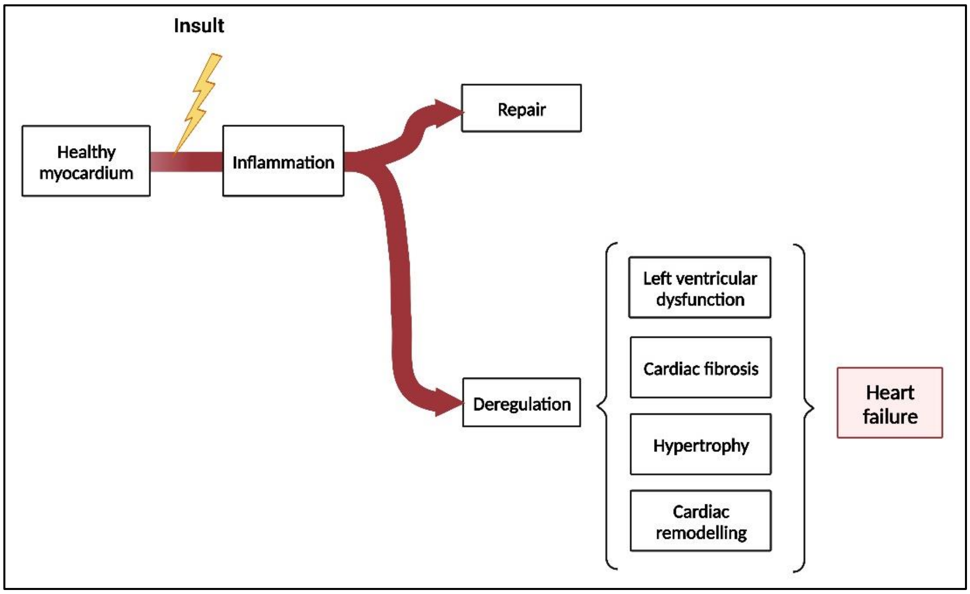

Figure 3: General implication of inflammation in heart failure development.

INFLAMMATORY RESPONSE TO AN ISCHAEMIC EVENT

An ischaemia-induced injury triggers an inflammatory response that can be divided into 3 phases (**Figure 4**)[28,57]:

1. **Acute phase**: Ischaemia causes death and damage of CMs and other cardiac cells (e.g., fibroblasts, ECs), as well as ECM degradation. Damage in ECs induces the loss of vessel integrity, augmenting its permeability and facilitating leukocyte infiltration[28]. Subsequently, damage-association molecular patterns (DAMPs) produced by cardiac cell death and ECM destruction, promote the synthesis of pro-inflammatory cytokines, chemokines and adhesion molecules. The release of these pro-inflammatory mediators takes place after DAMPs precipitate the activation of signalling pathways that activate the MAPK and NFκB pathways[28]. Inflammatory mediators produce a rapid leukocyte influx (mainly neutrophils and monocytes, but also T-lymphocytes) to the heart, which at the same time, amplifies the inflammatory response[60,61].

   Neutrophils are the first cells to arrive at the lesion[62], where they degrade ECM and contribute to the clearance of the wound by removing dead cells and debris[28,63]. Pro-inflammatory monocytes transdifferentiate into pro-inflammatory macrophages (M1). M1 macrophages clear dead cells by efferocytosis, but also secrete proteinases (cathepsins, matrix metalloproteinases) to promote tissue degradation[28,61]. Both cell types also produce pro-inflammatory cytokines (TNFα, interleukin [IL]-1, IL-6) to enhance immune response[28,60].

In parallel, after DAMP stimulation, fibroblasts secrete pro-inflammatory mediators, delaying their transdifferentiation into myofibroblasts and promoting ECM degradation[28]. It is worth mentioning that during this phase a provisional ECM, composed mainly of fibrin and fibronectin, is produced[28,32].
Of note, blood reperfusion after MI can induce reactive oxygen species that can contribute to the inflammatory response (ischaemia/reperfusion injury)[28].

2. **Reparative and proliferative phase**: Apoptotic neutrophils are phagocyted by macrophages, which are starting to shift towards a more anti-inflammatory phenotype (M2). The induction of macrophage differentiation to M2 is modulated by dead neutrophils, but also by dendritic cells and T-lymphocytes. M2 macrophages secrete anti-inflammatory cytokines, profibrotic and proangiogenic factors (IL-10, transforming growth factor β [TGF-β], vascular endothelial growth factor) to promote tissue repair[28,60,61,64].
The promotion of tissue neovascularisation is essential to the establishment of a new vessel network to provide nutrients and oxygen to the remaining cells. In response to proangiogenic factors, ECs from the infarct border zone create new vessels that extend to the injured region. Initially, those vessels lack SMCs and pericytes in their mural coat, but in the later stages of this phase, in response to platelet-derived growth factor, they acquire a mature mural coat, reducing leukocyte extravasation[28,32].
Another important feature of the reparative and proliferative phase is the activation of fibroblasts and the initiation of scar formation. Fibroblasts and other cells that can undergo mesenchymal transdifferentiation (SMCs, ECs, epicardial epithelial cells, pericytes) transdifferentiate into myofibroblasts in response to TGF-β and changes in the ECM composition[28,32,65]. These cells are implicated in the synthesis of new ECM components, such as collagens and fibronectin[32,65].
3. **Maturation phase**: In this last phase of the inflammatory response to ischaemia, scar maturation takes place. The new ECM components are cross-linked and the reparative cells remaining in the injured zone undergo apoptosis. Additionally, the secretion of antifibrotic mediators contributes to the termination of ECM formation and the reduction of fibroblast proliferation[28,32].

However, as stated previously, when inflammation does not resolve it becomes pathological. Indeed, if the injury cannot be resolved, macrophages recruit additional leukocytes to the affected area, resulting in a sustained inflammatory response, LV remodelling worsening, cardiac fibrosis promotion and CHF development. The exact mechanisms that trigger this response are poorly understood[57,59].

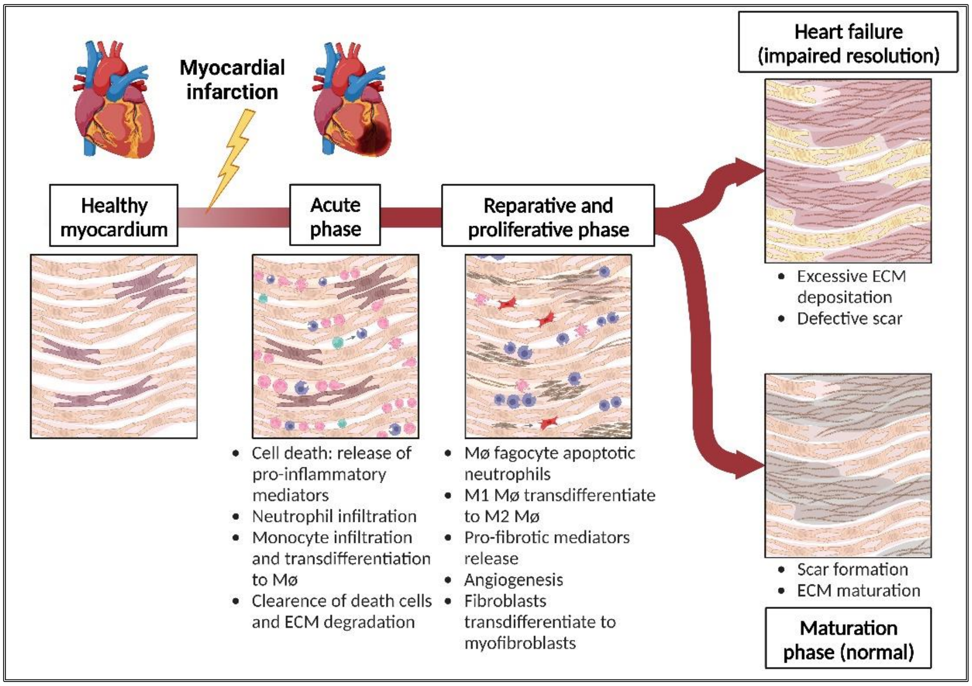

Figure 4: Inflammation after an ischaemic event.
ECM: extracellular matrix; **Mø**: macrophage

INFLAMMATORY RESPONSE IN NON-ISCHAEMIC CHRONIC HEART FAILURE

Even though it is known that low-grade non-resolving inflammation is present in CHF with a non-ischaemic background[57,58], the exact mechanisms by which inflammation affects cardiac remodelling and CHF development in these patients are not well understood.

Pressure overload (HTN-, HVD-related HF) is associated with LV hypertrophy and systolic and diastolic dysfunction. Further, the activation of the renin-angiotensin system, enhanced in HTN, leads to haemodynamic stress and hypertrophy development[64]. Noteworthy, inflammation is implicated in HTN pathophysiology[66]. Studies in mice where HF was induced by angiotensin II infusion or transverse-aortic construction described changes in the macrophage composition of the myocardium, with enrichment of those with a pro-inflammatory phenotype (M1)[64]. M1 macrophages release pro-inflammatory cytokines such as IL-1β or TNFα[58,59,64,67]. These cytokines are implicated in the deregulation of Ca^{2+} homeostasis in CMs, but also promote their hypertrophy, stiffness and apoptosis, all hallmarks of CHF[67]. TNFα and IL-1β upregulate the expression of the angiotensin I receptor and induce ECM remodelling, promoting fibrosis[58,59,67]. TNFα and angiotensin II (or activation of the renin-angiotensin system) induce TGF-β release by macrophages, enhancing fibroblasts' transdifferentiation into myofibroblasts[54,59,64,67]. Activated fibroblasts also produce TNFα and fibroblast growth factor, promoting hypertrophy[67]. Additionally, macrophages recruit T-lymphocytes, inducing fibrosis and adverse cardiac remodelling. Further, autoreactive T_{helper} cells with specificity for CM-expressed antigens promote hypertrophy and are related to CHF[61]. Thus, pressure overload induces leukocyte infiltration, pro-inflammatory cytokine release and cardiac fibrosis, ultimately leading to CHF.

In CHF due to DCM, there is also infiltration of immune cells, such as M1 macrophages, T-lymphocytes and B-lymphocytes to the myocardium. These immune cells release cytokines (e.g., TGF-β, IL-1β, TNFα) that promote adverse remodelling and cardiac fibrosis by promoting the activation and transdifferentiation of fibroblasts into myofibroblasts. Over time, myocardium stiffness increases, enhancing volume overload. This contributes to the worsening of LV dilation and CHF development[40,57,67]. Of note, auto-antibodies (autoimmunity) produced by B-lymphocytes (against β_1 receptor, M2 muscarinic receptor, adenine-nucleotide transporter, cardiac myosin, cardiac troponin I, Na^+/K^+ ATPase) have also been related to DCM development[40,54,61].

1.5.4. Haemostasis and platelet activation

Haemostasis is a highly regulated process that finalises in thrombi formation and the induction of tissue repair. The haemostatic system can be divided into three phases[68]:

1. **Primary haemostasis**: Blood vessel vasoconstriction at the injury site and platelet plug formation through platelet adhesion and aggregation.
2. **Secondary haemostasis**: Coagulation cascade activation as well as fibrin deposition and stabilisation.
3. **Tertiary haemostasis**: Dissolution of the fibrin clot through plasmin generation (fibrinolysis).

Thus, injury promotes vessel vasoconstriction and prothrombotic factors exposure (collagen, tissue factor [TF], etc.), triggering platelet activation and adhesion, and the formation of a platelet plug. Platelet adhesion occurs through the interaction of receptors in the platelet membrane and the endothelium. Specifically, ECs express von Willebrand factor (vWF) which binds to the glycoprotein complex Ib-IX on the platelet membrane. Once adhered, platelets activate and change shape, forming pseudopods that allow their aggregation and their adhesion into the injured area. Additionally, they express P-selectin and collagen receptors (integrin $\alpha_{IIb}\beta_3$) in their membrane and synthesise and secrete thromboxane A2 to enhance vasoconstriction and platelet aggregation. During platelet aggregation, integrin $\alpha_{IIb}\beta_3$ binds to vWF and circulating fibrinogen, which are involved in the platelet-plug formation. Simultaneously, the coagulation cascade is activated, which is related to thrombin generation and results in fibrin formation (thrombin cleaves fibrinogen into fibrin)[68,69]. Thrombi formation finalises when the clot is stabilised by fibrin deposition and cross-linking. Once healing has started, the clot starts to retract and degrade, and fibrin is cleaved by plasmin, the final step of the coagulation cascade (fibrinolysis)[68,70].

Independently of the underlying aetiology, CHF patients present an increased risk of thromboembolism due to enhanced platelet activation[61,71]. Altered levels of circulating markers of fibrin generation, fibrinolysis and platelet activation have been observed in these patients[71–73]. Moreover, CHF patients present alterations in all the components of Virchow's triad, namely ED, haemodynamic changes (blood stasis) and hypercoagulability[71].

As stated previously ED is a hallmark of CHF and is associated with a prothrombotic state[45]. Activated ECs have increased expression of cell adhesion molecules (enhanced immune cell recruitment), and altered expression of anti- and pro-thrombotic molecules (e.g., decreased expression of thrombomodulin and increased expression of PAI-1, TF and vWF)[46]. Blood stasis (i.e., lack or reduction of blood flow) promotes EC activation as well as the accumulation and activation of pro-thrombotic molecules, which in normal conditions circulate until their inactivation[74]. In CHF, blood stasis due to altered blood flow is the result of structural alterations in the heart. Dilated chambers, abnormalities in wall motion and impaired contractility result in thrombi formation[71,75]. This is of particular importance in those CHF patients with atrial fibrillation. This comorbidity, affecting around 25% of CHF patients, is related to an increased risk of thromboembolism due to impaired atrial contraction and thus inappropriate systemic perfusion[71,76]. Those characteristics (increased levels of prothrombotic molecules, chronic inflammation, stasis), together with altered fibrinolysis and platelet hyperreactivity induce hypercoagulability and increase thrombosis risk[71].

1.5.5. Cardiac hypertrophy

The main function of the heart is to maintain correct body perfusion in normal and stressful conditions. In haemodynamic overload, there is an enlargement (hypertrophy) of this organ to increase contractility and reduce ventricular wall stress. This occurs mainly through the enlargement of individual CMs (increased cytoplasmic volume and accumulation of organised sarcomeres) but other compensatory mechanisms such as changes in gene expression producing alterations in metabolism, contractility and CM survival also occur[77,78].

Depending on the inducing stimuli, hypertrophy can be physiological (e.g., exercise, pregnancy) or pathological (e.g., MI, chronic HTN). Both types are initially adaptive mechanisms to cardiac stress, albeit their underlying mechanisms differ. Physiological hypertrophy occurs when cardiac function is maintained over time, while pathological hypertrophy is accompanied by adverse cardiovascular events, including CHF (both HFpEF and HFrEF)[77]. Physiological hypertrophy is characterised by a mild increase in cardiac mass and individual CMs size (width and length). Hearts that undergo this process have a preserved or increased contractile function without fibrosis or cell death and, except for postnatal hypertrophy (normal body growth), it is fully reversible[77]. Mechanisms activated in this process are cell survival signalling, increased energy production and efficiency, angiogenesis proportional to the ventricular wall growth, antioxidant systems, mitochondrial quality control and CM proliferation and regeneration. On the contrary, in pathological hypertrophy, an initial compensatory mechanism inducing concentric/eccentric ventricle growth progresses to ventricular chamber dilation and wall thinning through the lengthening of individual CMs, contractile dysfunction and CHF. Mechanisms related to this process are cell death, fibrosis, dysregulation of Ca^{2+} handling proteins, mitochondrial dysfunction, metabolic reprogramming, reactivation of foetal gene expression, altered protein and mitochondrial quality control, altered sarcomere structure and insufficient angiogenesis[77].

1.5.6. Cardiac fibrosis

Cardiac fibrosis is a hallmark of CHF more frequently observed in HFrEF[50]. Cardiac fibrosis is, in short, the excessive deposition of ECM proteins in parenchymal cardiac tissues. Albeit it is in many cases a reparative mechanism, depending on the pathological context, fibrosis can be a deleterious reparative mechanism[50]. For example, as discussed previously, in a MI the sudden death of CMs stimulates inflammation and the activation of reparative myofibroblasts, which are implicated in the formation of a scar. This scar is not contractile, but maintains the structure of the myocardium, preventing mechanical complications such as cardiac rupture[28,32,50]. However, in systemic HTN there is a progressive deposition of ECM proteins, increasing myocardial stiffness and leading to diastolic dysfunction[32,50].

In the normal heart, CMs are surrounded by an interstitial ECM constituted of fibrillar collagens, glycoproteins, glycosaminoglycans and proteoglycans. This ECM, apart from providing a mechanical scaffold for CMs, is important for the transmission of their contractile force and for being a reservoir of growth factors, bioactive molecules and proteases[32,50,79]. Other cell types are enmeshed within the ECM, such as vascular ECs, immune cells (macrophages, mast cells and dendritic cells), SMCs, pericytes and fibroblasts[65]. Fibroblasts are the main ECM producer and represent one of the largest cell populations in the heart. In normal conditions, ECM undergoes a balanced turnover through the synthesis and degradation of its proteinaceous components (collagens, elastin) and the basement membrane[79].

After a detrimental stimulus, this balance becomes altered. Cardiac fibroblasts are activated and transdifferentiate into secretory, matrix-producing and contractile cells named myofibroblasts. This process is induced by the presence of soluble factors in the ECM, mainly TGF-β, although other factors such as platelet-derived growth factor and connective tissue growth factor are also involved[28,32,50,79,80]. Activated myofibroblasts produce large amounts of ECM proteins and enzymes (proteases, metalloproteinases, metalloproteinase inhibitors) that regulate ECM remodelling, inducing fibrosis (**Figure**

5)[50]. Fibrosis can affect cardiac function by increasing myocardial stiffness and altering electrical conduction (altered contractility)[32,79]. It is worth mentioning that, even though myofibroblasts are the main contributors to fibrosis, other cells such as immune cells, vascular cells and CMs participate in the process by secreting profibrotic mediators[50,79].

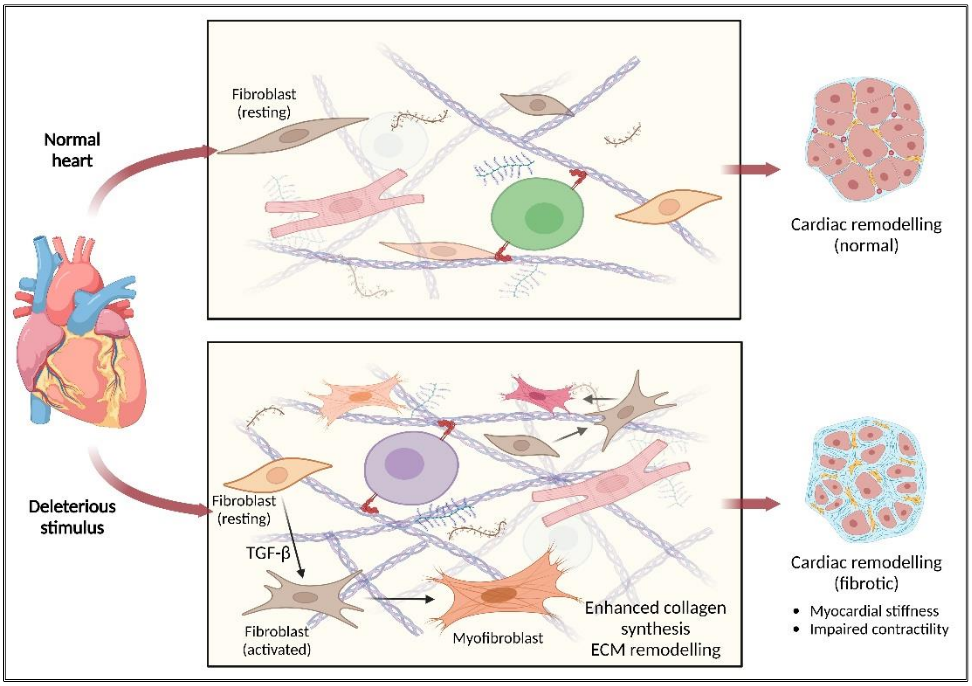

Figure 5: Cardiac remodelling.
ECM: extracellular matrix; **TGF-β**: transforming growth factor β

2. EXTRACELLULAR VESICLES

Extracellular microvesicles (MVs) are a heterogeneous population of small plasma membrane structures that, along with exosomes and apoptotic bodies, are part of the extracellular vesicles (EVs) family. They are released after activation stimuli[81] and have been found elevated in physiological and pathological states[82,83]. Additionally, these vesicle populations are classified depending on their size and biogenesis (**Figure 6**), with the exosomes being the smallest (40–150nm) and the apoptotic bodies being the largest (1–5µm)[84–86]. MVs have an intermediate size, ranging from 100nm to 1µm[84,85] and are characterised by presenting antigens derived from their parental cell in their membranes[82,87].

2.1. Biogenesis, cargo and uptake

Released by all eukaryotic cells[85], MVs have been detected in most human body fluids, including plasma and serum[85,87,88].

2.1.1. Biogenesis

As aforementioned, EVs subtypes have distinct biogenesis pathways, although sometimes overlapping mechanisms occur[89]. Exosomes are intraluminal vesicles within multivesicular bodies, released after multivesicular bodies are fused with the membrane of the parental cell. In contrast, MVs are generated by membrane blebbing, while apoptotic bodies are formed during membrane disintegration (**Figure 6**)[84,90].

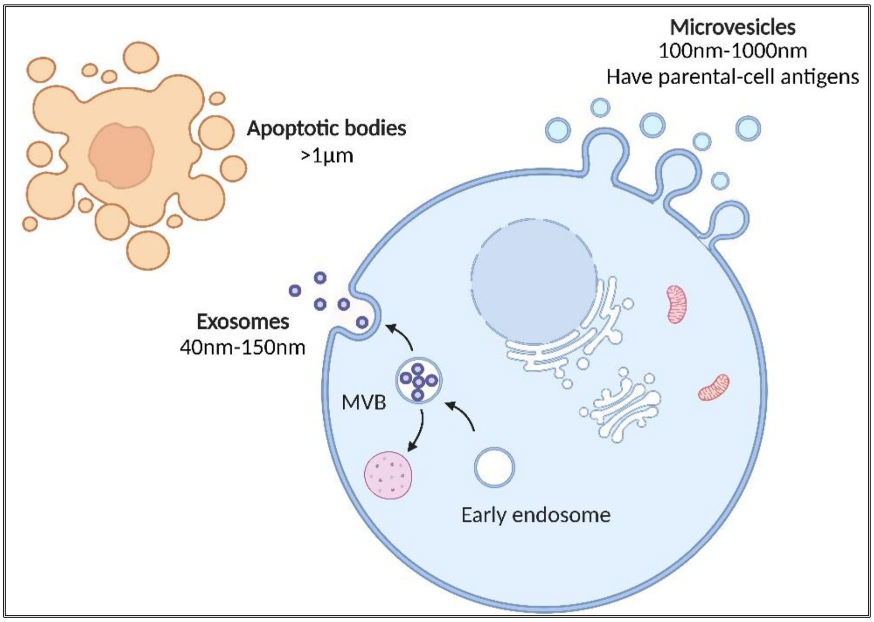

Figure 6: Extracellular vesicle biogenesis. Adapted from Raposo *et al.* (2013), *J Cell Biol*.[86]
MVB: multivesicular body

Biogenesis of MVs occurs by blebbing of the membrane of the parental cell and is the result of changes in membrane lipidic content and cytoskeleton rearrangements[89,91]. It is noteworthy that, as MVs obtain the membrane from their parental cell, they carry parental antigens that allow the characterisation of their cellular origin[82,87].

- **Changes in plasma membrane lipidic content**: During MVs formation, the membrane phospholipid distribution changes, mainly through the exposure of phosphatidylserine (PS) to the outer leaflet, which causes the membrane's physical bending. In the resting cell, the lipidic composition of the membrane's inner and outer leaflet is asymmetric. The outer leaflet is enriched in phosphatidylcholine and sphingomyelin, while the inner leaflet is enriched in PS and phosphatidylethanolamine. This asymmetry is maintained through the activity of the complementary phospholipid transporters flippase, floppase and scramblase. Thus, if PS or phosphatidylethanolamine move to the outer leaflet, they are back-transported to the inner leaflet by flippase. However, in cell activation a floppase induces the reverse mechanism, facilitating membrane bending and blebbing. Therefore, PS externalisation after cell activation results from its rapid floppase-mediated translocation to the outer leaflet and the Ca^{2+}-mediated inhibition of flippase[91,92]. Interestingly, not all MVs present PS in their membrane[93–96], suggesting additional formation mechanisms. Indeed, MVs can be generated even when membrane asymmetry is maintained[89]. In that sense, MVs are rich in cholesterol, suggesting that their formation could occur in lipid-rafts[97]. In fact, in cholesterol-depleted neutrophils or ECs, MVs generation is impaired[98,99]. Similarly, ceramide synthesis in the outer leaflet, inducing membrane bending through its cone-shaped structure, is sufficient for MVs release[92,100,101].
- **Cytoskeleton reorganisation**: Cytoskeleton rearrangement and contractility are crucial for MVs release. Several pathways related to GTPase signalling are involved in this process (**Figure 7**). On one side, ARF6 activates PLD and recruits ERK to the membrane, where ERK phosphorylates and activates

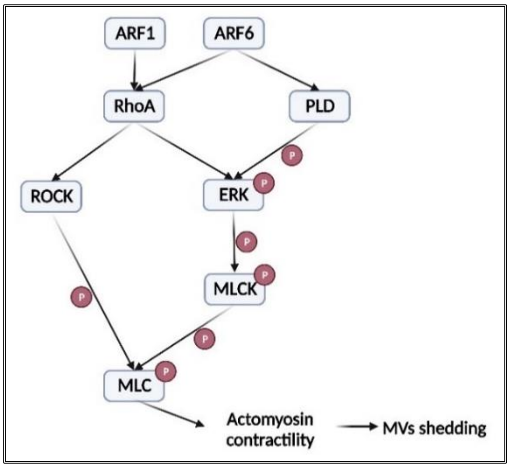

Figure 7: Pathways implicated in cytoskeleton reorganisation in MVs biogenesis. Adapted from Sedgwick *et al.* (2015), Sci. Rep[104]

ARF1/6: ADP ribosylation factor 1/6; **ERK**: extracellular signal-regulated kinase; **MLC**: myosin light chain; **MLCK**: myosin light chain kinase; **MVs**: extracellular microvesicles; **PLD**: phospholipase D; **RhoA**: Ras homolog family member A; **ROCK**: Rho-associated protein kinase

MLCK. MLCK, in turn, phosphorylates MLC to facilitate actomyosin-based contractility. MLC is enriched at the "necks" of the forming vesicles, and its contraction induces their release by fission[92,102,103]. MVs membrane-fission can also occur through a parallel pathway involving proteins from the Rho family. Either ARF6 or ARF1 can activate RhoA. Then, RhoA can induce the activation of MLC through two different pathways: it can activate ROCK, which then phosphorylates MLC and induces MVs shedding, or it activates ERK which activates MLCK through phosphorylation, who then activates MLC to induce MVs release[92,104,105]. Other pathways related to MVs biogenesis (involving proteins such as ARRDC1, ESCRT, ALIX, etc.) are being unravelled, but are, at the moment, poorly understood[92].

2.1.2. Molecular cargo

Apart from their membrane lipidic composition or their membrane proteins, MVs carry several molecule types in their lumen, including nucleotides, desoxyribonucleic acid (DNA), non-coding ribonucleic acid (RNA) (microRNA [miRNA], long non-coding RNA, messenger RNA [mRNA] and transfer RNA, among others), proteins and enzymes, bioactive lipids, certain metabolites, signalling components, transcription factors and even mitochondria (**Figure 8**)[106–109].

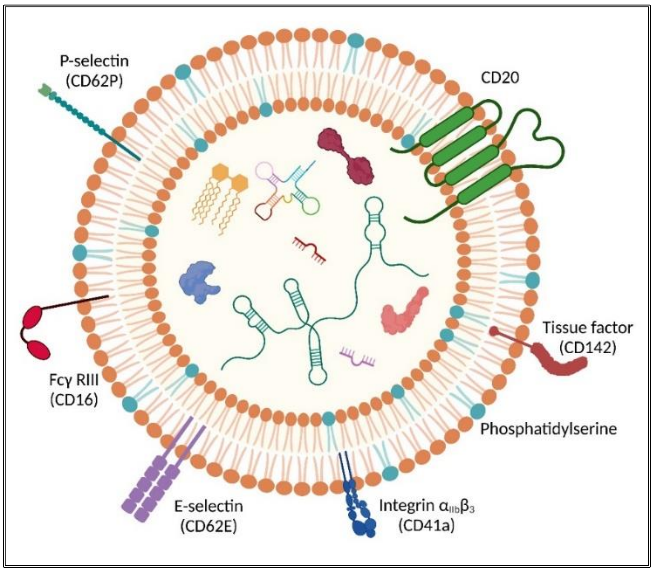

Figure 8: Extracellular microvesicle cargo.

How proteins or nucleic acids are sorted into MVs is not well-known, albeit active sorting seems to be the main mechanism, as exosomes contain diverse RNA species compared to their parental cell[109,110]. Cargo sorting is linked to intracellular trafficking, which is related to MVs formation[111]. Nevertheless, even though how cargo is selected and specifically transported to sites of MVs formation is unknown, these mechanisms involve proteins related to MVs biogenesis[106,111]. For instance, ARF6, implicated in MVs pinching and shedding, has been found to promote the selective enrichment of proteins such as MHC-I or β-integrin into MVs[103,112].

Nucleic acid cargo trafficking to EVs is unclear too. Yet, multiple mechanisms are implicated in RNA selection and packaging, including RNA-specific sequence motifs or secondary configuration, and RNA affinity to membrane lipids or RNA-binding proteins[106,109]. Additionally, evidence points out that molecule ratio (enrichment) could facilitate its loading[113,114] or that post-translational and post-transcriptional modifications in both RNA species and RNA-binding proteins are involved in RNA cargo loading[106,109,115].

2.1.3. Uptake

The clearance rate of EVs is variable. EVs have been detected in circulation in a time window that ranges from 5–15 minutes to at least 10–18 hours[116–119]. In addition, this time frame is affected by the individual's physiological state[120,121], as in physically untrained individuals increased levels of platelet-derived EVs (pEVs) were detected up to 2 hours after exercise, whereas pEVs levels returned to baseline within 2 hours in trained subjects[121].

Albeit EVs clearance is not completely understood, increasing evidence points out that the majority of EVs are removed from circulation by cellular uptake. The principal routes are endocytosis (clathrin-, caveolin- and lipid raft-mediated), micropinocytosis, phagocytosis and membrane fusion[106,111,122]. Depending on the cell type and its ligands, EVs uptake leads to their internalisation into vesicle trafficking pathways, leading them to recycling endosomes or to lysosomes, to induce cargo recycling or degradation, respectively. Alternatively, EVs cargo can be released into the target cell cytoplasm by the fusion of the EVs with the cell membrane. Interestingly, EVs can remain bound to the membrane of the recipient cell and not be internalised, as occurs with EVs involved in antigen presentation[109,111].

Detection of EVs by recipient cells occurs by recognition of membrane composition or surface protein profile, such as the presence of PS or receptors in their membrane[106,109,123–127]. EVs' uptake mechanism seems to be dependent on their cargo contents, with EVs rich in microRNAs internalised faster than those poor in this cargo[128]. This suggests that endocytosis of EVs may be a cell-cell communication mechanism rather than a clearance-only pathway.

2.2. Functional role

Circulating EVs are surrogate biomarkers of cell origin and functional status, as well as effectors of cell-cell communication through the delivery of their cargo. Since the publication of Barry *et al.* in 1997[129], it is known that EVs are not only elevated in physiological and pathological states[82] but also have a functional role. Certainly, EVs are involved in haemostasis, vascular tone, inflammation and angiogenesis, among others (**Figure 9**)[130]. Their involvement in these processes occurs mainly through their participation in cell-cell communication. Specifically, thanks to their membrane cargo they are recognised and internalised by specific target cells. As target cells can be both, adjacent or distant from the shedding cell, EVs can transfer their bioactive molecules in an autocrine and/or paracrine manner[131,132]. Furthermore, EVs can arrive at localisations that migrating or circulating cells cannot reach[111,133]. For instance, pEVs have been observed in body fluids where platelets are normally not found[133], such as the synovial fluid or the lymph in rheumatoid arthritis patients[134,135]. The implication of EVs in some hallmarks of CHF are summarised below.

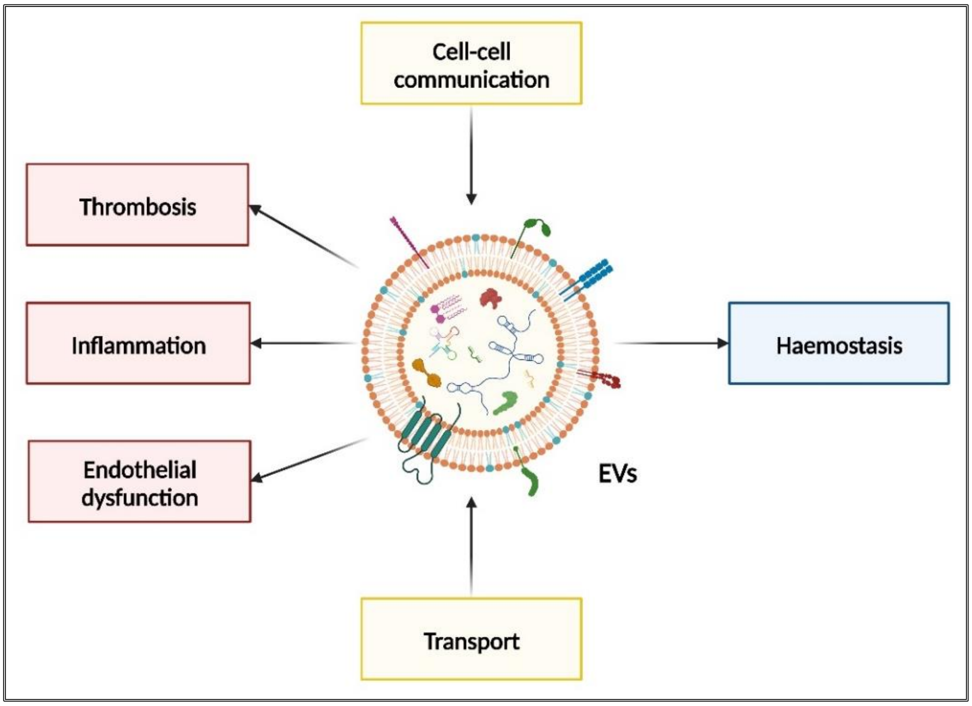

Figure 9: Functional roles of extracellular vesicles.
EVs: extracellular vesicles

2.2.1. Endothelial dysfunction

Endothelial dysfunction (ED) can be induced by EVs. Increased endothelial-derived EVs (eEVs) shedding has been observed in pathologies with altered endothelium, such as HTN[136,137], atherosclerosis[85,138] or CHF[139,140]. Moreover, eEVs are a biomarker of ED[141].

Endothelial function is affected by EVs through the promotion of coagulation and inflammation, as well as through the impairment of NO production[142]. EVs from erythrocytes, eEVs or pEVs affect vascular tone by decreasing NO bioavailability or inducing vasodilation. This occurs by producing reactive oxygen species, such as superoxide[143–146], affecting the regulation of eNOS or NADPH oxidase[144,147–149] or inducing the expression of cyclooxygenase-2 and prostacyclin[129]. Additionally, eEVs contribute to vascular permeability, enhancing ECs apoptosis and monocyte adhesion[150–152]. Of note, altered and slow shear stress is also related to the development of ED and is associated with the enhancement of eEVs biogenesis[153].

2.2.2. Haemostasis and thrombosis

Likewise, EVs have been related to coagulation and thrombi formation[154]. EVs have a procoagulant surface as they have negatively charged phospholipids in their membrane (such as PS), giving them the capacity to bind and activate coagulation factors like the tenase (factors IXa and Xa) and prothrombinase (factors Xa and Va) complexes, leading to thrombin generation[81,155]. In fact, PS in pEVs confers them with a 50–100 fold enhanced coagulation compared to activated platelets[156]. Other proteins like TF, factors VIII and Va, P-selectin, PSGL1, integrin $\alpha_{IIb}\beta_3$, PDI or vWF have also been detected in EVs surface, conferring them additional prothrombotic potential[137,155,157–159]. Moreover, their cargo also has prothrombotic capacity, as pEVs carrying arachidonic acid (thromboxane A2 precursor) can activate platelets and ECs[152]. Besides, EVs expose antithrombotic factors in their membrane, promoting plasmin generation and thus fibrinolysis. For example, EVs carrying tPA, TFPI, uPA, uPAR or PAI-1, among other factors, have been found[155,160,161]. Therefore, the final activity of EVs depends on the balance of the procoagulant and anticoagulant molecules they carry[155].

2.2.3. Inflammation

By modulating and regulating the immune system, EVs can stimulate or suppress the immune response[162]. Moreover, they are involved in the development of inflammatory and autoimmune diseases[162,163].

Certainly, EVs are related to inflammation through several mechanisms. On one side, they are implicated in antigen presentation, promoting both the activation, differentiation and maturation of immune cells, but also the suppression of their roles. On the other side, they can induce pro- and anti-inflammatory responses by transferring their cargo[92,162,164].

Antigen presentation by EVs has been related to immune cell activation and stimulation, but also to immune suppression[165]. For instance, EVs released by dendritic cells stimulate T-lymphocyte proliferation[166], while EVs shed by placental cells modulate the immune system and induce tolerance to foetal cells[167]. In pathological states, EVs can be pro- and anti-inflammatory too[92,162,164]. Tumour cell-derived EVs, when uptaken by immune cells, provoke an immune response against cancer cells. They deliver tumour-associated antigens, which will be used in antigen presentation and the induction of a tumour-specific T-lymphocyte stimulation[164,168]. At the same time, tumoral EVs attenuate the immune system by promoting tolerance to cancer cells[169]. Similarly, EVs are related to autoimmune diseases by carrying auto-antigens that can activate autoreactive T-lymphocytes[162,170].

As aforesaid, EVs also modulate inflammation by transferring their cargo[92,162,164,170]. For example, pEVs can deliver 12-lipooxigenase to mast cells, enhancing the production of the anti-inflammatory mediator lipoxin A4[171], while EVs from pancreatic islets of patients with diabetes mellitus type 1 contain γ-interferon and stimulate monocytes and autoreactive B- and T-lymphocytes, inducing pancreatic cell-destruction[163]. Likewise, hypoxia-induced EVs transfer *miR-23a* and TGF-β to natural killer cells, inducing the suppression of their activation[172].

Although the implicated mechanisms and their cargo composition are still being unravelled, increased levels of EVs from immune cells, among other cell types, have been observed in diseases where the immune system is involved, such as atherosclerosis[85,138,159], obesity[173] or autoimmune diseases[163,174], among others.

2.3. Methods for the analysis of extracellular vesicles

The study of EVs is possible by utilising several techniques, which are outlined in **Tables 4** and **5**. EV analysis requires their isolation and characterisation. Isolation techniques are normally based on size separation. Centrifugation is the most used, as it is easy and permits multiple sample processing. Characterisation methods rely on different properties of EVs, and the gold-standard method nowadays is flow cytometry, as it allows for parental cell determination through the recognition of EVs' surface antigens. For these reasons, these are the techniques utilised in this thesis. Other techniques and considerations for EV analysis are adressed below.

2.3.1. Preanalytical considerations

Isolation and characterisation of EVs are dependent on the biofluid or tissue used as a sample source. Thus, if EVs are to be purified from blood, cell culture medium or tissue, protocols to follow are distinct. In addition, the usage intent of the isolated EVs has to be considered, as the purity and quantity of the EVs needed for a clinical biomarker assessment or a mechanistic study are different[83,175]. This thesis will focus on techniques relevant to the EVs study in plasma, as the analysed EVs come from liquid biopsies (plasma) and isolated EVs have been used for clinical characterisation.

It is important to consider additional preanalytical factors that could affect EV analysis[83]. EVs can be isolated from either plasma or serum. However, serum induces platelet activation during clot formation, which is a known factor of pEVs production[88,176]. Further, the anticoagulant used also affects the number of EVs in the samples[177]. Given that heparin can bind EVs, block EV uptake and activate platelets, the use of heparin-based anticoagulants is discouraged. Instead, anticoagulants such as trisodium citrate or ethylenediaminetetraacetic acid are normally selected, when considering downstream analysis (heparin interferes with polymerase chain reaction [PCR])[176,178]. Trisodium citrate at 0.109mol/L is the most commonly used anticoagulant and has been recommended by the International Society on Thrombosis and Homeostasis[176]. Time of blood withdrawal, needle gauge, and blood handling after acquisition are also important. Recommendations are to obtain blood in fasting subjects with similar circadian time, as food intake can modulate EV production[179] and levels of large EVs with specific surface molecules vary during the day[180]. To minimise shear forces, which can induce EVs shedding, use of high-gauge needles and avoidance of butterfly systems is advised. In the same line, after venipuncture, removal of cuff and discard of the first millilitres of blood is recommended to eliminate pressure activation effects as well as fibroblast contamination[176,178].

2.3.2. Isolation

Several isolation methods relying on different biophysical properties of EVs, such as size, shape, charge, density and antigen exposure are used in EV analysis. Some of the most used techniques for EV isolation are listed in **Table 4**.

CENTRIFUGATION

Centrifugation and specifically differential centrifugation is the most used technique for EV isolation[181]. Differential centrifugation allows for EV enrichment and partial purification according to particle size and is sometimes pursued along other methods such as filtration[178]. Although several protocols are available, differential centrifugation normally consists of a first centrifugation at a low speed (200–1,500g) to remove cells[182], and a second centrifugation at a higher speed to pellet either large EVs (10,000–20,000g) or small EVs (100,000–200,000g)[176,178].

Differential centrifugation is widely used, as it allows for EV isolation without samples pre-treatment, permits processing multiple samples simultaneously and does not require specific equipment or great technical expertise[181]. However, it also has some drawbacks as it does not permit total purification of EVs given that the pellet will also contain protein aggregates and other contaminants of similar size. This can be improved by resuspending the pellet in phosphate buffer and then re-centrifuging it (washing the pellet), albeit this can reduce the isolation yield[178]. Some large EVs can also be eliminated in the first low-speed centrifugation and/or centrifugation-related EV aggregation can occur[176,178,182], lowering the concentration of isolated EVs. The use of differential centrifugation in the clinical setting is not feasible as it is laborious, time-consuming and has low throughput.

Centrifugation-related methods to improve the purity of isolated EVs have also been developed, relying on density to separate particles present in the sample[178,183]. Separation by density gradients can be pursued using, for example, a sucrose or an iodixanol gradient (OptiPrep™)[178]. A density gradient separates particles according to their flotation densities, which differ between proteins and vesicles[178], and even between vesicle types[183]. Proteins and aggregates will remain at the bottom of the tube, while vesicles will float upward until they reach their equilibrium density, which is reported between 1.1–1.19g/ml[178].

Table 4: Methods for EVs isolation.

METHOD	ADVANTAGES	DISADVANTAGES	REFERENCE
Centrifugation	- Sample pre-processing is not required. - Multiple samples can be processed in parallel. - Other isolation methods can be used in parallel. - Does not require special equipment or highly specialised personnel. - Standardised protocols available.	- Low throughput. - Labour intensive. - Time-consuming. - Total purification is not possible (same-sized particles co-isolated). - Low yield (easy to lose EVs in sequential centrifugations). - Not feasible in clinical use (non-scalable).	175,176,178,181,182
Filtration	- Sample pre-processing is not required. - Other isolation methods can be used in parallel. - Does not require special equipment or highly specialised personnel.	- EVs are not enriched in the solution (low concentration). - Low yield (EVs can adhere to the filter). - EVs can break or deform. - Not feasible in clinical use (non-scalable).	175,178,183
Size-exclusion chromatography	- High recovery rate. - High reproducibility. - EVs retain their biological activity. - Does not require special equipment or specialised personnel.	- Labour intensive. - Low yield. - Does not allow total purification of EVs (same-sized particles co-isolated).	175,182,184,185
Immunocapture assays	- Isolation and enrichment of specific EVs populations. - Multiple samples can be processed in parallel. - Clinically applicable.	- Loss of non-targeted EV populations. - Time-consuming. - Total purification is not possible (protein contaminants co-isolated). - Loss of EVs' biological activity - Expensive.	176,178,183
Precipitation	- Inexpensive. - Does not require special equipment or specialised personnel.	- Does not allow total purification of EVs (co-isolation of non-vesicular contaminants). - Complete removal of the precipitant agent is unlikely.	176,185–187

EVs: extracellular vesicles

2.3.3. Detection and characterisation

The characterisation of EVs after isolation can be pursued using several methods (**Table 5**). At the moment, the most used method is flow cytometry, which is detailed below.

FLOW CYTOMETRY

Flow cytometry is commonly used for EV studies. Even though it was first designed for cell analysis, it is being actively adapted for EV analysis, with flow cytometers capable of detecting smaller particles being designed every day.

Flow cytometry is a flow-based technique where individual particles pass through a flow-through chamber that is illuminated by several lasers (**Figure 10**). When each particle is illuminated by a laser beam, it refracts light. Light scattered at 20º is collected by the forward scatter. This measurement provides information on particle size, with larger particles refracting more light than smaller ones. Light refracted at a 90º angle to the excitation line is collected in the side scatter, and provides information about the particle's complexity (granularity and internal structures).

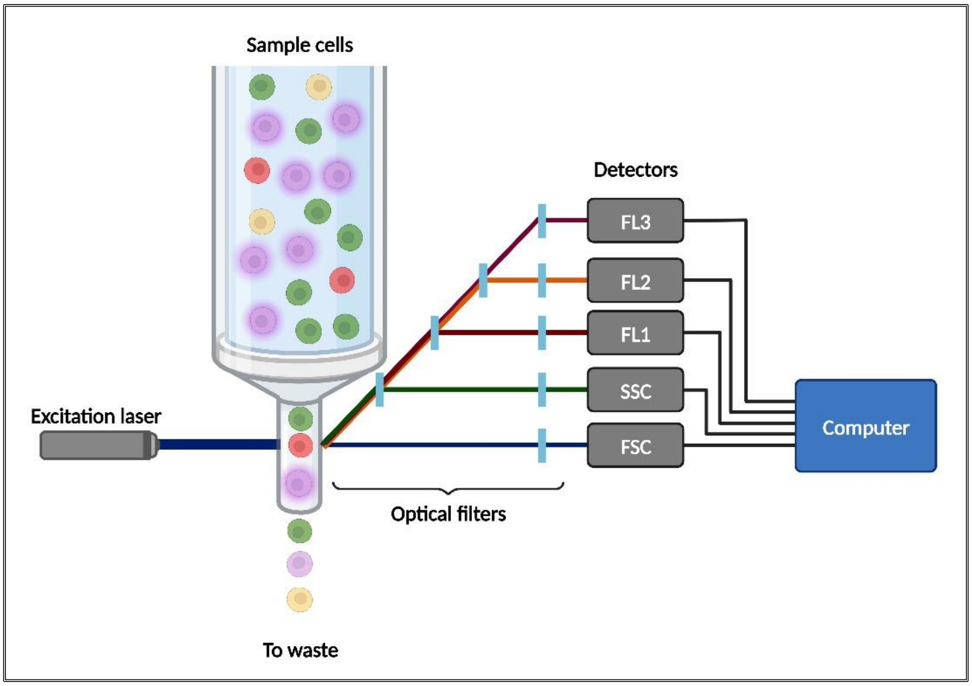

Figure 10: Schematic flow cytometry set-up.
FL1/2/3: fluorescence channel 1/2/3; **FSC**: forward scatter; **SSC**: side scatter

Table 5: Methods for EVs characterisation.

METHOD	ADVANTAGES	DISADVANTAGES	REFERENCES
BIOCHEMICAL APPROACHES			
Immunoblotting: Dot blot, western blot	- Detection of surface proteins. - Proteins separated by size. - Isolation purity determination by targeting non-EV proteins (e.g., HDL).	- Time-consuming. - Non-scalable. - Semi-quantitative. - Individual EVs content cannot be determined. - Large sample volume required.	178,188
Immunosorbent assays: ELISA	- Standardised. - Commercially available. - Quantitative. - Scalable. - Clinically applicable.	- Antibody-dependent protein recognition. - Limited number of recognised antigens per sample. - Expensive.	188
PHYSICAL APPROACHES			
Flow cytometry	- Size determination. - Particle complexity determination (granularity and internal structures). - Surface antigens determination using fluorochromes. - Sample concentration determination.	- Size determination pursued by comparison with commercially available polystyrene beads, with a different refractory index. - Swarming effect. - Small EVs difficult to analyse (<300nm).	175,176,188–191
Electron microscopy: SEM, TEM, Cryo-TEM	- Individual EVs' size and morphology determination. - TEM allows EV interior observation.	- Sample processing needed: EV morphology can be modified (solved using Cryo-TEM). - EVs sample concentration cannot be calculated (small number of EVs analysable per sample).	175,176,188
Atom force microscopy	- Sample can be analysed in solution (sample drying and labelling are not required). - Size, concentration and mechanical properties determination.	- Requires specialised equipment and trained personnel. - Low throughput.	175,188
Dynamic light scattering	- Size distribution determination.	- Extensive sample processing: uniform EVs size in samples is required.	175,178,188
Nanoparticle tracking analysis	- Sample concentration determination. - EVs size determination. - Fast.	- Small number of EVs analysed. - Sample contamination can induce concentration miscalculation.	175,176,178,188
Tunable resistive pulsing	- EVs size determination.	- Challenging to use. - Nanopore obstruction by EVs can occur.	176,178,188

Cryo-TEM: cryogenic TEM; **ELISA**: enzyme-linked immunosorbent assay; **EVs**: extracellular vesicles; **HDL**: high density lipoprotein; **SEM**: scanning electron microscopy; **TEM**: transmission electron microscopy

Particles can be labelled with fluorochromes excited at different wavelengths, providing more specific quantitative and qualitative data, like cell surface receptors or intracellular molecules. This, for instance, enables discrimination of cell types of similar size and complexity. Most instruments use separated channels and detectors for emitted light, which allows the use of more than one fluorochrome simultaneously[189].

In EVs studies, flow cytometry provides information on EVs' size and concentration[176,188]. Additionally, as EVs can be labelled with more than one fluorochrome (a maximum of 3 fluorochromes per particle due to their size), flow cytometry allows for the identification of specific EV subpopulations[176,188].

Albeit this methodology is widely used in EV studies, it is not hindrance-free. Size determination is pursued by comparing EVs' refractive index to that obtained by polystyrene beads. However, EVs typically scatter 10-fold less light than polystyrene beads, hampering size calculation. Also, smaller EVs often pass through the flow-through chamber collectively, instead of individually (swarming effect), resulting in a combined scattering signal that is counted as a single larger particle. This leads to inaccurate measurements of sample concentration[176,188]. At the moment, sizes below 300nm are particularly challenging. For this reason, is important to calibrate instruments and confirm individual particle detection using serial dilutions. Moreover, using proper sample and fluorescence controls and ensuring the removal of unbound fluorochromes is necessary[175,176]. Several studies addressing these problems[190,191], as well as international society recommendation guidelines[192,193], have been published.

At the moment, and considering the limitations of the aforestated methods, the International Society for Extracellular Vesicles recommends the use of more than one method when characterising EVs, normally a combination of high-resolution imaging of isolated EVs (electronic microscopy, atomic force microscopy) with size and concentration measurements (nanoparticle tracking analysis, flow cytometry). In parallel, initiatives to standardise reporting of isolation and characterisation, such as the EV-TRACK[194], MISEV2018[192] or MIFlowCyt-EV[193] are becoming indispensable in EVs studies.

3. MicroRNAs

MicroRNAs (miRNAs), molecular components carried by EVs, are small non-coding RNAs with an average length of 22 nucleotides. They have been implicated in gene expression regulation, mainly through gene silencing and repressing[195], although some studies have shown they can also activate gene expression and transcription[196,197].

Given their role as transcription regulators, miRNAs have been thoroughly studied in several diseases, where they have been found deregulated. In fact, they have been associated with disease development, prognosis and stratification[198–200]. Cardiovascular disease is also affected by miRNA deregulation, with several cardiovascular pathologies such as coronary and peripheral artery disease, MI or stroke, among others, presenting miRNA alterations[201–203]. Indeed, miRNA deregulation has also been observed in CHF, affecting several mechanisms related to this disease[204].

Apart from their direct role in disease pathogenesis, nowadays there is a great focus on determining the putative roles and utility of miRNAs as biomarkers of disease[205].

3.1. Biogenesis, release and clearance

MicroRNAs are codified throughout the genome, with the vast majority codified in intergenic regions, namely introns of both, coding and non-coding transcripts[195]. Nevertheless, miRNAs can also be codified in exons or intragenic regions. Some miRNAs are transcribed as one long transcript or close to each other, creating miRNA clusters. miRNAs are also grouped into families depending on the similarity of their seed sequences, which are comprised of 2–8 nucleotides and are responsible for mRNA targeting. miRNAs in the same cluster are generally co-transcribed and share the same seed, although this is not universal[195,205,206].

3.1.1. Biogenesis

The general mechanism of miRNA biogenesis in animal cells is through what is known as the miRNA canonical biogenesis pathway. This path is not the only mechanism of miRNA synthesis, as several non-canonical pathways have been described (**Figure 11**)[205].

MicroRNA CANONICAL PATHWAY

The general miRNA biogenesis pathway has 3 steps:

1. The pri-miRNA, the transcribed immature miRNA sequence that can be thousands of nucleotides long, is processed to pre-miRNA by the complex formed by DGCR8 and Drosha. This occurs when DGCR8 recognises the N6-methyladenylated GGCA motif of the pri-miRNA and Drosha cleaves the pri-miRNA duplex at the base of the hairpin. The resulting pre-miRNAs are hairpin-shaped sequences between 60–100 nucleotides long[195,205].

2. The pre-miRNA is transported to the cytoplasm by XPO5 in a Ran-GTPase-mediated manner, where it is recognised by DICER, an exonuclease[195,205].
3. DICER cleaves the terminal loop of the pre-miRNA and generates the miRNA mature form, which has a length of approximately 22 nucleotides[195,205]. At this point, however, there is still a double-chain molecule that must be transferred to the Argonaute-protein family as a monocatenary sequence. For this reason, a strand selection takes place, based on the thermodynamic stability of the 5’ ends of the miRNA duplex, or due to a 5’ uracil at nucleotide position 1. The strand with lower 5’ stability or with a 5’ uracil, known as the guide strand, is preferentially loaded into AGO2. The other strand, known as the passenger strand, is separated from the guide strand through various mechanisms according to their degree of complementarity. When no mismatches between both sequences exist, the passenger strand is cleaved by AGO2 and degraded, producing a strong strand bias. In cases where there are central mismatches, miRNAs duplexes not loaded to AGO2, are passively unwound and degraded. Functional miRNAs coupled to AGO2 become the miRNA-induced silencing complex (miRISC)[205,207].

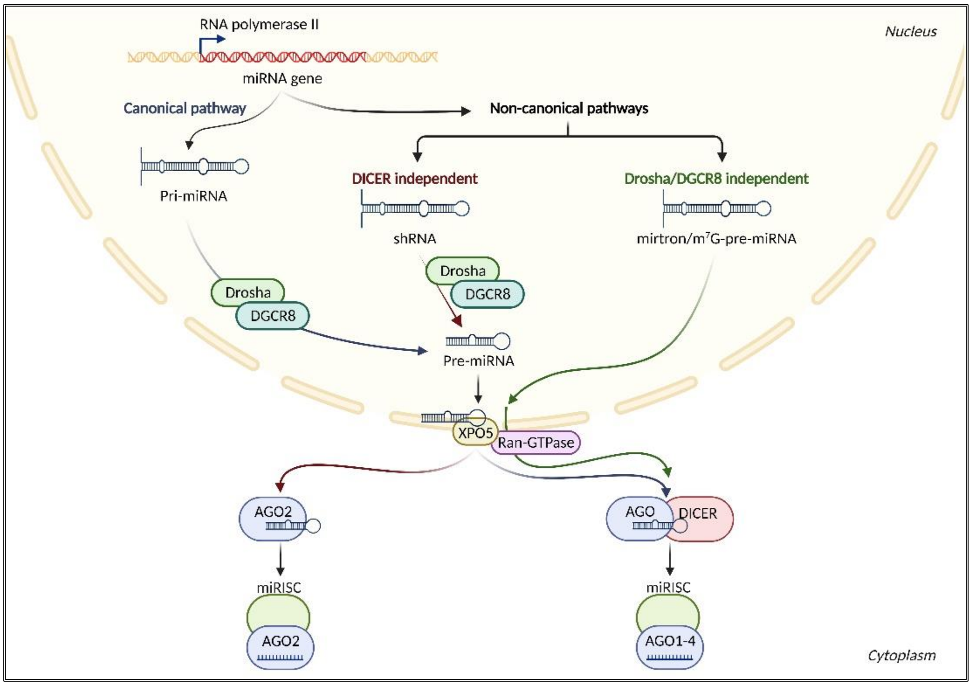

Figure 11: MicroRNA biogenesis.

AGO: argonaute; **DGCR8**: DiGeorge syndrome critical region 8; **m^{7}G-pre-miRNA**: 7-methylguanosine-capped pre-miRNA; **miRISC**: miRNA-induced silencing complex; **miRNA**: microRNA; **Ran-GTPase**: RAS-related nuclear protein-guanosine-5’-triphosphate-ase; **shRNA**: short-hairpin RNA; **RNA**: ribonucleic acid; **XPO5**: exportin 5

MicroRNA NON-CANONICAL PATHWAYS

Multiple non-canonical pathways have been elucidated. These pathways require proteins involved in the canonical pathway, and can be divided into 2 main pathways[205]:

- **Drosha/DGCR8-independent pathway**: Processes pre-miRNAs that resemble DICER substrates, such as mirtrons or 7-methylguanosine-capped pre-miRNAs. These pre-miRNAs are exported directly to the cytoplasm by XPO1, without being cleaved by Drosha. Once in the cytoplasm, DICER cleaves the terminal loop of the pre-miRNA and generates the mature form.
- **DICER-independent pathway**: Processes endogenous short-hairpin RNAs. These pre-miRNAs are processed by Drosha and are transported to the cytoplasm by XPO5/Ran-GTPase. Once there, given that their size is too small to be processed by DICER, pre-miRNAs are processed by AGO2.

3.1.2. Circulating microRNAs

As EVs, miRNAs have been detected in several biofluids[208], including plasma and serum[209]. The release of miRNAs into circulation occurs in several ways. Passive leakage by cell death (apoptosis, necrosis), active secretion in EVs or by being carried by proteins, including lipoproteins[109,110,210,211]:

- **miRNAs loaded into EVs**: The specific mechanisms through which miRNAs are loaded to EVs are currently poorly understood[106,109]. Evidence suggests that both passive and active loading occurs, with the latest likely being the predominant mechanism, as some studies have found some EVs enriched in miRNAs different from those observed in the parental cell[212]. Recent studies have observed that miRNA-loading can occur in parallel to EV biogenesis, with lipids implicated in MVs biogenesis, such as ceramide, promoting miRNA sorting into these EVs[109,213]. Others have identified specific motifs enriched in miRNAs targeted to EVs. For example, the GGAG motif is enriched in exosomal miRNAs and is related to the hnRNPA2B1 ribonucleoprotein, which is involved in the miRNA-loading of EVs[109,214]. Other motifs or specific secondary RNA structures are recognised by other RNA-binding proteins, such as AGO2, annexin A2, or SYNCRIP, contributing to miRNA loading[109,110]. Post-transcriptional modifications are also likely to be involved. Some miRNAs uridylated in the 3'-end are enriched in EVs, while miRNAs with adenylated 3'-end are mainly found in cells[109,115].
- **miRNAs carried by lipoproteins**: miRNAs can be carried by high-density (higher proportion) and low-density lipoproteins (HDLs and LDLs, respectively)[210,215]. Each lipoprotein carries a distinct pattern of miRNA, but miRNAs loaded in LDLs are similar to those carried by EVs[216,217].
- **miRNAs carried by ribonucleoproteins in circulation**: Some studies have pointed out that miRNAs in circulation are also transported by ribonucleoproteins[218], mainly from the AGO family (primarily AGO2)[219,220].

- **Passive leakage**: Upon cell injury or death, such that occurring after MI, cells can be disrupted and miRNAs liberated into circulation[221,222].

3.1.3. Clearance and/or internalisation

As miRNAs are mainly released to circulation into EVs, their clearance/internalisation is linked to EV uptake. Once in contact with their target cell, EVs can either fuse with the cell membrane and release their cargo into the cytoplasm, or can be internalised. If EVs are internalised, they are mainly directed to the lysosomes for degradation. Thus, to be functional, miRNAs need to escape this route. However, mechanisms related to this escape route are largely unknown[109,110]. HDL-bound miRNA can also be uptaken by target cells, but the efficiency and the pathways involved are not well-known and seem to differ between cell types[216,223].

3.2. Mechanism of action: epigenetic regulation

Once mature, miRNAs are implicated in gene regulation, which can result in reducing protein expression either completely or mildly[206]. Expression regulation occurs by the complementary binding of the miRNA to specific sequences of their target genes. Binding occurs mainly in the 3'-untranslated region (3'-UTR) of the target gene, albeit binding to the 5'-untranslated region (5'-UTR), coding or promoter sequence has also been described. Binding to the 3'-UTR induces translation repression and mRNA deadenylation and decapping, while binding to 5'-UTR or coding sequences induces silencing of gene expression. Interestingly, miRNA binding to promoter sequences has been associated with transcription induction[205]. miRNA-mRNA binding strength depends on the complementarity of the miRNA seed sequence with the target sequence. The strongest canonical (seed-matching) target sites are those that complement nucleotides 2–8 of the miRNA seed and have an adenine opposite the miRNA nucleotide 1 (known as t1A), but other canonical and non-canonical target sites have also been described[206]. Generally, miRNAs regulate gene expression by targeting cytoplasmatic mRNAs, even though studies have also demonstrated that they can also exert regulatory functions in the nucleus[197].

The binding of AGO to the 3'-UTR leads to gene silencing through translation repression and mRNA decay (**Figure 12**):

- **mRNA decay through mRNA deadenylation and decapping**: mRNA decay involves the recruitment of a scaffold protein member of the GW182 protein family (in humans, TNRC6A) by AGO. GW182 interacts with PABPC to recruit the PAN2-PAN3 and CCR4-NOT complexes, inducing mRNA deadenylation. Deadenylation promotes decapping by the DCP1-DCP2 complex, making the mRNA susceptible to rapid degradation by XRN1[205,206,224].
- **mRNA silencing through translation repression**: Inhibition of translation takes place by interfering with the function of eIF4A-I and eIF4A-II. The underlying

mechanism is unknown, but data indicates that miRISC induces their dissociation from the target mRNA, inhibiting ribosome scanning and the assembling of the eIF4F translation initiation complex[206,224].

Noteworthy, miRNAs can silence hundreds of genes, although with mild effects on each of them. In parallel, one gene can be regulated by multiple miRNAs. Moreover, a single pathway can be regulated by both, single or clusters of miRNAs. Cooperative repression can also occur by repressing neighbouring target sites on the target mRNA[206].

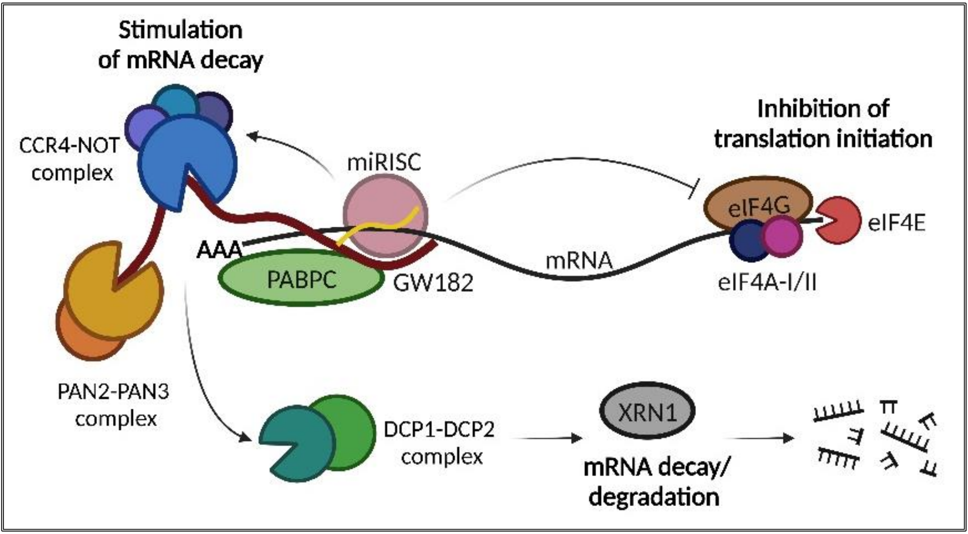

Figure 12: Gene silencing by miRNA. Adapted from Gebert *et al*., (2019), *Nat. Rev. Mol. Cell Biol*[206]
CCR4: carbon catabolite repressor protein 4; **DCP1/2**: mRNA-decapping enzyme subunit 1/2; **eiF4A-I/II**: eukaryotic initiation factor 4A-I/II; **EiF4E**: eukaryotic initiation factor 4E; **EiF4G**: eukaryotic initiation factor 4G; **GW182**: Glycine-Tryptophan protein of 182KDa; **miRISC**: miRNA-induced silencing complex; **mRNA**: messenger RNA; **NOT**: negative on TATA; **PABPC**: cytoplasmatic polyadenylate-binding protein; **PAN2/3**: poly(A)-nuclease deadenylation complex subunit 2/3; **RNA**: ribonucleic acid; **XRN1**: 5'-3' exoribonuclease 1

As gene regulators, miRNAs are involved in diverse physiological processes, hence when deregulated, they are associated with pathophysiological pathways and disease. In that line and as aforementioned, cardiac remodelling is the result of various mechanisms, including metabolic alterations, inflammation and cardiac hypertrophy and fibrosis[42]. Several miRNAs have been found altered in each of these processes, and thus contribute to HF development[225–228].

In that regard, miRNAs are recognised inflammation mediators that affect immune cells' function. Minimal changes in inflammation due to miRNA deregulation are associated with HF development, as inflammation is related to adverse remodelling and cardiac fibrosis, among others[226,229]. Likewise, miRNAs are implicated in metabolic homeostasis maintenance, and alterations in miRNAs have been associated with changes in metabolism and HF development[230,231]. For instance, in mice, alterations of the miR-199a/214 cluster are involved in the metabolic shift from fatty acid oxidation to glucose utilisation that takes place in the early stages of HF[232]. Similarly, hypertrophy can be exacerbated or suppressed by miRNAs[233,234], while several other miRNAs, such as *miR-21*, *miR-22* or *miR-101* have been associated with cardiac fibrosis by regulating the TGF-β pathway and other fibrosis-related mechanisms (e.g., PI3K-AKT pathway, ECM deposition)[80,235]. Therefore, through their role in gene regulation, individually or cooperatively, miRNAs are involved in CHF and hence are potential therapeutic targets as well as putative biomarkers[236].

3.3. Methods for the analysis of microRNAs

The study of miRNAs is possible through the use of various techniques, which have been summarised in **Tables 6** and **7**. Overall, two steps are necessary for miRNA analysis, isolation and characterisation. Isolation techniques using variations of the phenol-chloroform method are normally used, as it is an efficient method with commercial kits available. Quantitative real-time polymerase chain reaction (qRT-PCR) is the most used methodology to quantify and characterise miRNAs, as it is a specific, sensitive and reliable technique that does not require specialised personnel and uses equipment easily accessible in most research laboratories/institutes. For these reasons, these are the techniques used in this thesis. Other techniques and considerations for miRNA analysis are described below.

3.3.1. Preanalytical considerations

The sample source from where miRNAs are analysed influences their isolation and characterisation. In addition, protocols vary depending on the sample type and downstream applications. This thesis, given that the analysed miRNAs were obtained from liquid biopsies (blood), will focalise on the methodology suitable to this sample type.

MicroRNAs can be extracted from both, plasma and serum, but differences in miRNA levels have been observed between these sample types. Plasma is usually preferred and used as a miRNA source, as the coagulation occurring in serum preparation may release miRNAs from cellular components and change miRNA profiles. However, plasma contains cellular components (apoptotic or lysed cells) that can also increase miRNA count, and not all anticoagulants used in plasma preparation are adequate for downstream analysis, such as heparin, which inhibits PCR reactions[237,238]. Sample haemolysis, especially that of erythrocytes and platelets, is also important, as these cells can release miRNAs into the sample. To avoid this, high-gauge needle usage is recommended[208,237,238].

3.3.2. Extraction/isolation

Several methods can isolate miRNAs (**Table 6**), but choosing the best requires considering sample type, where the miRNA is expected to be found (in EVs, bound to proteins, etc.)

and downstream analysis[208]. Protocols based on chloroform-phenol isolation are the most widely used. It is based on the acid guanidinium thiocyanate-phenol-chloroform extraction, which fractionates efficiently RNA, DNA and proteins, and dissociates the majority of miRNA complexes. Several versions of this method exist and have been commercialised (e.g., miRVana™, miRNeasy, TRIzol™), where an additional purification with silica-beads columns (with nucleic acids affinity) is normally included. However, this type of extraction is time-consuming, can induce partial loss of RNA with a low GC content, and requires using toxic chemicals in high volumes (phenol) and specific equipment[208].

Table 6: microRNA isolation methods.

METHOD	ADVANTAGES	DISADVANTAGES	REFERENCES
Chloroform-phenol: miRVana™ miRNeasy TRIzol™	- Efficient separation of RNA, DNA and proteins. - Kits commercially available. - Highly specialised personnel not required.	- Time-consuming. - Loss of RNA with low GC content. - Use of toxic chemicals. - Specific equipment required (flow hood). - Non-scalable.	208
Precipitation: Mercury LN RT kit Immunoprecipitation	- Use of toxic chemicals not required. - Fast.	- miRNA loss (excess of protein-miRNA co-precipitation, incomplete protein denaturalisation).	208,239

DNA: desoxyribonucleic acid; **miRNA**: microRNA; **RNA**: ribonucleic acid

3.3.3. Detection and characterisation

Several methods are currently being developed to improve miRNA detection and identification (**Table 7**). qRT-PCR, the gold-standard method for miRNA analysis, is described below.

QUANTITATIVE REAL-TIME POLYMERASE CHAIN REACTION

Permitting individual miRNA characterisation, qRT-PCR is nowadays the most used method for miRNA quantification and identification. Its basic outline is the following: miRNA is reversely transcribed to complementary DNA (cDNA), which will be elongated and bound to either specific or universal primers. These primers permit the logarithmic amplification of the miRNA. Detection of the logarithmically increasing miRNA copies is achieved using fluorescent probes, which can be measured and used for miRNA detection and characterisation[240–242].

The elongation of miRNA's cDNA (primer binding) can be pursued by two different methods. One is the addition of a poly(A) tail before the retrotranscription, and the other is the stem-loop method[238,241,242]. In the latter, the target miRNA is retrotranscribed after annealing a stem-loop primer to its 3’ end, which is then used as a template for its amplification with a specific forward primer and a universal reverse primer or TaqMan™ probe[240,241]. Probe detection is normally performed using either SYBR® Green or Taqman™ probes, which are fluorescent. SYBR® Green is an intercalating fluorescent dye that binds to double-strand DNA. However, it is unspecific and can detect and characterise contaminating double-strand DNA or primer dimers as miRNAs. These false positives can be addressed by analysing the dissociation curve and monitoring the homogeneity of the amplified product[240,242]. Taqman™ probes are oligonucleotide probes labelled with a fluorophore and a quencher. During amplification, the probe is separated from the template, resulting in the cleavage of the fluorophore. This induces an increase in fluorescence that can be measured[240].

Table 7: microRNA detection and characterisation methods.

METHOD	ADVANTAGES	DISADVANTAGES	REFERENCES
HYBRIDISATION-BASED APPROACHES			
Microarray	- Multiple samples analysed in parallel. - Scalable. - Low-copy number molecule detection and identification.	- Expensive. - Complex data analysis.	241,242
Northern blotting	- Pre-miRNA and mature miRNA detection without amplification. - miRNA size determination. - Post-transcriptionally-added nucleotides detected.	- Semiquantitative. - Time-consuming. - Low throughput. - Low sensitivity.	240,242
AMPLIFICATION-BASED APPROACHES			
Sequencing	- Novel miRNAs detection. - miRNA mutations detection.	- Specialised equipment and highly trained personnel required. - Complex data analysis.	240,241,243
qRT-PCR	- Individual miRNA characterisation. - Multiple samples analysed in parallel. - High sensitivity. - High specificity.	- Relative quantification. - Low-medium throughput. - False positives occur easily.	238,240–242
ddPCR	- Low-frequency variants detection. - Absolute quantification. - Quantification without the need for a calibration curve. - Low sensitivity to PCR inhibitors.	- Quantification of contaminating-dsDNA. - Expensive. - Specialised equipment and highly trained personnel.	238,241

ddPCR: droplet digital PCR; **dsDNA**: double-strand desoxyribonucleic acid; **miRNA**: microRNA; **PCR**: polymerase chain reaction; **qRT-PCR**: quantitative real-time PCR

As it has high sensitivity and specificity, qRT-PCR is the gold-standard method for miRNA analysis. However, it is not limitation-free, as this technique provides relative quantification and has a low-medium throughput. Further, an inconsistent analysis and normalisation can affect negatively reproducibility, and false positives can occur easily during amplification[238,240–242].

4. EXTRACELLULAR VESICLES AND MICRORNAS IN CHRONIC HEART FAILURE

Given the difficulty of CHF to be recognised and diagnosed, as well as the complexity of patient stratification, several studies have focused on the search for differential cellular (EVs) and molecular (miRNAs) patterns with biomarker potential, unfortunately with contrasting results.

4.1. Extracellular vesicles

Several studies have focused on EVs in cardiovascular disease. However, there is little information on the involvement of EVs in CHF. A pioneering study of EVs in this patient population was carried out by Rössig *et al.*[244] in 2000. Authors observed that the serum of CHF patients contained “particles” that induced apoptosis and decreased cell viability when added to human umbilical vein endothelial cell cultures. Moreover, the effects of the particle-containing serum on the cells, correlated with the severity of CHF of the serum donor[244]. These initial observations in CHF patients were complemented by the studies of Garcia *et al.*[245], who found higher levels of EVs with markers of endothelial cell activation (vascular endothelial cadherin [CD144] and E-selectin [CD62E]) in CHF than in controls[245]. In the same study, authors evidenced that the circulating number of these eEVs decreased in CHF patients after heart transplantation[245]. These results support the idea that the pattern of circulating EVs (cEVs), related to pathologies such as CHF, can be modified with treatment. Indeed, a decrease in cEVs levels in CHF patients has been observed after vitamin C supplementation[246], immunoadsorption[247], or left ventricle assist device implantation[248–250].

In the last few years, several studies have focused on the relationship between cEVs and CHF (**Table A1**). In this respect, CHF patients have shown increased levels of cEVs with and without PS exposed on their surface (AV^+ and AV^-) from different cell-origin and activation status[139,249,251–256]. Some authors have suggested a potential value of cEVs to stratify CHF patients according to disease severity and outcome prediction. Thus, increased levels of cEVs of distinct phenotypic patterns have been found in CHF with various comorbidities, including subclinical hypothyroidism[253], insulin resistance[257] or metabolic syndrome[258]. In addition, cEVs seem to correlate with NYHA classification[139,258–261], and to discriminate patients suffering future cardiovascular events[139,252,262], CHF-related rehospitalisations[259] and CHF-related death[256,259]. Attempts to use cEVs to differentiate CHF according to their LVEF, namely HFpEF and HFrEF, have also been pursued, but mostly limited to cEVs of endothelial origin[254,261,263]. Patients with HFrEF have differential expression patterns of PECAM1 (CD31) and vascular endothelial cadherin (CD144) in eEVs compared to HFpEF[254,261,263].

4.2. Circulating microRNAs

In the last decade, circulating miRNAs have received increasing attention in the setting of clinical CHF and although results are still inconclusive, available findings suggest a potential value of miRNAs as disease biomarkers (**Table A2**).

In that sense, Tijsen and colleagues[264] reported that HF patients presented increased levels of *miR-423-5p* and that this miRNA had both, diagnostic and stratification potential[264]. Since then, studies have aimed to identify miRNAs that individually or in combination might discriminate CHF patients[265,266,275–284,267,285–294,268,295–304,269,305,270–274] or associate with disease severity[274,278,295,304,306,307] and prognosis[272,278,312–314,279,285,288,302,308–311]. However, most of the studies pursued until now have reached divergent conclusions. A wide range of miRNAs is available but a limited number of coincidences among studies have been identified, which makes the use of miRNAs as diagnostic and prognostic biomarkers in HF still a challenge. Further studies are therefore required to identify miRNAs, as well as the cellular and molecular processes in which they may be involved with pathophysiological relevance in HF.

Some clinical studies have also focused on the potential value of miRNAs to differentiate between CHF patients with reduced or preserved LVEF. Up to now, more than 20 miRNAs have been described to be differentially expressed between these two groups of patients. Still, reported results did not show coincident miRNAs[283,293,296,300,315–317]. As an example, a larger study comprising 2 validation cohorts, observed, in the screening stage, 41 differential miRNAs between HFrEF and HFpEF, with the best discriminative potential found for *miR-185-5p* and *miR-223-5p*. Whereas, in the validation stage, they highlight the discrimination power of an 8-miRNA panel (*miR-30a-5p*, *miR-106a-5p*, *miR-181a-2-3p*, *miR-191-5p*, *miR-193a-5p*, *miR-199b-5p*, *miR-486-5p* and *miR-660-5p*) that does not include *miR-185-5p* and *miR-223-5p*[317].

The relationship between CHF aetiology and miRNA patterns has also been investigated in recent years, especially focusing on discriminating patients with ischaemic[265,297,318–321], DCM[269–271,280,284,298], and HVD[276,281] origin. Regarding ischaemic origin, differential miRNA patterns have been related to HF development[290,318,321–323], and to the time of clinical manifestation of HF after the ischaemic event[322]. All these studies, albeit reporting miRNAs of potential value as biomarkers, do not provide any clue related to pathophysiological pathways.

Unfortunately, as mentioned previously, most of the studies pursued until now have reached contrasting conclusions. In the case of the *miR-423-5p,* reports where this miRNA has been found deregulated[267,272] and hence, corroborating Tijsen *et al.*[264] results, and investigations where this miRNA has not been detected or detected without differential patterns between analysed individuals[268,279,324] have been published.

Probably due to the complexity of this disease and its variable background, results from the studies pursued until now are variable. Assuredly, CHF is a complex entity with several background aetiologies, which can affect the type of miRNAs detected. Therefore, further research for miRNAs with biomarker potential and the unravelling of their pathophysiological role in this disease is necessary.

'Today we queried, questioned, and inquired. Promise me that come tomorrow, we will not stop asking why.'
- Gwenette Minnow Pea,
Ella Minnow Pea: A novel without letters, **Mark Dunn (2001)**

Hypothesis and Objectives

HYPOTHESIS

Nowadays, chronic heart failure (CHF) is one of the leading causes of morbidity and mortality in the industrialised world, affecting around 2% of the population over 65 years old. Moreover, its incidence is increasing due to the improved survival of ischaemic patients and the ageing of the general population.

With unspecific symptomatology associated with comorbidities, CHF recognition, diagnosis and stratification are challenging. Furthermore, CHF has the aggravating fact that once diagnosed, it is a disease with poor prognosis and survival. Although research to address its complex pathophysiology is actively underway, the mechanisms underlying the development of this disease are still poorly understood, and effective treatment options have been limited until recently. As such, biomarkers for early and accurate CHF diagnosis are scarce, and their utility to correctly predict patient outcome is controversial.

Therefore, it is crucial to progress in our understanding of the underlying pathophysiology to improve the early detection and stratification of CHF patients. Additionally, the discovery of new cellular and molecular biomarkers to detect and recognise CHF or its underlying causes early on would allow better and more personalised treatment strategies. As for the patients, early and accurate disease recognition would translate into the possibility to slow down the progression of the disease, diminishing the risk of hospitalisation, and overall gaining a better quality of life.

The **hypothesis of this thesis** is that by applying novel cellular and molecular technologies based on the determination of cellular activation and release of extracellular vesicles and characterisation of pathological traits of plasma epigenetic regulators of cell function, we could advance the understanding of CHF and characterise subtypes and severity of disease presentation.

OBJECTIVES

The specific objectives proposed to prove the hypothesis were:

Objective 1: To identify the differential pattern of circulating extracellular vesicles in chronic heart failure (CHF) patients.

Quantification and phenotypical characterisation by flow cytometry of the plasma extracellular vesicle patterns in CHF patients in comparison with age- and sex-matched individuals without CHF.

Objective 2: To explore the relationship between the differential extracellular vesicle pattern in aetiology and severity of CHF patients.

Analysis by statistical tools of the pathophysiological link of immune-cell-derived extracellular vesicle patterns with the ischaemic and non-ischaemic underlying aetiology and disease severity.

Objective 3: To characterise the differential circulating microRNA signature in CHF patients.

Investigation by untargeted quantitative real-time polymerase chain reaction of the differential profiles of microRNAs in CHF compared to age- and sex-matched individuals without CHF, and validation studies of the detected differential pattern.

Objective 4: To predict protein target genes of the CHF differential microRNA signature in plasma by *in silico* systems biology analysis.

Analysis of the putative role of microRNAs and their protein target genes in CHF pathogenesis by performing protein-protein interaction networks and enrichment pathway analysis.

"Whatever it is that you do, when you really want something, it's because that desire originated in the soul of the universe. It's your mission on earth."
-King Melchizedek,
The Alchemist, **Paulo Coelho (1988)**

Materials and methods

1. Study design

The study described in this thesis was performed in well-controlled CHF patients consecutively recruited at the cardiology department of the Hospital de la Santa Creu i Sant Pau in Barcelona (Spain), according to the inclusion criteria described below.

Patient information and biological samples were obtained at the patient inclusion in the study. Plasma samples were analysed for quantification and phenotypic characterisation of cEVs and identification of differential miRNA profiles in CHF. Studies were pursued in comparison with age- and sex-matched subjects without CHF, used as a reference group, and related them to the CHF aetiologic background and disease severity.

Based on *in silico* analysis and available literature, several miRNAs with differential pattern in CHF were selected. Using different bioinformatic tools, these epigenetic modulators were further investigated for identification of protein targets and protein-protein interactions in association with cardiac function (defined by LVEF), underlying aetiology and disease outcome (**Figure 13**).

The study protocol (Ref 16/44) was approved by the ethics committee for clinical research of the Hospital de la Santa Creu i Sant Pau and was conducted according to the Declaration of Helsinki. Written informed consent was obtained from all participants.

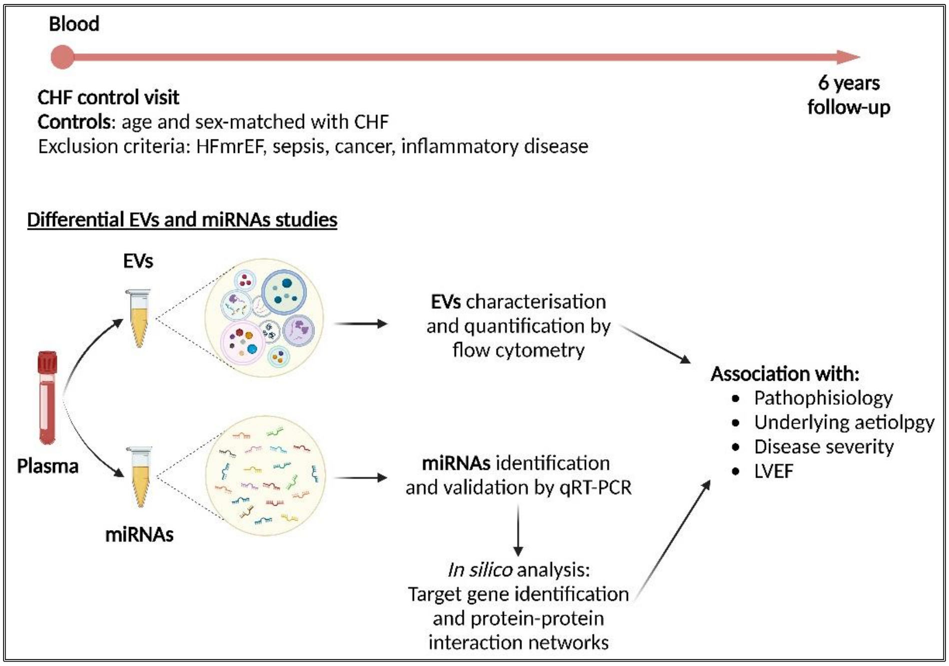

Figure 13: Schematic representation of the study design followed in this study.
CHF: chronic heart failure; **EVs**: extracellular vesicles; **HFmrEF**: heart failure with mildly reduced ejection fraction; **LVEF**: left ventricular ejection fraction; **miRNAs**: microRNAs; **qRT-PCR**: quantitative real-time polymerase chain reaction

2. Patients

This study is comprised of a total of 119 ambulatory patients with a clinical diagnosis of CHF (81 males/38 females; 67±11.8 years) and under guideline-directed medical therapy, who were consecutively recruited in the outpatient CHF unit of the Hospital de la Santa Creu i Sant Pau (Barcelona, Spain) between September 2016 and July 2018. Patients were followed-up until May 2022. Ischaemic aetiology affected 43 (36.1%) patients, while 76 (63.9%) had a non-ischaemic background. In addition, 59 (49.5%) CHF had HFpEF and 60 (50.5%) CHF had HFrEF.

A control group comprising a total of 60 individuals (34 males/26 females, 67.1±7.1 years) was also included, comprising sex- and age-matched controls without CHF. Demographic and clinical characteristics data, cardiovascular history and classical cardiovascular risk factors were obtained from all control individuals using a standardised report form at inclusion.

Details regarding demographic and clinical characteristics as well as cardiovascular history and classical cardiovascular risk factors of the subjects used in the studies can be found in the publications resulting from this thesis (**Articles 1** and **2**).

Patients with HFmrEF (40–50% LVEF) were excluded from the study. Importantly, neither patients nor control subjects had a history of cancer, sepsis or inflammatory disorders given that these conditions modify the total numbers of cEVs[325,326]. For the same reasons, pregnant women were also excluded[327].

3. Blood sampling and sample processing

Biological samples were collected after fasting and processed and stored immediately until patient recruitment was finalised. Blood was withdrawn from the cubital vein without a tourniquet using a 20-gauge needle after 10–14 hours of fasting into 3.8% sodium citrate Vacutainer® tubes. All samples were processed identically and within the first two hours.

As pictured in **Figure 14**, blood in sodium citrate tubes was used for EVs and miRNAs analysis. To avoid platelet activation, blood cells were eliminated by centrifugation (1,560g for 20 minutes [min] at 20ºC). To ensure the complete removal of cells and to obtain platelet-free plasma (PFP) a second centrifugation step was performed (1,500g for 10min at 20ºC). Aliquots of PFP were stored at −80ºC and unthawed until EVs or miRNA isolation and quantification took place.

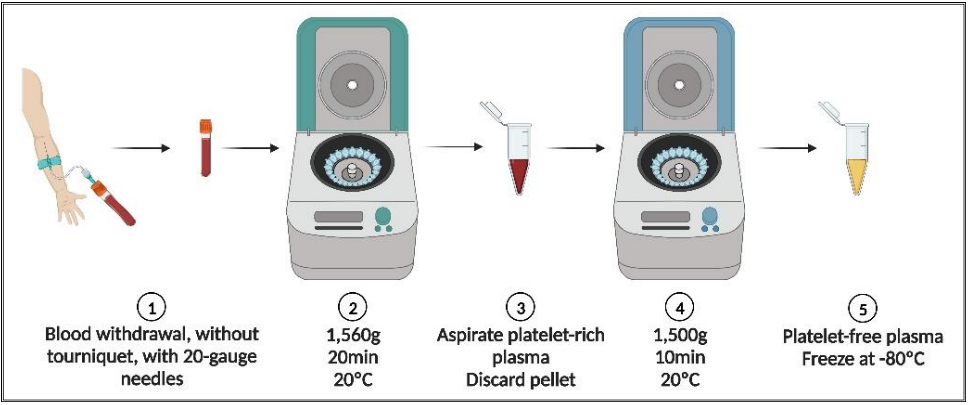

Figure 14: Schematic procedure for platelet-free plasma preparation.

4. Analysis of extracellular vesicles

Centrifugation was used for EV isolation, while flow cytometry was used for EV quantification and characterisation. Western blot was utilised to corroborate EVs surface markers. Detailed information on this methodology can be found in **Article 1**.

4.1. EVs isolation

As shown in **Figure 15**, EVs were isolated from PFP by a two-step high-speed centrifugation. The EVs-enriched pellet obtained after the first centrifugation, was washed with 0.22µm-filtered fresh citrate-phosphate buffered saline (PBS) solution and submitted to a second centrifugation and wash process. The remaining pellet (containing EVs) was resuspended in a final volume of 100µl citrate-PBS.

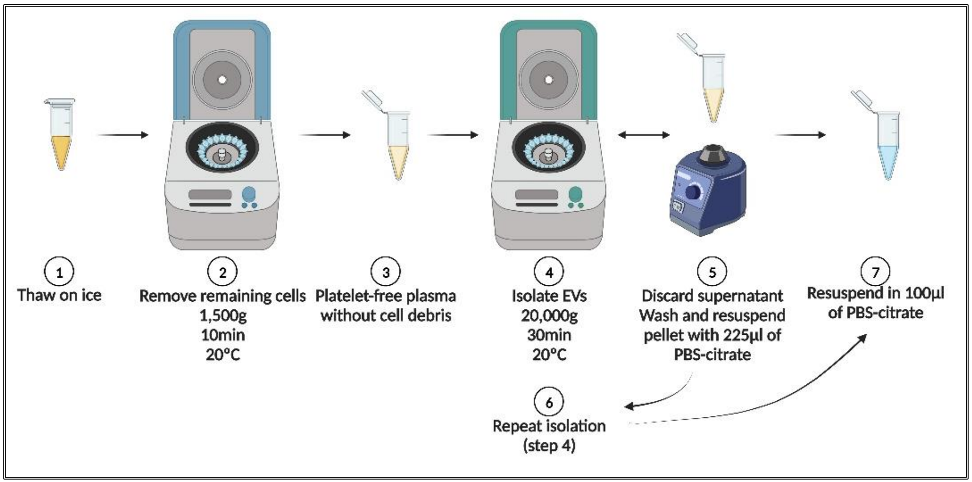

Figure 15: Schematic representation of EVs isolation.
EVs: extracellular vesicles; **PBS**: phosphate-buffered saline

4.2. EVs quantification and characterisation

FLOW CYTOMETRY

Three-label flow cytometric analysis for EVs quantification and characterisation was performed as described by Suades *et al.*[328,329] and shown in **Figure 16**. In short, each flow cytometry tube contained EVs pellets resuspended in PBS containing 2.5mmol of $CaCl_2$ (annexin binding buffer), which was labelled with annexin V (AV) and two specific monoclonal antibodies conjugated to different fluorochromes for flow cytometry detection. Of note, AV is a protein with a high affinity for PS. The specific antibodies used in this study are listed in **Table 8**.

The fluorescent signal was acquired in a FACSCantoII™ flow cytometer (Beckton Dickinson). Forward scatter, side scatter and fluorescence data were obtained with the settings in the logarithmic scale. As reported in **Article 1**, gate limits (0.1–1µm) were established following the criteria previously described[328,329]. EVs were identified and quantified based on their binding to AV and reactivity to cell-specific monoclonal antibodies. To identify positive marked events, fluorescence thresholds were set based on samples incubated with the same final concentration of isotype-matched control monoclonal antibodies.

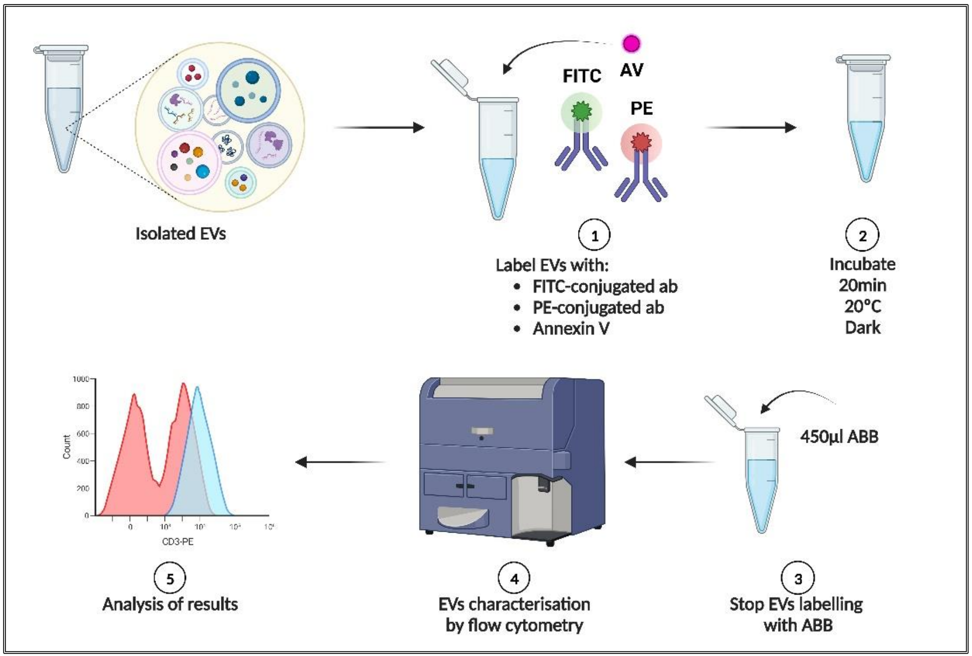

Figure 16: Schematic procedure for EVs characterisation and quantification by flow cytometry. **ab**: antibody; **ABB**: annexin binding buffer: **AV**: annexin V; **EVs**: extracellular vesicles; **FITC**: fluorescein isothiocyanate; **PE**: phycoerythrin

Data was analysed with the BD FACSDiva™ Software (Beckton Dickinson). The concentration (number of EVs per µl of plasma) was determined according to Nieuwland's procedure[330], based on the sample's volume, the flow cytometer's flow rate and the number of fluorescence-positive events (N):

$$\mathrm{EVs/\mu l} = \mathrm{N} \cdot \frac{V_f}{V_a} \cdot \frac{V_t}{FR} \cdot \frac{1}{V_i}$$

Where: V_f(µl)=final volume of washed EVs suspension, V_a(µl)=volume of washed EVs suspension used for each labelling analysis, V_t(µl)=volume of EVs before fluorescence-activated cell sorting analysis, FR(µl/min)=flow rate of the cytometer at "low flow" mode (the average volume of EVs suspension analysed in 1min), 1 is the µl unit of volume, and V_i(µl)=original volume of plasma used for EVs isolation.

WESTERN BLOT

The protein content of isolated EVs and cellular extracts was analysed by western blot. Detailed information on the protocol followed can be found in **Article 1**.

Briefly, EV protein extracts were obtained by lysis with Triton-X-100/TRIS-SDS buffer and overnight precipitation with cold acetone. Tissue and cell samples protein was extracted with RIPA buffer as detailed in **Article 1**. Protein content was quantified with the 2-D Quant Kit.

Protein samples were run in SDS-PAGE gels under denaturing or non-denaturing conditions depending on the used antibodies (**Table 9**). Once size-separated, proteins were transferred to a nitrocellulose membrane using the wet transfer method. Protein transfer was corroborated with Ponceau's Red staining. Membranes were blocked with either 5% BSA or 5% milk powder in TBS-Tween buffer, to prevent non-specific unions of the primary antibody. Then, membranes were incubated at adequate dilutions of the primary antibody. Primary antibodies were detected with a peroxidase-conjugated secondary antibody and developed by chemiluminescence. Chemiluminescent imaging analysis was performed with the ChemiDocTM XRS (Bio-Rad) using Quantity-One and Image Lab™ software (Bio-Rad).

Table 8: Antibodies used in flow cytometry for EVs characterisation.

	EXPRESSION	MARKER	ALTERNATIVE NAME	CONJUGATION	CLONE	DILUTION	HOST	COMPANY	CATALOGUE NUMBER
Annexin V	Widely expressed	PS^{+}	PS-binding protein	CF405	-	5µl (1:10)	-	Immunostep	ANXVCFB-200T
Leukocyte markers	Leukocytes	$CD45^{+}$	LCA	PE	MEM-28	5µl (1:10)	Mouse	Immunotools	21270454
	TL	$CD3^{+}$	TL co-receptor	FITC	HIT3b	5µl (1:10)	Mouse	Immunotools	21810033
	Activated lymphocytes	$CD29^{+}$	ITGB1/β1-integrin	FITC	HI29a	5µl (1:10)	Mouse	Immunotools	21810293
	Neutrophils, Mo	$CD11b^{+}$	MAC-1/αM-integrin	FITC	MEM-174	5µl (1:10)	Mouse	Immunotools	21279113
	Mo, Mø	$CD14^{+}$	LPS-receptor	PE	M5E2	5µl (1:100)	Mouse	BD Pharmingen	555398
	Granulocytes, neutrophils	$CD15^{+}$	Sialyl Lewis X	PE	MEM-158	5µl (1:10)	Mouse	Immunotools	21270154
	NK	$CD56^{+}$	NCAM1	FITC	B-A19	5µl (1:10)	Mouse	Immunotools	21810563
	NK; Mo	$CD16^{+}$	FcγRIII	FITC	HI16a	5µl (1:10)	Mouse	Immunotools	21810163

ABB: annexin binding buffer; **FcγRIII**: FCγ receptor type III; **FITC**: fluorescein isothiocyanate; **ITGB1**: integrin beta 1; **LCA**: leukocyte common antigen; **LPS**: lipopolysaccharide; **MAC-1**: macrophage antigen 1; **Mo**: monocyte; **Mø**: macrophage; **NCAM1**: neural cell adhesion molecule 1; **NK**: natural killer; **PE**: phycoerythrin; **PS**: phosphatidylserine; **TL**: T-lymphocyte

Table 9: Antibodies used in western blot for EVs characterisation.

	EXPRESSION	MARKER	ALTERNATIVE NAME	CLONE	DILUTION	DENATURING CONDITIONS	HOST	COMPANY	CATALOGUE NUMBER
Leukocyte markers	TL	CD3	TL co-receptor	Polyclonal	1:2000	Denaturing	Rabbit	Abcam	ab16044
	Neutrophils, Mo	CD11b	LCA	EP1345Y	1:1000	Denaturing	Rabbit	Abcam	ab52478
	Mo, Mø	CD14	MAC-1/αM-integrin	4B4F12	1:500	Non-denaturing	Mouse	Abcam	ab182032

LCA: leukocyte common antigen; **MAC-1**: macrophage antigen 1; **Mo**: monocyte; **Mø**: macrophage; **TL**: T-lymphocyte

5. Analysis of microRNAs

Extraction of miRNAs was pursued using a commercial version of the acid guanidinium thiocyanate-phenol-chloroform isolation method (miRNAeasy) while quantification and characterisation were performed by qRT-PCR. Detailed information on the methodology utilised can be found in **Article 2**.

5.1. microRNA extraction

The isolation of miRNAs was pursued using the 30/30 miRNeasy Serum/Plasma Advanced kit according to the manufacturer's protocol (Qiagen). In short, PFP samples were thawed until defrosted. Then, 200µl of plasma per sample were used, into which 25fmol of the exogenous miRNA *cel-miR-39-3p* were transferred. This spike-in control was used for normalisation in the expression analyses. Isolated miRNAs were resuspended in RNA-free water and stored at −80ºC.

5.1. microRNA amplification

To characterise and identify miRNAs, expression analyses were carried out by qRT-PCR, after miRNA retrotranscription to cDNA using the TaqMan™ Advanced miRNA cDNA Synthesis Kit (Applied Biosystems) following the manufacturer's recommendations.

5.1.1. MicroRNA profiling: expression analysis

The presence of specific miRNAs was tested by qRT-PCR (expression profiling). The amplification was pursued using microfluidic cards, commercially available platforms that include several (>100) Taqman™ chemistry-based miRNAs primer sets. Two types of microfluidic cards were used:

- **Low-density Taqman™ Advanced miRNA Human A Card microfluidic card** (Life Technologies): Contains 377 different human miRNAs, including 1 endogenous control (*hsa-miR-16-5p*). Additionally, it also comprises 1 exogenous control (*cel-miR-39-3p*) and 1 negative control (*ath-miR-159a*) that does not amplify in human samples.
- **Low-density Taqman™ Custom TaqMan® Array Advanced MicroRNA Cards microfluidic card** (Life Technologies): Contains 23 customised miRNAs and 1 endogenous control (*hsa-miR-16-5p*). Exogenous control *cel-miR-39-3p* for inter-sample expression normalisation was also included.

Sample preparation was pursued according to the manufacturer. Briefly, the miR-Amp reaction (final product of the cDNA preparation) was diluted 1:10 with RNAse-free water. Next, the sample was added to the qRT-PCR amplification mix, thoroughly mixed and introduced to the microfluidic card's reservoirs by centrifugation. miRNA amplification was pursued in an ABI PRISM 7900HT Sequence Detection System (Applied Biosystems).

The amplification thermocycler conditions consisted of **1)** enzyme activation (92ºC, 10min) and **2)** 40 cycles of denaturalisation (95ºC, 1 second) and annealing/extension (60ºC, 20 seconds).

A schematic diagram of the workflow followed during miRNA extraction, amplification and analysis, is shown in **Figure 17**.

5.1.2. Analysis of the data generated by qRT-PCR

In both phases, the amplification curves were analysed using the online tool Thermo Fisher Connect Dashboard (Life Technologies). Only miRNAs with Ct values Ct≤35 were considered. Ct values were obtained and processed by the standard curve method and normalised with the exogenous miRNA *cel-miR-39-3p*, according to the equation:

$$Ct = 2^{-(Ct_{target\ miRNA} - Ct_{exogeneous\ miRNA})}$$

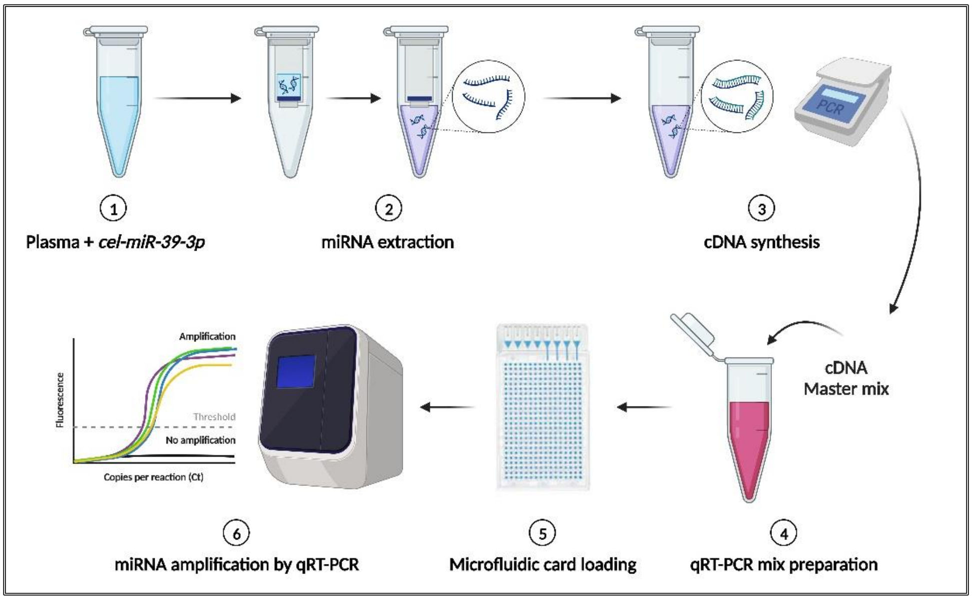

Figure 17: Workflow followed for microRNA extraction and amplification.
cDNA: complementary DNA; **DNA**: desoxyribonucleic acid; **miRNA**: microRNA; **qRT-PCR**: quantitative real-time polymerase chain reaction

6. *In silico* bioinformatics analyses

In silico analyses to discern the putative pathways related to the investigated miRNAs are described in detail in **Article 2**.

6.1. Algorithms for microRNAs' target-genes predictions

Putative target genes of miRNAs were predicted using four (4) different databases (**Table 10**), namely TargetScan[331], miRWalk[332], miRDB[333,334] and miRMap[335]. Only those target genes with a high likelihood to be regulated by miRNAs, according to their search algorithms, were considered. For this reason, only those target genes predicted by all used databases were used for analysis (network formation and pathway enrichment analysis).

6.2. Protein-protein interaction networks

Protein-protein interaction (PPI) networks are mathematical models of physical interactions (either transient or stable) between proteins. They provide information about relationships between proteins in protein complexes, putative roles of uncharacterised proteins or signalling pathways. In this study, PPIs were created in Cytoscape[336]. Cytoscape 3.0 is open-source software that integrates high-throughput data from several databases, between them STRING[337].

Once obtained, the curated target genes were introduced into Cytoscape. The STRING app integrated into this software was used to obtain a PPI, setting a confidence cut-off of 0.8 and the maximum number of additional interactions of 30. Once a PPI was generated, a community cluster strategy (GLay)[338] was applied to identify PPI-enriched clusters. Those clusters were further analysed to establish functional enrichments as described below.

6.3. Pathway enrichment analysis

Two different strategies were used for pathway enrichment analysis:

- **ShinyGO**: The curated target genes were introduced to the web-based software ShinyGO[339]. This platform was used to determine enriched Gene Ontology terms (Biological Process, Molecular Function, Cellular Component) related to predicted target genes, from which, the top 10 terms, sorted by average and rank (FDR and fold), were selected.
- **Clustering in Cytoscape**: Target genes included in each of the clusters generated from the PPI were used to pursue enrichment analysis using the STRING app of Cytoscape. Pathways considered were those excerpted from the KEGG database[340,341].

6.4. Individual microRNA pathway enrichment analysis

For individual miRNA pathway analysis, a repository-based gene database (RBGD) was created by querying "heart failure" to the STRING database in Cytoscape. Predicted targets of selected miRNAs (*miR-107* and *miR-139-5p*) were then matched to the RBGD gene list. Common genes and their neighbour-interacting genes were imported into ShinyGO for pathway enrichment analysis. Pathways considered were those excerpted from KEGG.

A list of all used bioinformatic tools can be found in **Table 10**. A schematic diagram of the *in silico* workflow is shown in **Figure 18**.

Table 10: Bioinformatic tools used for *in silico* analysis.

BIOINFORMATIC TOOL	ONLINE RESOURCE	REFERENCE
TargetScan	https://www.targetscan.org/vert_80/	331
miRWalk	http://mirwalk.umm.uni-heidelberg.de/	332
miRDB	http://www.mirdb.org/index.html	333,334
miRMap	https://mirmap.ezlab.org/	335
ShinyGO	http://bioinformatics.sdstate.edu/go/	339
Cytoscape	https://cytoscape.org/[1]	336
KEGG	https://www.genome.jp/kegg/	340,341

[1]Free software used after computer installation (it is not web-based software).

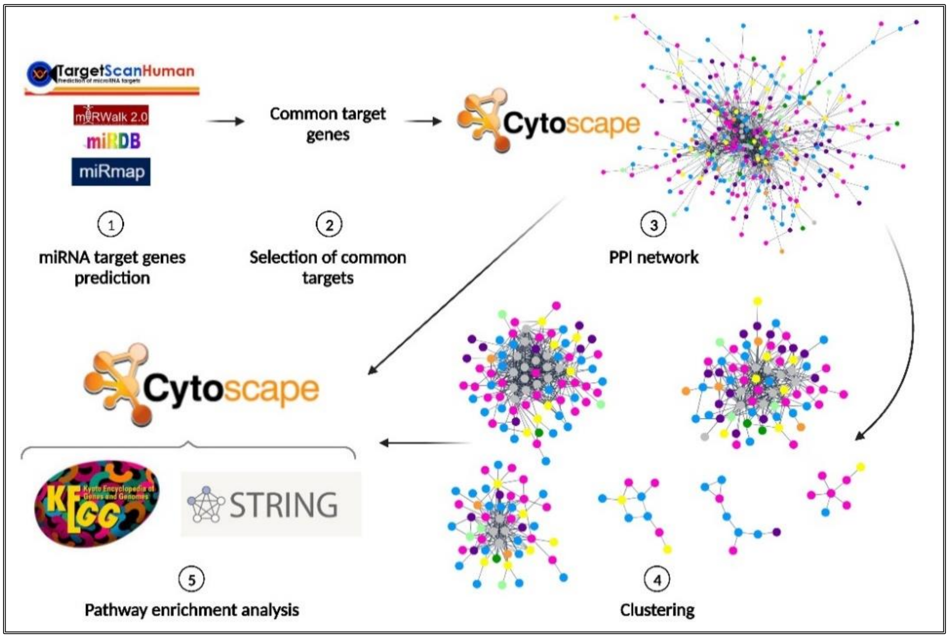

Figure 18: *In silico* analysis followed for enrichment pathway analysis.
miRNA: microRNA; **PPI**: protein-protein interaction

7. Statistical analyses

Statistical analyses were carried out using SPSS Statistical Analysis System (IBM Corp; Armonk). The normality of variables was assessed with the Shapiro-Wilk test. Analysis of qualitative variables was carried out utilising the chi-squared test considering the number of cases and percentages. According to the samples' non-normality, mean and median values of quantitative variables were compared with non-parametric tests. The statistical significances between groups were determined with U Mann-Whitney for non-paired variables. Correlation analyses were pursued using Spearman's correlation test. A $p<0.05$ was considered statistically significant.

Receiver operating characteristic (ROC) curve analyses for predicted probabilities were performed to identify threshold concentrations of EVs or miRNAs able to discriminate between groups, and the corresponding area under the curve (AUC) with its 95% confidence interval was calculated. Binary logistic regression models were pursued to estimate predicted probabilities using combinations of either EVs or miRNAs and other variables, such as NT-proBNP. A $p<0.05$ was considered statistically significant.

You become responsible, forever, for what you have tamed.
-Fox,
The Little Prince, **Antoine de Saint-Exupéry (1943)**

Results

The results of this thesis include two different articles:

ARTICLE 1

New Factors in Heart Failure Pathophysiology: Immunity cells release of extracellular vesicles

Alba Vilella-Figuerola, *Teresa Padró*, *Eulàlia Roig*, *Sònia Mirabet**, *Lina Badimon**
*Contributed equally to this work.

Published: Frontiers in Cardiovascular Medicine

Front. Cardiovasc. Med. 2022, 9, 939625, doi:10.3389/fcvm.2022.939625

Impact Factor (2021): 5.846

ARTICLE 2

Systems Biology in Chronic Heart Failure – Identification of Potential miRNA Regulators

***Alba Vilella-Figuerola**, Alex Gallinat, Rafael Escate, Sònia Mirabet, Teresa Padró*, Lina Badimon**
*Contributed equally to this work.

Published: International Journal of Molecular Sciences

Int. J. Mol. Sci. 2022, 23 (23), 15226, doi.org/10.3390/ijms232315226

Impact factor (2021): 6.208

ARTICLE 1

New Factors in Heart Failure Pathophysiology: Immunity cells release of extracellular vesicles

Alba Vilella-Figuerola; Teresa Padró; Eulàlia Roig; Sònia Mirabet*; Lina Badimon*
*Contributed equally to this work.

PUBLISHED: Frontiers in Cardiovascular Medicine

Front. Cardiovasc. Med. 2022, 9, 939625, doi:10.3389/fcvm.2022.939625

OBJECTIVE: To identify and characterise the pattern of immune-cell-derived extracellular vesicles in CHF patients and study their association with this disease.

HIGHLIGHTS:

- A differential EVs profile was identified in CHF patients in comparison to subjects without this disease.
- CHF patients have increased levels of EVs from total leukocytes ($CD45^+/AV^+$; $CD11b^+/AV^+$), monocytes ($CD16^+/AV^+$), neutrophils ($CD15^+/AV^+$; $CD29^+/CD15^+/AV^+$), T-lymphocytes ($CD3^+/AV^+$; $CD3^+/CD15^+/AV^+$) and natural killer cells ($CD56^+/AV^+$) when compared to control subjects.
- EVs from leukocytes ($CD45^+/AV^+$; $CD11b^+/AV^+$), activated neutrophils ($CD29^+/CD15^+/AV^+$) and T-lymphocytes ($CD3^+/AV^+$; $CD3^+/CD45^+/AV^+$) correlate positively with CHF severity (NYHA classification).
- CHF patients with an ischaemic background had higher levels of EVs shed by activated leukocytes ($CD29^+/AV^+$), lymphocytes ($CD3^+/AV^+$) and neutrophils ($CD15^+/CD29^+/AV^+$) than CHF patients with a non-ischaemic background.
- CHF patients with an ischaemic background and in the NYHA disease severity stages III–IV have an increased number of EVs from total leukocytes ($CD45^+/AV^+$; $CD11b^+/AV^+$) and T-lymphocytes ($CD3^+/AV^+$; $CD3^+/CD15^+/AV^+$) than ischaemic CHF patients with NYHA stage II. In addition, they presented more EVs derived from activated monocytes ($CD11b^+/CD14^+/AV^+$) and activated neutrophils ($CD15^+/CD29^+/AV^+$) than ischaemic CHF patients with NYHA stage II.
- The combination of EVs with the markers $CD11b^+/AV^+$ and $CD29^+/CD15^+/AV^+$ discriminates disease severity in ischaemic patients.

frontiers | Frontiers in Cardiovascular Medicine

TYPE Original Research
PUBLISHED 03 November 2022
DOI 10.3389/fcvm.2022.939625

Check for updates

OPEN ACCESS

EDITED BY
Kenneth Scott Campbell,
University of Kentucky, United States

REVIEWED BY
Raquel Guillamat-Prats,
LMU Munich University Hospital,
Germany
Diego Vinicius Santinelli Pestana,
Brigham and Women's Hospital
and Harvard Medical School,
United States
Takehiro Funamizu,
Juntendo University, Japan

*CORRESPONDENCE
Lina Badimon
lbadimon@santpau.cat

†These authors have contributed equally to this work

SPECIALTY SECTION
This article was submitted to Heart Failure and Transplantation, a section of the journal Frontiers in Cardiovascular Medicine

RECEIVED 09 May 2022
ACCEPTED 12 September 2022
PUBLISHED 03 November 2022

CITATION
Vilella-Figuerola A, Padró T, Roig E, Mirabet S and Badimon L (2022) New factors in heart failure pathophysiology: Immunity cells release of extracellular vesicles. *Front. Cardiovasc. Med.* 9:939625. doi: 10.3389/fcvm.2022.939625

New factors in heart failure pathophysiology: Immunity cells release of extracellular vesicles

Alba Vilella-Figuerola[1,2], Teresa Padró[1,3], Eulàlia Roig[4], Sònia Mirabet[3,4†] and Lina Badimon[1,3,5*†]

[1]Cardiovascular-Program ICCC, IR-Hospital Santa Creu i Sant Pau, IIB-Sant Pau, Barcelona, Spain, [2]Department of Biochemical and Molecular Biology, Universitat Autònoma de Barcelona, Barcelona, Spain, [3]Centro de Investigación Biomédica en Red Cardiovascular, Instituto de Salud Carlos III, Madrid, Spain, [4]Heart Failure Group, Department of Cardiology, Hospital Santa Creu i Sant Pau, Barcelona, Spain, [5]UAB-Chair Cardiovascular Research, Barcelona, Spain

Leukocyte-shed extracellular vesicles (EVs) can play effector roles in the pathophysiological mechanisms of different diseases. These EVs released by membrane budding of leukocytes have been found in high amounts locally in inflamed tissues and in the circulation, indicating immunity cell activation. These EVs secreted by immune cell subsets have been minimally explored and deserve further investigation in many areas of disease. In this study we have investigated whether in heart failure there is innate and adaptive immune cell release of EVs. Patients with chronic heart failure (cHF) (n = 119) and in sex- and age-matched controls without this chronic condition (n = 60). Specifically, EVs were quantified and phenotypically characterized by flow cytometry and cell-specific monoclonal antibodies. We observed that even in well medically controlled cHF patients (with guideline-directed medical therapy) there are higher number of blood annexin-V$^+$ (phosphatidylserine$^+$)-EVs carrying activated immunity cell-epitopes in the circulation than in controls ($p < 0.04$ for all cell types). Particularly, EVs shed by monocytes and neutrophils (innate immunity) and by T-lymphocytes and natural-killer cells (adaptive immunity) are significantly higher in cHF patients. Additionally, EVs-shed by activated leukocytes/neutrophils (CD11b$^+$, $p = 0.006$; CD29$^+$/CD15$^+$, $p = 0.048$), and T-lymphocytes (CD3$^+$/CD45$^+$, $p < 0.02$) were positively correlated with cHF disease severity (NYHA classification). Interestingly, cHF patients with ischemic etiology had the highest levels of EVs shed by lymphocytes and neutrophils ($p < 0.045$, all). In summary, in cHF patients there is a significant immune cell activation shown by high-release of EVs that is accentuated by clinical severity of cHF. These activated innate and adaptive immunity cell messengers may contribute by intercellular communication to the progression of the disease and to the common affectation of distant organs in heart failure (paracrine regulation) that contribute to the clinical deterioration of cHF patients.

KEYWORDS

extracellular microvesicles (EVs), chronic heart failure, immune cells, inflammation, liquid biopsies, extracellular vesicle (EV)

Introduction

Leukocyte-shed extracellular vesicles (EVs) can play effector roles in the pathophysiological mechanisms of different diseases. These EVs released by membrane budding of leukocytes have been found in high amounts locally in inflamed tissues and in the circulation, indicating immunity cell activation. These EVs secreted by immune cell subsets have been minimally explored and deserve further investigation in many areas of disease (1). Heart failure (HF) is a complex syndrome that accounts for a high proportion of cardiovascular death worldwide (2, 3). It is characterized by an impairment of the cardiac function due to genetic and environmental insults and comorbidities such as ischemic disease, that induce significant alterations of heart structure (left ventricle hypertrophy or dilation, fibrosis, maladaptive remodeling) and function (decreased cardiac output, increased end-diastolic pressure and diastolic or systolic dysfunction) (4). HF can be classified in HF with preserved ejection fraction (HFpEF), HF with reduced ejection fraction (HFrEF) and in HF with mildly reduced ejection fraction (HFmrEF), according to their echographic values of left ventricular ejection fraction (LVEF) (2, 5). Although these groups present common symptomatology, their pathophysiological mechanisms and therapeutic approaches are slightly different. In that sense, although this is not universal, the vast majority of HFrEF have underlying ischemic etiology, while HFpEF patients tend to develop HF due to hypertensive or heart valve disease (6, 7).

The systemic inflammation of these patients represents a chronic and non-resolving health impairment with the presence of elevated levels of circulating cytokines or pro-inflammatory mediators, such as TNFα, IL-β1, IL-6, or CRP (4, 8). Further to the raised levels of inflammatory biomarkers, another source of organ damage is the defective equilibrium between pro-inflammatory and anti-inflammatory immune-cell subsets, such as monocytes/macrophages, neutrophils, lymphocytes (B, Treg, Th), that often results in impaired repair processes (9–11). Several clinical trials have tried to target the on-going inflammation with neutral results (12, 13). The failure of these approaches suggests that the potentially involved pathways are not well understood, and that further research in the pathophysiology of the disease is needed. Indeed, HF is a spectrum of overlapping phenotypes that need to be more accurately classified.

Circulating extracellular microvesicles (EVs) are a heterogeneous population of extracellular vesicles with a size range between 20 and 1,000 nm. Composed of a phosphatidylserine-rich phospholipid bilayer that exposes transmembrane proteins and receptors from their parental cells, EVs are released after physiological stimuli such as cell activation, damage, stress, apoptotic or necrotic damage (14, 15). EVs play a role in physiology and pathophysiology since they are involved in various processes such as cell adhesion, communication (they carry miRNA, proteins and lipids), apoptosis, immune response, vascular function, remodeling, hemostasis or thrombosis (16). Their cargo reflects their parental cell condition and metabolic state and its numbers have been correlated with disease progression and severity (14, 16, 17). In cardiovascular disease, they have been related to several pathologies (18) including atherosclerosis (19–21), coronary artery disease (14), ischemia and myocardial infarction (22–24) and stroke (25).

To gain more insight in the pathophysiology of chronic HF (cHF), we aimed to investigate whether immune cells were activated in patients, even though treated according to guideline-directed medical therapy. Several studies have investigated endothelial-derived EVs in relation with cardiovascular risk factors and cardiovascular disease pathophysiology (26–29). However, to our knowledge, there are no studies investigating the type of immune cells that are activated and shed EVs in cHF.

In this study we have investigated whether in chronic heart failure there is innate and adaptive immune cell release of EVs and whether specific circulating EV patterns associate with the underlying cHF etiology (ischemic and non-ischemic) or the disease severity in cHF patients.

Materials and methods

Clinical study population

A total of 119 ambulatory patients with clinical diagnosis of cHF and under guideline-directed medical therapy were prospectively recruited in the outpatient HF unit of the Hospital de la Santa Creu i Sant Pau (Barcelona, Spain) between September 2016 and July 2018 and were followed-up until October 2019. During follow-up patients were treated according to international guidelines and at clinician discretion in the outpatient unit of our hospital. A control group was also included, comprising 60 sex- and age-matched controls without cHF. Baseline demographic data, classical cardiovascular risk factors and background medication of the study population (cHF and control groups) are shown in **Table 1**. Exclusion criteria were: HF with mildly reduced ejection fraction (40–50% of left ventricular ejection fraction [LVEF]), past history of cancer, inflammatory disorders, sepsis or infection. Pregnant women were also excluded. Characteristics of the cHF patients including biochemical and hematological data, cHF-etiology and cHF-severity (according to the New York

Abbreviations: AV, annexin V; cHF, chronic heart failure; EVs, extracellular microvesicles; HF-Isch, heart failure with an ischemic underlying etiology; HF-Nisch, heart failure with a non-ischemic underlying etiology; HFpEF, heart failure with preserved ejection fraction; HFrEF, heart failure with reduced ejection fraction; LVEF, left ventricle ejection fraction; NYHA, New York Heart Association.

TABLE 1 Patients and controls baseline characteristics.

	Controls $n = 60$	cHF $n = 119$	*P*-value controls-cHF
Demographic characteristics; mean ± SD			
Male/Female, n	34/26	81/38	0.133
Age, years	67.1 ± 7.1	67 ± 11.8	0.553
Systolic blood pressure, mmHg	144.8 ± 20.2	120.4 ± 19.1	**0.000**
Diastolic blood pressure, mmHg	83.7 ± 11.3	73.9 ± 11.1	**0.000**
Left ventricular ejection fraction,%	52–74†	45.59 ± 18.98	–
Risk factors; n (%)			
Smokers	10 (16)	13 (10.9)	0.278
Hypertension	33 (55)	82 (68.9)	0.067
Pulmonary hypertension	–	49 (41.1)	–
Diabetes mellitus	10 (16)	53 (44.5)	**0.000**
Dyslipidaemia	45 (75)	64 (53.7)	**0.004**
Chronic kidney disease	2 (3.3)	46 (38.6)	**0.000**
Atrial fibrillation	–	50 (42)	–
Background medication; n (%)			
Angiotensin-converting-enzyme inhibitors	19 (31.6)	48 (40.3)	0.333
Angiotensin II receptor blockers	9 (15)	35 (29.4)	0.054
Beta-blockers	2 (3.3)	100 (84)	**0.000**
Aldosterone antagonists	–	66 (55.4)	–
Diuretics‡	6 (10)	104 (87.3)	**0.000**
Angiotensin receptor neprilysin inhibitors	–	17 (14.2)	–
Ivabradine	–	14 (11.7)	–
Statins	37 (61.6)	77 (64.7)	0.690
Insulin	3 (5)	16 (13.4)	0.083
Anti-diabetic drugs	8 (13.3)	40 (33.6)	**0.004**
Antiplatelet agents	12 (20)	46 (38.6)	**0.012**
Anticoagulants	2 (3.3)	61 (51.2)	**0.000**
Anti-arrhythmic drugs	–	26 (21.8)	–

†LVEF normal range (excerpted from https://www.ncbi.nlm.nih.gov/books/NBK459131/ on 18/01/2021).
‡Includes: furosemide, hydrochlorothiazide, torasemide and indapamide.
SD, standard deviation; cHF, chronic heart failure. The statistically significant *p*-values are in bold.

Heart Association Classification [NYHA]) are given in **Table 2** and **Supplementary Tables 1**, **2**. NYHA classification system considers cardiac functionality and disease severity, dividing cHF in four categories (5). Briefly, NYHA I patients do not present limitations in their physical activity and daily activity does not cause breathlessness, fatigue or palpitations. NYHA II patients have a slight limitation of physical activity, and whereas they are comfortable at rest, ordinary activity produces breathlessness, fatigue or palpitations. Patients in NYHA III present a marked limitation of physical activity. Although they are comfortable at rest, less than ordinary physical activity results in breathlessness, fatigue or palpitations. Finally, NYHA IV patients are unable to carry on any physical activity without discomfort and can have symptoms at rest. In patients with ischemic etiology, ischemia was defined as history of a previous myocardial infarction, or in the absence of an acute ischemic event, if there was stenosis equal or greater than 75% in the common trunk or left anterior descending artery, as well as when stenosis was equal or greater than 75% in two or more of the principal coronary arteries.

The ethics committee at the Hospital de la Santa Creu i Sant Pau in Barcelona (Spain) approved the study (Ref 16/44) and it was conducted under the principles of the Declaration of Helsinki. A written informed consent was obtained from all participants prior recruitment.

Blood sampling, circulating extracellular vesicles isolation and characterization

Venous blood was withdrawn from the cubital vein without tourniquet using a 20-gauge needle after 10–14 h of fasting into 3.8% sodium citrate tubes (BD Vacutainer, Becton Dickinson).

TABLE 2 Clinical characteristics of cHF patients at baseline (n = 119).

Patients characteristics	
Clinical history; n(%) cHF etiology	
Ischemic	43 (36.1)
Non-ischemic	76 (63.9)
Hypertensive cardiomyopathy	19 (15.9)
Dilated cardiomyopathy	24 (20.1)
Hypertrophic cardiomyopathy	12 (10)
Heart valve disease	17 (14.2)
Other	4 (3.3)
New York Heart Association cHF stage	
NYHA I	0 (0)
NYHA II	52 (43.7)
NYHA III	66 (55.5)
NYHA IV	1 (0.8)
Hospitalizations in the 6 months prior study initiation	49 (41.1)
Re-events in the year prior study initiation	9 (7.6)
Percutaneous coronary intervention	4 (44.5)
Coronary artery bypass grafting	2 (22.2)
Medical treatment	3 (33.3)
Biochemistry; mean ± SD	
Hemoglobin, mg/dl	129.8 ± 18.5
Creatinine, mg/dl	1.3 ± 0.54
C-Reactive Protein, mg/ml	7.63 ± 11
NT-proBNP, pg/ml	2954.8 ± 4211.3
High-sensitive troponin T, ng/l	27.7 ± 20.9
Erythrocytes, 10^6/mm^3	3.98 ± 0.74
Platelets, 10^3/mm^3	173.2 ± 56.89
Leukocytes, mm^3	7426.1 ± 1950
Neutrophils, 10^9/L	4.74 ± 1.54
Monocytes, 10^9/L	0.75 ± 0.54
Major outcomes during follow-up; n (%)	
Cardiovascular event†	26 (21.8)
Stroke	8 (6.7)
Aortic dissection	1 (0.8)
AMI + Cardiogenic shock	3 (2.5)
HTx/HTx waiting list	10 (8.4)/1 (0.8)
CV death	7 (5.8)
Emergency hospital admission for cHF	16 (13.4)
Rehospitalisation for cHF	57 (47.8)
Aortic aneurism	1 (0.8)
Other death causes‡	10 (8.4)

†Includes patients that suffered a stroke, an aortic dissection, an AMI, a cardiogenic shock, a CV death (mainly due to cHF) or were admitted to the emergency department. It does not include patients that underwent a HTx.
‡Includes patients that died due to a septic shock, a hemorrhage or a non-successful HTx.
AMI, acute myocardial infarction; CV, cardiovascular; cHF, chronic heart failure; HTx, heart transplantation; NT-proBNP, N-terminal pro-hormone of brain natriuretic peptide; NYHA, New York Heart Association; SD, standard deviation.

All samples were processed identically and within the first 2 h. Blood was centrifuged at 1,560 g for 20 min at 20°C (Eppendorf 5810R GLOOB04932 centrifuge, A-4-81 rotor, Eppendorf) to avoid *in vitro* platelet activation. Platelet-poor plasma (PPP) was carefully aspirated, leaving about a 1 mm undisturbed layer on top of cells. A second centrifugation step was then performed at 1,500 g for 10 min at 20°C (Eppendorf 5415R centrifuge, FA45-24-11 rotor, Eppendorf) to ensure the complete removal of cells and obtain the platelet-free plasma (PFP). PFP aliquots were stored at −80°C until flow cytometry studies.

The EVs fraction was isolated from PFP by a two-step high-speed centrifugation, according to the procedure previously described (20, 24, 30). Specifically, PFP was thawed and centrifuged at 1,500 g for 10 min at 20°C (Eppendorf 5417R centrifuge, FA45-24-11 rotor, Eppendorf). Next, 250 µl of PFP were collected from the upper part of the vial and transferred to a new tube to pellet the EVs, and then centrifuged at 20,000 g for 30 min at 20°C (Eppendorf 5417R centrifuge, FA45-24-11 rotor, Eppendorf). The supernatant (225 µl) was discarded, and the EVs-enriched pellet was washed with 225 µl of citrate-phosphate buffered saline (PBS) solution (citrate-PBS; 1.4 mmol/L phosphate, 154 mmol/L NaCl, 10.9 mmol/L trisodium citrate, pH 7.4) before a second equal centrifugation (20,000 g, 30 min, 20°C) was pursued. Finally, the remaining pellets were resuspended in a final volume of 100 µl citrate-PBS.

Flow cytometric analysis of extracellular vesicles

Extracellular vesicles were phenotypically characterized by three-label flow cytometric analysis, performed as described previously (20, 24, 30). Washed EVs suspensions were diluted in PBS containing 2.5 mmol of $CaCl_2$ (Annexin binding buffer [ABB], BD Biosciences, San Jose). Afterward, combinations of CFBlue-conjugated annexin V (AV) (Immunostep, Salamanca, Spain) to detect phosphatidylserine, and two specific monoclonal antibodies (mAb) (**Supplementary Table 3**) labeled with fluorescein isothiocyanate (FITC) and phycoerythrin (PE), or the isotype-matched control mAb, were added. Samples were incubated for 20 min at 20°C in the dark and diluted with ABB before being immediately analyzed on a FACSCantoII™ (Becton Dickinson, Franklin Lakes, NJ, USA) flow cytometer.

Sample acquisition was performed during 1 min per sample at "low flow" rate. Forward scatter (FSC), side scatter (SSC), and fluorescence data were obtained with the settings in the logarithmic scale. Gate limits were established as follows with the same criteria previously described (20, 24, 30). The upper threshold for FSC was set with the Megamix-Plus FSC beads (BioCytex, Marseille, France). Megamix-Plus FSC beads for cytometer setting are a mix of beads of the following bead-equivalent diameters: 0.1, 0.3, 0.5, and 0.9 µm. According to the beads signal, the lower detection limit was placed as a threshold above the electronic background noise of the flow cytometer for FSC and the second logarithm for SSC. EVs within the established gate limits (>0.1 to 1 μm) were identified and quantified based on their binding to AV and reactivity to cell-specific mAb. To identify positive marked events, thresholds of fluorescence were also set based on samples incubated with the same final concentration of isotype-matched control mAb after titration experiments. AV binding level was corrected for auto-fluorescence using fluorescence signals obtained with EVs in a calcium-free buffer (PBS). Additional controls to correct for FITC-, PE- and CFBlue-fluorescence were also pursued (unstained and single-stained controls), as well as serial dilutions to ensure proper event detection and to prevent swarming. Finally, to corroborate the presence of EVs in the EVs suspension, 5% saponin-treated controls were performed (see **Supplementary Figure 1**). To reduce background noise, buffers were prepared on the same day and filtered through 0.22 μm pore-size filters under vacuum. EVs markers observed in cHF patients by flow cytometry were validated by western blot as described in **Supplementary material** and shown in **Supplementary Figure 2**.

Data was analyzed with BD FACSDiva™ Software (version 6.1.3, Becton Dickinson, Franklin Lakes, NJ, USA). The concentration (number of EVs per μl of plasma) was determined according to Nieuwland's procedure (31), based on sample's volume, flow cytometer's flow rate and the number of fluorescence-positive events (N), as follows: EVs/μl = N x (Vf/Va) x (Vt/FR) x (1/Vi), where Vf(μl) = final volume of washed EVs suspension, Va(μl) = volume of washed EVs suspension used for each labeling analysis, Vt(μl) = volume of EVs suspension before fluorescence-activated cell sorting analysis, FR(μl/min) = flow rate of the cytometer at low mode (the average volume of EVs suspension analyzed in 1 min), 1 is the μl unit of volume, and Vi(μl) = original volume of plasma used for EVs isolation.

Statistical analysis

Statistical analysis was performed using SPSS Statistical Analysis System (version 26.0, IBM Corp. Armonk, NY). Normality of variables was assessed with Saphiro–Wilks test. Descriptive analysis for qualitative variables was performed using number of cases and percentages, while for quantitative variables, mean ± SD were used except when specified. Frequencies of qualitative variables (clinical outcomes, risk factors, and medications) were compared between groups using Chi-squared analysis. Median values of quantitative variables were contrasted with non-parametric tests. Statistical significances between groups were determined with U Mann–Whitney tests. Correlation analyses were pursued using the Spearman correlation test. Receiver operating characteristic (ROC) curve analyses for predicted probabilities were performed to identify threshold concentrations of EVs able to discriminate between cHF NYHA stages, or between severity in ischemic patients, and the corresponding area under the curve (AUC) with its 95% confidence interval (CI) was calculated. Binary logistic regression models were pursued to estimate predicted probabilities for NYHA severity using combinations of EVs and/or the currently used biomarker NT-proBNP. A $p < 0.05$ was considered statistically significant. Sample size was determined using the GRANMO sample size calculator (version 7.12, April 2012). To detect mean differences in the number of EVs, a total of 126 subjects (controls and cHF) would be needed to complete the study (α risk = 0.05, beta risk = 0.2, two-sided test).

Results

Clinical characteristics of the study population

Mean age of cHF was 67 ± 12 years (68% of men). Sixty cHF patients presented reduced ejection fraction (HFrEF; LVEF < 40%; $n = 60$) while 59 (49.6%) had cHF with preserved ejection fraction (HFpEF; LVEF > 50%). Additionally, 52 (43.7%) cHF presented a less severe cHF symptomatology according to the NYHA classification (class II), while 66 (55.5%) and 1 (0.8%) were in the higher severity spectrum, being in the NYHA stages III and IV, respectively. Demographics, classical risk factors and background medication are shown in **Table 1**, while etiology, biochemistry data and follow-up events and outcomes are listed in **Table 2**. Demographical, pharmacological and classical risk factor data of cHF according to their ejection fraction or severity (NYHA classification) is disclosed in **Supplementary Tables 1**, **7**. Underlying etiology classification and clinical data of cHF according to these groups are listed in **Supplementary Tables 2**, **8**.

Immunity cell-derived circulating extracellular vesicles: Cell-origin and activation

Total levels of EVs-AV$^+$ shed by leukocytes were significantly higher in cHF patients than in controls. As shown in **Figure 1A**, EVs carrying the pan-leukocyte marker CD45$^+$, the T-lymphocyte co-receptor (CD3$^+$) or both (CD3$^+$/CD45$^+$), were significantly increased in cHF ($p < 0.0001$). In addition, patients had significantly higher amounts of monocyte- and neutrophil-derived AV$^+$-EVs carrying CD16$^+$ (receptor Fcγ III) and CD15$^+$ (sialyl Lewis X), respectively. EVs shed by natural-killer cells carrying the neural cell adhesion molecule-1 (CD56$^+$) were significantly elevated in cHF compared to controls.

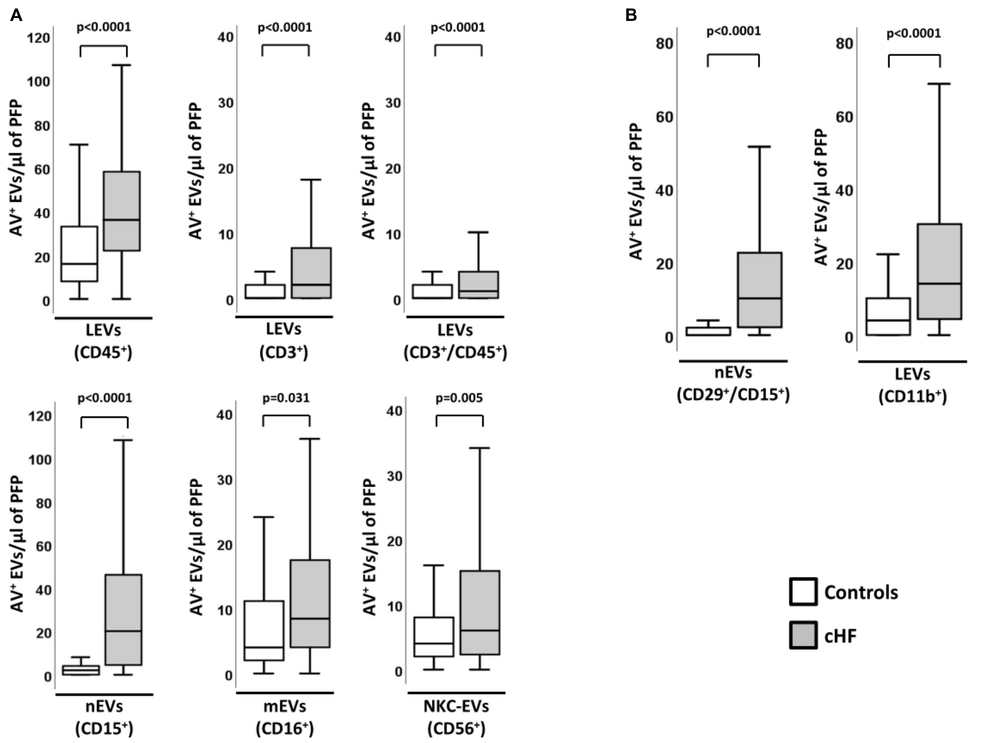

FIGURE 1

Cellular origin and distribution of AV^+ EVs in cHF and controls. **(A)** Distribution of EVs from total leukocytes ($CD45^+$), T-lymphocytes ($CD3^+$ and $CD3^+/CD45^+$), neutrophils ($CD15^+$), monocyte/macrophage ($CD16^+$) and natural-killer cells ($CD56^+$). **(B)** Distribution of EVs from activated neutrophils ($CD29^+/CD15^+$) and from activated leukocytes ($CD11b^+$). A $p < 0.05$ was considered significant (U Mann–Whitney test). AV^+, annexin V^+; cHF, chronic heart failure; EVs, extracellular microvesicles; LEVs, leukocyte-derived EVs; lEVs, lymphocyte-derived EVs; mEVs, monocyte-derived EVs; nEVs, neutrophil-derived EVs; NKC-EVs, natural-killer cells-derived EVs; PFP, platelet-free plasma.

In addition, cHF patients had significantly higher levels of EVs derived from activated immune cells (identified for the shedding of activation markers in EVs). Specifically, AV^+-EVs from activated leukocytes (integrin α-M; $CD11b^+$) and activated neutrophils (integrin β-1/sialyl Lewis X; $CD29^+/CD15^+$) were significantly increased in patients compared to controls (Figure 1B).

The activation of the immunity cells measured by EVs did not correlate with the number of blood leukocytes or CRP levels, indicating different pathophysiological pathways. Interestingly, circulating EVs from T-lymphocytes ($CD3^+/CD45^+/AV^+$) significantly correlated with the cardiac damage markers hsTnT and NT-proBNP, while levels of EVs from activated neutrophils ($CD29^+/CD15^+/AV^+$) and hsTnT and NT-proBNP showed a trend toward significance (Supplementary Table 4). cHF and control groups did not differ in the percentages of EVs shed by platelets ($CD41a^+$; αIIbβ 3-integrin).

Immune cell-derived circulating extracellular vesicles signature and chronic heart failure severity

Chronic heart failure patients with more severe form of disease (a higher score in the NYHA classification [NYHA III-IV]) had higher values of EVs derived from leukocytes ($CD45^+/AV^+$) and specifically those shed by T-lymphocytes ($CD3^+/AV^+$, $CD3^+/CD45^+/AV^+$). In addition, a significant increase in EVs from activated leukocytes ($CD11b^+/AV^+$) and activated neutrophils ($CD29^+/CD15^+/AV^+$) was observed in these patients, compared to those with NYHA II (Figure 2A). Interestingly, these differences were maintained when both groups were compared with controls (Supplementary Table 5).

Distribution of the cHF population according to disease severity (according to the NYHA classification) is given in Table 2. Patients' characteristics according to degree of

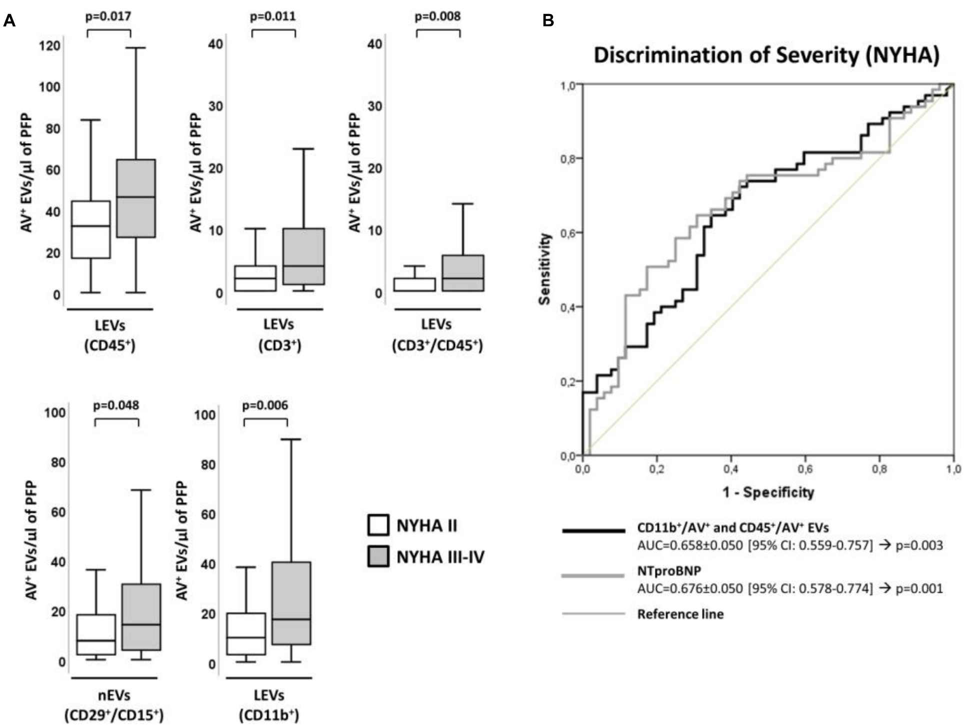

FIGURE 2
Distribution of AV$^+$-EVs of immune-cell origin considering disease severity according to NYHA. **(A)** Distribution of EVs from total leukocytes (CD45$^+$), T-lymphocytes (CD3$^+$ and CD3$^+$/CD45$^+$), activated leukocytes (CD11b$^+$) and from activated neutrophils (CD29$^+$/CD15$^+$). A $p < 0.05$ was considered significant (U Mann–Whitney test). **(B)** ROC curve analyses to evaluate EVs and NT-proBNP association to NYHA severity, with AUC indicated along its 95% CI. A $p < 0.05$ was considered significant. AUC, area under the curve; AV$^+$, annexin V$^+$; cHF, chronic heart failure; CI, confidence interval; EVs, extracellular microvesicles; LEVs, leukocyte-derived EVs; lEVs, lymphocyte-derived EVs; nEVs, neutrophil-derived EVs; NYHA, New York Heart Association; PFP, platelet-free plasma; ROC, receiver operating characteristic curve.

severity (NYHA II and NYHA III-IV stages) are shown in **Supplementary Tables 1**, **2**. Disease severity score according to NYHA correlated positively with hsTnT (rho = 0.200; $p = 0.031$) and NT-proBNP (rho = 0.313; $p = 0.001$).

Leukocyte-derived EVs subtypes showed a significant association to NYHA severity, evidencing their involvement in disease pathophysiology. By C-statistics analysis, the clustering of CD11b$^+$/AV$^+$ and CD45$^+$/AV$^+$ showed an AUC (AUC = 0.658 ± 0.050 [95% CI: 0.559–0.757]; $p = 0.003$) (**Supplementary Table 6**) similar to NT-proBNP (AUC = 0.676 ± 0.050 [95% CI: 0.578–0.774]; $p = 0.001$), hormone secreted by cardiomyocytes in the heart ventricles in response to stretching caused by increased ventricular blood volume that signals for a different pathophysiological pathway to that mapped by EVs (**Figure 2B** and **Supplementary Table 6**).

Interestingly, no differences in immune cell-derived EVs levels/phenotypes were detected in HFpEF and HFrEF patients. Instead, as expected, a negative correlation of NT-proBNP and LVEF was observed (rho = −0.222, $p = 0.015$). These results indicate that immune cell activation is a common feature in patients with both HFpEF and HFrEF. Demographic, biochemical and clinical classification of the patients according to their LVEF is shown in **Supplementary Tables 7–9**.

Circulating extracellular vesicles and chronic heart failure etiology: Ischemic and non-ischemic disease

Chronic heart failure patients with ischemic etiology (HF-Isch) presented increased levels of EVs. Specifically, EVs derived from T-lymphocytes (CD3$^+$/AV$^+$, $p = 0.045$) or carrying the leukocyte activation marker integrin β-1 (CD29$^+$/AV$^+$, $p = 0.025$) were significantly increased in HF-Isch compared to non-ischemic patients (HF-NIsch). Moreover, EVs from activated neutrophils ($CD29^+/CD15^+/AV^+$) displayed higher levels in HF-Isch compared to HF-NIsch, although this trend was non-significant ($p = 0.079$) (**Figure 3A**).

Within HF-Isch, different EVs profiles associated to disease severity (NYHA class). There were significantly higher levels of EVs derived from leukocytes ($CD45^+/AV^+$; $p = 0.013$), T-lymphocytes ($CD3^+/AV^+$ and $CD45^+/CD3^+/AV^+$; $p < 0.024$), and activated leukocytes, monocytes and neutrophils ($CD11b^+/AV^+$, $CD11b^+/CD14^+/AV^+$ and $CD29^+/CD15^+/AV^+$, respectively; $p < 0.05$) in severe disease patients. No differences associated to severity were detected in HF-NIsch (**Figure 4**). C-statistics analyses to assess the involvement of EVs in the pathophysiology and severity of disease in HF-Isch, showed that activated leukocytes ($CD11b^+/AV^+$) had the best discrimination power, with an AUC of 0.848 ± 0.058 (95% CI: 0.734–0.961; $p < 0.001$), followed by activated neutrophils ($CD29^+/CD15^+/AV^+$), with and AUC of 0.811 ± 0.065 (95% CI: 0.683–0.939; $p = 0.001$). Again, in an order of magnitude comparable to the contribution of disease showed by NT-proBNP, with an AUC of 0.816 + 0.071 (95% CI: 0.676–0.955; $p < 0.001$). When analyses were performed with the combined probabilities of EVs from activated leukocytes and neutrophils ($CD11b^+/AV^+$ and $CD29^+/CD15^+/AV^+$) the AUC increased to 0.858 ± 0.056 (95% CI: 0.747–0.968; $p < 0.001$), with a sensitivity and specificity of 80.0 and 83.3%, respectively. The addition of NT-proBNP to the analysis did not improve discrimination (AUC = 0.858 ± 0.056 [0.747–0.968]; $p < 0.001$) (**Figure 3B** and **Supplementary Table 10**) indicating two types of contribution to disease progression of EVs and NT-proBNP, respectively.

Extracellular vesicles shedding levels, considering elapsed time between any ischemic event and sample collection, was similar in those patients with longer elapsed time between ischemic event and blood withdrawal (more than 1 year: 7 ± 7 years) and those with lower time-periods (less than a year: 5 ± 2 months) (**Supplementary Table 11**).

Discussion

Heart failure is a complex syndrome where the heart is unable to maintain a correct blood supply to ensure that the metabolic needs of the body are met (2). This can occur due to structural and functional defects, which at the same time are the result of major pathogenic mechanisms like hemodynamic overload, ischemia-related dysfunction, or ventricular remodeling among others (32). cHF patients have shown in diverse studies to have a chronic and non-resolving inflammatory state (11, 33).

The immune system has an important role in the setting of structural and functional changes in many organs, especially when the immune reparative processes become impaired. The present study has aimed at obtaining information on the activation state of different immunity cells in cHF patients. We have demonstrated that cHF patients present differential EVs profiles in comparison to control subjects, observing increased levels of EVs derived from leukocytes in cHF, reflecting the chronic activation state of these cells.

We have specifically detected EVs derived from lymphocytes, neutrophils, monocytes/macrophages and natural-killer cells in cHF compared to controls. In addition, we have shown that numbers of these EVs, except those shed by natural-killer cells and monocytes, correlated with the severity of the symptomatology. The combination of EVs $CD11b^+/AV^+$ and $CD45^+/AV^+$ was able to discriminate between NYHA stages II and III-IV, with an AUC of 0.658, indicating the implication of the activation of these immunity cells in disease severity pathophysiology. We also found that EVs could discriminate the etiology of cHF, with those patients with underlying ischemic etiology presenting significantly increased immune cell shed EVs. Further, we observed that in these patients EVs from activated leukocytes in combination with those from activated neutrophils, had a high discriminative potential in assessing cHF severity similar to NT-proBNP that measures another component of disease pathophysiology. We did not observe, however, differences in immune-cell-derived EVs profiles depending on the LVEF of cHF patients, indicating that both HFpEF and HFrEF patients have activation of immunity cells.

Several studies have shown how EVs can signal pathophysiological pathways of cardiovascular disease progression. For instance, our group has recently demonstrated that EVs can predict the presence of atherosclerotic plaques and discriminate plaque composition in familial hypercholesterolemia (21, 34). Further, it is widely accepted that EVs can identify severity of various pathologies (30, 35) and predict cardiovascular events (24, 36, 37), including cardiovascular death (22, 30). In fact, some studies have already observed increased levels of EVs in cHF, such as EVs from endothelial cells carrying the marker $CD144^+$ (29).

Here, we have shown in patients under guideline-directed medical therapy that immunity cells are activated. The amount of EVs shed by neutrophils ($CD29^+/CD15^+/AV^+$), T-lymphocytes ($CD3^+/AV^+$ and $CD3^+/CD45^+/AV^+$) or carrying the activation marker $CD11b^+/AV^+$, positively correlates with disease severity. Further, we have shown for the first time that immune-cell-derived EVs associate to NYHA disease stage, and that immune cells are similarly activated in HFpEF and HFrEF patients. A non-resolving inflammation is a reported characteristic of HF (11, 38); in addition, our results indicate that there is an activated state of the innate and adaptive immune cells that may need be the target of future therapeutic interventions.

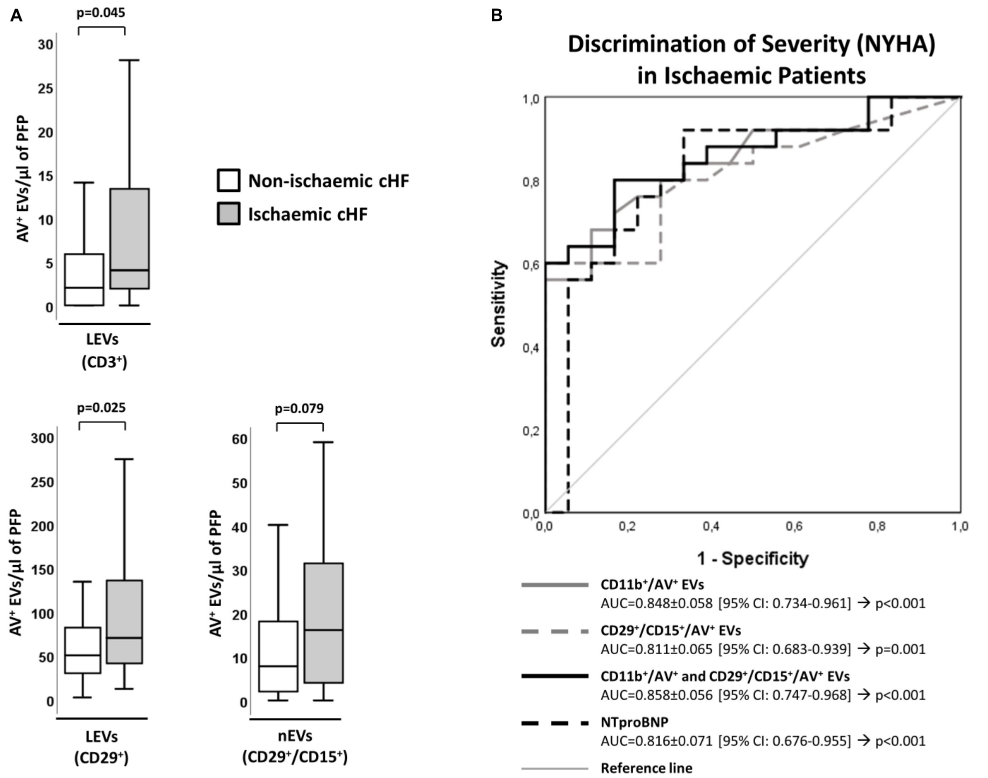

FIGURE 3
Distribution of AV$^+$-EVs from immune-cell origin considering disease etiology. **(A)** Distribution of EVs from T-lymphocytes (CD3$^+$), activated leukocytes (CD29$^+$) and from activated neutrophils (CD29$^+$/CD15$^+$). A $p < 0.05$ was considered significant (U Mann–Whitney test). **(B)** ROC curve analyses were used to evaluate the impact of EVs and combinations of EVs with NT-proBNP on HF severity (NYHA) in ischemic patients (AUC indicated along its 95% CI). A $p < 0.05$ was considered significant. AUC, area under the curve; AV$^+$, annexin V$^+$; cHF, chronic heart failure; CI, confidence interval; EVs, extracellular microvesicles; LEVs, leukocyte-derived EVs; lEVs, lymphocyte-derived EVs; nEVs, neutrophil-derived EVs; NYHA, New York Heart Association; PFP, platelet-free plasma; ROC, receiver operating characteristic curve.

Patients with cHF of ischemic origin have significantly higher numbers of EVs from T-lymphocytes and neutrophils. This is a pathophysiological indication of the increase in neutrophils in the myocardium after an initial insult (10). Neutrophils are of the first cells mobilized to the damaged myocardium, where they clear diseased cells, start the reparative macrophages (M1) induction and promote inflammation, tissue reparation and fibrosis (10, 11, 39). Following the neutrophil and macrophage wave, T-lymphocytes infiltrate the heart and promote wound healing. However, if this pro-inflammatory state is prolonged in time and is not switched to a more anti-inflammatory phenotype, maladaptive remodeling and fibrosis occur, promoting HF (11, 39). This crosstalk among cells in the damaged myocardium is mapped by the phenotypically characterized EVs.

As study limitations we should first mention that the relatively small cohort size included in the study has impeded the adjustment for comorbidities and medications; however, this is a hypothesis generating study. Second, by experimental design, we did not include patients with HF with mildly reduced ejection fraction, which could have provided additional insights in the pathophysiology of the disease. Third, it is also worth mentioning that the CD11b marker (integrin α-M) is expressed by activated cells and indicates the type of activated cell when is associated with another CD marker. Additionally, due to methodological issues we could not analyze EVs released by B lymphocytes, nor determine cell counts of all white blood cells analyzed. However, in view of our results, further studies addressing EVs from B cells are warranted.

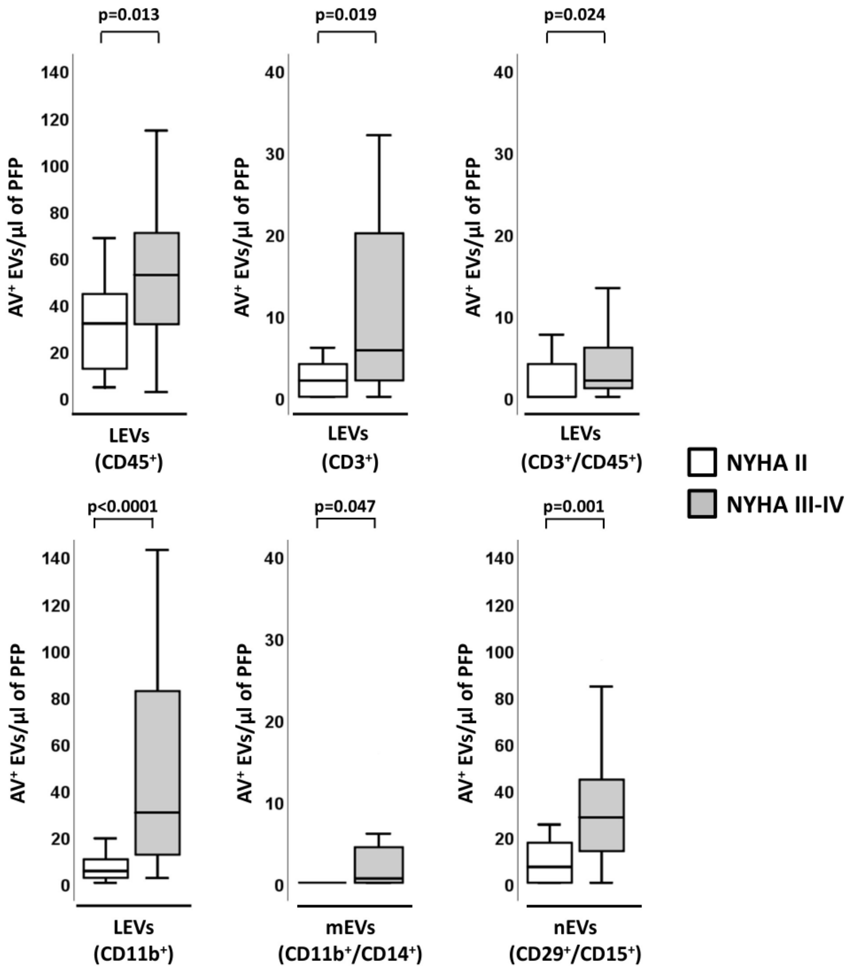

FIGURE 4
Distribution of AV$^+$-EVs of immune-cell origin considering disease severity in ischemic patients. Distribution of EVs of total leukocytes (CD45$^+$), T-lymphocytes (CD3$^+$ and CD3$^+$/CD45$^+$), activated leukocytes (CD11b$^+$) and from activated monocytes (CD11b$^+$/CD14$^+$) and activated neutrophils (CD29$^+$/CD15$^+$). A $p < 0.05$ was considered significant (U Mann–Whitney test). AV$^+$, annexin V$^+$; EVs, extracellular microvesicles; LEVs, leukocyte-derived EVs; lEVs, lymphocyte-derived EVs; mEVs, monocyte-derived EVs; nEVs, neutrophil-derived EVs; NYHA, New York Heart Association; PFP, platelet-free plasma.

Conclusion

In conclusion, HF is a complex syndrome where multiple pathophysiological pathways converge. In well treated chronic heart failure patients, immunity cells, both innate and adaptive immunity cells, are activated and release high number of circulating EVs. The released EVs may amplify the underlying inflammatory processes in these patients, affecting different tissues. Indeed, EVs are involved in crosstalk with other cells, acting as distant cell function regulators of targeted-receptor cells, even in distant organs.

Data availability statement

The data that support the findings of this study are available from the corresponding author upon reasonable request.

Ethics statement

The studies involving human participants were reviewed and approved by Ref 16/44; Ethics Committee of the Hospital de la Santa Creu i Sant Pau in Barcelona. The patients/participants provided their written informed consent to participate in this study.

Author contributions

LB, TP, ER, and SM designed the research. AV-F performed the experiments. AV-F, TP, and LB analyzed the results. AV-F, TP, SM, and LB wrote and revised the manuscript. All authors contributed to the article and approved the submitted version.

Funding

This work was supported by a Research Grant of the Spanish Society of Cardiology (SEC-2016) to LB; Spanish Ministry of Economy and Competitiveness of Science "Agencia Estatal de Investigación (AEI)" Proj Ref AEI/10.13039/501100011033-(PID2019-107160RB-I00) to LB; Institute of Health Carlos III (ISCIII) (Red RICORS TERAV- RD21/0017/0013 to LB; FIS PI19/01687 to TP); and cofounded by FEDER "Una Manera de Hacer Europa". AV-F was recipient of a research contract from the Cardiovascular Program-ICCC (IR-HSCSP). We thank Fundación Jesus Serra and Fundación de Investigación Cardiovascular (Barcelona, Spain) for their continuous support.

Acknowledgments

We are indebted to heart failure patients for their participation in the study and the physicians that contributed to recruitment. This work has been performed under the framework of the Doctoral Program in Biomedicine, Biochemistry and Molecular Biology of the Universitat Autònoma de Barcelona.

Conflict of interest

LB declares to have acted as SAB member of Sanofi, to have a Research Grant of AstraZeneca, to have received speaker fees of Sanofi and Bayer and to have founded the Spin-offs Glycardial Diagnostics SL and Ivastatin Therapeutics S (all unrelated to this work). TP declares to be co-founder of the Spin-offs Glycardial Diagnostics SL and Ivastatin Therapeutics S (all unrelated to this work).

The remaining authors declare that the research was conducted in the absence of any commercial or financial relationships that could be construed as a potential conflict of interest.

Publisher's note

All claims expressed in this article are solely those of the authors and do not necessarily represent those of their affiliated organizations, or those of the publisher, the editors and the reviewers. Any product that may be evaluated in this article, or claim that may be made by its manufacturer, is not guaranteed or endorsed by the publisher.

Supplementary material

The Supplementary Material for this article can be found online at: https://www.frontiersin.org/articles/10.3389/fcvm.2022.939625/full#supplementary-material

References

1. Ridger VC, Boulanger CM, Angelillo-Scherrer A, Badimon L, Blanc-Brude OP, Bochaton-Piallat M-L, et al. Microvesicles in vascular homeostasis and diseases position paper of the european society of cardiology (ESC) working group on atherosclerosis and vascular biology. *Thromb Haemost.* (2017) 117:1296–316. doi: 10.1160/TH16-12-0943

2. Kemp CD, Conte JV. The pathophysiology of heart failure. *Cardiovasc Pathol.* (2012) 21:365–71. doi: 10.1016/j.carpath.2011.11.007

3. Virani SS, Alonso A, Benjamin EJ, Bittencourt MS, Callaway CW, Carson AP, et al. Heart disease and stroke statistics—2020 update: a report from the American Heart Association. *Circulation.* (2020) 141:e139–596. doi: 10.1161/CIR.0000000000000746

4. Tanai E, Frantz S. Pathophysiology of heart failure. *Compr Physiol.* (2016) 6:187–214. doi: 10.1002/cphy.c140055

5. McDonagh TA, Metra M, Adamo M, Gardner RS, Baumbach A, Böhm M, et al. 2021 ESC Guidelines for the diagnosis and treatment of acute and chronic heart failure. *Eur Heart J.* (2021) 42:3599–726.

6. Campbell RT, McMurray JJV. Comorbidities and differential diagnosis in heart failure with preserved ejection fraction. *Heart Fail Clin.* (2014) 10:481–501. doi: 10.1016/j.hfc.2014.04.009

7. Lee DS, Gona P, Vasan RS, Larson MG, Benjamin EJ, Wang TJ, et al. Relation of disease pathogenesis and risk factors to heart failure with preserved or reduced ejection fraction: insights from the framingham heart study of the national heart, lung, and blood institute. *Circulation.* (2009) 119:3070–7. doi: 10.1161/CIRCULATIONAHA.108.815944

8. Testa M, Yeh M, Lee P, Fanelli R, Loperfido F, Berman JW, et al. Circulating levels of cytokines and their endogenous modulators in patients with mild to severe

congestive heart failure due to coronary artery disease or hypertension. *J Am Coll Cardiol.* (1996) 28:964–71. doi: 10.1016/S0735-1097(96)00268-9

9. Alvarez PA, Briasoulis A. Immune modulation in heart failure: the promise of novel biologics. *Curr Treat Options Cardiovasc Med.* (2018) 20:26. doi: 10.1007/s11936-018-0617-z

10. Kain V, Halade GV. Role of neutrophils in ischemic heart failure. *Physiol Genomics.* (2020) 205:107424. doi: 10.1016/j.pharmthera.2019.107424

11. Shirazi LF, Bissett J, Romeo F, Mehta JL. Role of inflammation in heart failure. *Curr Atheroscler Rep.* (2017) 19:27. doi: 10.1007/s11883-017-0660-3

12. Chung ES, Packer M, Lo KH, Fasanmade AA, Willerson JT. Randomized, double-blind, placebo-controlled, pilot trial of infliximab, a chimeric monoclonal antibody to tumor necrosis factor-α, in patients with moderate-to-severe heart failure: results of the anti-TNF therapy against congestive heart failure (ATTACH) trial. *Circulation.* (2003) 107:3133–40. doi: 10.1161/01.CIR.0000077913.60364.D2

13. Mann DL, McMurray JJV, Packer M, Swedberg K, Borer JS, Colucci WS, et al. Targeted anticytokine therapy in patients with chronic heart failure: results of the randomized etanercept worldwide evaluation (RENEWAL). *Circulation.* (2004) 109:1594–602. doi: 10.1161/01.CIR.0000124490.27666.B2

14. Boulanger CM, Loyer X, Rautou P-E, Amabile N. Extracellular vesicles in coronary artery disease. *Nat Rev Cardiol.* (2017) 14:259–72. doi: 10.1038/nrcardio.2017.7

15. Morel O, Jesel L, Freyssinet J-M, Toti F. Cellular mechanisms underlying the formation of circulating microparticles. *Arterioscler Thromb Vasc Biol.* (2011) 31:15–26. doi: 10.1161/ATVBAHA.109.200956

16. Suades R, Padró T, Badimon L. The role of blood-borne microparticles in inflammation and hemostasis. *Semin Thromb Hemost.* (2015) 41:590–606. doi: 10.1055/s-0035-1556591

17. Badimon L, Suades R, Fuentes E, Palomo I, Padró T. Role of platelet-derived microvesicles as crosstalk mediators in atherothrombosis and future pharmacology targets: a link between inflammation, atherosclerosis, and thrombosis. *Front Pharmacol.* (2016) 7:293. doi: 10.3389/fphar.2016.00293

18. Badimon L, Suades R, Vilella-Figuerola A, Crespo J, Vilahur G, Escate R, et al. Liquid biopsies: microvesicles in cardiovascular disease. *Antioxid Redox Signal.* (2020) 33:645–62. doi: 10.1089/ars.2019.7922

19. Leroyer AS, Isobe H, Lesèche G, Castier Y, Wassef M, Mallat Z, et al. Cellular origins and thrombogenic activity of microparticles isolated from human atherosclerotic plaques. *J Am Coll Cardiol.* (2007) 49:772–7. doi: 10.1016/j.jacc.2006.10.053

20. Suades R, Padró T, Vilahur G, Badimon L. Circulating and platelet-derived microparticles in human blood enhance thrombosis on atherosclerotic plaques. *Thromb Haemost.* (2012) 108:1208–19. doi: 10.1160/TH12-07-0486

21. Suades R, Padró T, Alonso R, Mata P, Badimon L. High levels of TSP1+/CD142+ platelet-derived microparticles characterise young patients with high cardiovascular risk and subclinical atherosclerosis. *Thromb Haemost.* (2015) 114:1310–21. doi: 10.1160/TH15-04-0325

22. Chiva-Blanch G, Bratseth V, Ritschel V, Andersen G, Halvorsen S, Eritsland J, et al. Monocyte-derived circulating microparticles (CD14+, CD14+/CD11b+ and CD14+/CD142+) are related to long-term prognosis for cardiovascular mortality in STEMI patients. *Int J Cardiol.* (2017) 227:876–81. doi: 10.1016/j.ijcard.2016.11.302

23. Sluijter JPG, Davidson SM, Boulanger CM, Buzás EI, De Kleijn DPV, Engel FB, et al. Extracellular vesicles in diagnostics and therapy of the ischaemic heart: position Paper from the working group on cellular biology of the heart of the european society of cardiology. *Cardiovasc Res.* (2018) 114:19–34. doi: 10.1093/cvr/cvx211

24. Suades R, Padró T, Crespo J, Ramaiola I, Martin-Yuste V, Sabaté M, et al. Circulating microparticle signature in coronary and peripheral blood of ST elevation myocardial infarction patients in relation to pain-to-PCI elapsed time. *Int J Cardiol.* (2016) 202:378–87. doi: 10.1016/j.ijcard.2015.09.011

25. Chiva-Blanch G, Suades R, Crespo J, Peña E, Padró T, Jiménez-Xarrié E, et al. Microparticle shedding from neural progenitor cells and vascular compartment cells is increased in ischemic stroke. *PLoS One.* (2016) 11:e0148176. doi: 10.1371/journal.pone.0148176

26. Berezin AE, Kremzer AA, Martovitskaya YV, Samura TA, Berezina TA. The predictive role of circulating microparticles in patients with chronic heart failure. *BBA Clin.* (2015) 3:18–24. doi: 10.1016/j.bbacli.2014.11.006

27. Berezin AE, Kremzer AA, Samura TA, Berezina TA. Altered signature of apoptotic endothelial cell-derived microvesicles predicts chronic heart failure phenotypes. *Biomark Med.* (2019) 13:737–50. doi: 10.2217/bmm-2018-0449

28. Berezin AE, Kremzer AA, Martovitskaya YV, Berezina TA, Gromenko EA. Pattern of endothelial progenitor cells and apoptotic endothelial cell-derived microparticles in chronic heart failure patients with preserved and reduced left ventricular ejection fraction. *EBioMedicine.* (2016) 4:86–94. doi: 10.1016/j.ebiom.2016.01.018

29. Nozaki T, Sugiyama S, Sugamura K, Ohba K, Matsuzawa Y, Konishi M, et al. Prognostic value of endothelial microparticles in patients with heart failure. *Eur J Heart Fail.* (2010) 12:1223–8. doi: 10.1093/eurjhf/hfq145

30. Sionis A, Suades R, Sans-Roselló J, Sánchez-Martínez M, Crespo J, Padró T, et al. Circulating microparticles are associated with clinical severity of persistent ST-segment elevation myocardial infarction complicated with cardiogenic shock. *Int J Cardiol.* (2018) 258:249–58. doi: 10.1016/j.ijcard.2017.10.044

31. Nieuwland R, Berckmans RJ, McGregor S, Böing AN, Romijn FPHTM, Westendorp RGJ, et al. Cellular origin and procoagulant properties of microparticles in meningococcal sepsis. *Blood.* (2000) 95:930–5. doi: 10.1182/blood.V95.3.930.003k46_930_935

32. Inamdar AA, Inamdar AC. Heart Failure: diagnosis, management and utilization. *J Clin Med.* (2016) 5:62. doi: 10.3390/jcm5070062

33. Biasucci LM, La Rosa G, Pedicino D, D'Aiello A, Galli M, Liuzzo G. Where does inflammation fit? *Curr Cardiol Rep.* (2017) 19:84. doi: 10.1007/s11886-017-0896-0

34. Chiva-Blanch G, Padró T, Alonso R, Crespo J, Perez De Isla L, Mata P, et al. Liquid biopsy of extracellular microvesicles maps coronary calcification and atherosclerotic plaque in asymptomatic patients with familial hypercholesterolemia: a computed tomographic angiography imaging study. *Arterioscler Thromb Vasc Biol.* (2019) 39:945–55. doi: 10.1161/ATVBAHA.118.312414

35. Gkaliagkousi E, Gavriilaki E, Yiannaki E, Vasileiadis I, Nikolaidou B, Lazaridis A, et al. Platelet microvesicles are associated with the severity of coronary artery disease: comparison between peripheral and coronary circulation. *J Thromb Thrombolysis.* (2021) 51:1138–43. doi: 10.1007/s11239-020-02302-5

36. Chiva-Blanch G, Crespo J, Suades R, Arderiu G, Padró T, Vilahur G, et al. CD142+/CD61+, CD146+ and CD45+ microparticles predict cardiovascular events in high risk patients following a Mediterranean diet supplemented with nuts. *Thromb Haemost.* (2016) 116:103–14. doi: 10.1160/TH16-02-0130

37. Chiva-Blanch G, Suades R, Crespo J, Vilahur G, Arderiu G, Padró T, et al. CD3+/CD45+ and SMA-α+ circulating microparticles are increased in individuals at high cardiovascular risk who will develop a major cardiovascular event. *Int J Cardiol.* (2016) 208:147–9. doi: 10.1016/j.ijcard.2016.01.211

38. Dick SA, Epelman S. Chronic heart failure and inflammation. What do we really know? *Circ Res.* (2016) 119:159–76. doi: 10.1161/CIRCRESAHA.116.308030

39. Dutka M, Bobiński R, Ulman-Włodarz I, Hajduga M, Bujok J, Pająk C, et al. Various aspects of inflammation in heart failure. *Heart Fail Rev.* (2020) 25:537–48. doi: 10.1007/s10741-019-09875-1

New Factors in Heart Failure Pathophysiology: Immunity cells release of extracellular vesicles

Supplementary Material

Alba Vilella-Figuerola[1,2], Teresa Padró[1,3], Eulàlia Roig[4], Sònia Mirabet[3,4†], Lina Badimon[1,3,5†*]

[1]Cardiovascular-Program-ICCC, IR-Hospital Santa Creu i Sant Pau, IIB-Sant Pau, Barcelona, Spain

2Biochemistry and Molecular Biology Department, Universitat Autònoma de Barcelona (UAB), Barcelona, Spain

[3]Centro de Investigación Biomédica en Red Cardiovascular, Instituto de Salud Carlos III, Madrid, Spain

[4]Heart Failure Group, Cardiology Department, Hospital Santa Creu i Sant Pau, Barcelona, Spain

[5]UAB-Chair Cardiovascular Research, Barcelona, Spain

[†]These authors have contributed equally to this work.

1 Supplementary Data

Western blot analysis of EVs

Isolated EVs were lysed with M2 buffer (50mmol/L TRIS pH 7.5, 150mmol/L NaCl, 1% SDS, 1% Triton-X-100, protease inhibitor) and the obtained protein was precipitated overnight at -20ºC, with 7 volumes of cold acetone. In addition, protein from human myocardial tissue, human monocytes and human platelets (with residual white cell fraction) was extracted with RIPA buffer (50mmol/L TRIS-HCl pH 6.8, 150mmol/L NaCl, 1% NP-40, 0.5% sodium deoxycholate, 0.5% SDS, protease inhibitor, adjusted to pH 8). Protein in the extracts was quantified with the 2-D Quant Kit (GE Healthcare, Germany).

Protein (5µg) from EVs lysates and myocardial tissue, monocyte and platelet-white blood cells extracts were loaded into SDS-PAGE (8% and 15%) gels under denaturing (CD3, CD11b) and non-denaturing (CD14) conditions. Protein detection was pursued using the antibodies listed in **Supplemental Table 3** as previously described(1).

Supplementary Material

Chemiluminescent imaging analysis was performed in the ChemiDocTM XRS (Bio-Rad Laboratories Inc) using the Quantity-One (version 4.6.8, Bio-Rad Laboratories Inc) and the Image Lab™ (version 6.0.1, Bio-Rad Laboratories Inc) software.

2 Extended Results

Clinical characteristics of the study population

Compared to controls, a higher number of cHF patients had chronic kidney disease (38.6% vs 3.3%, p<0.001) and diabetes (44.5% vs 16%, p<0.001), while 53.7% of cHF presented dyslipidaemia compared to 75% of controls (p=0.004). Also, 68.9% of cHF (55% of controls), suffered from hypertension (p=0.067). Regarding medication, cHF were treated with angiotensin-inhibition related drugs, beta-blockers and diuretics. In addition, more cHF patients were under antiplatelet, anticoagulant and anti-diabetic treatment (**Table 1**).

Ischaemic disease was the major cause of cHF, affecting 36.1% of the patients. Other major causes were dilated cardiomyopathy (20.1%), hypertensive cardiomyopathy (15.9%), heart valve disease (14.2%) and hypertrophic cardiomyopathy (10%) (**Table 2**). As presented in **Table 2**, 19 cHF patients had adverse cardiovascular events during follow-up, including acute myocardial infarction (1.6%), stroke (6.7%), aortic dissection (0.8%), cardiogenic shock (0.8%) and heart transplantation (8.4%; 1 of the patients had a previous stroke). In addition, 5.8% of the patients suffered a cardiovascular death, while other-cause death occurred in 8.4% of the cases. cHF-related hospitalisation occurred in 47.8% of cases and 13.4% of patients were admitted to the emergency department during follow-up.

3 Supplementary Tables

Supplemental table 1: Patients' characteristics at inclusion, considering New York Heart Association classification

	NHYA II n=52	NYHA III-IV n=67	P-value
DEMOGRAPHIC CHARACTERISTICS; mean±SD			
Male/Female, n	37/15	44/23	0.525
Age, years	66.37±12.72	67.61±11.18	0.639
Systolic blood pressure, mmHg	123.31±19.73	118.28±18.57	0.160
Diastolic blood pressure, mmHg	74.54±11.47	73.45±10.87	0.599
Left ventricular ejection fraction, %	45.67±19.24	45.52±18.92	0.964
RISK FACTORS; n (%)			
Smokers	6 (11.5)	7 (10.4)	0.850
Hypertension	35 (67.3)	47 (70.1)	0.740
Pulmonary hypertension	15 (28.8)	34 (50.7)	**0.008**
Diabetes mellitus	22 (42.3)	31 (46.2)	0.666
Dyslipidaemia	27 (51.9)	37 (55.2)	0.720
Chronic kidney disease	18 (34.6)	28 (41.7)	0.526
Atrial fibrillation	20 (38.4)	30 (44.7)	0.545
CLINICAL HISTORY; n (%)			
cHF aetiology			0.761
Ischaemic	18 (34.6)	25 (37.3)	
Non-ischaemic	34 (65.4)	42 (62.7)	
Hospitalisations in the 6 months prior study initiation	18 (43.7)	31 (42.3)	0.209
Re-events in the year prior study initiation	3 (5.7)	6 (8.9)	0.514
Percutaneous coronary intervention	2 (66.6)	2 (33.4)	0.343
Coronary artery bypass grafting	1 (33.4)	1 (16.6)	0.571
Medical treatment	0 (0)	3 (50)	0.134
BIOCHEMISTRY; mean±SD			
Haemoglobin, mg/dl	132.98±19.59	127.45±17.50	0.096
Creatinine, mg/dl	1.31±0.59	1.36±0.49	0.197
C-Reactive Protein, mg/ml	6.57±8.73	8.44±12.46	0.345
NT-proBNP, pg/ml	2173.38±4316.14	3561.28±4057.0	**0.001**
High-sensitive troponin T, ng/l	22.78±14.59	31.64±24.18	**0.041**
Erythrocytes, 10^6/mm^3	4.1±0.59	3.88±0.82	0.103
Platelets, 10^3/mm^3	178.12±51.26	169.28±61.12	0.326
Leukocytes, mm^3	7421.76±2172.93	7429.57±1773.26	0.541
Neutrophils, 10^9/L	4.74±1.15	4.74±1.77	0.891
Monocytes, 10^9/L	0.69±0.26	0.8±0.66	0.950

cHF: chronic heart failure; **NT-proBNP**: N-terminal pro-hormone of brain natriuretic peptide; **NYHA**: New York Heart Association; **SD**: standard deviation

Supplementary Material

Supplemental table 2: Follow-up events and outcomes, considering NYHA classification

MAJOR OUTCOMES DURING FOLLOW-UP; n (%)	NHYA II n=52	NYHA III-IV n=67	P-value
Cardiovascular event†	12 (23.1)	14 (20.9)	0.775
Stroke	3 (5.7)	5 (7.4)	0.714
Aortic dissection	1 (1.9)	0 (0)	0.254
AMI + Cardiogenic shock	2 (3.8)	1 (1.4)	0.417
HTx/HTx waiting list	0 (0)/1 (1.9)	10 (14.9)/0 (0)	**0.004**/0.254
CV death	3 (5.7)	4 (5.9)	0.963
Emergency hospital admission for cHF	6 (11.5)	10 (14.9)	0.591
Rehospitalisation	21 (40.3)	36 (53.7)	0.148
Aortic aneurism	0 (0)	1 (1.4)	0.376
Other death causes‡	2 (3.8)	8 (11.9)	0.114

†Includes patients that suffered a stroke, an aortic dissection, an AMI, a cardiogenic shock, a CV death (mainly due to cHF) or were admitted to the emergency department. It does not include patients that underwent a HTx.

‡Includes patients that died due to a septic shock, a haemorrhage or a non-successful HTx.

AMI: acute myocardial infarction; **CV**: cardiovascular; **cHF**: chronic heart failure; **HTx**: heart transplantation

Supplemental table 3: Cell surface molecules for extracellular microvesicle identification and characterisation

ANTIBODIES FOR FLOW CYTOMETRY ANALYSIS									
	EXPRESSION	**MARKER**	**ALTERNATIVE NAME**	**CONJUGATION**	**CLONE**	**DILUTION**	**HOST**	**COMPANY**	**CATALOGUE NUMBER**
Annexin V	Widely expressed	PS^{+}	PS-binding protein	CF405	-	5µl (1:10)	-	Immunostep	ANXVCFB-200T
Leukocyte markers	Lymphocytes T	$CD3^{+}$	T-cell coreceptor	FITC	HIT3b	5µl (1:10)	Mouse	Immunotools	21810033
	Leukocytes	$CD45^{+}$	LCA	PE	MEM-28	5µl (1:10)	Mouse	Immunotools	21270454
	Neutrophils, monocytes	$CD11b^{+}$	MAC-1/α-M integrin	FITC	MEM-174	5µl (1:10)	Mouse	Immunotools	21279113
	Monocytes, macrophages	$CD14^{+}$	LPS-receptor	PE	M5E2	5µl (1:100)	Mouse	BD Pharmingen	555398
	Activated lymphocytes	$CD29^{+}$	ITGBI	FITC	HI29a	5µl (1:10)	Mouse	Immunotools	21810293
	Granulocytes, neutrophils	$CD15^{+}$	Sialyl Lewis X	PE	MEM-158	5µl (1:10)	Mouse	Immunotools	21270154
	Natural killers	$CD56^{+}$	NCAM1	FITC	B-A19	5µl (1:10)	Mouse	Immunotools	21810563
	Natural killers, monocytes	$CD16^{+}$	FcγRIII	FITC	HI16a	5µl (1:10)	Mouse	Immunotools	21810163

*At staining (final volume of reagents: 50µl [5µl of isolated EVs, 5µl of Annexin V, ~5µl of antibody-FITC, ~5µl of antibody-PE, adjust to final a volume of 50µl with annexin binding buffer]).
FITC: Fluorescein isothiocyanate; **PE**: Phycoerythrin; **PS**: Phosphatidylserine; **LCA**: Leukocyte common antigen; **MAC-1**: Macrophage-1 Antigen; **LPS**: Lipopolysaccharide; **ITGB1**: Integrin β-1; **NCAM1**: Neural cell adhesion molecule-1; **FcγRIII**: Receptor Fcγ III.

ANTIBODIES FOR WESTERN BLOT ANALYSIS								
	EXPRESSION	**MARKER**	**ALTERNATIVE NAME**	**CLONE**	**DILUTION**	**HOST**	**COMPANY**	**CATALOGUE NUMBER**
Leukocyte markers	Lymphocytes T	CD3	T-cell coreceptor	Polyclonal	1:2000	Rabbit	Abcam	ab16044
	Neutrophils, monocytes	CD11b	MAC-1/α-M integrin	EP1345Y	1:1000	Rabbit	Abcam	ab52478
	Monocytes, macrophages	CD14	LPS-receptor	4B4F12	1:500	Mouse	Abcam	ab182032

LCA: Leukocyte common antigen; **MAC-1**: Macrophage-1 Antigen

Supplemental table 4: Association between AV$^+$-EVs and biochemical parameters

	Leukocytes		Neutrophils		Monocytes	
	Spearman's Rho	P-value	Spearman's Rho	P-value	Spearman's Rho	P-value
Cell-origin markers						
CD3$^+$	0.041	0.664	0.118	0.451	-0.004	0.978
CD45$^+$	0.034	0.720	0.095	0.550	0.085	0.593
CD3$^+$/CD45$^+$	0.069	0.464	0.176	0.259	0.067	0.670
CD14$^+$	-0.057	0.543	0.101	0.517	0.062	0.695
CD15$^+$	0.025	0.789	0.222	0.152	-0.067	0.670
CD56$^+$	-0.033	0.727	-0.014	0.927	0.055	0.727
CD16$^+$	0.051	0.787	-0.248	0.354	-0.003	0.991
CD16$^+$/CD14$^+$	-0.244	0.202	-0.350	0.201	-0.163	0.561
Activation markers						
CD11b$^+$	0.037	0.695	0.146	0.349	-0.152	0.329
CD11b$^+$/CD14$^+$	-0.072	0.450	0.120	0.461	-0.101	0.535
CD29$^+$	0.033	0.724	-0.027	0.865	0.170	0.276
CD29$^+$/CD15$^+$	0.045	0.630	0.213	0.171	0.032	0.837

	C-Reactive Protein		NT-proBNP		High-sensitive troponin T	
	Spearman's Rho	P-value	Spearman's Rho	P-value	Spearman's Rho	P-value
Cell-origin markers						
CD3$^+$	-0.082	0.381	0.220	**0.016**	0.147	0.113
CD45$^+$	-0.118	0.212	-0.055	0.558	0.091	0.331
CD3$^+$/CD45$^+$	-0.096	0.311	0.252	**0.006**	0.217	**0.020**
CD14$^+$	-0.089	0.343	0.123	0.183	0.053	0.573
CD15$^+$	0.063	0.504	0.162	0.081	0.084	0.372
CD56$^+$	-0.024	0.800	0.082	0.378	-0.045	0.633
CD16$^+$	-0.086	0.646	0.034	0.853	0.098	0.599
CD16$^+$/CD14$^+$	-0.011	0.953	-0.031	0.867	-0.140	0.462
Activation markers						
CD11b$^+$	0.060	0.526	0.145	0.116	0.082	0.382
CD11b$^+$/CD14$^+$	-0.017	0.858	0.108	0.252	0.133	0.161
CD29$^+$	-0.059	0.527	0.028	0.765	0.038	0.687
CD29$^+$/CD15$^+$	0.040	0.668	0.175	0.057	0.162	0.082

AV$^+$: annexin V$^+$; **EVs**: extracellular vesicles; **NTproBNP**: N-terminal pro-hormone of brain natriuretic peptide

Supplemental table 5: Comparison of EVs levels according to disease severity and controls.

mean±SD	NYHA II	NYHA III-IV	CTLs	P-value NYHA II vs III-IV	P-value NYHA II vs CTLs	P-value NYHA III-IV vs CTLs
$CD3^+/AV^+$	2 [0-4]	4 [1.04-10]	0 [0-2]	**0.017**	**0.009**	**0.000**
$CD45^+/AV^+$	32 [16.55-44]	46 [26.6-64]	16 [8-34]	**0.011**	**0.003**	**0.000**
$CD3^+/CD45^+/AV^+$	0 [0-2]	2 [0-5.7]	0 [0-2]	**0.008**	0.100	**0.000**
$CD11b^+/AV^+$	9.75 [2.94-19.5]	17.1 [6-42]	4 [0-10]	**0.006**	**0.001**	**0.000**
$CD29^+/CD15^+/AV^+$	7.6 [2-18]	14 [3.8-32]	0 [0-2]	**0.048**	**0.000**	**0.000**

CTLs: controls; **NYHA**: New York Heart Association; **SD**: standard deviation

Supplemental table 6: ROC curve analysis for the discrimination of NYHA severity classification

	AUC±SD (95% CI)	P-value	Sensitivity	Specificity
$CD11b^+/AV^+$	0.648±0.050 (0.549-0.746)	**0.006**	0.627	0.615
$CD45^+/AV^+$	0.637±0.051 (0.536-0.738)	**0.011**	0.646	0.558
$CD3^+/CD45^+/AV^+$	0.636±0.051 (0.536-0.737)	**0.011**	0.615	0.596
$CD3^+/AV^+$	0.626±0.051 (0.526-0.726)	**0.019**	0.552	0.654
$CD29^+/CD15^+/AV^+$	0.606±0.052 (0.504-0.707)	**0.048**	0.597	0.577
Clustered $CD11b^+/AV^+$ and $CD45^+/AV^+$	0.658±0.050 (0.559-0.757)	**0.003**	0.662	0.615
Clustered $CD11b^+/AV^+$ and $CD3^+/CD45^+/AV^+$	0.635±0.051 (0.535-0.735)	**0.012**	0.585	0.596
NT-proBNP	0.676±0.050 (0.578-0.774)	**0.001**	0.672	0.655
High sensitivity Troponin T	0.611±0.052 (0.508-0.713)	**0.041**	0.606	0.529
Clustered $CD11b^+/AV^+$ and NT-proBNP	0.702±0.049 (0.607-0.797)	**0.000**	0.716	0.615
Clustered $CD45^+/AV^+$ and NT-proBNP	0.705±0.048 (0.610-0.799)	**0.000**	0.677	0.712
Clustered $CD3^+/CD45^+/AV^+$ with NT-proBNP	0.691±0.049 (0.596-0.787)	**0.000**	0.631	0.673
Clustered $CD11b^+/AV^+$, $CD45^+/AV^+$ and NT-proBNP	0.704±0.048 (0.609-0.798)	**0.000**	0.738	0.615
Clustered $CD11b^+/AV^+$, $CD3^+/CD15^+/AV^+$ and NT-proBNP	0.690±0.049 (0.594-0.786)	**0.000**	0.677	0.615

AUC: area under the curve; **CI**: confidence interval; **SD**: standard deviation; **NT-proBNP**: N-terminal pro-hormone of brain natriuretic peptide; **NYHA**: New York Heart Association

Supplemental table 7: Patient characteristics depending on ejection fraction classification

	HFpEF n=59	HFrEF n=60	P-value
DEMOGRAPHIC CHARACTERISTICS; mean±SD			
Male/Female, n	31/28	50/10	**0.000**
Age, years	71.1±9.6	63±12.5	**0.000**
Systolic blood pressure, mmHg	128.3±16.6	112.7±18.3	**0.000**
Diastolic blood pressure, mmHg	76.3±8.9	71.5±12.5	**0.007**
Left ventricular ejection fraction, %	63±9	28.47±6.2	**0.000**
RISK FACTORS; n (%)			
Smokers	7 (11.8)	6 (10)	0.744
Hypertension	48 (81.3)	34 (56.6)	**0.004**
Pulmonary hypertension	22 (37.2)	27 (45)	0.268
Diabetes mellitus	23 (38.9)	30 (50)	0.227
Dyslipidaemia	35 (59.3)	29 (48.3)	0.229
Chronic kidney disease	26 (44)	20 (33.3)	0.289
Atrial fibrillation	31 (52.5)	19 (31.6)	**0.025**
BACKGROUND MEDICATION; n (%)			
Angiotensin-converting-enzyme inhibitors	22 (37.2)	26 (43.3)	0.502
Angiotensin II receptor blockers	23 (38.9)	12 (20)	**0.023**
Beta-blockers	40 (67.7)	60 (100)	**0.000**
Aldosterone antagonists	17 (28.8)	49 (81.6)	**0.000**
Diuretics[†]	52 (88.1)	52 (86.6)	0.809
Angiotensin receptor neprilysin inhibitors	0 (0)	17 (28.3)	**0.000**
Ivabradine	2 (3.3)	12 (20)	**0.005**
Statins	36 (61)	41 (68.3)	0.404
Insulin	5 (8.4)	11 (18.3)	0.115
Anti-diabetic drugs	20 (33.8)	20 (33.3)	0.948
Antiplatelet agents	14 (23.7)	32 (53.3)	**0.001**
Anticoagulants	34 (57.6)	27 (45)	0.148
Anti-arrhythmic drugs	13 (22)	13 (21.6)	0.961

[†]Includes: furosemide, hydrochlorothiazide, torasemide and indapamide.

HFpEF: heart failure with preserved ejection fraction; **HFrEF**: heart failure with reduced ejection fraction; **SD**: standard deviation

Supplementary Material

Supplemental table 8: Clinical characteristics of patients at baseline

	HFpEF n=59	HFrEF n=60	P-value
CLINICAL HISTORY; n (%)			
cHF aetiology			
Ischaemic	14 (23.7)	29 (48.3)	**0.005**
Non-ischaemic	45 (76.2)	31 (51.6)	
Hypertensive cardiomyopathy	16 (27.1)	3 (5)	**0.001**
Dilated cardiomyopathy	0 (0)	24 (40)	**0.000**
Hypertrophic cardiomyopathy	12 (20)	0 (0)	**0.001**
Heart valve disease	13 (22)	4 (6.6)	**0.017**
Other	4 (6.7)	0 (0)	**0.040**
New York Heart Association cHF stage			
NYHA I	0 (0)	0 (0)	1.000
NYHA II	25 (42.3)	27 (45)	0.773
NYHA III	34 (57.6)	32 (53.3)	0.637
NYHA IV	0 (0)	1 (1.6)	0.319
Hospitalisations in the 6 months prior study initiation	26 (44)	23 (38.3)	0.420
Re-events in the year prior study initiation	2 (3.3)	7 (11.6)	0.088
Percutaneous coronary intervention	0 (0)	4 (57.1)	0.151
Coronary artery bypass grafting	1 (50)	1 (14.3)	0.284
Medical treatment	1 (50)	2 (28.6)	0.571
BIOCHEMISTRY; mean±SD			
Haemoglobin, mg/dl	126.2±17.7	133.4±18.7	0.060
Creatinine, mg/dl	1.39±0.58	1.29±0.49	0.427
C-Reactive Protein, mg/ml	9.2±13.9	6.1±6.8	0.185
NT-proBNP, pg/ml	2782.6±4712.2	3124.1±3685.5	0.113
High-sensitive troponin T, ng/l	26.6±22.1	28.9±19.8	0.371
Erythrocytes, 10^6/mm^3	3.86±0.64	4.1±0.81	0.052
Platelets, 10^3/mm^3	168.9±49.6	177.4±63.4	0.462
Leukocytes, mm^3	7191±1744.8	7661.03±2124.9	0.377
Neutrophils, 10^9/L	4.39±1.09	5.03±1.79	0.133
Monocytes, 10^9/L	0.67±0.2	0.82±0.69	0.651

HFpEF: heart failure with preserved ejection fraction; **HFrEF**: heart failure with reduced ejection fraction; **NT-proBNP**: N-terminal pro-hormone of brain natriuretic peptide; **NYHA**: New York Heart Association; **SD**: standard deviation

Supplemental table 9: Follow-up outcome

MAJOR OUTCOMES DURING FOLLOW-UP; n (%)	HFpEF n=59	HFrEF n=60	P-value
Cardiovascular event†	11 (18.6)	15 (25)	0.402
Stroke	3 (5)	5 (8.3)	0.479
Aortic dissection	1 (1.6)	0 (0)	0.311
AMI + Cardiogenic shock	1 (1.6)	2 (3.3)	0.569
HTx/HTx waiting list	3 (5)/0 (0)	7 (11.6)/1 (1.6)	0.196/0.319
CV death	3 (5)	4 (6.6)	0.714
Emergency hospital admission for cHF	7 (11.8)	9 (15)	0.616
Rehospitalisation	29 (49.1)	28 (46.6)	0.786
Aortic aneurism	1 (1.6)	0 (0)	0.311
Other death causes‡	7 (11.8)	3 (5)	0.177

†Includes patients that suffered a stroke, an aortic dissection, an AMI, a cardiogenic shock, a CV death (mainly due to cHF) or were admitted to the emergency department. It does not include patients that underwent a HTx.

‡Includes patients that died due to a septic shock, a haemorrhage or a non-successful HTx.

AMI: acute myocardial infarction; **CV**: cardiovascular; **HFpEF**: heart failure with preserved ejection fraction; **HFrEF**: heart failure with reduced ejection fraction; **HTx**: heart transplantation

Supplementary Material

Supplemental table 10: ROC curve analysis for the discrimination of NYHA severity classification in ischaemic patients.

	AUC±SD (95% CI)	P-value	Sensitivity	Specificity
$CD11b^+/AV^+$	0.848±0.058 (0.734-0.961)	**0.000**	0.800	0.722
$CD29^+/CD15^+/AV^+$	0.811±0.065 (0.683-0.939)	**0.001**	0.760	0.722
$CD3^+/AV^+$	0.723±0.077 (0.573-0.873)	**0.013**	0.640	0.556
$CD45^+/AV^+$	0.714±0.081 (0.555-0.874)	**0.019**	0.667	0.778
$CD3^+/CD45^+/AV^+$	0.700±0.083 (0.537-0.864)	**0.029**	0.652	0.667
$CD11b^+/CD14^+/AV^+$	0.661±0.085 (0.493-0.828)	0.081	0.522	0.778
Clustered $CD11b^+/AV^+$ and $CD29^+/CD15^+/AV^+$	0.858±0.056 (0.747-0.968)	**0.000**	0.800	0.833
Clustered $CD11b^+/AV^+$ and $CD3^+/AV^+$	0.857±0.057 (0.746-0.968)	**0.000**	0.760	0.833
Clustered $CD29^+/CD15^+/AV^+$ and $CD3^+/AV^+$	0.812±0.065 (0.686-0.939)	**0.001**	0.760	0.722
NT-proBNP	0.816±0.071 (0.676-0.955)	**0.000**	0.800	0.722
High sensitivity Troponin T	0.640±0.082 (0.472-0.808)	0.127	0.600	0.588
Clustered $CD11b^+/AV^+$ and NT-proBNP	0.849±0.057 (0.737-0.961)	**0.000**	0.760	0.778
Clustered $CD29^+/CD15^+/AV^+$ with NT-proBNP	0.809±0.065 (0.681-0.937)	**0.001**	0.800	0.667
Clustered $CD3^+/AV^+$ and NT-proBNP	0.700±0.079 (0.545-0.855)	**0.027**	0.680	0.556
Clustered $CD11b^+/AV^+$, $CD29^+/CD45^+/AV^+$ and NT-proBNP	0.858±0.056 (0.747-0.968)	**0.000**	0.800	0.833
Clustered $CD11b^+/AV^+$, $CD3^+/AV^+$ and NT-proBNP	0.853±0.057 (0.741-0.965)	**0.000**	0.760	0.833

AUC: area under the curve; **CI**: confidence interval; **SD**: standard deviation; **NT-proBNP**: N-terminal pro-hormone of brain natriuretic peptide; **NYHA**: New York Heart Association

Supplemental table 11: EVs levels according myocardial infarction elapsed time in ischaemic cHF.

median [IQR]	AMI >1year before sample acquisition	AMI <1year before sample acquisition	P-value
$CD3^+/AV^+$	4.8 [1-13.8]	4 [1.47-13.42]	0.939
$CD45^+/AV^+$	45.8 [38.8-140]	38 [22-58]	0.337
$CD3^+/CD45^+/AV^+$	3.85 [1-5.85]	1.95 [0-6]	0.741
$CD11b^+/AV^+$	17.55 [15.55-24]	12 [6-40.92]	0.546
$CD14^+/AV^+$	2 [0-5.8]	3.8 [1.9-8]	0.335
$CD11b^+/CD14^+/AV^+$	0 [0-0]	0 [0-2]	0.093
$CD29^+/AV^+$	54 [31-91.75]	70.56 [44-135.45]	0.378
$CD15^+/AV^+$	36.6 [18-58.6]	26.49 [2-84]	0.755
$CD29^+/CD15^+/AV^+$	20 [11-32.05]	16.55 [2-37]	0.781
$CD56^+/AV^+$	4.85 [3-9.85]	8.75 [3.3-17.55]	0.378
$CD16^+/AV^+$	28 [28-28]	4.68 [4-15.56]	0.170
$CD16^+/CD14^+/AV^+$	0 [0-0]	0 [0-0]	0.684

AMI: acute myocardial infarction; **IQR**: interquartile range

3.1 Supplementary Figures

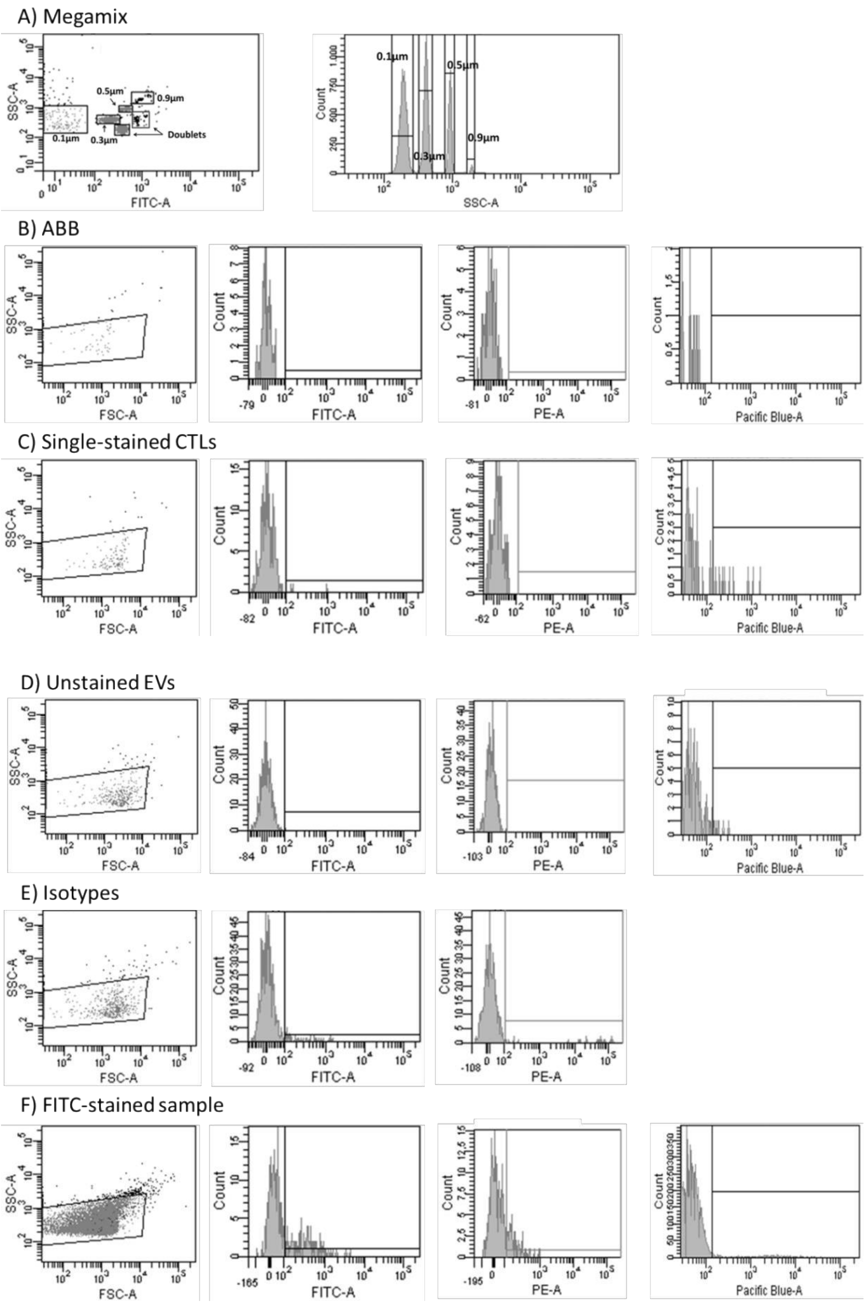

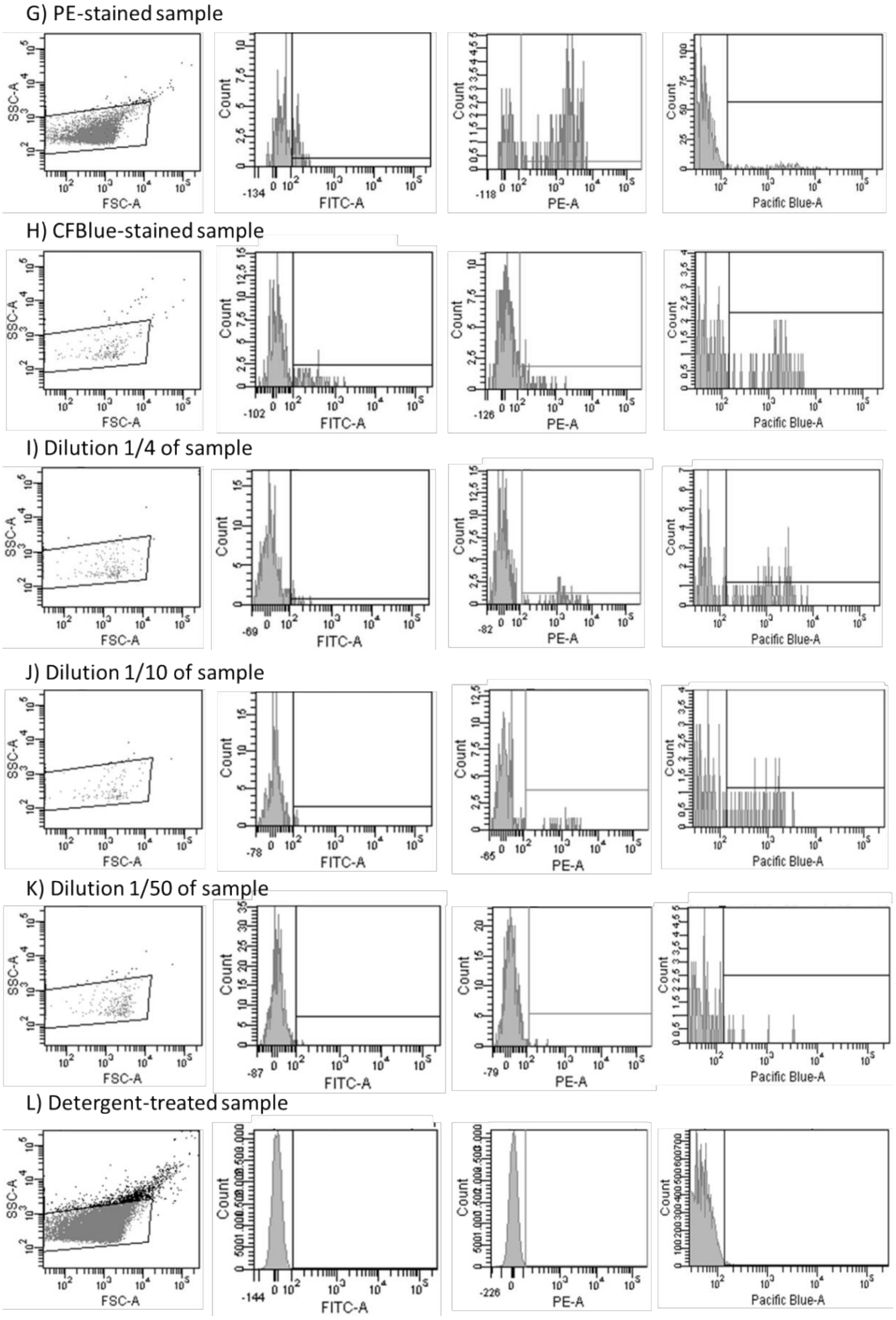
G) PE-stained sample
H) CFBlue-stained sample
I) Dilution 1/4 of sample
J) Dilution 1/10 of sample
K) Dilution 1/50 of sample
L) Detergent-treated sample
SSC-A
FSC-A
Count
FITC-A
PE-A
Pacific Blue-A

Supplementary Material

Supplemental Figure 1: **Flow cytometry controls for EVs analysis**. Representative FSC/SSC dot plots, and CFBlue (in the Pacific Blue channel), FITC and PE histograms of: **(A)** Megamix-Plus FSC beads; **(B)** Annexin Binding Buffer (ABB) only; **(C)** ABB with FITC-, PE-labelled antibodies and FCBlue-labelled Annexin V; **(D)** Unstained EVs; **(E)** FITC- and PE-labelled isotype controls; **(F)** FITC-stained sample; **(G)** PE-stained sample; **(H)** CFBlue-stained sample; **(I)** Dilution 1/4 of sample; **(J)** Dilution of 1/10 of sample; **(K)** Dilution of 1/50 of sample; **(L)** Detergent treated EVs sample (saponin 5% treatment in EVs-labelled with a FITC- and PE-antibody, as well as with FCBlue-labelled Annexin V). Note that the scale of the x axis in Pacific Blue histograms differs slightly from the x axis of FITC and PE histograms.

frontiers

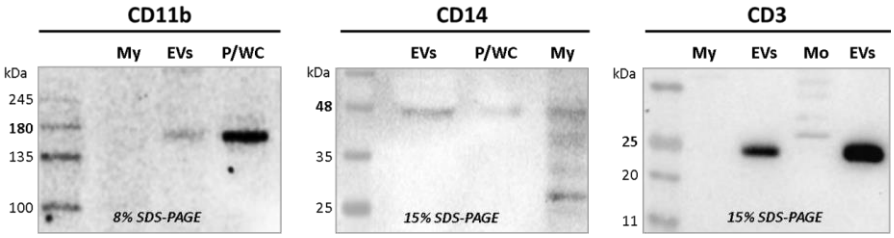

Supplemental Figure 2: **SDS-PAGE analysis to validate the markers determined by flow cytometry.** CD11b is expressed on the surface of many leukocytes (including monocytes, neutrophils, natural killer cells, granulocytes and macrophages) and it is found in P/WC extracts containing white cells and also in the EVs isolated from cHF patients' blood, but not in our control myocardium; CD14 (produced mostly by macrophages as part of the innate immune system) is found in the EVs, in less amount in the myocardium and in the control extract; CD3 (protein complex and T cell co-receptor that is involved in activating both cytotoxic T cell and T helper cells) is found in the EVs and not in the myocardial tissue or in monocytes.

EVs: extracellular microvesicles; **Mo**: monocytes; **My**: myocardium; **P/WC**: platelet-white blood cells extract

Supplementary Material

4 MiFlowCyt-EV: Author checklist

FRAMEWORK CRITERIA	COMPLETED CRITERIA
1.1 Preanalytical variables conforming to MISEV guidelines	Blood was collected from 119 chronic heart failure (cHF) individuals and 60 controls in 5ml 0.109M citrated plastic tubes (BD Vacutainer, Becton Dickinson) via antecubital vein puncture using a 20-gauge needle. Tubes were transported vertically at room temperature (RT). Within 2 hours of blood withdrawal; platelet-depleted plasma was prepared by centrifugation (Eppendorf 5810R GLOOB04932 centrifuge, A-4-81 rotor, Eppendorf) at 1,560g for 20 minutes at 20ºC. A second centrifugation was then pursued (Eppendorf 5415R centrifuge, FA45-24-11 rotor, Eppendorf) at 1,500g for 10 minutes at 20ºC. The first centrifugation step was done with 4.5mL whole blood in the 5mL 0.109M citrated plastic tubes (BD Vacutainer, Becton Dickinson). Supernatant was collected 1mm above the buffy coat. The second centrifugation step was pursued with 650µl platelet-depleted plasma in 1.5mL Eppendorf tubes (Thermo Fisher Scientific). 300µl x2 aliquots of platelet-depleted plasma were transferred to 1.5mL low-protein binding Eppendorf tubes (Thermo Fisher Scientific) and snap-frozen in liquid nitrogen before being stored at −80 °C.
1.2 Experimental design according to MIFlowCyt guidelines	**1.1 Aim**: To compare the concentration of EVs from different parental origin in platelet-free plasma between individuals with cHF and age-, sex- and risk factor-matched controls without cHF. We hypothesise that the concentration of immune-derived EVs will be increased in individuals with cHF, as cHF has been associated with chronic and non-resolving inflammation. **1.2 Keywords**: EVs; extracellular microvesicles, cHF; chronic heart failure; innate and immune cells, inflammation **1.3 Experimental variables**: EVs from 119 individuals with cHF and 60 non-cHF controls. There was no significant difference in age, sex or smoking-status between individuals with and without cHF. Scatter-based triggering was used for the detection of particles.
2.1 Sample staining details	The presence of EVs was determined using parental-cell specific antibody staining. 5µl of EVs suspension was diluted in 30µl of filtered PBS (through 0.22µm pores) containing 2.5mM of $CaCl_2$ (Annexin Binding Buffer [ABB], BD Biosciences, San José) and stained with 5µl of a FITC-conjugated antibody, 5µl of a PE-conjugated antibody and 5µl of CFBlue-conjugated annexin V (please see **Supplemental Table 3** for an overview of the antibodies/reagents and concentrations used) for 20 minutes at 20ºC and protected from light. Matched isotype controls, were incubated in the same conditions and concentration as the labelling antibodies.
2.2 Sample washing details	EVs isolated by a two-step centrifugation were resuspended in PBS-0.32% citrated buffer, previously filtrated in 0.22µm-pore filters. The isolation was pursued by centrifuging (Eppendorf 5417R centrifuge, FA45-24-11 rotor, Eppendorf) the samples at 20,000g for 30 minutes at 20ºC, washing the pellet with PBS-0.32% citrated buffer and re-centrifuging the samples at 20,000g for 30 minutes at 20ºC. Supernatant was discarded and the pellet with EVs was resuspended to a total volume of 100µl of filtered PBS-0.32% citrated buffer.

frontiers

FRAMEWORK CRITERIA	COMPLETED CRITERIA
	Thus, EV samples were washed before staining. Antibody labelling of EVs was stopped by diluting ten times the sample with buffer prior to FACS acquisition.
2.3 Sample dilution details	5µL of EV suspension was added to 15µL of reagents and 35µL of ABB (filtered PBS containing 2.5mM of $CaCl_2$), resulting in a 10-fold dilution. This 10-fold dilution was then diluted 10 times, with 50µL of sample added to 450µL of filtered ABB. EV concentration was semi-quantitatively estimated according to Nieuwland's formula(2) based on sample's volume (taking into account these dilutions), flow cytometer's flow rate and the number of fluorescence-positive events as described in **Methods** section.
3.1 Buffer alone controls	A buffer-only control of 0.22µm-filtered ABB (PBS containing 2.5mM of $CaCl_2$) was recorded at the same flow cytometer, with identical acquisition settings as all other samples, including triggering threshold, voltages, flow rate and acquisition time.
3.2 Buffer with reagent controls	A buffer with reagent control mimicking each of the used antibodies concentrations was recorded at the same flow cytometer and acquisition settings as all other samples, including triggering threshold, voltages, flow rate and acquisition time.
3.3 Unstained controls	Unstained controls were measured at the same dilution, as matched stained and isotype controls. Flow cytometer acquisition settings were maintained for all samples, including triggering threshold, voltages, flow rate and acquisition time.
3.4 Isotype controls	Isotype controls were used at the same concentration as matched stained controls and were recorded at the same dilution as matched stained and unstained controls and stained samples. Flow cytometer acquisition settings were maintained for all samples, including triggering threshold, voltages, flow rate and acquisition time.
3.5 Single-stained controls	Single-stained controls of all used antibodies/CFBlue-conjugated annexin (see **Supplemental Table 3**) were analysed to aid compensation of used antibodies in the FITC, PE and Pacific Blue channels when excited by the 488nm laser.
3.7 Serial dilutions	Samples were serially diluted 4 times, with the sample diluted 1/4, 1/10 and 1/50 in 0.22µm-filtered ABB.
3.8. Detergent treated EV-samples	Stained samples, diluted 100-fold, were treated with 5% saponin for 20 min at 20°C to test the lability of the used antibodies and annexin V.
4.1 Trigger Channel(s) and Threshold(s)	Based on the buffer alone control, detection was triggered on the 488nm laser excited FITC channel and the 405nm laser excited by Pacific Blue, determined using CTS beads (Becton Dickinson, Franklin Lakes, NJ, USA).
4.2 Flow Rate / Volumetric quantification	Flow rate was calculated by the mass discharge method and considered constant throughout the analysis (~20µL/min). The FACSCantoII "low flow" rate mode was used in all analyses.
4.3 Fluorescence Calibration	NA Cytometer CST beads (Becton Dickinson, Franklin Lakes, NJ, USA) controls to check cytometer performance were analysed each day. Megamix Plus FSC beads (BioCytex, Marseille, France), were also run to determine EVs size gates. Nevertheless, because our analysis only required a positive/negative epitope discrimination, standardisation of the strength/intensity of florescence was not

Supplementary Material

FRAMEWORK CRITERIA	COMPLETED CRITERIA
	implemented in this study.
4.4 Light Scatter Calibration	Cytometer CSTs (Becton Dickinson, Franklin Lakes, NJ, USA) controls to check flow cytometer performance were analysed each working day. Megamix Plus FSC beads (BioCytex, Marseille, France) were also run to determine and establish EVs size gate.
5.1 EV diameter/surface area/volume approximation	NA
5.2 EV refractive index approximation	NA
5.3 EV epitope number approximation	NA
6.1 Completion of MIFlowCyt checklist	Completed MIFlowCyt checklist file has been included.
6.2 Calibrated channel detection range	NA
6.3 EV number/concentration	EVs number was calculated following Nieuwland's formula(2), which takes into consideration sample's volume, flow cytometer's flow rate and the number of fluorescence-positive events (N), as follows: EVs/µl = N x (Vf/Va) x (Vt/FR) x (1/Vi), where Vf(µl)=final volume of washed EVs suspension, Va(µl)=volume of washed EVs suspension used for each labelling analysis, Vt(µl)=volume of EVs suspension before fluorescence-activated cell sorting analysis, FR(µl/min)=flow rate of the cytometer at low mode (the average volume of EVs suspension analysed in 1min), 1 is the µl unit of volume, and Vi(µl)=original volume of plasma used for EVs isolation.
6.4 EV brightness	NA

frontiers

5 MiFlowCyt: Compliant checklist

REQUIREMENT	COMPLETED CRITERIA
1.1. Purpose	To compare the concentration of EVs from different parental origin in platelet-free plasma between individuals with cHF and age-, sex- and risk factor-matched controls without cHF. We hypothesise that the concentration of immune-derived EVs will be increased in individuals with cHF, as cHF has been associated with chronic and non-resolving inflammation.
1.2. Keywords	Extracellular microvesicles, chronic heart failure; immune cells, inflammation
1.3. Experiment variables	EVs from 119 individuals with cHF and 60 non-cHF controls. There was no significant difference in age, sex or smoking-status between individuals with and without cHF. Scatter-based triggering was used for the detection of particles.
1.4. Organization name and address	Cardiovascular Program-ICCC Institut de Recerca de l'Hospital de la Santa Creu i Sant Pau Sant Antoni Maria Claret 167 08025 Barcelona Spain
1.5. Primary contact name and email address	Prof. Lina Badimon lbadimon@santpau.cat
1.6. Date or time period of experiment	10/01/2018 – 12/09/2019
1.7. Conclusions	cHF patients present increased levels of immune-derived EVs, which in addition correlate with severity, compared to non-cHF controls.
1.8. Quality control measures	Implemented quality control measures were cytometer CST beads (Becton Dickinson, Franklin Lakes, NJ, USA), which were run every working day to verify flow cytometer performance. Megamix Plus FSC beads (BioCytex, Marseille, France), were run each working day to determine EVs size gates.
2.1.1.1. Sample description	Washed EVs isolated from platelet-free plasma of cHF and non-cHF individuals.
2.1.1.2. Biological sample source description	Platelet-free plasma of cHF and non-cHF individuals.
2.1.1.3. Biological sample source organism description	Human
2.1.2.2. Environmental sample location	NA
2.3. Sample treatment description	EVs isolated by a two-step centrifugation were resuspended in PBS-0.32% citrated buffer, previously filtrated in 0.22µm-pore filters. The isolation was pursued by centrifuging (Eppendorf 5417R centrifuge, FA45-24-11 rotor, Eppendorf) the samples at 20,000g

Supplementary Material

REQUIREMENT	COMPLETED CRITERIA
	for 30 minutes at 20ºC, washing the pellet with PBS-0.32% citrated buffer and re-centrifuging the samples at 20,000g for 30 minutes at 20ºC. Supernatant was discarded and the pellet with EVs was resuspended to a total volume of 100µl of filtered PBS-0.32% citrated buffer.
2.4. Fluorescence reagent(s) description	EVs were triple-labelled with a combination of 3 fluorochromes, two corresponding to FITC- and PE-conjugated antibodies and the third one to FCBlue-conjugated annexin V, respectively. Used reagents are listed and characterised in **Supplemental Table 3**.
3.1. Instrument manufacturer	Becton Dickinson
3.2. Instrument model	FACSCantoII™
3.3. Instrument configuration and settings	EVs gating was optimised for detection as previously described(3–5). Additional information is included in this **Supplementary material**.
4.1. List-mode data files	NA Despite data has not been uploaded to a public repository, it will be available upon request to the authors.
4.2. Compensation description	Single-stained controls of all used antibodies/CFBlue-conjugated annexin (see **Supplemental Table 3**) were analysed to aid compensation of used antibodies in the FITC, PE and Pacific Blue channels when excited by the 488nm laser.
4.3. Data transformation details	NA Data transformation was not applied. Data from .cfs files were analysed by statistical software (SPSS version 26.0, IBM Corp. Armonk, NY).
4.4.1. Gate description	How gates were established and specific examples can be found in **Supplemental Figure 1**.
4.4.2. Gate statistics	Plots show the total number of events recorded for 1 minute at “low mode” flow rate.
4.4.3. Gate boundaries	More information and images can be found in **Supplemental Figure 1**.

6 Supplementary references

1. Lugano R, Peña E, Badimon L, Padró T. Aggregated low-density lipoprotein induce impairment of the cytoskeleton dynamics through urokinase-type plasminogen activator/urokinase-type plasminogen activator receptor in human vascular smooth muscle cell. J Thromb Haemost. 2012 Oct;10(10):2158–67.

2. Nieuwland R, Berckmans RJ, McGregor S, Böing AN, Romijn FPHTM, Westendorp RGJ, et al. Cellular origin and procoagulant properties of microparticles in meningococcal sepsis. Blood. 2000 Feb 1;95(3):930–5.

3. Suades R, Padró T, Vilahur G, Badimon L. Circulating and platelet-derived microparticles in human blood enhance thrombosis on atherosclerotic plaques. Thromb Haemost. 2012;108(6):1208–19.

4. Suades R, Padró T, Crespo J, Ramaiola I, Martin-Yuste V, Sabaté M, et al. Circulating microparticle signature in coronary and peripheral blood of ST elevation myocardial infarction patients in relation to pain-to-PCI elapsed time. Int J Cardiol. 2016 Jan 1;202:378–87.

5. Sionis A, Suades R, Sans-Roselló J, Sánchez-Martínez M, Crespo J, Padró T, et al. Circulating microparticles are associated with clinical severity of persistent ST-segment elevation myocardial infarction complicated with cardiogenic shock. Int J Cardiol. 2018 May 1;258:249–58.

ARTICLE 2

Systems Biology in Chronic Heart Failure – Identification of Potential miRNA Regulators

Alba Vilella-Figuerola; Alex Gallinat; Rafael Escate; Sònia Mirabet; Teresa Padró*; Lina Badimon*
*Contributed equally to this work.

PUBLISHED: International Journal of Molecular Sciences

Int. J. Mol. Sci. 2022, 23 (23), 15226, doi.org/10.3390/ijms232315226

OBJECTIVE: Identification and characterisation of the microRNA-pattern in chronic heart failure patients (CHF) patients and study their role in the pathophysiology of this disease.

HIGHLIGHTS:

- A downregulated profile of 8 microRNAs (miRNAs) is identified and validated in CHF patients in comparison to subjects without this disease.
- miRNAs *let-7a-5p*, *miR-107*, *miR-125a-5p*, *miR-139-5p*, *miR-150-5p*, *miR-30b-5p* and *miR-342-3p* define 7 clusters and work cooperatively in pathways related to cell cycle, and RAS, PI3K-AKT, TGF-β and chemokine signalling.
- Combinations of miRNAs *let-7a-5p*, *miR-107*, *miR-125a-5p*, *miR-139-5p*, *miR-150-5p*, *miR-30b-5p* and *miR-342-3p* (included in clusters 1–4) discriminate between HFpEF and HFrEF, and between ischaemic and non-ischaemic CHF.
- Combinations of miRNAs *miR-107*, *miR-139-5p* and *miR-150-5p* (included in clusters 5+7) discriminate between HFpEF and HFrEF.
- miRNAs *miR-107*, *miR-139-5p* and *miR-150-5p* are involved in pathways related to focal adhesions, ubiquitin-mediated proteolysis, and RAS, PI3K-AKT, TGF-β, NOTCH, Wnt, Hippo, thyroid hormone and cytokine signalling. Pathways specifically related to these miRNAs were involved in cardiomyopathy development (hypertrophic, dilated and arrhythmogenic), aldosterone-regulated sodium reabsorption, vascular SMCs contraction and leukocyte migration.
- miRNAs *let-7a-5p*, *miR-125a-5p*, *miR-30b-5p* and *miR-342-3p* (not included in clusters with discriminative power) are involved in pathways related to cellular senescence, EGFR tyrosine kinase inhibitor and endocrine resistance, as well as with prolactin, PI3K-AKT, ErbB, TGF-β and JAK-STAT signalling. Pathways

specifically related to these miRNAs were involved in metabolism (glucagon signalling, lipolysis regulation and carbohydrate digestion and absorption) and inflammation (inflammatory mediator regulation of TRP channels).

- *miRNA-139-5p* and *miRNA-107* are overrepresented in the generated clusters and participate in the MAPK and PI3K-AKT signalling.
- *miRNA-139-5p* individually discriminates between ischaemic and non-ischaemic CHF.

International Journal of *Molecular Sciences*

MDPI

Article

Systems Biology in Chronic Heart Failure—Identification of Potential miRNA Regulators

Alba Vilella-Figuerola [1,2], Alex Gallinat [1,2], Rafael Escate [1,3], Sònia Mirabet [3,4], Teresa Padró [1,3,†] and Lina Badimon [1,3,5,*,†]

1 Cardiovascular-Program-ICCC, IR-Hospital Santa Creu i Sant Pau, IIB-Sant Pau, 08025 Barcelona, Spain
2 Biochemistry and Molecular Biology Department, Universitat Autònoma de Barcelona (UAB), 08193 Cerdanyola del Vallès, Spain
3 Centro de Investigación Biomédica en Red Cardiovascular (CIBER-CV), Instituto de Salud Carlos III, 28029 Madrid, Spain
4 Heart Failure Group, Cardiology Department, Hospital Santa Creu i Sant Pau, 08025 Barcelona, Spain
5 Chair Cardiovascular Research, Universitat Autònoma de Barcelona (UAB), 08025 Barcelona, Spain
* Correspondence: lbadimon@santpau.cat; Tel.: +34-935-565-882; Fax: +34-935-565-559
† These authors contributed equally to this work.

Abstract: Heart failure (HF) is a complex disease entity with high clinical impact, poorly understood pathophysiology and scantly known miRNA-mediated epigenetic regulation. We have analysed miRNA patterns in patients with chronic HF (cHF) and a sex- and age-matched reference group and pursued an in silico system biology analysis to discern pathways involved in cHF pathophysiology. Twenty-eight miRNAs were identified in cHF that were up-regulated in the reference group, and eight of them were validated by RT-qPCR. In silico analysis of predicted targets by STRING protein-protein interaction networks revealed eight cluster networks (involving seven of the identified miRNAs) enriched in pathways related to cell cycle, Ras, chemokine, PI3K-AKT and TGF-β signaling. By ROC curve analysis, combined probabilities of these seven miRNAs (*let-7a-5p*, *miR-107*, *miR-125a-5p*, *miR-139-5p*, *miR-150-5p*, *miR-30b-5p* and *miR-342-3p*; clusters 1–4 [C:1–4]), discriminated between HF with preserved ejection fraction (HFpEF) and HF with reduced ejection fraction (HFrEF), and ischaemic and non-ischaemic aetiology. A combination of *miR-107*, *miR-139-5p* and *miR-150-5p*, involved in clusters 5 and 7 (C:5+7), discriminated HFpEF from HFrEF. Pathway enrichment analysis of miRNAs present in C:1–4 (*let-7a-5p*, *miR-125a-5p*, *miR-30b-5p* and *miR-342-3p*) revealed pathways related to HF pathogenesis. In conclusion, we have identified a differential signature of down-regulated miRNAs in the plasma of HF patients and propose novel cellular mechanisms involved in cHF pathogenesis.

Keywords: miRNA; chronic heart failure; network; enrichment pathways; pathophysiology

check for updates

Citation: Vilella-Figuerola, A.; Gallinat, A.; Escate, R.; Mirabet, S.; Padró, T.; Badimon, L. Systems Biology in Chronic Heart Failure—Identification of Potential miRNA Regulators. *Int. J. Mol. Sci.* **2022**, *23*, 15226. https://doi.org/10.3390/ijms232315226

Academic Editors: Michael T. Chin and Claudio de Lucia

Received: 11 October 2022
Accepted: 1 December 2022
Published: 3 December 2022

1. Introduction

Heart failure (HF), affecting 1–2% of the world's population over the age of 65, is one of the leading causes of mortality and morbidity [1,2]. It is a complex disease where the heart is unable to meet the metabolic demands of the body [3,4]. Chronic HF (cHF) has several underlying aetiologies (ischaemic disease, dilated cardiomyopathy, hypertrophy cardiomyopathy, hypertension, heart valve disease, etc.) that produce alterations in heart structure (left ventricle hypertrophy or dilation, cardiac fibrosis, heart remodelling) and function (abnormal cardiac output, diastolic dysfunction), leading to common symptomatology [3]. The underlying pathological mechanisms that conduce to cHF are not completely understood, but several biological pathways are involved in the progression of the disease [5].

Plasma sample analysis allows the easy acquisition of biologic material, such as microRNAs (miRNAs) that may assist in disease characterisation and patient risk stratification.

Further, some plasma miRNAs provide prognosis information [6–8] (such as HF development after AMI [6]), or help in disease diagnosis [9,10], (as biomarkers of childhood dilated cardiomyopathy [9]). miRNAs are short RNA sequences (18–22 nucleotides long) that are involved in the regulation and control of RNA expression [11]. Given their role as transcriptional regulators, miRNAs are being thoroughly studied in several conditions [12]. Because of their stability and accessibility in blood, there is a great interest to determine the miRNA role in HF.

Some miRNAs have been related to cardiovascular (CV) disease pathogenesis [13,14] and the potential of others (e.g., *miR-423-5p*) as biomarkers for HF has been explored [15]. In that sense, we have previously determined that, in familial hypercholesterolaemia patients, up-regulated expression of miRNA *miR-133a* was associated with CV disease clinical event presentation. Further, we detected that this miRNA was mechanistically associated with atherosclerosis development [16]. Using a similar approach, we have investigated whether plasma miRNAs could show a differential pattern of expression in patients with cHF. Further, we performed an *in silico* systems biology analysis to predict protein targets of the identified differential miRNA signature and highlight those proteins involved in biological processes and molecular pathways with a higher probability to contribute to the pathophysiology of chronic heart failure.

2. Results

2.1. Differential miRNA Signature in cHF

We comparatively analysed the plasma levels of 377 miRNAs in cHF patients and reference subjects (RS). Of these 377 miRNAs, 167 were consistently detected in both groups. Differential expression analyses between cHF and RS showed that 28 of these miRNAs presented statistically significant differences and a fold-change ($\log_2$) higher than ± 0.38 between groups. Of these, the top 15 miRNAs presenting an area under the curve (AUC) ≥ 0.7 after C-statistics analysis and a fold-change >1.7 (0.75 in $\log_2$) were selected for further analysis. Three of the top-fifteen miRNAs were of the same family (*let-7a-5p*, *let-7f-5p* and *let-7g-5p*) and have been reported to be involved in the regulation of common pathways [17]. Therefore, only miRNA *let-7a-5p*, with the best AUC among them, was further analysed. In addition, and considering the probability of a low detection level, we excluded those miRNAs that according to miRBase presented a number of reads in the lowest 25% range (Figure 1 and Supplemental Table S1).

Thus, nine miRNAs (*let-7a-5p*, *miR-107*, *miR-125a-5p*, *miR-139-5p*, *miR-150-5p*, *miR-224-5p*, *miR-30b-5p*, *miR-335-5p* and *miR-342-3p*) were further selected for validation. Additionally, we selected two miRNAs (*miR-16-5p* and *miR-223-3p*) that had similar expression values between groups as negative controls.

These selected miRNAs were further validated by RT-qPCR using customised cards in larger cHF (n = 46) and RS (n = 26) groups. Differences between groups reached statistical power in eight miRNAs (*let-7a-5p*, *miR-107*, *miR-125a-5p*, *miR-139-5p*, *miR-150-5p*, *miR-30b-5p*, *miR-335-5p* and *miR-342-3p*), being all down-regulated in cHF compared to RS. Differential expression of *miR-224-5p*, although showing a similar trend, did not reach statistical significance. Negative controls (*miR-16-5p* and *miR-223-3p*) maintained similar expression between groups (Figure 2 and Supplemental Table S2).

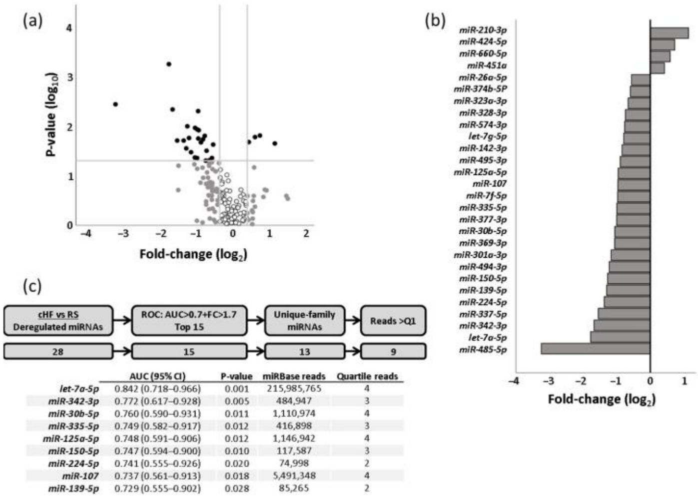

	AUC (95% CI)	P-value	miRBase reads	Quartile reads
let-7a-5p	0.842 (0.718–0.966)	0.001	215,985,765	4
miR-342-3p	0.772 (0.617–0.928)	0.005	484,947	3
miR-30b-5p	0.760 (0.590–0.931)	0.011	1,110,974	4
miR-335-5p	0.749 (0.582–0.917)	0.012	416,898	3
miR-125a-5p	0.748 (0.591–0.906)	0.012	1,146,942	4
miR-150-5p	0.747 (0.594–0.900)	0.010	117,587	3
miR-224-5p	0.741 (0.555–0.926)	0.020	74,998	2
miR-107	0.737 (0.561–0.913)	0.018	5,491,348	4
miR-139-5p	0.729 (0.555–0.902)	0.028	85,265	2

Figure 1. miRNA profiling in cHF patients and reference subjects. (**a**) miRNA profiling as a dot plot in a Cartesian graph. *x*-axis represents $\log_2$ (fold-change) and *y*-axis represents $\log_{10}$ (median concentration *p*-value). miRNAs with 1.3-fold changes in concentration level (greater than 0.38 [$\log_2$ (1.3)] and less than 0.38 [$\log_2$ (1/1.3)]) and significant *p*-value are shown in solid black dots. miRNAs with 1.3-fold changes in concentration level (greater than 0.38 [$\log_2$ (1.3)] and less than 0.38 [$\log_2$ (1/1.3)]) but non-significant *p*-value are shown in solid grey dots. miRNAs with less than 1.3-fold changes in concentration level (lower than 0.38 [$\log_2$ (1.3)] and higher than 0.38 [$\log_2$ (1/1.3)]) and non-significant *p*-value are shown in black circles. (**b**) Bar graph indicating changes in the expression of miRNAs between patients and reference subjects. (**c**) Schematic workflow for miRNA selection. AUC: area under the curve; cHF: chronic heart failure; FC: fold-change; Q1: first (lowest) quartile; RS: reference subjects; ROC: receiver operating characteristic curve.

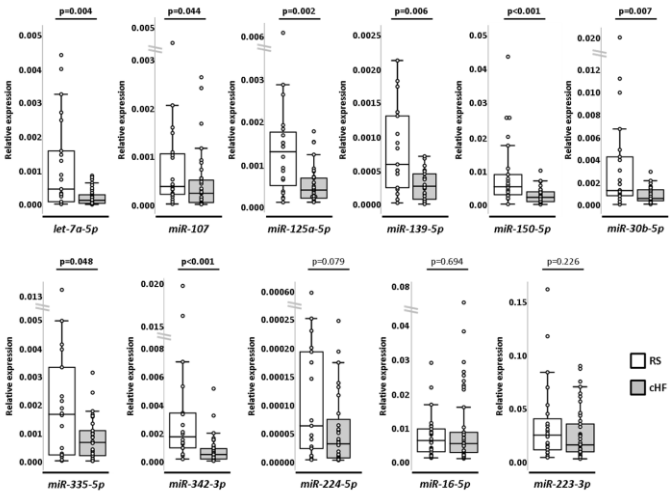

Figure 2. Box and whisker plots of selected miRNAs analysed in cHF ($n = 46$) and RS ($n = 26$). U Mann–Whitney test. A *p*-value < 0.05 was considered significant. cHF: chronic heart failure; RS: reference subjects.

2.2. In Silico System Biology Analysis and Target Prediction

Gene-targets of the differential miRNA signature (577 genes) were obtained with the combination of four different miRNA-target prediction algorithms (TargetScan, miRmap, miRWalk and miRDB [18–22]). All validated miRNAs were included in target data mining (*let-7a-5p*, *miR-107*, *miR-125a-5p*, *miR-139-5p*, *miR-150-5p*, *miR-30b-5p* and *miR-342-3p*), except *miR-335-5p*, given that, for this miRNA, only one target was obtained after combining predictions of all four algorithms used. The resulting targets were analysed using the ShinyGO web-based software [23] for pathway enrichment analysis (Table 1). Gene ontology (GO) annotations for biological processes of predicted targets, sorted by average and rank (FDR and fold), revealed significant enrichment in pathways related to coronary vasculature morphogenesis and development (GO:0060977 and GO:0060976, respectively; FDR < 0.001, both), TGF-β signalling regulation (GO:0030511 and GO:1903846; FDR < 0.001, both) and with ventricular and cardiac septum development (GO:0003281 and GO:0003279, respectively; FDR < 0.001, both).

Table 1. Pathway enrichment analysis of GO terms in ShinyGo, sorted by average ranks (FDR and fold).

GO TERMS	Gene Number (Pathway Gene Number)	Fold Enrichment	Enrichment FDR
Biological Process			
Presynapse assembly	11 (52)	8.3	1.02×10^{-5}
Coronary vasculature morphogenesis	6 (16)	14.8	1.79×10^{-4}
Presynapse organisation	11 (55)	7.9	1.83×10^{-5}
Coronary vasculature development	9 (46)	7.7	1.95×10^{-4}
Synaptic membrane adhesion	7 (28)	9.8	3.69×10^{-4}
Positive regulation of TGF-β signalling pathway	7 (30)	9.2	5.32×10^{-4}
Positive regulation of cellular response to TGF-β stimulus	7 (30)	9.2	5.32×10^{-4}
Ventricular septum development	11(72)	6.0	1.92×10^{-4}
Cardiac septum development	14 (108)	5.1	7.89×10^{-5}
Ventricular compact myocardium morhogenesis	4 (8)	19.7	1.23×10^{-3}
Molecular Function			
SMAD binding	14 (80)	6.9	2.44×10^{-6}
RNA strand annealing activity	3 (5)	23.7	5.10×10^{-3}
Insulin-like growth factor I binding	4 (13)	12.1	7.17×10^{-3}
β-catenin binding	13 (89)	5.7	2.58×10^{-5}
RNA stem-loop binding	4 (14)	11.3	9.53×10^{-3}
Poly-purine tract binding	6 (29)	8.1	2.71×10^{-3}
Transcription factor binding	42 (596)	2.7	2.36×10^{-6}
Poly(G) binding	3 (8)	14.8	1.80×10^{-2}
DNA-binding transcription repressor activity. RNA polymerase II-specific	21 (333)	2.4	4.50×10^{-3}
3,5-cyclic-AMP phosphodiesterase activity	4 (16)	9.8	1.52×10^{-2}
Cellular Component			
Cytoplasmic ribonucleoprotein granule	23 (272)	3.3	5.56×10^{-5}
GABA-ergic synapse	9 (74)	4.8	4.56×10^{-3}
Ribonucleoprotein granule	23 (288)	3.1	1.29×10^{-4}
Node of Ranvier	4 (15)	10.5	1.10×10^{-2}
Filopodium	11 (119)	3.6	7.40×10^{-3}
Glutamatergic synapse	25 (358)	2.7	4.44×10^{-4}
Site of polarised growth	15 (196)	3.0	6.17×10^{-3}
Chromatin	76 (1316)	2.2	8.70×10^{-9}
Adherens junction	14 (180)	3.0	7.33×10^{-3}
Heterochromatin	8 (77)	4.1	1.62×10^{-2}

Additionally, a protein-protein interaction (PPI) network, including all 577 predicted targets, was built according to data from the STRING database [24] using Cytoscape [25]. The resulting network revealed a highly connected nodule involving 273 targets from all included miRNAs (Figure 3a). We then applied a community cluster strategy to identify PPI-enriched nodules [26] and ran a functional overrepresentation analysis upon pathways from the KEGG database [27,28]. Clusters with fewer than five nodes were excluded from the analysis. As a result, eight clusters were identified from the main connected component of the network (Figure 3b). Noteworthy, four clusters included targets from all query miRNAs (clusters 1–4) and were the ones selected for more specific pathway analysis. As depicted in Supplemental Table S3, the identified clusters aggregate functionally related genes. Highly significant enrichment for focal adhesions (hsa04510; FDR < 0.001), chemokine, Ras and PI3K-AKT signalling pathways (hsa04062, hsa04014 and hsa04151, respectively; FDR < 0.001, all) was found for cluster 1. Also, strong enrichments in cell cycle (hsa04110; FDR < 0.001), cellular senescence (hsa04218; FDR < 0.001) and TGF-β signalling (hsa04350; FDR < 0.001) were detected for cluster 2. For clusters 3 and 4, only marginal enrichments were found in genes involved in RNA transport (hsa03013; FDR < 0.001), Wnt and Hippo signalling pathways (hsa04310 and hsa04390, respectively; FDR < 0.001).

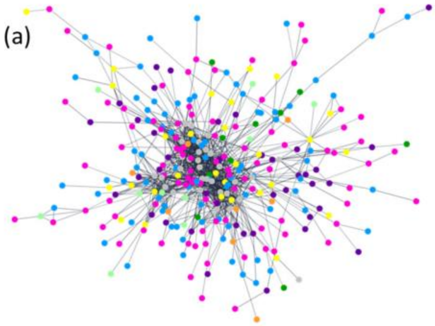

(c)

	CLUSTER 1	2	3	4	5	6	7	8	9	10	11	12	13	Total nodes
let-7a-5p	8	14	10	4	0	1	0	0	1	1	0	0	1	40
miR-107	22	16	10	17	4	5	1	1	1	2	1	1	0	81
miR-125a-5p	1	2	5	1	0	0	0	0	0	0	1	0	0	10
miR-139-5p	27	19	18	13	3	2	5	3	1	1	1	1	1	95
miR-150-5p	7	7	5	6	2	0	1	0	1	0	0	0	0	29
miR-30b-5p	1	4	1	2	0	0	0	0	0	0	0	0	0	8
miR-342-3p	2	3	1	3	0	0	0	1	0	0	0	0	0	10
Added by STRING	15	10	2	4	0	0	0	0	0	0	0	0	0	31
Total nodes	83	75	52	50	9	8	7	5	4	4	3	2	2	304

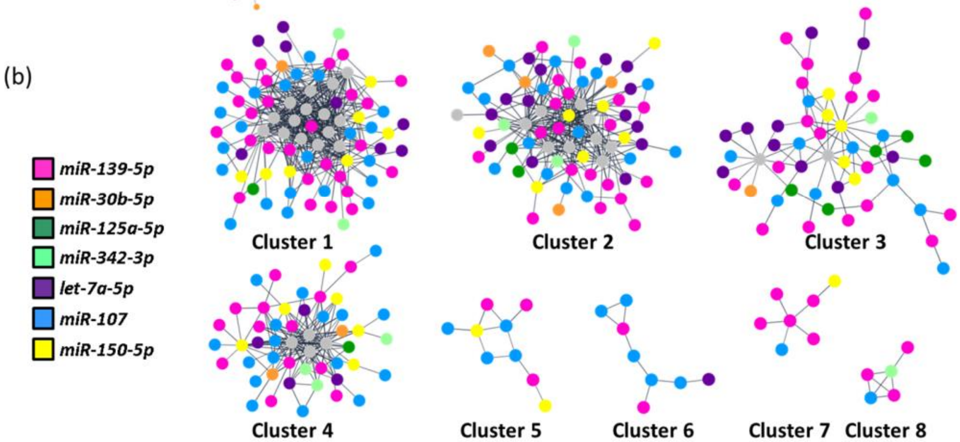

Figure 3. miRNA clustering and enrichment analysis. (**a**) PPI network of the circulating miRNA signature in cHF. Only interactions with a confidence score higher than 0.8 were considered. Node colours represent targeting miRNA. Grey nodes correspond to STRING-added nodes. (**b**) Community clusters identified within the main connected component of the PPI network. Clusters with less than 5 genes were excluded. (**c**) Table with number of target genes regulated by each miRNA, per cluster. cHF: chronic heart failure; PPI: protein-protein interaction.

2.3. Association of Clusters with cHF Subtypes

Considering that the networks obtained in the PPI analysis associated with specific pathways, we analysed if clustered miRNAs provided new information to differentiate between HF subtypes. As shown in Table 2, we observed that C-statistics analysis of the combined probabilities of those miRNAs with a role in clusters 1–4 (including miRNAs *let-7a-5p*, *miR-107*, *miR-125a-5p*, *miR-139-5p*, *miR-150-5p*, *miR-30b-5p* and *miR-342-3p*; from now on "C:1–4") differentiated between patients with HF with preserved ejection fraction (HFpEF) and HF with reduced ejection fraction (HFrEF) (AUC: 0.725 ± 0.102 [95% Confidence Interval (CI): 0.526–0.925]; $p = 0.047$) and between cHF underlying aetiologies (ischaemic vs. non-ischaemic; AUC: 0.789 ± 0.088 [95% CI: 0.617–0.962]; $p = 0.019$), but not need for rehospitalisation ($p = 0.880$).

Table 2. ROC curve analysis of miRNAs according to their cluster formation.

	AUC ± SD (95% CI)	*p*-Value	Sensitivity	Specificity
(a) Differentiation of Ejection Fraction				
Clusters 1–4 miRNAs *	0.725 ± 0.102 (0.526–0.925)	**0.047**	0.769	0.643
Cluster 5 and 7 miRNAs: *miR-107 + miR-139-5p + miR-150-5p*	0.782 ± 0.083 (0.618–0.945)	**0.007**	0.722	0.714
Cluster 6 miRNAs: *miR-107 + miR-139-5p + let-7a-5p*	0.582 ± 0.112 (0.363–0.802)	0.467	0.571	0.538
Cluster 8 miRNAs: *miR-107 + miR-139-5p + miR-342-3p*	0.690 ± 0.097 (0.500–0.881)	0.068	0.611	0.643
(b) Differentiation of Underlying Aetiology				
Cluster 1–4 miRNAs *	0.789 ± 0.088 (0.617–0.962)	**0.019**	0.737	0.750
Cluster 5 and 7 miRNAs: *miR-107 + miR-139-5p + miR-150-5p*	0.643 ± 0.118 (0.410–0.875)	0.216	0.696	0.667
Cluster 6 miRNAs: *miR-107 + miR-139-5p + let-7a-5p*	0.691 ± 0.126 (0.443–0.939)	0.124	0.684	0.625
Cluster 8 miRNAs: *miR-107 + miR-139-5p + miR-342-3p*	0.645 ± 0.106 (0.438–0.853)	0.193	0.636	0.500
(c) Differentiation of Need for Rehospitalisation				
Clusters 1–4 miRNAs *	0.518 ± 0.118 (0.287–0.749)	0.880	0.471	0.600
Cluster 5 and 7 miRNAs: *miR-107 + miR-139-5p + miR-150-5p*	0.695 ± 0.092 (0.514–0.877)	0.080	0.636	0.600
Cluster 6 miRNAs: *miR-107 + miR-139-5p + let-7a-5p*	0.641 ± 0.107 (0.432–0.850)	0.228	0.588	0.600
Cluster 8 miRNAs: *miR-107 + miR-139-5p + miR-342-3p*	0.700 ± 0.093 (0.518–0.882)	0.074	0.591	0.600

* Includes all miRNAs: *let-7a-5p*, *miR-107*, *miR-125a-5p*, *miR-139-5p*, *miR-150-5p*, *miR-30b-5p* and *miR-342-3p*. Numbers in bold indicate statistical significance. (a) Ejection fraction: HFrEF (LVEF < 40; $n = 24$) and HFpEF (LVEF ≥ 50; $n = 22$); (b) Background aetiology: ischaemic ($n = 14$) and non-ischaemic ($n = 32$); (c) Need for rehospitalisation: rehospitalised ($n = 32$) and non-rehospitalised ($n = 14$). AUC: area under the curve; CI: confidence interval; HFpEF: heart failure with preserved ejection fraction; HFrEF: heart failure with reduced ejection fraction; LVEF: left ventricular ejection fraction; ROC: receiver operating characteristic; SD: standard deviation.

Similarly, the combined probabilities of miRNAs in clusters 5 and 7 (*miR-107*, *miR-139-5p* and *miR-150-5p*; from now on "C:5+7") could differentiate between HFpEF and HFrEF (AUC: 0.782 ± 0.083 [95% CI: 0.618–0.945]; $p = 0.007$), but not between background aetiologies ($p = 0.216$). These miRNAs presented a tendency to discriminate the need for rehospitalisation, but it did not reach statistical significance ($p = 0.080$).

The combined probabilities of miRNAs involved in cluster 6 (*miR-107*, *miR-139-5p* and *let-7a-5p*) did not differentiate between ejection fractions ($p = 0.467$), underlying aetiology ($p = 0.124$) or need for rehospitalisation ($p = 0.228$). The combination of miRNAs included in cluster 8 (*miR-107*, *miR-139-5p* and *miR-342-3p*) presented a borderline tendency to differentiate between cHF ejection fraction groups ($p = 0.068$) and the need for rehospitalisation (p = 0.074). They could not, however, discriminate between background aetiologies (p = 0.193).

To study if the miRNAs implicated in the clusters with discriminatory potential associated with specific pathways, we performed two other PPI networks. Specifically, we compared if the miRNAs included in C:5+7 (*miR-107*, *miR-139-5p* and *miR-150-5p*) and the miRNAs not included in these clusters but present in C:1–4 (*let-7a-5p*, *miR-125a-5p*, *miR-30b-5p* and *miR-342-3p*; from now on "Differential miRNAs [DiffmiR]") were enriched in different biological pathways. Further, we analysed if those divergent pathways could be associated with the discriminatory differences observed between C:1–4 and C:5+7.

Thus, two PPI networks were generated in Cytoscape with data from STRING [24]. Networks for C:5+7 and DiffmiR were created with 408 and 189 predicted target genes, respectively. The new resulting networks included 204 predicted targets for C:5+7 and 63 for DiffmiR (Figures 4a and 5a). To identify PPI-enriched nodules, we applied a community cluster strategy [26], as described above, and pursued a functional overrepresentation analysis upon pathways from the KEGG database [27,28]. Only clusters with more than five nodes were considered for analysis.

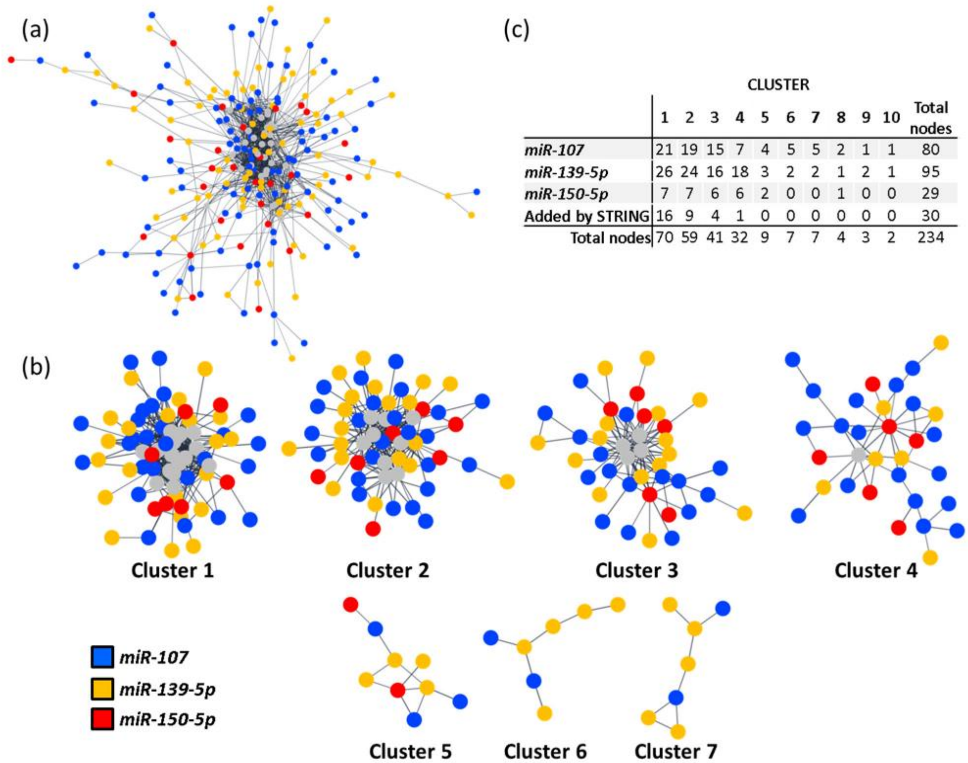

CLUSTER	1	2	3	4	5	6	7	8	9	10	Total nodes
miR-107	21	19	15	7	4	5	5	2	1	1	80
miR-139-5p	26	24	16	18	3	2	2	1	2	1	95
miR-150-5p	7	7	6	6	2	0	0	1	0	0	29
Added by STRING	16	9	4	1	0	0	0	0	0	0	30
Total nodes	70	59	41	32	9	7	7	4	3	2	234

Figure 4. miRNA in C:5+7 clustering and enrichment analysis. (**a**) PPI network of the miRNAs included in clusters 5 and 7 (C:5+7) of the main PPI network. Only interactions with a confidence score higher than 0.8 were considered. Node colour represents targeting miRNA. Grey nodes correspond to STRING-added nodes. (**b**) Community clusters identified within the main connected component of the C:5+7 PPI network. Clusters with fewer than five genes were excluded. (**c**) Table with number of target genes regulated by each miRNA, per cluster. C:5+7: miRNAs included in clusters 5 and 7 of the main PPI network (includes *miR-107*, *miR-139-5p* and *miR-150-5p*); PPI: protein-protein interaction.

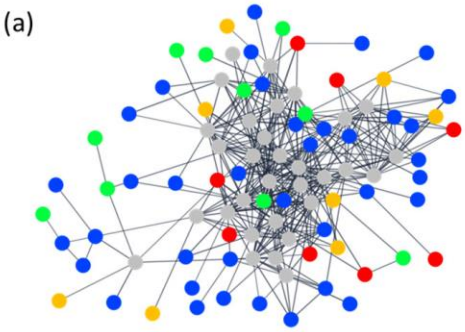

(c)

	CLUSTER 1	2	3	4	5	Total nodes
let-7a-5p	8	6	13	5	5	37
miR-125a-5p	5	2	0	0	3	10
miR-30b-5p	1	1	4	2	0	8
miR-342-3p	2	1	2	2	1	8
Added by STRING	9	4	12	5	1	31
Total nodes	25	14	31	14	10	94

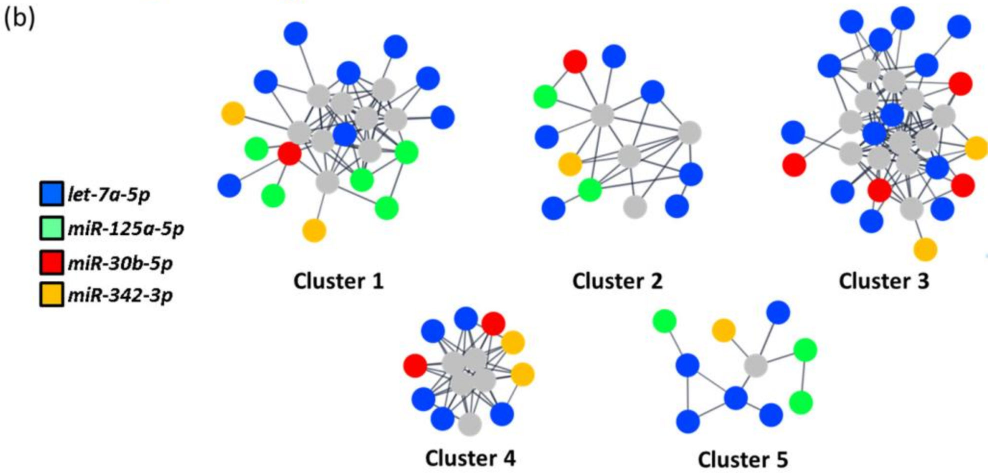

Figure 5. miRNA in DiffmiR clustering and enrichment analysis. (**a**) PPI network of the miRNAs included in C:1–4 but not in C:5+7 of the main PPI network (DiffmiR). Only interactions with a confidence score higher than 0.8 were considered. Node colour represents targeting miRNA. Grey nodes correspond to STRING-added nodes. (**b**) Community clusters identified within the main connected component of the DiffmiR network. Clusters with fewer than five genes were excluded. (**c**) Table with number of target genes regulated by each miRNA, per cluster. C:1–4: miRNAs included in clusters 1–4 of the main PPI network (includes *let-7a-5p*, *miR-107*, *miR-125a-5p*, *miR-139-5p*, *miR-150-5p*, *miR-30b-5p* and *miR-342-3p*); C:5+7: miRNAs included in clusters 5 and 7 of the main PPI network (includes *miR-107*, *miR-139-5p* and *miR-150-5p*); DiffmiR: miRNAs included in clusters 1–4 but not in clusters 5 and 7 of the main PPI network (includes *let-7a-5p*, *miR-125a-5p*, *miR-30b-5p* and *miR-342-3p*); PPI: protein-protein interaction.

As a result, seven clusters were generated from the main connected component of the C:5+7 network (Figure 4b). Of these, five clusters included targets from the three involved miRNAs and were selected for pathway enrichment analysis (Supplemental Table S4). Cluster 1 was significantly enriched in focal adhesions (hsa04510; FDR < 0.001), and Ras, chemokine and PI3K-AKT signalling pathways (hsa04014, hsa04062 and hsa04151, respectively; FDR < 0.001 all). Cluster 2 was enriched in Notch, TGF-β and thyroid hormone signalling pathways (hsa04330, hsa04350 and hsa04919, respectively; FDR < 0.001, all), as well as cell cycle (hsa04110; FDR < 0.001). Cluster 3 was enriched in pathways related to ubiquitin-mediated proteolysis (hsa04120; FDR < 0.001), and Wnt and Hippo signalling pathways (hsa04310 and hsa04390, respectively; FDR < 0.0002, both). Clusters 4 and 5 were marginally enriched in RNA transport (hsa03013; FDR < 0.001) and taste transduction (hsa04742; FDR < 0.001).

From the main connected component of the DiffmiR, five clusters were generated (Figure 5b). Only those clusters with target genes of the four miRNAs included in the analysis were selected for pathway enrichment analysis (clusters 1–2). Cluster 1 was enriched in prolactin, PI3K-AKT, ErbB and JAK-STAT signalling pathways (hsa04917, hsa04151, hsa04012 and hsa04630, respectively; FDR < 0.001, all), as well as in EGFR tyrosine kinase inhibitor resistance (hsa01521; FDR < 0.001) and endocrine resistance (hsa01522; FDR < 0.001). Cluster 2 was enriched in cellular senescence (hsa04218; FDR < 0.001) and TGF-β signalling pathway (hsa04350; FDR < 0.001) (Supplemental Table S5).

These results were then compared with the pathways obtained in the pathway enrichment analysis of the PPI including all miRNAs (*let-7a-5p*, *miR-107*, *miR-125a-5p*, *miR-139-5p*, *miR-150-5p*, *miR-30b-5p* and *miR-342-3p*; Figure 3). Only those pathways unique to C:1–4, C:5+7 or DiffmiR, as well as common between C:1–4 and C:5+7/DiffmiR (Figure 6), were considered.

DESCRIPTION - KEGG	FDR value	Fold enrichment
Thyroid hormone signalling pathway	3.24×10^{-12}	10.08
Endocrine and other factor-regulated calcium reabsorption	0.0045	5.66
Thermogenesis	0.0080	2.18
ECM-receptor interaction	0.0162	3.41

DESCRIPTION - KEGG	FDR value	Fold enrichment
Inflammatory mediator regulation of TRP channels	3.35×10^{-5}	4.26
Carbohydrate digestion and absorption	0.0047	4.55
Regulation of lipolysis in adipocytes	0.0068	3.70
Glucagon signalling pathway	0.0199	1.98

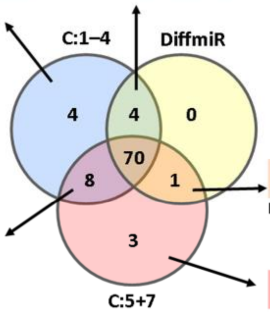

DESCRIPTION - KEGG	FDR value	Fold enrichment
Leukocyte transendothelial migration	3.89×10^{-9}	8.26
Vascular smooth muscle contraction	4.18×10^{-5}	4.51
Arrhythmogenic right ventricular cardiomyopathy	6.2×10^{-4}	5.26
Aldosterone-regulated sodium reabsorption	0.0012	8.11
Hypertrophic cardiomyopathy	0.0118	3.37
Dilated cardiomyopathy	0.0137	3.16
Hedgehog signalling pathway	0.0057	6.38
RNA transport	8.56×10^{-5}	3.75

DESCRIPTION - KEGG	FDR value	Fold enrichment
Necroptosis	1.6×10^{-4}	2.68

DESCRIPTION - KEGG	FDR value	Fold enrichment
Viral myocarditis	0.0439	3.64
Spliceosome	0.0115	3.03
Taste transduction	1.38×10^{-5}	4.94

Figure 6. Venn diagram of enriched pathways identified for each group of miRNAs. C:1–4: miRNAs included in clusters 1–4 of the main PPI network (includes *let-7a-5p*, *miR-107*, *miR-125a-5p*, *miR-139-5p*, *miR-150-5p*, *miR-30b-5p* and *miR-342-3p*); C:5+7: miRNAs included in clusters 5 and 7 of the main PPI network (includes *miR-107*, *miR-139-5p* and *miR-150-5p*); DiffmiR: miRNAs included in clusters 1–4 but not in clusters 5 and 7 of the main PPI network (includes *let-7a-5p*, *miR-125a-5p*, *miR-30b-5p* and *miR-342-3p*).

Thus, the C:5+7 network was enriched in leukocyte transendothelial migration (hsa04670; FDR < 0.001), vascular smooth muscle contraction (hsa04270; FDR < 0.001), arrhythmogenic right ventricular, hypertrophic and dilated cardiomyopathy (hsa05412, hsa05410, hsa05414, respectively; FDR < 0.02, all), aldosterone-regulated sodium reabsorption (hsa04960; FDR = 0.0012), viral myocarditis (hsa05416; FDR = 0.043), hedgehog signalling pathway (hsa04340; FDR = 0.0057), RNA transport (hsa03013; FDR < 0.001), spliceosome (hsa03040; FDR = 0.0115) and taste transduction (hsa04742; FDR < 0.001).

The DiffmiR network was enriched in glucagon signalling pathway (hsa04922; FDR = 0.019), inflammatory mediator regulation of TRP channels (hsa04750; FDR < 0.001), carbohydrate digestion and absorption (hsa04973; FDR = 0.0047) and regulation of lipolysis in adipocytes (hsa04923; FDR = 0.0068).

2.4. miR-107 and miR-139 Were Overrepresented in All Clusters

When the weight of each miRNA in each cluster of the main PPI network was considered (Figure 3a), we observed that *miR-107* and *miR-139-5p* were overrepresented, with 81 (26.4%) and 95 (31.25%) of all clustered protein-coding genes targeted by these miRNAs, respectively (Figure 3c). Therefore, *miR-107* and *miR-139-5p* were analysed individually to better understand their specific contribution to cHF pathophysiology.

In silico analysis querying "heart failure" to STRING Pubmed in Cytoscape [25] resulted in a repository-based list of 837 genes related to HF (repository-based gene database [RBGD]). The 81 and 95 targets of *miR-107* and *miR-139-5p*, respectively, were matched individually to the RBGD list (Supplemental Figure S1). Using this approach, we found three protein-coding genes regulated by *miR-107* and nine regulated by *miR-139-5p* that were also identified as genes with a role in HF, according to the repository-derived data included in the RBGD list (Table 3).

Table 3. Clustered miRNA targets detected in the STRING-generated heart failure database.

miRNA	Target	Cluster
miR-107	ESR1	1
miR-107	BDNF	1
miR-107	MFN2	4
miR-139-5p	DMD	1
miR-139-5p	ROCK2	1
miR-139-5p	MAPK8	1
miR-139-5p	GNB1	1
miR-139-5p	ROCK1	1
miR-139-5p	IGF1R	1
miR-139-5p	SMARCA4	2
miR-139-5p	NOTCH1	2
miR-139-5p	PDE3A	12

These 12 common protein-coding genes and their RBGD-based neighbouring interacting genes (101 for *miR-107* and 176 for *miR-139-5p*) were selected and analysed with ShinyGO [23] to determine their putative pathways. Using the KEGG database [27,28], we observed that both miRNAs participated in the pathways PI3K-AKT signalling (hsa04151; FDR < 0.001; both miRNAs) and MAPK signalling (hsa04010; FDR < 0.001; both miRNAs) (Figure 7a,b).

2.5. Association of Individual Plasma miRNAs with Aetiology and with Left Ventricular Ejection Fraction in cHF Patients

A study of individual miRNAs showed that *miR-139-5p* presented differential expression patterns between cHF patients with and without underlying ischaemic aetiology ($p = 0.022$), but not for left ventricular ejection fraction (LVEF) levels (Figure 8 and Supplemental Tables S6 and S7). miRNA plasma levels did not show statistically significant changes between patients with different degrees of severity according to the New York Heart Association (NYHA) classification.

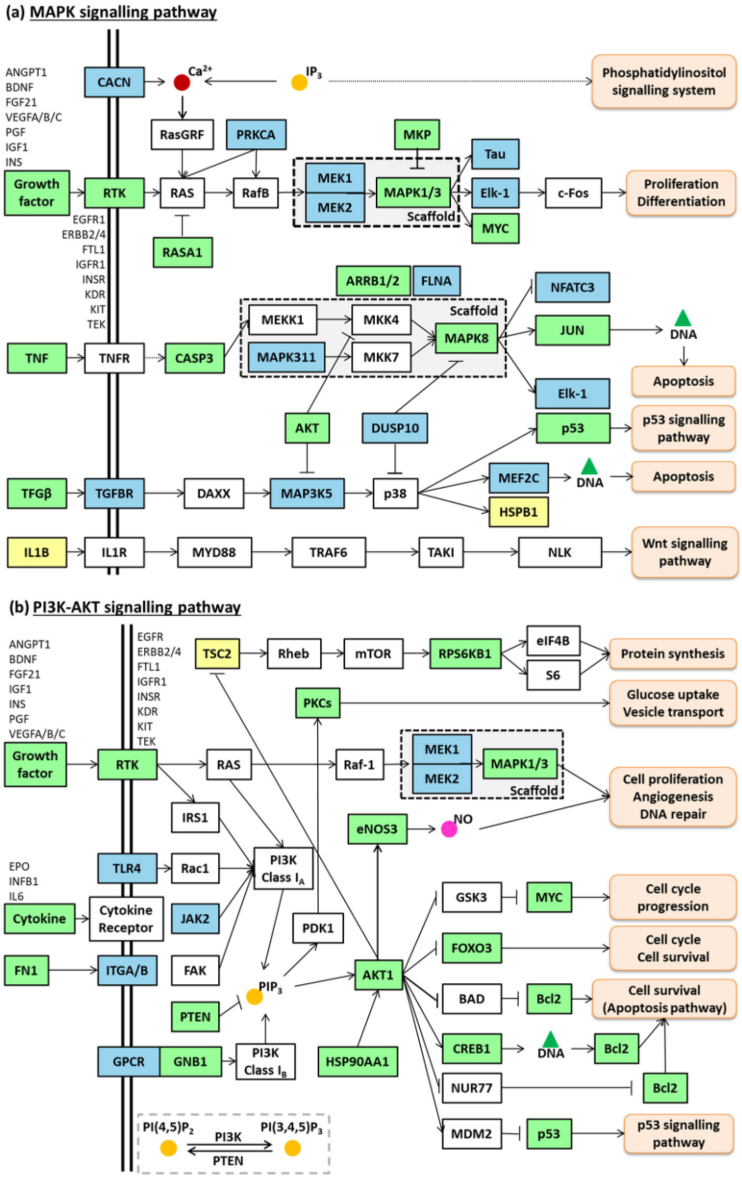

Figure 7. *miR-107* and *miR-139-5p* common pathways. (**a**) MAPK signalling pathway. (**b**) PI3K-AKT signalling pathway. Coloured nodes correspond to target genes and their neighbouring genes. In blue: *miR-139-5p* target genes and their neighbouring genes; in yellow: *miR-107* target genes and their neighbouring genes; in green: *miR-139-5p* and *miR-107* common target genes and their neighbouring genes; in white: additional nodes for pathway completion. Unframed gene names correspond to targeted genes included under a broader category such as "growth factor", "RTK" or "cytokine". Adapted from pathways "MAPK signalling pathway (hsa04010)" and "PI3K-AKT signalling pathway (hsa04151)" generated in the KEGG database.

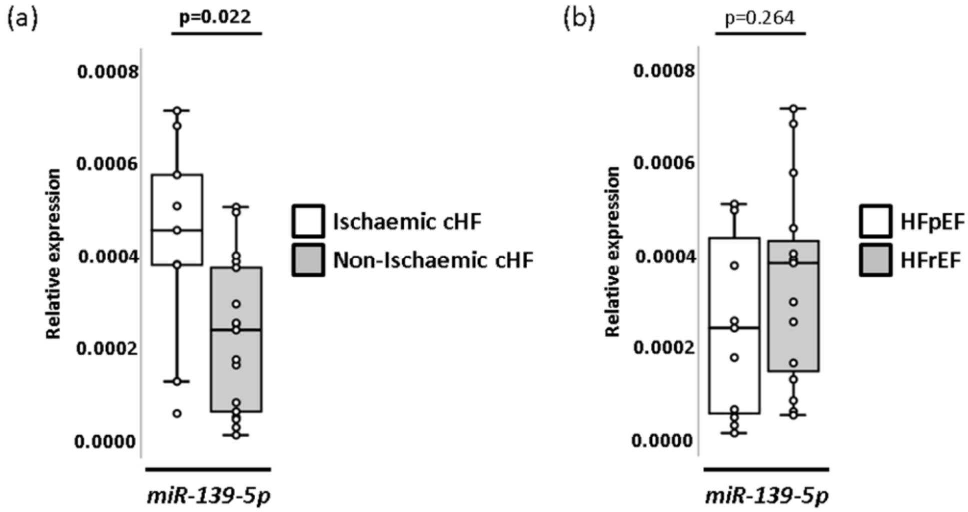

Figure 8. miRNAs patterns associations with cHF underlying aetiology and ejection fraction. (**a**) Box and whisker plots of miRNA *miR-139-5p* in cHF patients according to underlying aetiology (ischaemic and non-ischaemic). (**b**) Box and whisker plots of miRNA *miR-139-5p* in cHF patients according to ejection fraction (HFpEF and HFrEF). A $p < 0.05$ was considered significant. cHF: chronic heart failure; HFpEF: heart failure with preserved ejection fraction; HFrEF: heart failure with reduced ejection fraction.

3. Discussion

Heart failure is a highly frequent disease with a complex pathophysiology [3]. Circulating miRNAs are emerging as tools to facilitate disease diagnosis, prognosis, risk stratification and management [6–10]. In addition, miRNAs have a role in gene expression regulation and are, therefore, involved in disease pathogenesis [12,13]. In this study, we have used a non-targeted approach to miRNA identification and investigated plasma samples of cHF patients. We have studied the putative role of miRNAs in cHF pathogenesis through gene regulation by pursuing an in silico enrichment pathway analysis. Additionally, we analysed if these miRNAs were individually related to pathways associated with cHF pathogenesis.

In this study, we have identified the presence of a down-regulated eight-miRNA pattern in the plasma of cHF patients in comparison to a group of reference subjects. Specifically, circulating levels of miRNAs *let-7a-5p*, *miR-107*, *miR-125a-5p*, *miR-139-5p*, *miR-150-5p*, *miR-30b-5p*, *miR-335-5p* and *miR-342-3p* were significantly lower in cHF than in the RS group. Predicted target genes of seven of these miRNAs (*let-7a-5p*, *miR-107*, *miR-125a-5p*, *miR-139-5p*, *miR-150-5p*, *miR-30b-5p* and *miR-342-3p*) clustered and were related to several pathways, including cell cycle, cellular senescence, or Ras, chemokine, PI3K-AKT and TGF-β signalling pathways. Interestingly, we found that, when miRNAs were considered according to their clusterisation, they had discriminative value. Specifically, we observed that the best discrimination for ejection fraction types (HFpEF and HFrEF) was obtained with those miRNAs regulating cluster 5 and 7 (*miR-107*, *miR-139-5p* and *miR-150-5p*; C:5+7), followed by those miRNAs involved in clusters 1–4 (*let-7a-5p*, *miR-107*, *miR-125a-5p*, *miR-139-5p*, *miR-150-5p*, *miR-30b-5p* and *miR-342-3p*; C:1–4). The latest miRNA combination also differentiated background aetiology, but the combination of *miR-107*, *miR-139-5p* and *miR-150-5p* (C:5+7) did not. For this reason, we explored if miRNAs in C:1–4 but not in C:5+7 were related to specific pathways that could explain this difference. Thus, the cluster involving *let-7a-5p*, *miR-125a-5p*, *miR-30b-5p* and *miR-342-3p*

(DiffmiR), associated with metabolic (glucagon signalling pathway, lipolysis regulation and carbohydrate digestion and absorption) and inflammatory pathways (inflammatory mediator regulation of TRP channels). In contrast, miRNAs in the C:5+7 had gene targets involved in cardiomyopathy-related pathways (hypertrophic, dilated and arrhythmogenic cardiomyopathies), aldosterone-regulated sodium reabsorption, vascular smooth muscle cell contraction, or leukocyte trans-endothelial migration.

In contrast to our findings at the systemic level, *let-7a-5p* was found up-regulated in plasma from the coronary sinus of cHF patients when compared to controls [29]; although differences between both studies could relate to the plasmatic sample origin. Our study could reflect systemic changes in cHF, whereas those miRNA patterns in the coronary sinus could be more related to pathological alterations in the heart [29]. In agreement with our results, Ellis and colleagues [30] detected down-regulated levels of *miR-150-5p* in the plasma of cHF in comparison to controls [30]. Similarly, Scrutinio et al. [31] reported *miR-150-5p* to be down-regulated in cHF patients with severe symptomatology in comparison to cHF with mild symptomatology and to controls, being *miR-150-5p* associated with an increased risk of death, heart transplantation or left ventricular assist devices implantation [31]. Furthermore, the serum levels of *miR-150-5p* have been reported to be significantly decreased in acute myocardial infarction (AMI) patients compared to controls, with AMI patients who developed cHF presenting the lowest levels [32]. The same study suggested that *miR-150-5p* was able to predict post-AMI cHF when combined with brain natriuretic peptide (BNP)[32] and that *miR-150-5p* was independently associated with post-AMI cHF through multivariate analysis including age, BNP and LVEF [32]. Although we did find a negative correlation of this miRNA with LVEF, we did not observe an association of *miR-150-5p* with ischaemic disease. This could be due to the sample type (plasma instead of serum) [33], or to the fact that we compared those patients with cHF due to an AMI with those patients that developed cHF due to other reasons, such as heart valve disease or cardiac hypertrophy, which could also affect *miR-150-5p* levels.

In contrast, we observed that miRNA *miR-139-5p* was up-regulated in the plasma of those patients with underlying ischaemic disease in comparison with those with underlying non-ischaemic disease. Divergent results were found by Voellenkle et al., who observed similar levels of this miRNA (from peripheral blood mononuclear cells [PBMCs]) between cHF with ischaemic and non-ischaemic backgrounds [34]. Nevertheless, in agreement with our findings, the authors described down-regulated levels of *miR-139-5p* in cHF [34]. The difference in ischaemia-related *miR-139-5p* response between blood cells and plasma samples suggests that a tissue origin other than blood accounts for circulating *miR-139-5p* in patients who suffered an AMI. In this respect, Ming et al. have reported decreased levels of *miR-139-5p* in left ventricle tissue of patients with hypertrophic cardiomyopathy and demonstrated an anti-hypertrophic effect mediated by this miRNA through the regulation of IGF-R1 and c-Jun [35]. It is known that IFG-R1 is a component of both MAPK and PI3K-Akt signalling pathways [36]. Interestingly, the assessment of miRNAs in-cluster individual weight in our study evidenced the presence of *miR-139-5p* and *miR-107* in all clusters. Further, the in silico analysis revealed that both miRNAs were implicated in the MAPK and PI3K-AKT signalling pathways. Voellenkle et al. also detected *miR-107* down-regulation in cHF compared to their controls [34]. Some reports have associated this miRNA with metabolism and cardiac function [37], as well as angiogenesis [38] or hypoxia [39]. Further, some reports indicate that *miR-107* regulates gene expression through the PI3K-AKT and MAPK pathways [40,41], in correlation with our in silico results. Moreover, *miR-30b-5p* was found to be deregulated in HF compared to both, healthy subjects and patients with shortness of breath [30].

To our knowledge, this is the first time *miR-335-5p* has been identified in patients recruited in a heart failure clinic, that is, patients with clinical evidence and diagnosis of chronic heart failure. Some studies including ischaemic patients detected a down-regulation of this miRNA in acute ischaemia [6] or during a three-month post-myocardial infarction period [42]. The latter study suggested *miR-335-5p* together with five other miRNAs as potential markers of deleterious left ventricular remodelling, but it did not provide evidence of changes in patients with established chronic heart failure. Studies in animal models have also related this miRNA with atherosclerosis [43] or ventricular remodelling [42,44,45], with apparently controversial findings. Thus, studies in mice have associated *miR-335-5p* overexpression with a reduction of atherosclerotic plaque vulnerability and angiogenesis promotion [46]. In contrast, this miRNA was found up-regulated in rat and mouse models of pulmonary hypertension, where the induced right ventricular remodelling was linked to increased *miR-335-5p* expression and its blockade alleviated remodelling [45]. Interestingly, contrasting results were observed in a model of sepsis-induced myocardial injury [44]. Long and colleagues observed that up-regulated levels of this miRNA ameliorated myocardial injury by reducing apoptosis and Ca^{2+} overload [44]. Nevertheless, we need to take into consideration that miRNA patterns in animal models may not reflect a human profile [47] and that all those studies reflect an acute injury rather than a chronic disease. Similarly, little is known about *miR-342-3p*. To this respect, Ellis et al. observed down-regulated levels of *miR-342-3p* in cHF in comparison to healthy subjects or patients with shortness of breath [30], but no association of this miRNA with background aetiology or ejection fraction in cHF has been reported.

The in silico analysis we performed with the validated miRNAs (main PPI network) revealed an enrichment of several pathways, including cell cycle, cellular senescence, and Ras, chemokine, PI3K-AKT and TGF-β signalling pathways. Multiple pathophysiological mechanisms are involved in HF. Among them, cHF patients are characterised by presenting an unresolving inflammatory state, endothelial dysfunction and cardiac remodelling (including cardiac fibrosis, hypertrophy and apoptosis). In agreement with our results, Ras/MAPK and PI3K-AKT signalling have been previously related to cardiac hypertrophy and HF [36,48]. Similarly, the TGF-β and PI3K-AKT pathways have been related to cardiac fibrosis [49–51]. Further, HF patients are characterised for presenting an unresolved inflammatory state, where chemokine levels are increased [52] and innate immunity cell increase their release of extracellular vesicles [53].

It is widely accepted that in HF there is a change in cardiac metabolism. In the healthy heart, cardiomyocytes produce energy mainly through fatty acid oxidation. However, in the failing heart, energy production swifts to a glucose-based metabolism (glycolysis and anaplerosis) and other forms of metabolism, such as the use of lactate, branched-chain amino acids and ketone bodies [54]. Although by in silico analysis we evidenced that miRNA-target genes in the DiffmiR cluster were associated with metabolism (glucagon signalling pathway, lipolysis regulation and carbohydrate digestion and absorption), a specific implication of these metabolic pathways in metabolic remodelling in cHF is, as far as we know, still undetermined. However, alterations in the glucagon signalling pathway (compromising cAMP signalling in cardiomyocytes) and increased levels of adipocyte lipolysis, have been detected in HF [55,56]. Further, suppression of HF development was observed in a mice model fed with a strict carbohydrate-restricted diet [57].

4. Materials and Methods

4.1. Study Design

Patients with cHF treated by guideline-directed medical therapy (GDMT) were prospectively recruited in the outpatient HF unit of the Hospital de la Santa Creu i Sant Pau (Barcelona, Spain) from September 2016 to July 2018 (n = 58). Patients with LVEF between 40% and 50% (mildly reduced LVEF; HFmrEF), past history of cancer, inflammatory disorders, sepsis or infection were excluded from the study. Pregnant women were also excluded. A group of reference subjects of age- and sex-matched subjects without cHF (n = 26) was also analysed.

A quantitative Low-density TaqMan™ Advanced miRNA Human A Card was run on 28 patients, 14 patients with preserved LVEF (HFpEF; LVFE $\geq$ 50%), and 14 with reduced LVEF (HFrEF; LVFE < 40%) (Table 4).

Table 4. Baseline characteristics of cHF patients and reference subjects in the miRNA selection.

	cHF *n* = 28	Reference Subjects *n* = 16	*p*-Value
Demographic Characteristics; mean ± SD			
Male/Female, *n*	14/14	10/6	0.423
Age, years	69 ± 12	67 ± 8	0.222
Systolic blood pressure, mmHg	119 ± 20	140 ± 17	0.001
Diastolic blood pressure, mmHg	75 ± 11	79± 11	0.191
Left ventricular ejection fraction,%	43 ± 20	52–74 *	-
Clinical History; *n* (%)			
cHF aetiology			
Ischaemic	7 (25)	-	-
Non-ischaemic	21 (75)	-	-
Hypertensive cardiomyopathy	7 (25)	-	-
Dilated cardiomyopathy	7 (25)	-	-
Heart valve disease	7 (25)	-	-
Hypertrophic cardiomyopathy	0 (0)	-	-
Left ventricular ejection fraction			
HFpEF	14 (50)	-	-
HFrEF	14 (50)	-	-
New York Heart Association cHF stage			
NYHA I	0 (0)	-	-
NYHA II	11 (39.2)	-	-
NYHA III	17 (60.7)	-	-
NYHA IV	0 (0)	-	-
Risk factors; *n* (%)			
Smokers	0 (0)	0 (0)	-
Hypertension	18 (64.2)	10 (62.5)	0.906
Pulmonary hypertension	18 (64.2)		-
Diabetes mellitus	14 (50)	2 (12.5)	0.013
Dyslipidaemia	14 (50)	13 (81.2)	0.041
Chronic kidney disease	12 (42.8)	0 (0)	0.002
Atrial fibrillation	11 (39.2)		-
Background medication; *n* (%)			
Angiotensin-converting-enzyme inhibitors	13 (46.4)	8 (50)	0.820
Angiotensin II receptor blockers	10 (35.7)	3 (18.7)	0.235
Angiotensin receptor neprilysin inhibitors	4 (14.20)		-
Beta-blockers	24 (85.7)	1 (6.2)	0.000
Aldosterone antagonists	18 (64.2)	-	
Diuretics	26 (92.8)	1 (6.2)	0.000
Ivabradine	3 (10.7)	-	-
Statins	19 (67.8)	12 (75)	0.617
Insulin	4 (14.2)	1 (6.2)	0.419
Anti-diabetic drugs	10 (35.7)	2 (12.5)	0.096
Antiplatelet agents	7 (25)	5 (31.2)	0.654
Anticoagulants	16 (57.1)	0 (0)	0.000
Anti-arrhythmic drugs	6 (21.4)	-	-

cHF: chronic heart failure; HFpEF: heart failure with preserved ejection fraction; HFrEF: heart failure with reduced ejection fraction; NYHA: New York Heart Association; SD: standard deviation. Numbers in bold indicate statistical significance. * LVEF normal range (excerpted from https://www.ncbi.nlm.nih.gov/books/NBK459131/, on 18 January 2021).

The reference-subject group comprised 16 sex- and age-matched subjects without cHF. Baseline demographic and biochemical data, classical CV risk factors, background medication and clinical outcomes of cHF patients and reference subjects are included in Tables 4 and 5. A schematic diagram of the study design is shown in Figure 9.

Table 5. Biochemical and clinical outcomes of cHF patients in the miRNA selection.

	cHF *n* = 28
Biochiemistry; mean ± SD	
Haemoglobin, mg/dL	133 ± 19
Creatinine, mg/dL	1.24 ± 0.41
C-Reactive Protein, mg/mL	10.11 ± 12.99
NT-proBNP, pg/mL	3834 ± 4602
High-sensitive troponin T, ng/L	28 ± 17
Platelets, $10^3/mm^3$	164 ± 47
Erythrocytes, $10^6/mm^3$	4.1 ± 0.7
Leukocytes, mm^3	7723 ± 2283
Osteopontin, ng/mL	99.06 ± 35.78
Major outcomes during follow-up; *n* (%)	
Cardiovascular event [1]	12 (42.8)
Stroke	3 (10.7)
AMI	2 (7.1)
HTx	6 (21.4)
Cardiovascular death	5 (17.8)
Emergency hospital admission for cHF	9 (32.1)
Rehospitalisation for cHF	19 (67.8)
Aortic aneurism	0 (0)
Other death causes [2]	8 (28.5)

AMI: acute myocardial infarction; cHF: chronic heart failure; HTx: heart transplantation; NT-proBNP: N-terminal prohormone of brain natriuretic peptide; SD: standard deviation. [1.] Includes patients that suffered a stroke, an AMI, a cardiovascular death (mainly due to cHF), or were admitted to the emergency department. It does not include patients that underwent HTx or patients that were rehospitalised. [2.] Includes patients that died due to a septic shock, a haemorrhage, or a non-successful HTx.

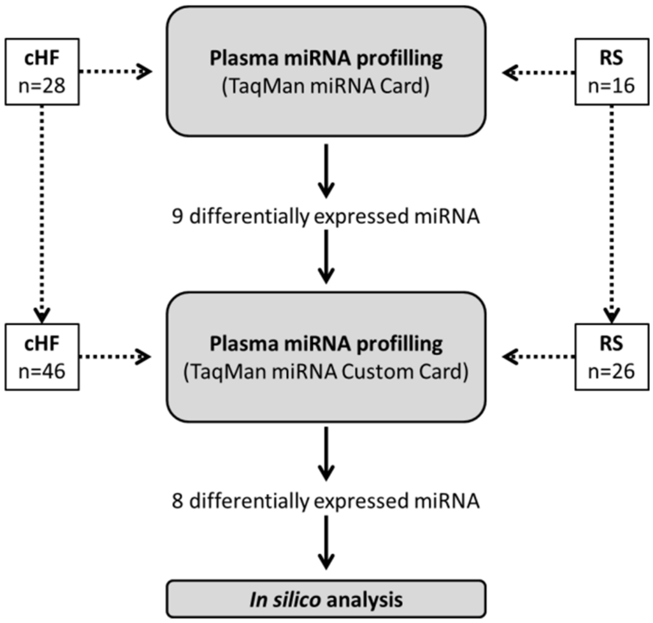

Figure 9. Schematic diagram of the study design. cHF: chronic heart failure; RS: reference subjects.

The identified differential miRNAs were validated using the quantitative Low-density Custom TaqMan® Array Advanced MicroRNA Cards in cHF patients (*n* = 58). Patients consistently expressing miRNA species in plasma were further investigated (n = 46). Samples of the reference subjects were similarly processed (n = 26). HFrEF affected 52.2% of patients, and 30.4% of cHF had ischaemic disease as the underlying cause of cHF. Clinical and biochemical characteristics, as well as clinical outcomes of these groups, are shown in Tables 6 and 7.

Table 6. Baseline characteristics of cHF patients and reference subjects in the miRNA validation.

	cHF n **= 46**	**Reference Subjects** n **= 26**	***p*-Value**
Demographic characteristics; mean ± SD			
Male/Female, n	31/15	17/9	0.862
Age, years	69 ± 11	66 ± 8	0.128
Systolic blood pressure, mmHg	118 ± 19	140 ± 18	**0.000**
Diastolic blood pressure, mmHg	75 ± 10	83 ± 14	**0.009**
Left ventricular ejection fraction, %	43 ± 17	52–74 *	
Clinical history; n (%)			
cHF aetiology			
Ischaemic	14 (30.4)	-	-
Non-ischaemic	32 (69.6)	-	-
Hypertensive cardiomyopathy	9 (19.6)	-	-
Dilated cardiomyopathy	12 (26.1)	-	-
Heart valve disease	8 (17.4)	-	-
Hypertrophic cardiomyopathy	3 (6.5)	-	-
Left ventricular ejection fraction			
HFpEF	22 (47.8)	-	-
HFrEF	24 (52.2)	-	-
New York Heart Association cHF stage			
NYHA I	0 (0)	-	-
NYHA II	17 (36.9)	-	-
NYHA III	29 (63.1)	-	-
NYHA IV	0 (0)	-	-
Risk factors; n (%)			
Smokers	1 (2.1)	4 (15.3)	**0.034**
Hypertension	34 (73.9)	16 (61.5)	0.274
Pulmonary hypertension	23 (50)	-	-
Diabetes mellitus	24 (52.2)	4 (15.3)	**0.002**
Dyslipidaemia	25 (54.3)	17 (65.3)	0.264
Chronic kidney disease	18 (39.1)	0 (0)	**0.000**
Atrial fibrillation	24 (52.2)	-	-
Background medication; n (%)			
Angiotensin-converting-enzyme inhibitors	21 (45.6)	12 (46.1)	0.967
Angiotensin II receptor blockers	14 (30.4)	5 (19.2)	0.300
Angiotensin receptor neprilysin inhibitors	5 (10.8)	-	-
Beta-blockers	40 (86.9)	1 (3.8)	**0.000**
Aldosterone antagonists	28 (60.8)	-	-
Diuretics	43 (93.4)	2 (7.6)	**0.000**
Ivabradine	4 (8.6)	-	-
Statins	32 (69.6)	15 (57.6)	0.309
Insulin	6 (13)	1 (3.8)	0.206
Anti-diabetic drugs	14 (30.4)	3 (11.5)	0.070
Antiplatelet agents	13 (28.2)	5 (19.2)	0.395
Anticoagulants	29 (63.1)	1 (3.8)	**0.000**
Anti-arrhythmic drugs	10 (21.7)	-	-

cHF: chronic heart failure; HFpEF: heart failure with preserved ejection fraction; HFrEF: heart failure with reduced ejection fraction; NYHA: New York Heart Association; SD: standard deviation. Numbers in bold indicate statistical significance. * LVEF normal range (excerpted from https://www.ncbi.nlm.nih.gov/books/NBK459131/, on 18 January 2021).

Table 7. Biochemical and clinical outcomes of cHF patients in the miRNA validation.

	cHF *n* = 46
Biochemistry; mean ± SD	
Haemoglobin, mg/dL	132 ± 19
Creatinine, mg/dL	1.27 ± 0.44
C-Reactive Protein, mg/mL	9.78 ± 15.34
NT-proBNP, pg/mL	3278 ± 3931
High-sensitive troponin T, ng/L	28 ± 17
Platelets, $10^3/mm^3$	156 ± 53
Erythrocytes, $10^6/mm^3$	4 ± 0.8
Leukocytes, mm^3	7588 ± 2064
Osteopontin, ng/mL	100.17± 41.72
Major outcomes during follow-up; *n* (%)	
Cardiovascular event [1]	24 (52.2)
Stroke	7 (15.2)
AMI	2 (4.3)
HTx	7 (15.2)
Cardiovascular death	9 (19.6)
Emergency hospital Admission for cHF	16 (34.7)
Rehospitalisation for cHF	32 (69.6)
Aortic aneurism	1 (2.1)
Other death causes [2]	11 (23.9)

AMI: acute myocardial infarction; cHF: chronic heart failure; HTx: heart transplantation; NT-proBNP: N-terminal prohormone of brain natriuretic peptide; SD: standard deviation. [1.] Includes patients that suffered a stroke, an AMI, a cardiovascular death (mainly due to cHF), or were admitted to the emergency department. It does not include patients that underwent HTx or patients that were rehospitalised. [2.] Includes patients that died due to a septic shock, a haemorrhage, or a non-successful HTx.

4.2. Blood Sampling

After 10–14 h of fasting, venous blood was withdrawn without tourniquet into 3.8% sodium citrate tubes. All samples were processed identically and within the first 2 h. Firstly, blood was centrifuged at 1560× *g* for 20 min at room temperature to eliminate blood cells and generate platelet-poor plasma (PPP). Secondly, to obtain platelet-free plasma (PFP), samples were centrifuged at 1500× *g* for 10 min at room temperature. Finally, aliquots were stored at −80 °C until miRNA analyses were performed.

4.3. miRNA Extraction, cDNA Synthesis and Analysis

The isolation of miRNA from PFP was performed using the miRNeasy Serum/Plasma Advanced kit (217201; Qiagen; Hilden, Germany) following the provider's instructions. During miRNA extraction, and according to the manufacturer's directions, all samples were spiked-in with 25 fmol of the exogenous miRNA *cel-miR-39-3p*.

miRNAs were transcribed and pre-amplified using the TaqMan™ Advanced miRNA cDNA Synthesis Kit (A28007; Applied Biosystems; Foster City, CA, USA), and then profiled. For the initial miRNA identification and selection studies, miRNAs were profiled with the Low-density TaqMan™ Advanced miRNA Human A Card (A34714; Life Technologies; Carlsbad, CA, USA). This array focuses on highly characterised miRNAs [58]. Specifically, it contains 377 different human miRNAs, including 1 endogenous control (*hsa-miR-16-5p*). Additionally, it also comprises 1 exogenous control (*cel-miR-39-3p*) and 1 negative control (*ath-miR-159a*) that does not amplify in human samples. Validated miRNAs were profiled using the Low-density Custom TaqMan® Array Advanced MicroRNA Cards (Life Technologies; Carlsbad, CA, USA) (Supplemental Table S8). Taqman RT-qPCR amplification was performed in an ABI PRISM 7900HT Sequence Detection System (Applied Biosystems; Foster City, CA, USA) and the amplification curves were analysed using the Thermo Fisher Connect Dashboard (Life Technologies; Carlsbad, CA, USA). Only miRNAs with an expression threshold below 35 Ct cycles were considered. Ct values were obtained and processed by the standard curve method and normalised with the exogenous miRNA *cel-miR-39-3p*, according to the equation $2^{-(\mathrm{Ct\,[target]}-\mathrm{Ct\,[exogenous]})}$.

4.4. In Silico Systems Biology Analysis

Putative target genes of the selected miRNAs were determined using the databases TargetScan, miRmap, miRWalk and miRDB [18–22]. Considered target genes were those with a high likelihood to be regulated by miRNA according to their search algorithms. For each miRNA, only those targets predicted in all four databases were selected for gene-network analysis.

Initial enrichment pathway analysis of curated target lists of the identified miRNAs was pursued with the web-based software ShinyGO [23]. The top-10 Gene Ontology terms, sorted by average and rank (FDR and fold), were selected.

Additionally, the curated target lists were imported into Cytoscape 3.0 (online free available platform) [25] to build protein-protein interaction (PPI) networks according to the STRING database interaction data [24]. A confidence cut-off was set to 0.8, and the maximum number of additional interactions was limited to 30. In order to identify PPI-enriched clusters, a community cluster strategy (GLay) [26] was applied to the main connected component of each network. The resulting clusters were then analysed for functional enrichments according to the pathway annotations from the KEGG database [27,28].

For individual miRNA pathway analysis, a repository-based gene database (RBGD) was created by querying "heart failure" to the STRING Pubmed database interaction data (bioinformatics tool of the Cytoscape platform). Predicted targets of selected miRNAs were then matched to the RBGD list. Common genes and their neighbour interacting genes were imported to ShinyGO for pathway enrichment analysis. A schematic diagram of the protocol used can be found in Supplemental Figure S1.

4.5. Statistical Analysis

Sample normality was assessed with the Shapiro–Wilks test. Qualitative variables were described using the number of cases and percentages and analysed with the Chi-squared test, while quantitative variables were described using the median [interquartile range] and analysed with the U Mann–Whitney test. Receiver Operating Characteristic (ROC) curve analyses and the corresponding area under the curve (AUC), along with its 95% confidence interval (CI) were calculated to determine the discrimination potential of miRNAs (patients vs. reference subjects), and AUCs values (with cut-offs $\geq$0.7 and $\leq$0.3) were used for miRNA selection. Additionally, ROC curves for predicted probabilities were pursued to identify expression thresholds of miRNAs between patients and reference subjects, between cHF types (HFpEF and HFrEF), background aetiology (ischaemic and non-ischaemic), or need for rehospitalisation during the 4–6 years of follow-up, and the corresponding area under the AUC with its 95% CI was calculated. A $p < 0.05$ was considered statistically significant. SPSS Statistical Analysis System (version 26.0, IBM Corp; Armonk, NY, USA) was utilised.

5. Conclusions

In conclusion, in this hypothesis-generating study, we have identified and validated a differential pattern of eight miRNAs that are down-regulated in the systemic circulation of cHF patients. Additionally, we have shown by in silico analysis and systems biology approaches that these miRNAs are, when considered as a cluster, involved in molecular mechanisms and signalling pathways related to cHF. Nevertheless, further research on this topic, including pursuing mechanistic studies to validate our results, is warranted to corroborate these findings as well as to improve the understanding of cHF pathophysiology.

Study Limitations

This study is not free of limitations. Comparisons were pursued between cHF and a reference group of healthy subjects. This latter group was used to determine baseline miRNA levels for comparison purposes, as there are no established "normal" miRNA levels. Further studies to identify the effect of miRNAs in other populations are warranted.

Supplementary Materials: The following supporting information can be downloaded at: https://www.mdpi.com/article/10.3390/ijms232315226/s1.

Author Contributions: Conceptualization, L.B., T.P. and S.M.; methodology, A.V.-F., A.G. and R.E.; software, A.V.-F., A.G. and R.E.; formal analysis, A.V.-F., A.G., R.E., T.P. and L.B.; investigation, T.P. and L.B.; data curation, A.V.-F., A.G., R.E., T.P. and L.B.; writing—original draft, A.V.-F., A.G., R.E., T.P. and L.B.; writing—review & editing, A.V.-F., A.G., R.E., T.P., S.M. and L.B.; supervision, T.P. and L.B.; project administration, T.P. and L.B.; funding acquisition, T.P. and L.B. All authors have read and agreed to the published version of the manuscript.

Funding: This work was supported by a Research Grant of the Spanish Society of Cardiology (SEC-2016) to L.B.; Spanish Ministry of Economy and Competitiveness of Science "Agencia Estatal de Investigación (AEI)" Proj Ref AEI/10.13039/501100011033-[PID2019-107160RB-I00] to L.B.; Institute of Health Carlos III (ISCIII) [Red RICORS TERAV-RD21/0017/0013 to L.B.; FIS PI19/01687 to T.P.]; and cofounded by FEDER "Una Manera de Hacer Europa". The H2020-JTI-IMI2-2017-13-two-stage Project "TRANSBIOLINE 821283" to L.B. & T.P. We thank Fundación Jesus Serra and Fundación de Investigación Cardiovascular (Barcelona, Spain) for their continuous support. A.V.-F. is a pre-doctoral fellow recipient of a research contract from the Cardiovascular Program-ICCC (IR-HSCSP). A.G. is a pre-doctoral fellow from BES-2017-081378.

Institutional Review Board Statement: The local ethics committee for clinical research approved the study (Ref. 16/44). Written informed consent was obtained from all participants before the initiation of the study and all research was conducted following the Declaration of Helsinki.

Informed Consent Statement: Informed consent was obtained from all subjects involved in the study before inclusion.

Data Availability Statement: The data that support the findings of this study are available from the corresponding author upon reasonable request.

Acknowledgments: We are indebted to heart failure patients for their participation in the study and the physicians that contributed to recruitment. This work has been performed under the framework of the Doctoral Program in Biomedicine, Biochemistry and Molecular Biology of the Universitat Autònoma de Barcelona.

Conflicts of Interest: L.B. declares to have acted as a SAB member of Sanofi, Ionnis, Pfizer and NovoNordisk; to have a Research Grant from AstraZeneca; to have received speaker fees from Sanofi and Bayer and to have founded the Spin-offs Glycardial Diagnostics SL and Ivastatin Therapeutics S (all unrelated to this work). T.P. declares to be a co-founder of the Spin-offs Glycardial Diagnostics SL and Ivastatin Therapeutics S (all unrelated to this work). The remaining authors have nothing to disclose.

References

1. Ponikowski, P.; Voors, A.A.; Anker, S.D.; Bueno, H.; Cleland, J.G.F.; Coats, A.J.S.; Falk, V.; González-Juanatey, J.R.; Harjola, V.P.; Jankowska, E.A.; et al. 2016 ESC Guidelines for the Diagnosis and Treatment of Acute and Chronic Heart Failure. *Eur. Heart J.* **2016**, *37*, 2129–2200. [CrossRef] [PubMed]
2. Groenewegen, A.; Rutten, F.H.; Mosterd, A.; Hoes, A.W. Epidemiology of Heart Failure. *Eur. J. Heart Fail.* **2020**, *22*, 1342–1356. [CrossRef] [PubMed]
3. Kemp, C.D.; Conte, J.V. The Pathophysiology of Heart Failure. *Cardiovasc. Pathol.* **2012**, *21*, 365–371. [CrossRef] [PubMed]
4. Pfeffer, M.A.; Shah, A.M.; Borlaug, B.A. Heart Failure with Preserved Ejection Fraction in Perspective. *Circ. Res.* **2019**, *124*, 1598–1617. [CrossRef] [PubMed]
5. Capote, L.; Nyakundi, R.; Martinez, B.; Lymperopoulos, A. Pathophysiology of Heart Failure. In *Pathophysiology and Pharmacotherapy of Cardiovascular Disease*; Springer International Publishing: Cham, Switzerland, 2015; pp. 37–55. ISBN 9783319159614.
6. Liang, J.; Bai, S.; Su, L.; Li, C.; Wu, J.; Xia, Z.; Xu, D. A Subset of Circulating MicroRNAs Is Expressed Differently in Patients with Myocardial Infarction. *Mol. Med. Rep.* **2015**, *12*, 243–247. [CrossRef]
7. Finicelli, M.; Squillaro, T.; Galderisi, U.; Peluso, G. Micro-RNAs: Crossroads between the Exposure to Environmental Particulate Pollution and the Obstructive Pulmonary Disease. *Int. J. Mol. Sci.* **2020**, *21*, 7221. [CrossRef]

8. Luo, F.; Liu, W.; Bu, H. MicroRNAs in Hypertrophic Cardiomyopathy: Pathogenesis, Diagnosis, Treatment Potential and Roles as Clinical Biomarkers. *Heart Fail. Rev.* **2022**, *27*, 2211–2221. [CrossRef]
9. Jiao, M.; You, H.-Z.; Yang, X.-Y.; Yuan, H.; Li, Y.-L.; Liu, W.-X.; Jin, M.; Du, J. Circulating MicroRNA Signature for the Diagnosis of Childhood Dilated Cardiomyopathy. *Sci. Rep.* **2018**, *8*, 724. [CrossRef]
10. Li, M.; Zhang, J. Circulating MicroRNAs: Potential and Emerging Biomarkers for Diagnosis of Cardiovascular and Cerebrovascular Diseases. *Biomed Res. Int.* **2015**, *2015*, 730535. [CrossRef]
11. O'Brien, J.; Hayder, H.; Zayed, Y.; Peng, C. Overview of MicroRNA Biogenesis, Mechanisms of Actions, and Circulation. *Front. Endocrinol. (Lausanne).* **2018**, *9*, 402. [CrossRef]
12. De Rosa, R.; Polito, M.V.; Benvenga, R.; De Angelis, E.; Piscione, F.; Galasso, G. MicroRNAs and Cardiovascular Diseases: From Bench to Bedside. *Transl. Med. @ UniSa* **2017**, *17*, 12–18.
13. Deng, J.; Zhong, Q. Advanced Research on the MicroRNA Mechanism in Heart Failure. *Int. J. Cardiol.* **2016**, *220*, 61–64. [CrossRef]
14. Zhao, Y.; Yan, M.; Chen, C.; Gong, W.; Yin, Z.; Li, H.; Fan, J.; Zhang, X.A.; Wang, D.W.; Zuo, H. MiR-124 Aggravates Failing Hearts by Suppressing CD151-Facilitated Angiogenesis in Heart. *Oncotarget* **2018**, *9*, 14382–14396. [CrossRef]
15. Tijsen, A.J.; Creemers, E.E.; Moerland, P.D.; De Windt, L.J.; Van Der Wal, A.C.; Kok, W.E.; Pinto, Y.M. MiR423-5p as a Circulating Biomarker for Heart Failure. *Circ. Res.* **2010**, *106*, 1035–1039. [CrossRef]
16. Escate, R.; Padró, T.; Suades, R.; Camino, S.; Muñiz, O.; Diaz-Diaz, J.L.; Sionis, A.; Mata, P.; Badimon, L. High MiR-133a Levels in the Circulation Anticipates Presentation of Clinical Events in Familial Hypercholesterolaemia Patients. *Cardiovasc. Res.* **2021**, *117*, 109–122. [CrossRef]
17. Obad, S.; dos Santos, C.O.; Petri, A.; Heidenblad, M.; Broom, O.; Ruse, C.; Fu, C.; Lindow, M.; Stenvang, J.; Straarup, E.M.; et al. Silencing of MicroRNA Families by Seed-Targeting Tiny LNAs. *Nat. Genet.* **2011**, *43*, 371–378. [CrossRef] [PubMed]
18. Agarwal, V.; Bell, G.W.; Nam, J.-W.; Bartel, D.P. Predicting Effective MicroRNA Target Sites in Mammalian MRNAs. *Elife* **2015**, *4*, e05005. [CrossRef]
19. Vejnar, C.E.; Zdobnov, E.M. MiRmap: Comprehensive Prediction of MicroRNA Target Repression Strength. *Nucleic Acids Res.* **2012**, *40*, 11673–11683. [CrossRef] [PubMed]
20. Liu, W.; Wang, X. Prediction of Functional MicroRNA Targets by Integrative Modeling of MicroRNA Binding and Target Expression Data. *Genome Biol.* **2019**, *20*, 18. [CrossRef]
21. Chen, Y.; Wang, X. MiRDB: An Online Database for Prediction of Functional MicroRNA Targets. *Nucleic Acids Res.* **2020**, *48*, D127–D131. [CrossRef] [PubMed]
22. Sticht, C.; De La Torre, C.; Parveen, A.; Gretz, N. MiRWalk: An Online Resource for Prediction of MicroRNA Binding Sites. *PLoS ONE* **2018**, *13*, e0206239. [CrossRef] [PubMed]
23. Ge, S.X.; Jung, D.; Yao, R. ShinyGO: A Graphical Gene-Set Enrichment Tool for Animals and Plants. *Bioinformatics* **2020**, *36*, 2628–2629. [CrossRef] [PubMed]
24. Szklarczyk, D.; Gable, A.L.; Nastou, K.C.; Lyon, D.; Kirsch, R.; Pyysalo, S.; Doncheva, N.T.; Legeay, M.; Fang, T.; Bork, P.; et al. The STRING Database in 2021: Customizable Protein-Protein Networks, and Functional Characterization of User-Uploaded Gene/Measurement Sets. *Nucleic Acids Res.* **2021**, *49*, D605–D612. [CrossRef]
25. Shannon, P.; Markiel, A.; Ozier, O.; Baliga, N.S.; Wang, J.T.; Ramage, D.; Amin, N.; Schwikowski, B.; Ideker, T. Cytoscape: A Software Environment for Integrated Models of Biomolecular Interaction Networks. *Genome Res.* **2003**, *13*, 2498–2504. [CrossRef] [PubMed]
26. Su, G.; Kuchinsky, A.; Morris, J.H.; States, D.J.; Meng, F. GLay: Community Structure Analysis of Biological Networks. *Bioinformatics* **2010**, *26*, 3135–3137. [CrossRef]
27. Kanehisa, M.; Goto, S. KEGG: Kyoto Encyclopedia of Genes and Genomes. *Nucleic Acids Res.* **2000**, *28*, 27–30. [CrossRef]
28. Kanehisa, M.; Furumichi, M.; Sato, Y.; Ishiguro-Watanabe, M.; Tanabe, M. KEGG: Integrating Viruses and Cellular Organisms. *Nucleic Acids Res.* **2021**, *49*, D545–D551. [CrossRef]
29. Marques, F.Z.; Vizi, D.; Khammy, O.; Mariani, J.A.; Kaye, D.M. The Transcardiac Gradient of Cardio-MicroRNAs in the Failing Heart. *Eur. J. Heart Fail.* **2016**, *18*, 1000–1008. [CrossRef]
30. Ellis, K.L.; Cameron, V.A.; Troughton, R.W.; Frampton, C.M.; Ellmers, L.J.; Richards, A.M. Circulating MicroRNAs as Candidate Markers to Distinguish Heart Failure in Breathless Patients. *Eur. J. Heart Fail.* **2013**, *15*, 1138–1147. [CrossRef] [PubMed]
31. Scrutinio, D.; Conserva, F.; Passantino, A.; Iacoviello, M.; Lagioia, R.; Gesualdo, L. Circulating MicroRNA-150-5p as a Novel Biomarker for Advanced Heart Failure: A Genome-Wide Prospective Study. *J. Hear. Lung Transplant.* **2017**, *36*, 616–624. [CrossRef]
32. Lin, X.; Zhang, S.; Huo, Z. Serum Circulating MiR-150 Is a Predictor of Post-Acute Myocardial Infarction Heart Failure. *Int. Heart J.* **2019**, *60*, 280–286. [CrossRef] [PubMed]
33. Mompeón, A.; Ortega-Paz, L.; Vidal-Gómez, X.; Costa, T.J.; Pérez-Cremades, D.; Garcia-Blas, S.; Brugaletta, S.; Sanchis, J.; Sabate, M.; Novella, S.; et al. Disparate MiRNA Expression in Serum and Plasma of Patients with Acute Myocardial Infarction: A Systematic and Paired Comparative Analysis. *Sci. Rep.* **2020**, *10*, 5373. [CrossRef] [PubMed]
34. Voellenkle, C.; van Rooij, J.; Cappuzzello, C.; Greco, S.; Arcelli, D.; Di Vito, L.; Melillo, G.; Rigolini, R.; Costa, E.; Crea, F.; et al. MicroRNA Signatures in Peripheral Blood Mononuclear Cells of Chronic Heart Failure Patients. *Physiol. Genom.* **2010**, *42*, 420–426. [CrossRef]
35. Ming, S.; Shui-yun, W.; Wei, Q.; Jian-hui, L.; Ru-tai, H.; Lei, S.; Mei, J.; Hui, W.; Ji-zheng, W. MiR-139-5p Inhibits Isoproterenol-Induced Cardiac Hypertrophy by Targetting c-Jun. *Biosci. Rep.* **2018**, *38*, BSR20171430. [CrossRef]

36. Nakamura, M.; Sadoshima, J. Mechanisms of Physiological and Pathological Cardiac Hypertrophy. *Nat. Rev. Cardiol.* **2018**, *15*, 387–407. [CrossRef]
37. Rech, M.; Kuhn, A.R.; Lumens, J.; Carai, P.; van Leeuwen, R.; Verhesen, W.; Verjans, R.; Lecomte, J.; Liu, Y.; Luiken, J.J.F.P.; et al. AntagomiR-103 and -107 Treatment Affects Cardiac Function and Metabolism. *Mol. Ther. Nucleic Acids* **2019**, *14*, 424–437. [CrossRef] [PubMed]
38. Li, Y.; Mao, L.; Gao, Y.; Baral, S.; Zhou, Y.; Hu, B. MicroRNA-107 Contributes to Post-Stroke Angiogenesis by Targeting Dicer-1. *Sci. Rep.* **2015**, *5*, 13316. [CrossRef]
39. Kulshreshtha, R.; Ferracin, M.; Wojcik, S.E.; Garzon, R.; Alder, H.; Agosto-Perez, F.J.; Davuluri, R.; Liu, C.-G.; Croce, C.M.; Negrini, M.; et al. A MicroRNA Signature of Hypoxia. *Mol. Cell. Biol.* **2007**, *27*, 1859–1867. [CrossRef]
40. Fan, Q.; Wu, M.; Li, C.; Li, J. MiR-107 Aggravates Oxygen-Glucose Deprivation/Reoxygenation (OGD/R)-Induced Injury Through Inactivating PI3K-AKT Signalling Pathway by Targeting FGF9/FGF12 in PC12 Cells. *J. Stroke Cerebrovasc. Dis.* **2022**, *31*, 106295. [CrossRef]
41. Niu, C.-C.; Lin, S.-S.; Yuan, L.-J.; Lu, M.-L.; Ueng, S.W.N.; Yang, C.-Y.; Tsai, T.-T.; Lai, P.-L. Upregulation of MiR-107 Expression Following Hyperbaric Oxygen Treatment Suppresses HMGB1/RAGE Signaling in Degenerated Human Nucleus Pulposus Cells. *Arthritis Res. Ther.* **2019**, *21*, 42. [CrossRef]
42. Charrier, H.; Cuvelliez, M.; Dubois-Deruy, E.; Mulder, P.; Richard, V.; Bauters, C.; Pinet, F. Integrative System Biology Analyses Identify Seven MicroRNAs to Predict Heart Failure. *Non-Coding RNA* **2019**, *5*, 22. [CrossRef] [PubMed]
43. An, F.; Yin, Y.; Ju, W. Long Noncoding RNA DANCR Expression and Its Predictive Value in Patients with Atherosclerosis. *Bioengineered* **2022**, *13*, 6919–6928. [CrossRef] [PubMed]
44. Long, X.; Huang, Y.; He, J.; Zhang, X.; Zhou, Y.; Wei, Y.; Tang, Y.; Liu, L. Upregulation of MiR-335 Exerts Protective Effects against Sepsis-induced Myocardial Injury. *Mol. Med. Rep.* **2021**, *24*, 806. [CrossRef] [PubMed]
45. Ma, H.; Ye, P.; Zhang, A.K.; Yu, W.D.; Lin, S.; Zheng, Y.G. Upregulation of MiR-335-5p Contributes to Right Ventricular Remodeling via Calumenin in Pulmonary Arterial Hypertension. *Biomed Res. Int.* **2022**, *2022*, 9294148. [CrossRef] [PubMed]
46. Sun, B.; Meng, M.; Wei, J.; Wang, S. Long Noncoding RNA PVT1 Contributes to Vascular Endothelial Cell Proliferation via Inhibition of MiR-190a-5p in Diagnostic Biomarker Evaluation of Chronic Heart Failure. *Exp. Ther. Med.* **2020**, *19*, 3348–3354. [CrossRef] [PubMed]
47. Vegter, E.L.; Ovchinnikova, E.S.; Sillj, H.H.W.; Meems, L.M.G.; Van Der Pol, A.; Van Der Velde, A.R.; Berezikov, E.; Voors, A.A.; Boer, R.A.D.; Van Der Meer, P. Rodent Heart Failure Models Do Not Reflect the Human Circulating MicroRNA Signature in Heart Failure. *PLoS ONE* **2017**, *12*, e0177242. [CrossRef] [PubMed]
48. Matsuda, T.; Jeong, J.I.; Ikeda, S.; Yamamoto, T.; Gao, S.; Babu, G.J.; Zhai, P.; Del Re, D.P. H-Ras Isoform Mediates Protection Against Pressure Overload-Induced Cardiac Dysfunction in Part Through Activation of AKT. *Circ. Hear. Fail.* **2017**, *10*, e003658. [CrossRef] [PubMed]
49. Qin, W.; Cao, L.; Massey, I.Y. Role of PI3K/Akt Signaling Pathway in Cardiac Fibrosis. *Mol. Cell. Biochem.* **2021**, *476*, 4045–4059. [CrossRef] [PubMed]
50. Ghafouri-Fard, S.; Khanbabapour Sasi, A.; Hussen, B.M.; Shoorei, H.; Siddiq, A.; Taheri, M.; Ayatollahi, S.A. Interplay between PI3K/AKT Pathway and Heart Disorders. *Mol. Biol. Rep.* **2022**, *49*, 9767–9781. [CrossRef] [PubMed]
51. Frangogiannis, N.G. Cardiac Fibrosis. *Cardiovasc. Res.* **2021**, *117*, 1450–1488. [CrossRef]
52. Hanna, A.; Frangogiannis, N.G. Inflammatory Cytokines and Chemokines as Therapeutic Targets in Heart Failure. *Cardiovasc. Drugs Ther.* **2020**, *34*, 849–863. [CrossRef]
53. Vilella-Figuerola, A.; Padró, T.; Roig, E.; Mirabet, S.; Badimon, L. New Factors in Heart Failure Pathophysiology: Immunity Cells Release of Extracellular Vesicles. *Front. Cardiovasc. Med.* **2022**, *9*, 939625. [CrossRef] [PubMed]
54. Miranda-Silva, D.; Lima, T.; Rodrigues, P.; Leite-Moreira, A.; Falcão-Pires, I. Mechanisms Underlying the Pathophysiology of Heart Failure with Preserved Ejection Fraction: The Tip of the Iceberg. *Heart Fail. Rev.* **2021**, *26*, 453–478. [CrossRef]
55. Petersen, K.M.; Bøgevig, S.; Holst, J.J.; Knop, F.K.; Christensen, M.B. Hemodynamic Effects of Glucagon: A Literature Review. *J. Clin. Endocrinol. Metab.* **2018**, *103*, 1804–1812. [CrossRef] [PubMed]
56. Kintscher, U.; Foryst-Ludwig, A.; Haemmerle, G.; Zechner, R. The Role of Adipose Triglyceride Lipase and Cytosolic Lipolysis in Cardiac Function and Heart Failure. *Cell Rep. Med.* **2020**, *1*, 100001. [CrossRef]
57. Nakamura, M.; Odanovic, N.; Nakada, Y.; Dohi, S.; Zhai, P.; Ivessa, A.; Yang, Z.; Abdellatif, M.; Sadoshima, J. Dietary Carbohydrates Restriction Inhibits the Development of Cardiac Hypertrophy and Heart Failure. *Cardiovasc. Res.* **2021**, *117*, 2365–2376. [CrossRef]
58. Kozomara, A.; Birgaoanu, M.; Griffiths-Jones, S. MiRBase: From MicroRNA Sequences to Function. *Nucleic Acids Res.* **2019**, *47*, D155–D162. [CrossRef] [PubMed]

SUPPLEMENTAL MATERIAL

Systems Biology in Chronic Heart Failure – Identification of Potential miRNAs Regulators

Vilella-Figuerola A[1,2], Gallinat A[1,2], Escate R[1,3], Mirabet S[3,4], Padró T[1,3,†] Badimon L[1,3,5,†*]

[1]Cardiovascular-Program-ICCC, IR-Hospital Santa Creu i Sant Pau, IIB-Sant Pau, Barcelona, Spain
[2]Biochemistry and Molecular Biology Department, Universitat Autònoma de Barcelona (UAB), Barcelona, Spain
[3]Centro de Investigación Biomédica en Red Cardiovascular, Instituto de Salud Carlos III, Madrid, Spain
[4]Heart Failure Group, Cardiology Department, Hospital Santa Creu i Sant Pau, Barcelona, Spain
[5]UAB-Chair Cardiovascular Research, Barcelona, Spain
[†]This authors contributed equally to this work.

***Correspondence**:
Prof. Lina Badimon
lbadimon@santpau.cat
Cardiovascular Program-ICCC
Research Institute Hospital de la Santa Creu i Sant Pau
Sant Antoni M[a] Claret 167, 08025 Barcelona, Spain
Phone: +34.935565882
Fax: +34.935565559

Keywords: miRNA, chronic heart failure, network, enrichment pathways, pathophysiology

SUPPLEMENTAL FIGURES

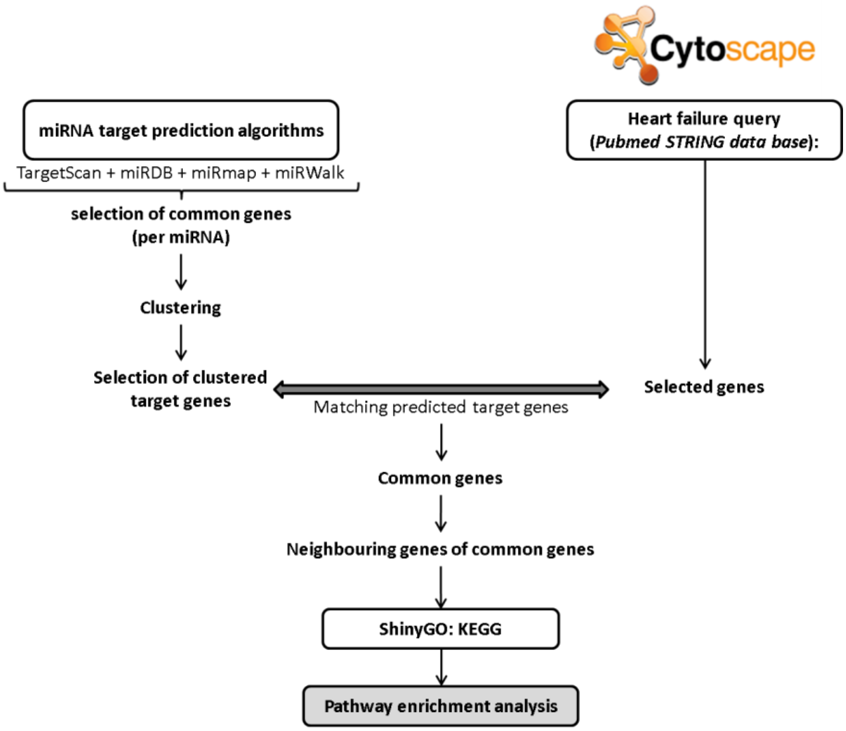

Supplemental Figure S1: Schematic representation of the *in silico* analysis of individual miRNAs.

SUPPLEMENTAL TABLES

Supplemental Table S1: miRNA selection strategy

	Fold-change (log_2)	AUC±SD (95% CI)	P-value	Same family	miRBase reads	Quartile reads
let-7a-5p	**−1.777**	**0.842±0.063 (0.718–0.966)**	**0.001**	**1**	**215,985,765**	**4**
miR-485-5p	−3.245	0.823±0.085 (0.657–0.989)	0.004	0	3,168	1
miR-342-3p	**−1.675**	**0.772±0.079 (0.617–0.928)**	**0.005**	**0**	**484,947**	**3**
miR-30b-5p	**−1.058**	**0.760±0.087 (0.590–0.931)**	**0.011**	**0**	**1,110,974**	**3**
miR-335-5p	**−0.995**	**0.749±0.086 (0.582–0.917)**	**0.012**	**0**	**416,898**	**3**
miR-125a-5p	**−0.957**	**0.748±0.080 (0.591–0.906)**	**0.012**	**0**	**1,146,942**	**3**
miR-150-5p	**−1.270**	**0.747±0.078 (0.594–0.900)**	**0.010**	**0**	**117,587**	**2**
miR-337-5p	−1.548	0.741±0.093 (0.558–0.923)	0.020	0	4,424	1
miR-224-5p	**−1.370**	**0.741±0.095 (0.555–0.926)**	**0.020**	**0**	**74,998**	**2**
miR-494-3p	−1.223	0.740±0.085 (0.574–0.907)	0.018	0	11,622	1
let-7g-5p	−0.791	0.739±0.082 (0.579–0.899)	0.016	1	50,508,337	4
let-7f-5p	−0.973	0.739±0.082 (0.579–0.899)	0.016	1	115,380,455	4
miR-107	**−0.968**	**0.737±0.090 (0.561–0.913)**	**0.018**	**0**	**5,491,348**	**4**
miR-495-3p	−0.894	0.730±0.087 (0.560–0.900)	0.021	0	20,270	1
miR-139-5p	**−1.299**	**0.729±0.088 (0.555–0.902)**	**0.028**	**0**	**85,265**	**2**
miR-301a-3p	−1.168	0.726±0.096 (0.539–0.914)	0.034	0	81,204	2
miR-26a-5p	−0.558	0.726±0.086 (0.557–0.895)	0.024	0	28,542,742	4
miR-328-3p	−0.740	0.722±0.097 (0.532–0.911)	0.032	0	26,824	1
miR-142-3p	−0.840	0.720±0.082 (0.559–0.881)	0.019	0	160,986	3
miR-377-3p	−1.001	0.701±0.087 (0.530–0.872)	0.044	0	4,424	1
miR-374b-5p	−0.593	0.701±0.088 (0.530–0.873)	0.044	0	491,420	3
miR-369-3p	−1.062	0.701±0.095 (0.514–0.887)	0.043	0	11,211	1
miR-574-3p	−0.763	0.700±0.092 (0.521–0.879)	0.050	0	125,985	3
miR-323a-3p	−0.659	0.697±0.091 (0.518–0.875)	0.049	0	603	1
miR-451a	0.421	0.286±0.080 (0.130–0.442)	0.021	0	1,666,621	4
miR-424-5p	0.726	0.269±0.080 (0.113–0.426)	0.016	0	861,807	3
miR-660-5p	0.591	0.263±0.085 (0.096–0.431)	0.017	0	91,879	2
miR-210-3p	1.137	0.253±0.091 (0.075–0.432)	0.023	0	66,359	2

AUC: area under the curve; **CI**: confidence interval; **SD**: standard deviation. **In bold**: selected miRNAs.
Selection strategy: 1) Selection of top 15 best miRNAs according to AUC and fold-change. 2) Elimination of miRNAs from the same family (miRNAs with better AUC selected). 3) Elimination of miRNAs with low number of reads (4^{th} quantile).

Supplemental Table S2: Expression values of analysed miRNAs

miRNA	CTL (*n*=26) median [IQR]	cHF (*n*=46) median [IQR]	*p*-value	Fold-change (log_2)
let-7a-5p	0.00045 [0.00008–0.00158]	0.00012 [0.00003–0.0003]	**0.004**	0.266 (−1.911)
miR-107	0.00004 [0.00002–0.0001]	0.00002 [0.000003–0.00005]	**0.044**	0.620 (−0.689)
miR-125a-5p	0.00121 [0.00041–0.00167]	0.00031 [0.00012–0.00059]	**0.002**	0.252 (−1.987)
miR-139-5p	0.00006 [0.00002–0.00013]	0.00003 [0.00001–0.00005]	**0.006**	0.456 (−1.133)
miR-150-5p	0.00521 [0.00288–0.0088]	0.0021 [0.00083–0.00372]	**0.000**	0.403 (−1.312)
miR-30b-5p	0.00123 [0.00077–0.0042]	0.00053 [0.00032–0.00136]	**0.007**	0.430 (−1.217)
miR-335-5p	0.00165 [0.00021–0.00331]	0.00065 [0.00019–0.00107]	**0.048**	0.397 (−1.334)
miR-342-3p	0.0017 [0.00092–0.00338]	0.00045 [0.00013–0.00087]	**0.000**	0.264 (−1.921)
miR-224-5p	0.00006 [0.00002–0.00019]	0.00003 [0.00001–0.00007]	0.079	0.486 (−1.040)
miR-16-5p	0.00603 [0.0027–0.00943]	0.00511 [0.00249–0.00843]	0.694	0.847 (−0.240)
miR-223-3p	0.0243 [0.01047–0.03971]	0.01508 [0.00857–0.03479]	0.226	0.621 (−0.688)

cHF: chronic heart failure; **CTL**: controls; **IQR**: interquartile range
Bold indicates statistical significance.

Supplemental Table S3: Pathways identified by enrichment analysis included in Figure 3

	DESCRIPTION - KEGG	FDR value	Genes (background genes)	Fold enrichment
CLUSTER 1				
hsa04510	Focal adhesion	$5.52x10^{-21}$	21 (198)	10.61
hsa04062	Chemokine signalling pathway	$3.89x10^{-20}$	20 (186)	10.75
hsa04014	Ras signalling pathway	$4.27x10^{-20}$	21 (226)	9.29
hsa04151	PI3K-Akt signalling pathway	$4.67x10^{-19}$	23 (350)	6.57
hsa04917	Prolactin signalling pathway	$1.60x10^{-17}$	14 (69)	20.29
hsa01522	Endocrine resistance	$2.05x10^{-17}$	15 (95)	15.79
hsa04926	Relaxin signalling pathway	$3.37x10^{-17}$	16 (128)	12.5
hsa04915	Oestrogen signalling pathway	$1.66x10^{-15}$	15 (133)	11.28
hsa01521	EGFR tyrosine kinase inhibitor resistance	$2.11x10^{-15}$	13 (78)	16.67
hsa04012	ErbB signalling pathway	$4.02x10^{-15}$	13 (83)	15.66
hsa04935	Growth hormone synthesis, secretion and action	$8.07x10^{-15}$	14 (118)	11.86
hsa04015	Rap1 signalling pathway	$1.82x10^{-14}$	16 (202)	7.92
hsa04810	Regulation of actin cytoskeleton	$2.82x10^{-14}$	16 (209)	7.66
hsa04722	Neurotrophin signalling pathway	$1.24x10^{-13}$	13 (114)	11.4
hsa04912	GnRH signalling pathway	$2.20x10^{-13}$	12 (89)	13.48
hsa04933	AGE-RAGE signalling pathway in diabetic complications	$5.44x10^{-13}$	12 (98)	12.24
hsa04910	Insulin signalling pathway	$6.05x10^{-13}$	13 (133)	9.77
hsa04010	MAPK signalling pathway	$1.77x10^{-12}$	16 (288)	5.56
hsa04370	VEGF signalling pathway	$2.44x10^{-12}$	10 (57)	17.54
hsa04071	Sphingolipid signalling pathway	$2.53x10^{-12}$	12 (116)	10.34
hsa04919	Thyroid hormone signalling pathway	$3.24x10^{-12}$	12 (119)	10.08
hsa04611	Platelet activation	$4.01x10^{-12}$	12 (122)	9.84
hsa04068	FoxO signalling pathway	$6.05x10^{-12}$	12 (127)	9.45
hsa04520	Adherens junction	$8.53x10^{-12}$	10 (67)	14.93
hsa04660	T cell receptor signalling pathway	$1.30x10^{-11}$	11 (101)	10.89
hsa04550	Signalling pathways regulating pluripotency of stem cells	$1.54x10^{-11}$	12 (140)	8.57
hsa04921	Oxytocin signalling pathway	$2.84x10^{-11}$	12 (149)	8.05
hsa04664	Fc epsilon RI signalling pathway	$1.92x10^{-10}$	9 (66)	13.64
hsa04625	C-type lectin receptor signalling pathway	$2.67x10^{-10}$	10 (102)	9.8
hsa04072	Phospholipase D signalling pathway	$3.70x10^{-10}$	11 (147)	7.48
hsa04150	mTOR signalling pathway	$4.77x10^{-10}$	11 (151)	7.28
hsa04540	Gap junction	$1.43x10^{-09}$	9 (87)	10.34
hsa05418	Fluid shear stress and atherosclerosis	$2.03x10^{-09}$	10 (130)	7.69
hsa04371	Apelin signalling pathway	$2.14x10^{-09}$	10 (131)	7.63
hsa04929	GnRH secretion	$3.09x10^{-09}$	8 (63)	12.7
hsa04670	Leukocyte transendothelial migration	$8.23x10^{-09}$	9 (109)	8.26
hsa04662	B cell receptor signalling pathway	$1.36x10^{-08}$	8 (78)	10.26
hsa04720	Long-term potentiation	$8.54x10^{-08}$	7 (64)	10.94
hsa04024	cAMP signalling pathway	$1.16x10^{-07}$	10 (208)	4.81
hsa04650	Natural killer cell mediated cytotoxicity	$2.93x10^{-07}$	8 (121)	6.61
hsa04210	Apoptosis	$5.46x10^{-07}$	8 (132)	6.06
hsa04211	Longevity regulating pathway	$5.58x10^{-07}$	7 (87)	8.05
hsa04270	Vascular smooth muscle contraction	$5.64x10^{-07}$	8 (133)	6.02
hsa04530	Tight junction	$1.76x10^{-06}$	8 (156)	5.13
hsa04144	Endocytosis	$4.14x10^{-06}$	9 (241)	3.73
hsa04666	Fc gamma R-mediated phagocytosis	$1.18x10^{-05}$	6 (90)	6.67
hsa04723	Retrograde endocannabinoid signalling	$1.32x10^{-05}$	7 (145)	4.83
hsa04218	Cellular senescence	$1.61x10^{-05}$	7 (150)	4.67
hsa05142	Chagas disease	$1.91x10^{-05}$	6 (99)	6.06
hsa04928	Parathyroid hormone synthesis, secretion and action	$2.34x10^{-05}$	6 (103)	5.83
hsa04022	cGMP-PKG signalling pathway	$2.53x10^{-05}$	7 (162)	4.32
hsa04066	HIF-1 signalling pathway	$2.69x10^{-05}$	6 (106)	5.66
hsa04668	TNF signalling pathway	$3.52x10^{-05}$	6 (112)	5.36
hsa04960	Aldosterone-regulated sodium reabsorption	$8.51x10^{-05}$	4 (37)	10.81
hsa04261	Adrenergic signalling in cardiomyocytes	$1.50x10^{-04}$	6 (147)	4.08
hsa04657	IL-17 signalling pathway	$1.80x10^{-04}$	5 (92)	5.43
hsa04930	Type II diabetes mellitus	$1.80x10^{-04}$	4 (46)	8.7

	DESCRIPTION - KEGG	FDR value	Genes (background genes)	Fold enrichment
hsa04750	Inflammatory mediator regulation of TRP channels	$1.90x10^{-04}$	5 (94)	5.32
hsa04630	JAK-STAT signalling pathway	$2.20x10^{-04}$	6 (160)	3.75
hsa04620	Toll-like receptor signalling pathway	$2.60x10^{-04}$	5 (101)	4.95
hsa04659	Th17 cell differentiation	$2.60x10^{-04}$	5 (101)	4.95
hsa01524	Platinum drug resistance	$7.90x10^{-04}$	4 (70)	5.71
hsa04918	Thyroid hormone synthesis	$9.60x10^{-04}$	4 (74)	5.41
hsa05412	Arrhythmogenic right ventricular cardiomyopathy	0.001	4 (76)	5.26
hsa04310	Wnt signalling pathway	0.0016	5 (154)	3.25
hsa04350	TGF-β signalling pathway	0.0019	4 (91)	4.4
hsa05414	Dilated cardiomyopathy	0.0022	4 (95)	4.21
hsa04621	NOD-like receptor signalling pathway	0.0026	5 (174)	2.87
hsa04931	Insulin resistance	0.0034	4 (107)	3.74
hsa04961	Endocrine and other factor-regulated calcium reabsorption	0.0045	3 (53)	5.66
hsa04923	Regulation of lipolysis in adipocytes	0.0047	3 (54)	5.56
hsa04152	AMPK signalling pathway	0.0049	4 (120)	3.33
hsa05017	Spinocerebellar ataxia	0.0074	4 (135)	2.96
hsa04714	Thermogenesis	0.008	5 (229)	2.18
hsa04920	Adipocytokine signalling pathway	0.0088	3 (69)	4.35
hsa04141	Protein processing in endoplasmic reticulum	0.0142	4 (165)	2.42
hsa04658	Th1 and Th2 cell differentiation	0.0158	3 (87)	3.45
hsa04512	ECM-receptor interaction	0.0162	3 (88)	3.41
hsa05410	Hypertrophic cardiomyopathy	0.0166	3 (89)	3.37
hsa04922	Glucagon signalling pathway	0.0229	3 (101)	2.97
hsa04973	Carbohydrate digestion and absorption	0.0375	2 (44)	4.55
CLUSTER 2				
hsa04110	Cell cycle	$3.13x10_{-14}$	14 (120)	11.67
hsa04218	Cellular senescence	$7.40x10_{-11}$	12 (150)	8
hsa04350	TGF-β signalling pathway	$2.47x10_{-10}$	10 (91)	10.99
hsa04659	Th17 cell differentiation	$2.89x10_{-07}$	8 (101)	7.92
hsa04550	Signalling pathways regulating pluripotency of stem cells	$2.12x10^{-06}$	8 (140)	5.71
hsa01522	Endocrine resistance	$2.58x10^{-06}$	7 (95)	7.37
hsa04310	Wnt signalling pathway	$3.76x10^{-06}$	8 (154)	5.19
hsa04919	Thyroid hormone signalling pathway	$9.76x10^{-06}$	7 (119)	5.88
hsa04068	FoxO signalling pathway	$1.38x10^{-05}$	7 (127)	5.51
hsa04330	Notch signalling pathway	$3.56x10^{-05}$	5 (52)	9.62
hsa04390	Hippo signalling pathway	$3.56x10^{-05}$	7 (153)	4.58
hsa04933	AGE-RAGE signalling pathway in diabetic complications	$3.56x10^{-05}$	6 (98)	6.12
hsa04520	Adherens junction	$9.10x10^{-05}$	5 (67)	7.46
hsa04371	Apelin signalling pathway	0.0017	5 (131)	3.82
hsa04917	Prolactin signalling pathway	0.0017	4 (69)	5.8
hsa04115	p53 signalling pathway	0.0019	4 (72)	5.56
hsa04630	JAK-STAT signalling pathway	0.0036	5 (160)	3.13
hsa05142	Chagas disease	0.0052	4 (99)	4.04
hsa04926	Relaxin signalling pathway	0.0125	4 (128)	3.13
hsa05418	Fluid shear stress and atherosclerosis	0.0129	4 (130)	3.08
hsa04658	Th1 and Th2 cell differentiation	0.0347	3 (87)	3.45
hsa04657	IL-17 signalling pathway	0.0395	3 (92)	3.26
CLUSTER 3				
hsa03013	RNA transport	$9.30x10^{-05}$	7 (160)	4.38
CLUSTER 4				
hsa04120	Ubiquitin mediated proteolysis	$3.14x10^{-08}$	9 (135)	6.67
hsa04310	Wnt signalling pathway	$1.22x10^{-06}$	8 (154)	5.19
hsa04390	Hippo signalling pathway	0.00015	6 (153)	3.92
hsa04340	Hedgehog signalling pathway	0.0086	3 (47)	6.38
hsa04550	Signalling pathways regulating pluripotency of stem cells	0.0128	4 (140)	2.86

Supplemental Table S4: Pathways identified by enrichment analysis of miRNAs included in Figure 4

	DESCRIPTION - KEGG	FDR value	Genes (background genes)	Fold enrichment
CLUSTER 1				
hsa04014	Ras signalling pathway	$5.82x10^{-17}$	18 (226)	7.96
hsa04510	Focal adhesion	$1.31x10^{-16}$	17 (198)	8.59
hsa04062	Chemokine signalling pathway	$5.14x10^{-13}$	14 (186)	7.53
hsa04151	PI3K-Akt signalling pathway	$5.14x10^{-13}$	17 (350)	4.86
hsa04012	ErbB signalling pathway	$1.19x10^{-12}$	11 (83)	13.25
hsa04810	Regulation of actin cytoskeleton	$1.62x10^{-12}$	14 (209)	6.70
hsa04520	Adherens junction	$4.71x10^{-12}$	10 (67)	14.93
hsa01521	EGFR tyrosine kinase inhibitor resistance	$1.72x10^{-11}$	10 (78)	12.82
hsa04015	Rap1 signalling pathway	$1.72x10^{-11}$	13 (202)	6.44
hsa04722	Neurotrophin signalling pathway	$1.72x10^{-11}$	11 (114)	9.65
hsa01522	Endocrine resistance	$7.0x10^{-11}$	10 (95)	10.53
hsa04917	Prolactin signalling pathway	$1.31x10^{-10}$	9 (69)	13.04
hsa04010	MAPK signalling pathway	$6.06x10^{-10}$	13 (288)	4.51
hsa04370	VEGF signalling pathway	$9.97x10^{-10}$	8 (57)	14.04
hsa04625	C-type lectin receptor signalling pathway	$2.4x10^{-9}$	9 (102)	8.82
hsa04670	Leukocyte transendothelial migration	$3.89x10^{-9}$	9 (109)	8.26
hsa04071	Sphingolipid signalling pathway	$5.46x10^{-9}$	9 (116)	7.76
hsa04935	Growth hormone synthesis, secretion and action	$6.13x10^{-9}$	9 (118)	7.63
hsa04068	FoxO signalling pathway	$1.1x10^{-8}$	9 (127)	7.09
hsa04926	Relaxin signalling pathway	$1.14x10^{-8}$	9 (128)	7.03
hsa05418	Fluid shear stress and atherosclerosis	$1.27x10^{-8}$	9 (130)	6.92
hsa04910	Insulin signalling pathway	$1.5x10^{-8}$	9 (133)	6.77
hsa04912	GnRH signalling pathway	$1.5x10^{-8}$	8 (89)	8.99
hsa04915	Oestrogen signalling pathway	$1.5x10^{-8}$	9 (133)	6.77
hsa04550	Signalling pathways regulating pluripotency of stem cells	$2.14x10^{-8}$	9 (140)	6.43
hsa04933	AGE-RAGE signalling pathway in diabetic complications	$2.88x10^{-8}$	8 (98)	8.16
hsa04072	Phospholipase D signalling pathway	$3.07x10^{-8}$	9 (147)	6.12
hsa04921	Oxytocin signalling pathway	$3.37x10^{-8}$	9 (149)	6.04
hsa04660	T cell receptor signalling pathway	$3.38x10^{-8}$	8 (101)	7.92
hsa04919	Thyroid hormone signalling pathway	$1.03x10^{-7}$	8 (119)	6.72
hsa04611	Platelet activation	$1.21x10^{-7}$	8 (122)	6.56
hsa04150	mTOR signalling pathway	$5.35x10^{-7}$	8 (151)	5.30
hsa04664	Fc epsilon RI signalling pathway	$1.16x10^{-6}$	6 (66)	9.09
hsa04144	Endocytosis	$1.32x10^{-6}$	9 (241)	3.73
hsa04024	cAMP signalling pathway	$4.82x10^{-6}$	8 (208)	3.85
hsa04530	Tight junction	$8.49x10^{-6}$	7 (156)	4.49
hsa04929	GnRH secretion	$1.93x10^{-5}$	5 (63)	7.94
hsa04650	Natural killer cell mediated cytotoxicity	$2.62x10^{-5}$	6 (121)	4.96
hsa04371	Apelin signalling pathway	$3.94x10^{-5}$	6 (131)	4.58
hsa04210	Apoptosis	$4.06x10^{-5}$	6 (132)	4.55
hsa04270	Vascular smooth muscle contraction	$4.18x10^{-5}$	6 (133)	4.51
hsa04662	B cell receptor signalling pathway	$4.72x10^{-5}$	5 (78)	6.41
hsa04540	Gap junction	$7.7x10^{-5}$	5 (87)	5.75
hsa04218	Cellular senescence	$7.78x10^{-5}$	6 (150)	4.00
hsa04666	Fc gamma R-mediated phagocytosis	$8.79x10^{-5}$	5 (90)	5.56
hsa04657	IL-17 signalling pathway	$9.61x10^{-5}$	5 (92)	5.43
hsa04022	cGMP-PKG signalling pathway	$1.1x10^{-4}$	6 (162)	3.70
hsa04659	Th17 cell differentiation	$1.4x10^{-4}$	5 (101)	4.95
hsa04066	HIF-1 signalling pathway	$1.7x10^{-4}$	5 (106)	4.72
hsa04668	TNF signalling pathway	$2.2x10^{-4}$	5 (112)	4.46
hsa04720	Long-term potentiation	$3.4x10^{-4}$	4 (64)	6.25
hsa04920	Adipocytokine signalling pathway	$4.5x10^{-4}$	4 (69)	5.80
hsa05412	Arrhythmogenic right ventricular cardiomyopathy	$6.2x10^{-4}$	4 (76)	5.26
hsa04211	Longevity regulating pathway	0.001	4 (87)	4.60
hsa04350	TGF-β signalling pathway	0.0012	4 (91)	4.40
hsa04960	Aldosterone-regulated sodium reabsorption	0.0012	3 (37)	8.11
hsa04621	NOD-like receptor signalling pathway	0.0014	5 (174)	2.87

	DESCRIPTION - KEGG	FDR value	Genes (background genes)	Fold enrichment
hsa05142	Chagas disease	0.0015	4 (99)	4.04
hsa04620	Toll-like receptor signalling pathway	0.0016	4 (101)	3.96
hsa04928	Parathyroid hormone synthesis, secretion and action	0.0018	4 (103)	3.88
hsa04931	Insulin resistance	0.002	4 (107)	3.74
hsa04930	Type II diabetes mellitus	0.0021	3 (46)	6.52
hsa04723	Retrograde endocannabinoid signalling	0.0058	4 (145)	2.76
hsa04261	Adrenergic signalling in cardiomyocytes	0.006	4 (147)	2.72
hsa01524	Platinum drug resistance	0.0065	3 (70)	4.29
hsa04310	Wnt signalling pathway	0.0069	4 (154)	2.60
hsa04630	JAK-STAT signalling pathway	0.0078	4 (160)	2.50
hsa04141	Protein processing in endoplasmic reticulum	0.0087	4 (165)	2.42
hsa04658	Th1 and Th2 cell differentiation	0.0112	3 (87)	3.45
hsa05410	Hypertrophic cardiomyopathy	0.0118	3 (89)	3.37
hsa05414	Dilated cardiomyopathy	0.0137	3 (95)	3.16
hsa04110	Cell cycle	0.025	3 (120)	2.50
hsa04152	AMPK signalling pathway	0.025	3 (120)	2.50
hsa04217	Necroptosis	0.0428	3 (149)	2.01
hsa05416	Viral myocarditis	0.0439	2 (55)	3.64
hsa04390	Hippo signalling pathway	0.0451	3 (153)	1.96
CLUSTER 2				
hsa04330	Notch signalling pathway	$1.44x10^{-6}$	6 (52)	11.54
hsa04350	TGF-β signalling pathway	$1.44x10^{-6}$	7 (91)	7.69
hsa04110	Cell cycle	$5.51x10^{-6}$	7 (120)	5.83
hsa04919	Thyroid hormone signalling pathway	$5.51x10^{-6}$	7 (119)	5.88
hsa04218	Cellular senescence	$2.2x10^{-4}$	6 (150)	4.00
hsa04310	Wnt signalling pathway	$2.4x10^{-4}$	6 (154)	3.90
hsa01522	Endocrine resistance	$3.2x10^{-4}$	5 (95)	5.26
hsa04659	Th17 cell differentiation	$3.7x10^{-4}$	5 (101)	4.95
hsa04520	Adherens junction	0.0012	4 (67)	5.97
hsa04550	Signalling pathways regulating pluripotency of stem cells	0.0013	5 (140)	3.57
hsa04068	FoxO signalling pathway	0.0095	4 (127)	3.15
hsa05418	Fluid shear stress and atherosclerosis	0.0099	4 (130)	3.08
hsa04917	Prolactin signalling pathway	0.0159	3 (69)	4.35
hsa04658	Th1 and Th2 cell differentiation	0.0273	3 (87)	3.45
hsa04933	AGE-RAGE signalling pathway in diabetic complications	0.0355	3 (98)	3.06
hsa04024	cAMP signalling pathway	0.0374	4 (208)	1.92
hsa04066	HIF-1 signalling pathway	0.0415	3 (106)	2.83
CLUSTER 3				
hsa04120	Ubiquitin mediated proteolysis	$2.34x10^{-12}$	11 (135)	8.15
hsa04310	Wnt signalling pathway	$6.6x10^{-6}$	7 (154)	4.55
hsa04390	Hippo signalling pathway	$6.18x10^{-5}$	6 (153)	3.92
hsa04340	Hedgehog signalling pathway	0.0057	3 (47)	6.38
hsa04550	Signalling pathways regulating pluripotency of stem cells	0.007	4 (140)	2.86
CLUSTER 4				
hsa03013	RNA transport	$8.56x10^{-5}$	6 (160)	3.75
hsa03040	Spliceosome	0.0115	4 (132)	3.03
CLUSTER 5				
hsa04742	Taste transduction	$1.38x10^{-5}$	4 (81)	4.94

Supplemental Table S5: Pathways identified by enrichment analysis of miRNAs included in Figure 5

	DESCRIPTION - KEGG	FDR value	Genes (background genes)	Fold enrichment
CLUSTER 1				
hsa04917	Prolactin signalling pathway	$1.02x10^{-13}$	9 (69)	13.04
hsa01522	Endocrine resistance	$4.11x10^{-11}$	8 (95)	8.42
hsa01521	EGFR tyrosine kinase inhibitor resistance	$5.55x10^{-10}$	7 (78)	8.97
hsa04151	PI3K-Akt signalling pathway	$5.55x10^{-10}$	10 (350)	2.86
hsa04012	ErbB signalling pathway	$6.43x10^{-10}$	7 (83)	8.43
hsa04630	JAK-STAT signalling pathway	$8.82x10^{-10}$	8 (160)	5.00
hsa04933	AGE-RAGE signalling pathway in diabetic complications	$1.55x10^{-9}$	7 (98)	7.14
hsa04062	Chemokine signalling pathway	$2.29x10^{-9}$	8 (186)	4.30
hsa04935	Growth hormone synthesis, secretion and action	$4.45x10^{-9}$	7 (118)	5.93
hsa04068	FoxO signalling pathway	$6.54x10^{-9}$	7 (127)	5.51
hsa04926	Relaxin signalling pathway	$6.54x10^{-9}$	7 (128)	5.47
hsa04915	Oestrogen signalling pathway	$7.42x10^{-9}$	7 (133)	5.26
hsa04659	Th17 cell differentiation	$6.3x10^{-8}$	6 (101)	5.94
hsa04625	C-type lectin receptor signalling pathway	$6.35x10^{-8}$	6 (102)	5.88
hsa05418	Fluid shear stress and atherosclerosis	$1.98x10^{-7}$	6 (130)	4.62
hsa04210	Apoptosis	$2.08x10^{-7}$	6 (132)	4.55
hsa04550	Signalling pathways regulating pluripotency of stem cells	$2.82x10^{-7}$	6 (140)	4.29
hsa04912	GnRH signalling pathway	$9.96x10^{-7}$	5 (89)	5.62
hsa04510	Focal adhesion	$1.42x10^{-6}$	6 (198)	3.03
hsa05142	Chagas disease	$1.46x10^{-6}$	5 (99)	5.05
hsa04015	Rap1 signalling pathway	$1.52x10^{-6}$	6 (202)	2.97
hsa04660	T cell receptor signalling pathway	$1.53x10^{-6}$	5 (101)	4.95
hsa04066	HIF-1 signalling pathway	$1.89x10^{-6}$	5 (106)	4.72
hsa04722	Neurotrophin signalling pathway	$2.62x10^{-6}$	5 (114)	4.39
hsa04014	Ras signalling pathway	$2.65x10^{-6}$	6 (226)	2.65
hsa04071	Sphingolipid signalling pathway	$2.73x10^{-6}$	5 (116)	4.31
hsa04910	Insulin signalling pathway	$4.94x10^{-6}$	5 (133)	3.76
hsa04370	VEGF signalling pathway	$6.37x10^{-6}$	4 (57)	7.02
hsa04921	Oxytocin signalling pathway	$7.9x10^{-6}$	5 (149)	3.36
hsa04929	GnRH secretion	$8.67x10^{-6}$	4 (63)	6.35
hsa04664	Fc epsilon RI signalling pathway	$9.84x10^{-6}$	4 (66)	6.06
hsa04920	Adipocytokine signalling pathway	$1.11x10^{-5}$	4 (69)	5.80
hsa04662	B cell receptor signalling pathway	$1.72x10^{-5}$	4 (78)	5.13
hsa04211	Longevity regulating pathway	$2.56x10^{-5}$	4 (87)	4.60
hsa04657	IL-17 signalling pathway	$3.13x10^{-5}$	4 (92)	4.35
hsa04750	Inflammatory mediator regulation of TRP channels	$3.35x10^{-5}$	4 (94)	4.26
hsa04620	Toll-like receptor signalling pathway	$4.28x10^{-5}$	4 (101)	3.96
hsa04931	Insulin resistance	$5.18x10^{-5}$	4 (107)	3.74
hsa04668	TNF signalling pathway	$6.09x10^{-5}$	4 (112)	3.57
hsa04919	Thyroid hormone signalling pathway	$7.57x10^{-5}$	4 (119)	3.36
hsa04611	Platelet activation	$8.22x10^{-5}$	4 (122)	3.28
hsa04371	Apelin signalling pathway	$1.0x10^{-4}$	4 (131)	3.05
hsa04010	MAPK signalling pathway	$1.2x10^{-4}$	5 (288)	1.74
hsa04930	Type II diabetes mellitus	$1.3x10^{-4}$	3 (46)	6.52
hsa04150	mTOR signalling pathway	$1.6x10^{-4}$	4 (151)	2.65
hsa04217	Necroptosis	$1.6x10^{-4}$	4 (149)	2.68
hsa04218	Cellular senescence	$1.6x10^{-4}$	4 (150)	2.67
hsa01524	Platinum drug resistance	$3.9x10^{-4}$	3 (70)	4.29
hsa04024	cAMP signalling pathway	$5.0x10^{-4}$	4 (208)	1.92
hsa04540	Gap junction	$7.0x10^{-4}$	3 (87)	3.45
hsa04658	Th1 and Th2 cell differentiation	$7.0x10^{-4}$	3 (87)	3.45
hsa04152	AMPK signalling pathway	0.0017	3 (120)	2.50
hsa04723	Retrograde endocannabinoid signalling	0.0028	3 (145)	2.07
hsa04072	Phospholipase D signalling pathway	0.0029	3 (147)	2.04
hsa04530	Tight junction	0.0034	3 (156)	1.92
hsa04621	NOD-like receptor signalling pathway	0.0044	3 (174)	1.72
hsa04973	Carbohydrate digestion and absorption	0.0047	2 (44)	4.55

	DESCRIPTION - KEGG	FDR value	Genes (background genes)	Fold enrichment
hsa04923	Regulation of lipolysis in adipocytes	0.0068	2 (54)	3.70
hsa04810	Regulation of actin cytoskeleton	0.007	3 (209)	1.44
hsa04720	Long-term potentiation	0.0092	2 (64)	3.13
hsa04520	Adherens junction	0.0098	2 (67)	2.99
hsa04666	Fc gamma R-mediated phagocytosis	0.0165	2 (90)	2.22
hsa04922	Glucagon signalling pathway	0.0199	2 (101)	1.98
hsa04928	Parathyroid hormone synthesis, secretion and action	0.0205	2 (103)	1.94
hsa04650	Natural killer cell mediated cytotoxicity	0.0274	2 (121)	1.65
hsa04261	Adrenergic signalling in cardiomyocytes	0.0391	2 (147)	1.36
hsa04310	Wnt signalling pathway	0.042	2 (154)	1.30
hsa04022	cGMP-PKG signalling pathway	0.0458	2 (162)	1.23
hsa04141	Protein processing in endoplasmic reticulum	0.0471	2 (165)	1.21
CLUSTER 2				
hsa04218	Cellular senescence	1.85×10^{-5}	5 (150)	3.33
hsa04350	TGF-β signalling pathway	4.21×10^{-5}	4 (91)	4.40
hsa04144	Endocytosis	8.0×10^{-4}	4 (241)	1.66
hsa04659	Th17 cell differentiation	0.0013	3 (101)	2.97
hsa04933	AGE-RAGE signalling pathway in diabetic complications	0.0013	3 (98)	3.06
hsa05142	Chagas disease	0.0013	3 (99)	3.03
hsa04110	Cell cycle	0.0019	3 (120)	2.50
hsa04371	Apelin signalling pathway	0.0023	3 (131)	2.29
hsa04550	Signalling pathways regulating pluripotency of stem cells	0.0026	3 (140)	2.14
hsa04390	Hippo signalling pathway	0.0032	3 (153)	1.96
hsa04010	MAPK signalling pathway	0.0168	3 (288)	1.04
hsa04520	Adherens junction	0.0168	2 (67)	2.99
hsa04722	Neurotrophin signalling pathway	0.0423	2 (114)	1.75
hsa04926	Relaxin signalling pathway	0.0481	2 (128)	1.56

Supplemental Table S6: Expression values of analysed miRNAs according to underlying aetiology of cHF

miRNA	Ischaemic cHF (*n*=14) median [IQR]	Non-ischaemic cHF (*n*=32) median [IQR]	*p*-value	Fold-change ($\log_2$)
let-7a-5p	0.0001 [0.00006–0.00019]	0.00012 [0.00001–0.00043]	0.821	0.847 (−0.239)
miR-107	0.00002 [0.000002–0.00007]	0.00002 [0.000004–0.00005]	0.808	0.804 (−0.315)
miR-125a-5p	0.00012 [0.00006–0.00037]	0.00032 [0.00015–0.00061]	0.084	0.354 (−1.497)
miR-139-5p	0.00005 [0.00004–0.00006]	0.00002 [0.00001–0.00004]	**0.022**	1.929 (0.948)
miR-150-5p	0.0026 [0.00098–0.00357]	0.00173 [0.00054–0.00407]	0.412	1.503 (0.588)
miR-30b-5p	0.00054 [0.00018–0.00121]	0.00053 [0.00035–0.00136]	0.473	1.016 (0.023)
miR-335-5p	0.00083 [0.00008–0.00156]	0.00064 [0.00023–0.00098]	0.741	1.289 (0.367)
miR-342-3p	0.00028 [0.00007–0.00059]	0.00046 [0.00022–0.0009]	0.169	0.611 (−0.710)

cHF: chronic heart failure; **IQR**: interquartile range
Bold indicates statistical significance.

Supplemental Table S7: Expression values of analysed miRNAs according to cHF ejection fraction

miRNA	HFpEF (*n*=22) median [IQR]	HFrEF (*n*=24) median [IQR]	*p*-value	Fold-change (log_2)
let-7a-5p	0.00014 [0.00002–0.0003]	0.00011 [0.00004–0.00024]	0.947	1.209 (0.274)
miR-107	0.00001 [0.000002–0.00004]	0.00003 [0.00001–0.00009]	0.185	0.492 (−1.023)
miR-125a-5p	0.00031 [0.00015–0.00048]	0.00028 [0.00011–0.00062]	0.952	1.086 (0.119)
miR-139-5p	0.00002 [0.000004–0.00005]	0.00004 [0.00001–0.00005]	0.264	0.624 (−0.681)
miR-150-5p	0.00151 [0.00068–0.00293]	0.00278 [0.00098–0.00407]	0.130	0.546 (−0.874)
miR-30b-5p	0.00036 [0.00021–0.00092]	0.00107 [0.00038–0.00156]	0.075	0.336 (−1.572)
miR-335-5p	0.00065 [0.00032–0.00099]	0.00059 [0.00006–0.00144]	0.726	1.102 (0.140)
miR-342-3p	0.0004 [0.00006–0.00087]	0.00047 [0.00013–0.0009]	0.601	0.849 (−0.236)

cHF: chronic heart failure; **HFpEF**: heart failure with preserved ejection fraction; **HFrEF**: heart failure with reduced ejection fraction; **IQR**: interquartile range

Supplemental Table S8: Selected miRNAs

microRNA	miRbase ID	ThermoFisher ID	MiRbase sequence
let-7a-5p	MIMAT0000062	478575_mir	ugagguaguagguuguauaguu
miR-16-5p	MIMAT0000069	477860_mir	uagcagcacguaaauauuggcg
miR-107	MIMAT0000104	478254_mir	agcagcauuguacagggcuauca
miR-125a-5p	MIMAT0000443	477884_mir	ucccugagacccuuuaaccuguga
miR-139-5p	MIMAT0000250	478312_mir	ucuacagugcacgugucuccagu
miR-150-5p	MIMAT0000451	477918_mir	ucucccaacccuuguaccagug
miR-223-3p	MIMAT0000280	477983_mir	ugucaguuugucaaauacccca
miR-224-5p	MIMAT0000281	477986_mir	ucaagucacuagugguuccguuuag
miR-30b-5p	MIMAT0000420	478007_mir	uguaaacauccuacacucagcu
miR-335-5p	MIMAT0000765	478324_mir	ucaagagcaauaacgaaaaaugu
miR-342-3p	MIMAT0000753	478044_mir	ucucacacagaaaucgcacccgu
cel-miR-39-3p*	MIMAT0000010	478293_mir	ucaccggguguaaaucagcuug

*miRNA used for normalisation

'And how am I supposed to take that? As a compliment, maybe? After all, it's my story you're talking about.'
'No, no, it's mine. You just appear in it.'
-Capricon and Fenoglio,
Inkheart, **Cornelia Funke (2003)**

Discussion

Chronic heart failure (CHF) is a complex clinical syndrome with a diverse aetiological background that involves many pathophysiological mechanisms[8,12,21]. It is known that several pathways play a role in adverse heart remodelling and disease progression, such as endothelial dysfunction, inflammation, cardiac fibrosis and hypertrophy, among others[41,42]. However, the underlying cellular and molecular players that provoke CHF are still insufficiently elucidated.

Extracellular vesicles (EVs) are small lipid-bilayer membrane vesicles that are released by most cell types and contain a complex cargo of nucleic acids and proteins from the parental cells[157]. There is increasing scientific evidence that EVs exert multifaceted roles in the homeostasis of health and disease. EVs mostly act as bioactive effectors in cell-cell communication and are involved in the regulation of a range of biological processes through the transfer of specific biomolecular cargos to recipient cells[85]. Concerning the EV cargo in nucleic acids, distinct RNA classes have been found, including functional messenger RNA and non-coding RNA such as microRNAs (miRNAs), long non-coding RNAs and circular RNAs, among others[107,342]. In agreement, both EVs and miRNAs, are considered emerging tools that can facilitate disease diagnosis and prognosis, patient stratification and management[83,200,234]. However, their clinical usefulness needs to be fully investigated. Therefore, in this thesis, to gain more insight into the pathophysiology of CHF, we investigated circulating EVs and miRNAs in patients with CHF.

Several studies have found that EVs are associated with disease development, and increased levels of circulating EVs have been detected in several cardiovascular conditions[83,87]. In this regard, the Badimon's group has demonstrated altered EVs levels in various cardiac pathologies including myocardial infarction (MI)[343–346], cardiogenic shock[347] or stroke[348]. In addition, previous studies of our group have evidenced increased EV shedding in subjects at high cardiovascular risk, such as old subjects with >3 cardiovascular risk factors[349] or with genetic diagnostic of familial hypercholesterolaemia[350]. To notice, in this latter group of patients, circulating EVs derived from immune and endothelial cells were particularly elevated compared to patients with secondary hypercholesterolaemia[350]. In addition, EVs have been found to be potential surrogate markers to predict the presence and composition of atherosclerotic plaques in high cardiovascular-risk patients[351,352].

To date, studies of EVs in CHF have focused primarily on their role in endothelial dysfunction, a well-known hallmark of vascular dysfunction. Increased levels of EVs shed by endothelial cells have been observed in CHF in comparison to healthy controls[139,249,251–253], reflecting the impairment of the endothelium. In addition, some previous studies have evidenced an association between endothelial cell-derived EVs and CHF severity, as well as prediction of future cardiovascular events, CHF-related rehospitalisation and CHF-related death[139,252,259]. On the contrary, the relationship of EVs with other underlying causes of CHF is still largely unexplored and poorly understood.

The immune system and inflammatory processes have an important role in the setting of structural and functional changes in many organs, including the heart[54,55]. This is of special importance when the immune reparative processes become impaired, as occurs in CHF patients, who normally present a chronic unresolved inflammatory state[56]. Therefore, one of the aims of this thesis is to gain information on the activation state of different immune cells in CHF patients by investigating the differential pattern of circulating EVs derived from these cells. In short, we have demonstrated that EVs shed by different immune cells are heightened in CHF patients in comparison with a sex- and an age-matched control group without CHF, reflecting the chronic activation state of these cells in CHF. Specifically, we evidenced increased numbers of EVs from leukocytes (carrying the general leukocyte marker $CD45^+$ [leukocyte common antigen]), and from specific subtypes including monocytes, neutrophils, T-lymphocytes and natural-killer cells (NKs). Further, we detected elevated numbers of immune-cell-derived EVs carrying activated immune cell epitopes in CHF patients. After myocardial injury, large numbers of immune cells migrate into the heart, where they participate in the healing of the affected tissue. Neutrophils and monocytes are key players in the initial inflammation phases, promoting tissue degradation and removing dead cells while inducing a pro-inflammatory state[28,63]. T-lymphocytes are also recruited during the inflammatory phase, although in lower numbers than neutrophils or macrophages[353], in response to cytokines produced by dendritic cells[354]. The role of NKs in the post-injury myocardium has been less explored, but available studies suggest that NKs protect against cardiac fibrosis by limiting collagen deposition and preventing the accumulation of other immune cells in the heart[61,355].

As discussed above, levels of EVs relate to disease severity[346]. Expanding the understanding of CHF, the results of this thesis provide evidence that the increase in EV-shedding by immune cells, specifically by T-lymphocytes and neutrophils, is associated with the severity in CHF symptomatology as defined by NYHA stages. Inflammation is associated with CHF severity, and inflammatory markers such as C-reactive protein or TNFα correlate with NYHA stages[356,357]. Moreover, inflammation markers have predictive value in CHF patients[358]. In agreement, leukocyte-derived EVs not only associate with NYHA stages but can also discriminate between severity degrees to a similar extent that NT-proBNP, which measures another component of disease pathophysiology. Of note, the differential profile of immune-cell-derived EVs was not associated to left ventricular ejection fraction (LVEF) in the CHF patients, which may indicate that all CHF patients have activation of immune cells, independently of suffering HFrEF and HFpEF.

Levels of EVs not only correlate with disease severity but also associate with the underlying aetiology leading to CHF development. Thus, the EV profiles analysed evidenced that CHF patients with an ischaemic background had significantly increased levels of EVs from T-lymphocytes and activated neutrophils carrying the cell-epitope marker β1-integrin (CD29). In fact, in the initial inflammation stages after a MI, neutrophils are highly present in the myocardium, where they contribute removing cell debris and promoting ECM remodelling[28]. However, defective clearance of neutrophils from the injured myocardium is associated with heart failure development[63,359], due to prolonged ongoing inflammation, maladaptive remodelling and fibrosis[360]. In addition to macrophages, T-lymphocytes are key immune cell components maintaining the low-grade non-resolving inflammation in CHF, independently of the disease aetiology[353]. Thus, it is reported that T-lymphocytes are involved in antigen presentation and induction of cardiac fibrosis both in ischaemic and non-ischaemic CHF patients[353]. Extending these findings, the presence of higher levels of EVs carrying the CD3 surface epitope in CHF patients with an ischaemic background strongly supports the relevance of T-lymphocytes in the myocardial remodelling post-MI and their active role in the pathological evolution towards heart failure. To our knowledge, the role of neutrophils in non-ischaemic CHF has not been addressed before. Therefore, the results of this thesis strongly support the view that the immune cell behaviour in the damaged myocardium is mapped by the phenotypical characterisation of EVs.

Besides being increased in pathologic conditions and being potential biomarker sources, EVs are characterised by transporting proteins, lipids and nucleic acids, including miRNAs[106,107]. Circulating miRNAs are highly stable and actively transported by binding to RNA-binding proteins resistant to nuclease degradation, and more importantly, entrapped in EVs[220,361]. Once delivered to their target cell, miRNAs can regulate gene expression and induce a cellular response. Certainly, many miRNAs have been related to cardiac remodelling[225,226], such as *miR-21* which has been associated with cardiac fibrosis and cardiac hypertrophy[233] or *miR-122* which is related to inflammation and cardiac fibrosis[362]. At the same time, given their simple accessibility in the blood (for example being transported in EVs), miRNAs are becoming the focus of interest in various studies searching for biomarkers[205]. Several authors are determining their potential in diagnosis and patients' stratification, and even prognosis and risk determination[200].

One of the aims of this thesis was to investigate the putative role of circulating miRNAs in the regulation of pathways associated with CHF pathogenesis. Using a non-targeted approach to miRNA identification, we have identified the presence of 8 downregulated circulating miRNAs in CHF. These miRNAs, namely *let-7a-5p*, *miR-107*, *miR-125a-5p*, *miR-139-5p*, *miR-150-5p*, *miR-30b-5p*, *miR-335-5p* and *miR-342-3p*, were lower in plasma of CHF patients compared to a sex- and age-matched reference group. In agreement with our untargeted discovery study, seven of the miRNAs (except for *miR-335-5p*), have been found dysregulated in patients with established CHF in different studies[265,268,275,278,289,314,321,363].

MicroRNAs mostly regulate genes cooperatively[206]. For this reason, studies analysing the role of multiple miRNAs in regulating signalling pathways are of great relevance, since they can help to better understand the pathophysiological processes in which they are involved and their potential clinical value. In this thesis, we have performed an *in silico* systems biology analysis using 4 different publicly available platforms (TargetScan, miRmap, miRWalk, and miRDB)[331–333,335] to identify the predicted protein targets of the identified differential miRNA signature. Briefly, 557 target genes were identified for 7 of the 8 miRNAs. *miR-335-5p* was excluded from further target-gene data mining studies since only one target was obtained after combining the predictions of all 4 algorithms. Interestingly, protein-protein interaction (PPI) analysis resulted in a highly connected network involving 49% of the identified targets, suggesting a high cooperative regulation of molecular signalling processes by the 7-miRNA differential signature identified in CHF. Noteworthy, previous studies investigating various of the identified miRNAs have related them to molecular pathways and processes associated with cardiac remodelling, such as inflammation (*miR-150-5p*, *miR-125a-5p*, *miR-342-3p*)[229,364–366], endothelial dysfunction (*miR-335-5p*)[367] and metabolic alterations (*miR-107*)[368]. In addition, *miR-125a-5p* has been associated to cardiac fibrosis[369], and *miR-107*, *miR-30b-5p*, *miR-139-5p* and *miR-342-3p* to cardiac hypertrophy[370–372].

To better understand the PPI networks regulated by the differential miRNA signature in CHF, a community cluster strategy was applied to identify PPI-enriched nodules[338], and thereafter a functional overrepresentation analysis upon pathways from the KEGG database was performed[340,341]. As a result, 8 different clusters were identified. Four of the clusters (clusters 1–4) included targets from the 7 miRNAs, which supports the concept that the differential miRNA signature cooperatively regulates molecular pathways involved in CHF pathophysiology, such as cellular senescence and Ras, chemokine, PI3K-AKT and TGF-β signalling pathways. Interestingly, the combination of these miRNAs discriminated CHF background aetiology (ischaemic and non-ischaemic) and LVEF type (HFrEF and HFpEF).

Ras/MAPK and PI3K-AKT signalling pathways have been reported to be involved in hypertrophy development[77,373], and both PI3K-AKT and TGF-β have been related to cardiac fibrosis[374,375]. Noteworthy, cardiac hypertrophy and cardiac fibrosis occur in both, ischaemic and non-ischaemic CHF[32,50,77]. After a MI, hypertrophy of the remaining cardiomyocytes takes place to compensate for the loss of cellular mass[77], while in hypertension or heart valve disease, cardiomyocyte hypertrophy occurs to compensate for volume overload[31,33,34], leading to CHF. Similarly, excessive extracellular matrix deposition after an ischaemic injury or in response to systemic hypertension results in cardiac fibrosis, which increases myocardial stiffness and induces CHF development[32,50]. However, as the underlying cause differs, the exact mechanisms involved in this process may be slightly different[32,376]. Unfortunately, the specific mechanisms inducing hypertrophy and fibrosis in each of these aetiologies are underexplored, but differential fine-tunning regulation by miRNAs could well be implicated in these processes and would support their discriminative potential.

As mentioned previously, inflammation is an important hallmark of CHF patients, who present ongoing and non-resolving inflammation[56]. This is reflected by an increase of cytokines in CHF[54], or increased levels of immune-derived EV, as we observe in these patients. Moreover, cytokine signalling is not only involved in inflammation but is also associated with the development of cardiac fibrosis and hypertrophy[50,377]. Thus, the miRNA-differential signature in CHF patients could regulate cytokine signalling and influence cardiac fibrosis and hypertrophy, in parallel to their direct regulation through the TGF-β and Ras/MAPK pathways. As inflammation occurs in both ischaemic and non-ischaemic CHF[57,58], miRNAs could regulate these pathways in CHF patients independently of the underlying aetiology. Further studies are needed to decipher whether the individual miRNA-specific contribution to the highly complex inflammatory process might explain their differential discriminatory potential.

Cellular senescence, another pathway enriched in our *in silico* analysis, is also related to both cardiac hypertrophy and fibrosis, and in CHF it has been associated with mitochondrial dysfunction[378]. Mitochondrial dysfunction is related to the metabolic alterations observed in CHF, characterised by a shift from fatty acid oxidation-based to a more glycolysis-based metabolism[51,52]. Interestingly, target genes of some of the miRNAs participating in the differential signature (*let-7a-5p*, *miR-125a-5p*, *miR-30b-5p* and *miR-342-3p*; cluster DiffmiR) were enriched in pathways related to metabolism, namely glucagon signalling pathway, carbohydrate digestion and absorption, and regulation of lipolysis in adipocytes. In this respect, studies have demonstrated that CHF patients have defects in the glucagon signalling pathway and enhanced levels of adipocyte lipolysis[379,380].

Interestingly, the other three miRNAs (*miR-107*, *miR-139-5p* and *miR-150-5p*; clusters 5+7) were not involved in the regulation of metabolic-related pathways when analysed separately. This could explain their inability to discriminate between aetiologies. These three miRNAs (clusters 5+7), however, were associated with pathways related to non-ischaemic cardiomyopathies that can evolve to CHF, namely hypertrophic and dilated cardiomyopathy. Additional enriched pathways involving clusters 5+7 were related to blood pressure regulation, such as vascular smooth muscle contraction or aldosterone-regulated sodium reabsorption, and inflammation, like leukocyte transendothelial migration. This group of miRNAs (clusters 5+7) could discriminate between HFpEF and HFrEF, and the observed associated pathways reflect this finding. Both, hypertension and hypertrophic cardiomyopathy are more frequently observed in HFpEF[38,381], while dilated cardiomyopathy is associated with HFrEF[39]. Additionally, leukocyte transendothelial migration is one of the initial processes involved in atherosclerosis[382], which at the same time is one underlying cause of ischaemic heart disease[23]. Even though ischaemic heart disease can lead to both, HFpEF and HFrEF, atherosclerosis-related ischaemia is more predominantly observed in HFrEF[24,25].

Therefore, the findings of this thesis strongly support the view that miRNAs cooperatively regulate several pathophysiological mechanisms involved in CHF development. In parallel, pathway regulation by each specific miRNA may differ, allowing the modulation fine-tuning of the affected mechanisms.

In summary, the results of this thesis provide evidence that CHF patients have increased levels of immune-cell-derived EVs that reflect a chronic and unresolving inflammation. The EVs differential profile relates to disease severity and the underlying aetiology and thus associates with CHF pathophysiology. In addition, CHF patients have a differential profile of 8 downregulated miRNAs in plasma that associates with several disease hallmarks, including inflammation, endothelial dysfunction, cardiac hypertrophy, cardiac fibrosis and altered metabolism, which are factors associated with disease pathophysiology. Importantly, the results obtained in this thesis provide an in-depth knowledge on the contribution of the immune cell system to CHF. The high release of immune-cell-derived EVs, accentuated by the clinical severity of CHF, reflects a substantial immune cell activation in these patients. These activated innate and adaptive immune cell messengers would contribute by carrying differential patterns of miRNAs through the circulation to the progression of the disease and to the common affectation of distant organs (paracrine regulation) that contribute to the clinical deterioration of CHF patients.

'I — I hardly know, sir, just at present — at least I know who I WAS when I got up this morning, but I think I must have been changed several times since then.'
-Alice,
Alice in Wonderland, **Lewis Carroll (1865)**

Conclusions

The conclusions of this thesis are the following:

1. **1.** Chronic heart failure patients (CHF) under guideline-directed medical therapy have a higher number of annexin V^{+} (phosphatidylserine^{+}) circulating immune-cell-derived extracellular vesicles (EVs) in the circulation than controls.

2. The number of EVs shed by T-lymphocytes and neutrophils correlated with the severity of the CHF symptomatology.

3. CHF patients with ischaemic background had higher levels of EVs originating from T-lymphocytes and neutrophils than CHF with non-ischaemic aetiology.

4. A downregulated pattern of eight 8 microRNAs was identified in the plasma of CHF in comparison to a reference control group.

5. Target proteins of 7 of the 8 differential miRNAs were organised in different clusters participating in molecular mechanisms and signalling pathways related to CHF.

6. Target genes of miRNAs *let-7a-5p*, *miR-30b-5p*, *miR-107*, *miR-125a-5p*, *miR-139-5p*, *miR-150-5p* and *miR-342-3p*, when clustered, could discriminate between ischaemic and non-ischaemic background and between CHF ejection fraction groups.

GENERAL CONCLUSIONS

In summary, the results of this thesis provide evidence of a specific pattern of circulating extracellular vesicles and microRNAs that associate with the underlying pathophysiology of chronic heart failure. The observed changes in the plasma pattern of circulating extracellular vesicles and microRNAs may contribute to a better understanding of mechanisms involved in chronic heart failure development and to a more accurate disease recognition, diagnosis and phenotyping.

"Every book, has a soul. The soul of the person who wrote it and of those who read it and lived and dreamed with it. Every time a book changes hands, every time someone runs his eyes down its pages, its spirit grows and strengthens."
The shadow of the wind, **Carlos Ruiz Zafón (2001)**

References

1. Kemp, C. D. & Conte, J. V. The pathophysiology of heart failure. *Cardiovasc. Pathol.* **21**, 365–371 (2012).

2. Tanai, E. & Frantz, S. Pathophysiology of heart failure. *Compr. Physiol.* **6**, 187–214 (2016).

3. McDonagh, T. A. *et al.* 2021 ESC Guidelines for the diagnosis and treatment of acute and chronic heart failure. *Eur. Heart J.* **42**, 3599–3726 (2021).

4. Ponikowski, P. *et al.* 2016 ESC Guidelines for the diagnosis and treatment of acute and chronic heart failure. *Eur. Heart J.* **37**, 2129–2200 (2016).

5. James, S. L. *et al.* Global, regional, and national incidence, prevalence, and years lived with disability for 354 diseases and injuries for 195 countries and territories, 1990–2017: a systematic analysis for the Global Burden of Disease Study 2017. *Lancet* **392**, 1789–1858 (2018).

6. Groenewegen, A., Rutten, F. H., Mosterd, A. & Hoes, A. W. Epidemiology of heart failure. *Eur. J. Heart Fail.* **22**, 1342–1356 (2020).

7. Savarese, G. *et al.* Global burden of heart failure: a comprehensive and updated review of epidemiology. *Cardiovasc. Res.* **118**, 3272–3287 (2023).

8. Metra, M. & Teerlink, J. R. Heart failure. *Lancet (London, England)* **390**, 1981–1995 (2017).

9. Sicras-Mainar, A., Sicras-Navarro, A., Palacios, B., Varela, L. & Delgado, J. F. Epidemiology and treatment of heart failure in Spain: the HF-PATHWAYS study. *Rev. Esp. Cardiol.* **75**, 31–38 (2022).

10. Farré, N. *et al.* Real world heart failure epidemiology and outcome: A population-based analysis of 88,195 patients. *PLoS ONE* **12**, e0172745 (2017).

11. Arrigo, M. *et al.* Acute heart failure. *Nat. Rev. Dis. Primer* **6**, 16 (2020).

12. Inamdar, A. A. & Inamdar, A. C. Heart Failure: Diagnosis, Management and Utilization. *J. Clin. Med.* **5**, 62 (2016).

13. Campbell, R. T. & McMurray, J. J. V. Comorbidities and Differential Diagnosis in Heart Failure with Preserved Ejection Fraction. *Heart Fail. Clin.* **10**, 481–501 (2014).

14. Dunlay, S. M., Roger, V. L. & Redfield, M. M. Epidemiology of heart failure with preserved ejection fraction. *Nat. Rev. Cardiol.* **14**, 591–602 (2017).

15. Hunt, S. A. *et al.* ACC/AHA guidelines for the evaluation and management of chronic heart failure in the adult: executive summary. *J. Am. Coll. Cardiol.* **38**, 2101–2113 (2001).

16. Sarhene, M. *et al.* Biomarkers in heart failure: the past, current and future. *Heart Fail. Rev.* **24**, 867–903 (2019).

17. Castiglione, V. *et al.* Biomarkers for the diagnosis and management of heart failure.

Heart Fail. Rev. **27**, 625–643 (2022).

18. Pfeffer, M. A., Shah, A. M. & Borlaug, B. A. Heart Failure with Preserved Ejection Fraction in Perspective. *Circ. Res.* **124**, 1598–1617 (2019).
19. Takeishi, Y. Biomarkers in Heart Failure. *Int. Heart J.* **55**, 474–481 (2014).
20. Nair, N. Epidemiology and pathogenesis of heart failure with preserved ejection fraction. *Rev. Cardiovasc. Med.* **21**, 531–540 (2020).
21. Ziaeian, B. & Fonarow, G. C. Epidemiology and aetiology of heart failure. *Nat. Rev. Cardiol.* **13**, 368–378 (2016).
22. Padro, T. *et al.* ESC Working Group on Coronary Pathophysiology and Microcirculation position paper on 'coronary microvascular dysfunction in cardiovascular disease'. *Cardiovasc. Res.* **116**, 741–755 (2020).
23. Libby, P. *et al.* Atherosclerosis. *Nat. Rev. Dis. Primer* **5**, 56 (2019).
24. Del Buono, M. G. *et al.* Coronary Microvascular Dysfunction Across the Spectrum of Cardiovascular Diseases: JACC State-of-the-Art Review. *J. Am. Coll. Cardiol.* **78**, 1352–1371 (2021).
25. Camici, P. G., Tschöpe, C., Di Carli, M. F., Rimoldi, O. & Van Linthout, S. Coronary microvascular dysfunction in hypertrophy and heart failure. *Cardiovasc. Res.* **116**, 806–816 (2020).
26. Leancă, S. A. *et al.* Left Ventricular Remodeling after Myocardial Infarction: From Physiopathology to Treatment. *Life* **12**, 1111 (2022).
27. Frangogiannis, N. G. Pathophysiology of myocardial infarction. *Compr. Physiol.* **5**, 1841–1875 (2015).
28. Prabhu, S. D. & Frangogiannis, N. G. The biological basis for cardiac repair after myocardial infarction. *Circ. Res.* **119**, 91–112 (2016).
29. Lloyd-Jones, D. M. *et al.* Lifetime risk for developing congestive heart failure: The Framingham Heart Study. *Circulation* **106**, 3068–3072 (2002).
30. Díez, J. & Butler, J. Growing Heart Failure Burden of Hypertensive Heart Disease: A Call to Action. *Hypertension* **80**, 13–21 (2023).
31. Messerli, F. H., Rimoldi, S. F. & Bangalore, S. The Transition From Hypertension to Heart Failure: Contemporary Update. *JACC. Heart failure* **5**, 543–551 (2017).
32. Frangogiannis, N. G. The extracellular matrix in myocardial injury, repair, and remodeling. *J. Clin. Investig.* **127**, 1600–1612 (2017).
33. Slivnick, J. & Lampert, B. C. Hypertension and Heart Failure. *Heart Fail. Clin.* **15**, 531–541 (2019).
34. Gaasch, W. H. & Meyer, T. E. Left Ventricular Response to Mitral Regurgitation.

Circulation **118**, 2298–2303 (2008).

35. Uretsky, S. & Wolff, S. D. Cardiovascular Magnetic Resonance in Valvular Heart Disease–Related Heart Failure. *Heart Fail. Clin.* **17**, 103–108 (2021).

36. Maron, B. J. & Maron, M. S. Hypertrophic cardiomyopathy. *Lancet* **381**, 242–255 (2013).

37. Becker, R. C., Owens, A. P. & Sadayappan, S. Tissue-level inflammation and ventricular remodeling in hypertrophic cardiomyopathy. *J. Thromb. Thrombolysis* **49**, 177–183 (2020).

38. Antunes, M. de O. & Scudeler, T. L. Hypertrophic cardiomyopathy. *IJC Heart Vasc.* **27**, 100503 (2020).

39. Giri, P., Mukhopadhyay, A., Gupta, M. & Mohapatra, B. Dilated cardiomyopathy: a new insight into the rare but common cause of heart failure. *Heart Fail. Rev.* **27**, 431–454 (2022).

40. Schultheiss, H. P. *et al.* Dilated cardiomyopathy. *Nat. Rev. Dis. Primer* **5**, 32 (2019).

41. Cohn, J. N., Ferrari, R. & Sharpe, N. Cardiac remodeling—concepts and clinical implications: a consensus paper from an international forum on cardiac remodeling. *J. Am. Coll. Cardiol.* **35**, 569–582 (2000).

42. Azevedo, P. S., Polegato, B. F., Minicucci, M. F., Paiva, S. A. R. & Zornoff, L. A. M. Cardiac Remodeling: Concepts, Clinical Impact, Pathophysiological Mechanisms and Pharmacologic Treatment. *Arq. Bras. Cardiol.* **106**, 62–69 (2016).

43. Giannitsi, S., Maria, B., Bechlioulis, A. & Naka, K. Endothelial dysfunction and heart failure: A review of the existing bibliography with emphasis on flow mediated dilation. *JRSM Cardiovasc. Dis.* **8**, 204800401984304 (2019).

44. Alem, M. M. Endothelial dysfunction in chronic heart failure: Assessment, findings, significance, and potential therapeutic targets. *Int. J. Mol. Sci.* **20**, 3198 (2019).

45. Zuchi, C. *et al.* Role of endothelial dysfunction in heart failure. *Heart Fail. Rev.* **25**, 21–30 (2020).

46. Bochenek, M. L. & Schäfer, K. Role of Endothelial Cells in Acute and Chronic Thrombosis. *Hamostaseologie* **39**, 128–139 (2019).

47. Katz, S. D. *et al.* Vascular endothelial dysfunction and mortality risk in patients with chronic heart failure. *Circulation* **111**, 310–314 (2005).

48. Elkayam, U., Khan, S., Mehboob, A. & Ahsan, N. Impaired endothelium-mediated vasodilation in heart failure: Clinical evidence and the potential for therapy. *J. Card. Fail.* **8**, 15–20 (2002).

49. Schiattarella, G. G., Sequeira, V. & Ameri, P. Distinctive patterns of inflammation across the heart failure syndrome. *Heart Fail. Rev.* **26**, 1333–1344 (2021).

50. Frangogiannis, N. G. Cardiac fibrosis. *Cardiovasc. Res.* **117**, 1450–1488 (2021).

51. Lopaschuk, G. D., Karwi, Q. G., Tian, R., Wende, A. R. & Abel, E. D. Cardiac Energy Metabolism in Heart Failure. *Circ. Res.* **128**, 1487–1513 (2021).

52. Miranda-Silva, D., Lima, T., Rodrigues, P., Leite-Moreira, A. & Falcão-Pires, I. Mechanisms underlying the pathophysiology of heart failure with preserved ejection fraction: the tip of the iceberg. *Heart Fail. Rev.* **26**, 453–478 (2021).

53. Zhou, B. & Tian, R. Mitochondrial dysfunction in pathophysiology of heart failure. *J. Clin. Investig.* **128**, 3716–3726 (2018).

54. Mann, D. L. Innate immunity and the failing heart: The cytokine hypothesis revisited. *Circ. Res.* **116**, 1254–1268 (2015).

55. Dutka, M. *et al.* Various aspects of inflammation in heart failure. *Heart Fail. Rev.* **25**, 537–548 (2020).

56. Murphy, S. P., Kakkar, R., McCarthy, C. P. & Januzzi, J. L. Inflammation in Heart Failure: JACC State-of-the-Art Review. *J. Am. Coll. Cardiol.* **75**, 1324–1340 (2020).

57. Adamo, L., Rocha-Resende, C., Prabhu, S. D. & Mann, D. L. Reappraising the role of inflammation in heart failure. *Nat. Rev. Cardiol.* **17**, 269–285 (2020).

58. Hanna, A. & Frangogiannis, N. G. Inflammatory Cytokines and Chemokines as Therapeutic Targets in Heart Failure. *Cardiovasc. Drugs Ther.* **34**, 849–863 (2020).

59. Zhang, Y., Bauersachs, J. & Langer, H. F. Immune mechanisms in heart failure. *Eur. J. Heart Fail.* **19**, 1379–1389 (2017).

60. Zimmer, A., Bagchi, A. K., Vinayak, K., Bello-Klein, A. & Singal, P. K. Innate immune response in the pathogenesis of heart failure in survivors of myocardial infarction. *Am. J. Physiol. Heart Circ. Physiol.* **316**, H435–H445 (2019).

61. Strassheim, D., Dempsey, E. C., Gerasimovskaya, E., Stenmark, K. & Karoor, V. Role of inflammatory cell subtypes in heart failure. *J. Immunol. Res.* **2019**, 2164017 (2019).

62. Castillo, E. C., Vázquez-Garza, E., Yee-Trejo, D., García-Rivas, G. & Torre-Amione, G. What Is the Role of the Inflammation in the Pathogenesis of Heart Failure? *Curr. Cardiol. Rep.* **22**, 139 (2020).

63. Kain, V. & Halade, G. V. Role of neutrophils in ischemic heart failure. *Physiol. Genomics* **205**, 107424 (2020).

64. Dick, S. A. & Epelman, S. Chronic heart failure and inflammation. What do we really know? *Circ. Res.* **119**, 159–176 (2016).

65. Frangogiannis, N. G. The inflammatory response in myocardial injury, repair, and remodelling. *Nat. Rev. Cardiol.* **11**, 255–265 (2014).

66. McMaster, W. G., Kirabo, A., Madhur, M. S. & Harrison, D. G. Inflammation,

Immunity, and Hypertensive End-Organ Damage. *Circ. Res.* **116**, 1022–1033 (2015).

67. Van Linthout, S. & Tschöpe, C. Inflammation – Cause or Consequence of Heart Failure or Both? *Curr. Heart Fail. Rep.* **14**, 251–265 (2017).

68. Periayah, M. H., Halim, A. S. & Mat Saad, A. Z. Mechanism Action of Platelets and Crucial Blood Coagulation Pathways in Hemostasis. *International journal of hematology-oncology and stem cell research* **11**, 319–327 (2017).

69. Gando, S., Levi, M. & Toh, C.-H. Disseminated intravascular coagulation. *Nature reviews. Disease primers* **2**, 16037 (2016).

70. Marieb, E. N. *Anatomía y Fisiología Humana*. (Addison Wesley, 2008).

71. Kim, J. H., Shah, P., Tantry, U. S. & Gurbel, P. A. Coagulation Abnormalities in Heart Failure: Pathophysiology and Therapeutic Implications. *Curr. Heart Fail. Rep.* **13**, 319–328 (2016).

72. Thomas, I., EncisoSilva, J., Schlueter, M. & Greenberg, B. Anticoagulation Therapy and NOACs in Heart Failure. in *Handbook of Experimental Pharmacology* **243**, 515–535 (Springer New York LLC, 2016).

73. De Lorenzo, F., Saba, N. & Kakkar, V. V. Blood Coagulation in Patients with Chronic Heart Failure. *Drugs* **63**, 565–576 (2003).

74. López, J. A. & Chen, J. Pathophysiology of venous thrombosis. *Thromb. Res.* **123 Suppl 4**, S30-4 (2009).

75. Lip, G. Y. & Gibbs, C. R. Does heart failure confer a hypercoagulable state? Virchow's triad revisited. *J. Am. Coll. Cardiol.* **33**, 1424–1426 (1999).

76. Carlisle, M. A., Fudim, M., DeVore, A. D. & Piccini, J. P. Heart Failure and Atrial Fibrillation, Like Fire and Fury. *JACC Heart Fail.* **7**, 447–456 (2019).

77. Nakamura, M. & Sadoshima, J. Mechanisms of physiological and pathological cardiac hypertrophy. *Nat. Rev. Cardiol.* **15**, 387–407 (2018).

78. Ali, H., Braga, L. & Giacca, M. Cardiac regeneration and remodelling of the cardiomyocyte cytoarchitecture. *FEBS J.* **287**, 417–438 (2020).

79. Creemers, E. E. & Van Rooij, E. Function and Therapeutic Potential of Noncoding RNAs in Cardiac Fibrosis. *Circ. Res.* **118**, 108–118 (2016).

80. Zhao, Y., Du, D., Chen, S., Chen, Z. & Zhao, J. New Insights into the Functions of MicroRNAs in Cardiac Fibrosis: From Mechanisms to Therapeutic Strategies. *Genes (Basel).* **13**, 1390 (2022).

81. Zarà, M. *et al.* Biology and role of extracellular vesicles (EVs) in the pathogenesis of thrombosis. *Int. J. Mol. Sci.* **20**, 2840 (2019).

82. Suades, R., Padró, T. & Badimon, L. The Role of Blood-Borne Microparticles in Inflammation and Hemostasis. *Semin. Thromb. Hemost.* **41**, 590–606 (2015).

83. Badimon, L. *et al.* Liquid Biopsies: Microvesicles in Cardiovascular Disease. *Antioxid. Redox Signal.* **33**, 645–662 (2020).

84. Sluijter, J. P. G. *et al.* Extracellular vesicles in diagnostics and therapy of the ischaemic heart: Position Paper from the Working Group on Cellular Biology of the Heart of the European Society of Cardiology. *Cardiovasc. Res.* **114**, 19–34 (2018).

85. Suades, R., Greco, M. F., Padró, T. & Badimon, L. Extracellular Vesicles as Drivers of Immunoinflammation in Atherothrombosis. *Cells* **11**, 1845 (2022).

86. Raposo, G. & Stoorvogel, W. Extracellular vesicles: Exosomes, microvesicles, and friends. *J. Cell Biol.* **200**, 373–383 (2013).

87. Boulanger, C. M., Loyer, X., Rautou, P.-E. & Amabile, N. Extracellular vesicles in coronary artery disease. *Nat. Rev. Cardiol.* **14**, 259–272 (2017).

88. Palviainen, M. *et al.* Extracellular vesicles from human plasma and serum are carriers of extravesicular cargo—Implications for biomarker discovery. *PLoS ONE* **15**, e0236439 (2020).

89. Van Niel, G., D'Angelo, G. & Raposo, G. Shedding light on the cell biology of extracellular vesicles. *Nat. Rev. Mol. Cell Biol.* **19**, 213–228 (2018).

90. Mathieu, M., Martin-Jaular, L., Lavieu, G. & Théry, C. Specificities of secretion and uptake of exosomes and other extracellular vesicles for cell-to-cell communication. *Nat. Cell Biol.* **21**, 9–17 (2019).

91. Morel, O., Jesel, L., Freyssinet, J.-M. & Toti, F. Cellular mechanisms underlying the formation of circulating microparticles. *Arterioscler. Thromb. Vasc. Biol.* **31**, 15–26 (2011).

92. Ortega, M. A. *et al.* An Updated View of the Importance of Vesicular Trafficking and Transport and Their Role in Immune-Mediated Diseases: Potential Therapeutic Interventions. *Membranes (Basel)* **12**, 552 (2022).

93. Shet, A. S. *et al.* Sickle blood contains tissue factor-positive microparticles derived from endothelial cells and monocytes. *Blood* **102**, 2678–2683 (2003).

94. Connor, D. E., Exner, T., Ma, D. D. F. & Joseph, J. E. The majority of circulating platelet-derived microparticles fail to bind annexin V, lack phospholipid-dependent procoagulant activity and demonstrate greater expression of glycoprotein Ib. *Thromb. Haemost.* **103**, 1044–1052 (2010).

95. Arraud, N. *et al.* Extracellular vesicles from blood plasma: Determination of their morphology, size, phenotype and concentration. *J. Thromb. Haemost.* **12**, 614–627 (2014).

96. Arraud, N., Gounou, C., Turpin, D. & Brisson, A. R. Fluorescence triggering: A general strategy for enumerating and phenotyping extracellular vesicles by flow cytometry. *Cytometry A* **89**, 184–195 (2016).

97. Biró, E. *et al.* The phospholipid composition and cholesterol content of platelet-derived microparticles: a comparison with platelet membrane fractions. *J. Thromb. Haemost.* **3**, 2754–2763 (2005).

98. Del Conde, I., Shrimpton, C. N., Thiagarajan, P. & López, J. A. Tissue-factor-bearing microvesicles arise from lipid rafts and fuse with activated platelets to initiate coagulation. *Blood* **106**, 1604–1611 (2005).

99. Burger, D. *et al.* Endothelial microparticle formation by angiotensin II is mediated via ang II receptor type I/NADPH Oxidase/rho kinase pathways targeted to lipid rafts. *Arterioscler. Thromb. Vasc. Biol.* **31**, 1898–1907 (2011).

100. Bianco, F. *et al.* Acid sphingomyelinase activity triggers microparticle release from glial cells. *EMBO J.* **28**, 1043–1054 (2009).

101. Menck, K. *et al.* Neutral sphingomyelinases control extracellular vesicles budding from the plasma membrane. *J. Extracell. Vesicles* **6**, 1378056 (2017).

102. Abels, E. R. & Breakefield, X. O. Introduction to Extracellular Vesicles: Biogenesis, RNA Cargo Selection, Content, Release, and Uptake. *Cell. Mol. Neurobiol.* **36**, 301–312 (2016).

103. Clancy, J. W., Schmidtmann, M. & D'Souza-Schorey, C. The ins and outs of microvesicles. *FASEB BioAdvances* **3**, 399–406 (2021).

104. Sedgwick, A. E., Clancy, J. W., Olivia Balmert, M. & D'Souza-Schorey, C. Extracellular microvesicles and invadopodia mediate non-overlapping modes of tumor cell invasion. *Sci. Rep* **5**, 14748 (2015).

105. Souza-Schorey, C. & Schorey, J. S. Regulation and mechanisms of extracellular vesicle biogenesis and secretion. *Essays Biochem.* **62**, 125–133 (2018).

106. Sedgwick, A. E. & D'Souza-Schorey, C. The biology of extracellular microvesicles. *Traffic* **19**, 319–327 (2018).

107. Murillo, O. D. *et al.* exRNA Atlas Analysis Reveals Distinct Extracellular RNA Cargo Types and Their Carriers Present across Human Biofluids. *Cell* **177**, 463–477 (2019).

108. Boudreau, L. H. *et al.* Platelets release mitochondria serving as substrate for bactericidal group IIA-secreted phospholipase a to promote inflammation. *Blood* **124**, 2173–2183 (2014).

109. O'Brien, K., Breyne, K., Ughetto, S., Laurent, L. C. & Breakefield, X. O. RNA delivery by extracellular vesicles in mammalian cells and its applications. *Nat. Rev. Mol. Cell Biol.* **21**, 585–606 (2020).

110. Han, C., Yang, J., Sun, J. & Qin, G. Extracellular vesicles in cardiovascular disease: Biological functions and therapeutic implications. *Pharmacol. Ther.* **233**, 108025 (2022).

111. van Niel, G. *et al.* Challenges and directions in studying cell–cell communication by

extracellular vesicles. *Nat. Rev. Mol. Cell Biol.* **23**, 369–382 (2022).

112. Muralidharan-Chari, V. *et al.* ARF6-Regulated Shedding of Tumor Cell-Derived Plasma Membrane Microvesicles. *Curr. Biol.* **19**, 1875–1885 (2009).

113. de Jong, O. G. *et al.* Cellular stress conditions are reflected in the protein and RNA content of endothelial cell-derived exosomes. *J. Extracell. Vesicles* **1**, 18396 (2012).

114. Squadrito, M. L. *et al.* Endogenous RNAs Modulate MicroRNA Sorting to Exosomes and Transfer to Acceptor Cells. *Cell Rep.* **8**, 1432–1446 (2014).

115. Koppers-Lalic, D. *et al.* Nontemplated nucleotide additions distinguish the small RNA composition in cells from exosomes. *Cell Rep.* **8**, 1649–1658 (2014).

116. Augustine, D. *et al.* Dynamic release and clearance of circulating microparticles during cardiac stress. *Circ. Res.* **114**, 109–113 (2014).

117. Boyle, L. J. *et al.* Impact of reduced daily physical activity on conduit artery flow-mediated dilation and circulating endothelial microparticles. *Journal of Applied Physiology* **115**, 1519–1525 (2013).

118. van den Goor, J. M. *et al.* Retransfusion of pericardial blood does not trigger systemic coagulation during cardiopulmonary bypass. *Eur. J. Cardio-thoracic Surg.* **31**, 1029–1036 (2007).

119. Vince, R. V., Chrismas, B., Midgley, A. W., McNaughton, L. R. & Madden, L. A. Hypoxia mediated release of endothelial microparticles and increased association of S100A12 with circulating neutrophils. *Oxid. Med. Cell. Longev.* **2**, 2–6 (2009).

120. Sossdorf, M., Otto, G. P., Claus, R. A., Gabriel, H. H. & Lósche, W. Release of pro-coagulant microparticles after moderate endurance exercise. *Platelets* **21**, 389–391 (2010).

121. Sossdorf, M., Otto, G. P., Claus, R. A., Gabriel, H. H. W. & Lösche, W. Cell-derived microparticles promote coagulation after moderate exercise. *Med. Sci. Sports Exerc.* **43**, 1169–1176 (2011).

122. Mulcahy, L. A., Pink, R. C. & Carter, D. R. F. Routes and mechanisms of extracellular vesicle uptake. *J. Extracell. Vesicles* **3**, 24641 (2014).

123. Flaumenhaft, R. Formation and fate of platelet microparticles. *Blood Cells Mol. Dis.* **36**, 182–187 (2006).

124. Litvack, M. L., Post, M. & Palaniyar, N. IgM promotes the clearance of small particles and apoptotic microparticles by macrophages. *PLoS ONE* **6**, 0017223 (2011).

125. Pacheco, P., White, D. & Sulchek, T. Effects of Microparticle Size and Fc Density on Macrophage Phagocytosis. *PLoS ONE* **8**, e60989 (2013).

126. Dasgupta, S. K. *et al.* Lactadherin and clearance of platelet-derived microvesicles. *Blood* **113**, 1332–1339 (2009).

127. Loyer, X., Vion, A.-C., Tedgui, A. & Boulanger, C. M. Microvesicles as cell-cell messengers in cardiovascular diseases. *Circ. Res.* **114**, 345–353 (2014).

128. Alexy, T., Rooney, K., Weber, M., Gray, W. D. & Searles, C. D. TNF-alters the release and transfer of microparticle-encapsulated miRNAs from endothelial cells. *Physiol. Genomics* **46**, 833–840 (2014).

129. Barry, O. P., Praticò, D., Lawson, J. A. & FitzGerald, G. A. Transcellular activation of platelets and endothelial cells by bioactive lipids in platelet microparticles. *J. Clin. Investig.* **99**, 2118–2127 (1997).

130. Curtis, A. M. *et al.* Endothelial microparticles: Sophisticated vesicles modulating vascular function. *Vascular Medicine (United Kingdom)* **18**, 204–214 (2013).

131. Berumen Sánchez, G., Bunn, K. E., Pua, H. H. & Rafat, M. Extracellular vesicles: mediators of intercellular communication in tissue injury and disease. *Cell Commun. Signal.* **19**, 104 (2021).

132. Tkach, M. & Théry, C. Communication by Extracellular Vesicles: Where We Are and Where We Need to Go. *Cell* **164**, 1226–1232 (2016).

133. Puhm, F., Boilard, E. & Machlus, K. R. Platelet Extracellular Vesicles: Beyond the Blood. *Arterioscler. Thromb. Vasc. Biol.* **41**, 87–96 (2021).

134. Knijff-Dutmer, E. A. J., Koerts, J., Nieuwland, R., Kalsbeek-Batenburg, E. M. & Van De Laar, M. A. F. J. Elevated levels of platelet microparticles are associated with disease activity in rheumatoid arthritis. *Arthritis & Rheumatism* **46**, 1498–1503 (2002).

135. Tessandier, N. *et al.* Platelets Disseminate Extracellular Vesicles in Lymph in Rheumatoid Arthritis. *Arterioscler. Thromb. Vasc. Biol.* **40**, 929–942 (2020).

136. Helbing, T., Olivier, C., Bode, C., Moser, M. & Diehl, P. Role of microparticles in endothelial dysfunction and arterial hypertension. *World J. Cardiol.* **6**, 1135–1139 (2014).

137. Lugo-Gavidia, L. M. *et al.* Role of Microparticles in Cardiovascular Disease: Implications for Endothelial Dysfunction, Thrombosis, and Inflammation. *Hypertension* **77**, 1825–1844 (2021).

138. Giró, O. *et al.* Extracellular vesicles in atherothrombosis and cardiovascular disease: Friends and foes. *Atherosclerosis* **330**, 61–75 (2021).

139. Nozaki, T. *et al.* Prognostic value of endothelial microparticles in patients with heart failure. *Eur. J. Heart Fail.* **12**, 1223–1228 (2010).

140. Berezin, A. Pattern of Microvesicles in Heart Failure: Novel Biomarker of Endothelial Dysfunction and Vascular Reparation. *Biomarkers J.* **04**, 16 (2018).

141. Zhang, J. Biomarkers of endothelial activation and dysfunction in cardiovascular diseases. *Rev. Cardiovasc. Med.* **23**, 73 (2022).

142. Hromada, C., Mühleder, S., Grillari, J., Redl, H. & Holnthoner, W. Endothelial

extracellular vesicles-promises and challenges. *Front. Physiol.* **8**, 275 (2017).

143. Boulanger, C. M. *et al.* Circulating Microparticles From Patients With Myocardial Infarction Cause Endothelial Dysfunction. *Circulation* **104**, 2649–2652 (2001).

144. Brodsky, S. V., Zhang, F., Nasjletti, A. & Goligorsky, M. S. Endothelium-derived microparticles impair endothelial function in vitro. *Am. J. Physiol. Heart Circ. Physiol.* **286**, H1910–H1915 (2004).

145. Donadee, C. *et al.* Nitric Oxide Scavenging by Red Blood Cell Microparticles and Cell-Free Hemoglobin as a Mechanism for the Red Cell Storage Lesion. *Circulation* **124**, 465–476 (2011).

146. Camus, S. M. *et al.* Circulating cell membrane microparticles transfer heme to endothelial cells and trigger vasoocclusions in sickle cell disease. *Blood* **125**, 3805–3814 (2015).

147. Jansen, F. *et al.* High glucose condition increases NADPH oxidase activity in endothelial microparticles that promote vascular inflammation. *Cardiovasc. Res.* **98**, 94–106 (2013).

148. Densmore, J. C. *et al.* Endothelium-derived microparticles induce endothelial dysfunction and acute lung injury. *Shock* **26**, 464–471 (2006).

149. Han, X. *et al.* Circulating microparticles are associated with plaque burden and cause eNOS uncoupling in patients with carotid atherosclerosis. *Front. Pharmacol.* **13**, 976644 (2022).

150. Chatterjee, V. *et al.* Endothelial microvesicles carrying Src-rich cargo impair adherens junction integrity and cytoskeleton homeostasis. *Cardiovasc. Res.* **116**, 1525–1538 (2020).

151. Edrissi, H., Schock, S. C., Hakim, A. M. & Thompson, C. S. Microparticles generated during chronic cerebral ischemia increase the permeability of microvascular endothelial barriers in vitro. *Brain Res.* **1634**, 83–93 (2016).

152. Barry, O. P., Praticò, D., Savani, R. C. & FitzGerald, G. A. Modulation of monocyte-endothelial cell interactions by platelet microparticles. *J. Clin. Investig.* **102**, 136–144 (1998).

153. Feng, S. *et al.* Endothelial microparticles: A mechanosensitive regulator of vascular homeostasis and injury under shear stress. *Front. Cell Dev. Biol.* **10**, 980112 (2022).

154. Zifkos, K., Dubois, C. & Schäfer, K. Extracellular Vesicles and Thrombosis: Update on the Clinical and Experimental Evidence. *Int. J. Mol. Sci.* **22**, 9317 (2021).

155. Vallier, L. *et al.* Microparticles and Fibrinolysis. *Semin. Thromb. Hemost.* **43**, 129–134 (2017).

156. Sinauridze, E. I. *et al.* Platelet microparticle membranes have 50- to 100-fold higher specific procoagulant activity than activated platelets. *Thromb. Haemost.* **97**, 425–

434 (2007).

157. Badimon, L. *et al.* Microvesicles in Atherosclerosis and Angiogenesis: From Bench to Bedside and Reverse. *Front. Cardiovasc. Med.* **4**, 77 (2017).

158. Jy, W. *et al.* Endothelial microparticles induce formation of platelet aggregates via a von Willebrand factor/ristocetin dependent pathway, rendering them resistant to dissociation. *J. Thromb. Haemost.* **3**, 1301–1308 (2005).

159. Badimon, L. *et al.* Extracellular vesicles in atherothrombosis: From biomarkers and precision medicine to therapeutic targets. *Immunological reviews* **312**, 6–19 (2022).

160. Lacroix, R. *et al.* Activation of plasminogen into plasmin at the surface of endothelial microparticles: A mechanism that modulates angiogenic properties of endothelial progenitor cells in vitro. *Blood* **110**, 2432–2439 (2007).

161. Lacroix, R. & Dignat-George, F. Microparticles as a circulating source of procoagulant and fibrinolytic activities in the circulation. *Thromb. Res.* **129**, S27–S29 (2012).

162. Robbins, P. D., Dorronsoro, A. & Booker, C. N. Regulation of chronic inflammatory and immune processes by extracellular vesicles. *J. Clin. Investig.* **126**, 1173–1180 (2016).

163. Lu, M. *et al.* The Role of Extracellular Vesicles in the Pathogenesis and Treatment of Autoimmune Disorders. *Front. Immunol.* **12**, 566299 (2021).

164. Marar, C., Starich, B. & Wirtz, D. Extracellular vesicles in immunomodulation and tumor progression. *Nature Immunology* **22**, 560–570 (2021).

165. Lindenbergh, M. F. S. & Stoorvogel, W. Antigen Presentation by Extracellular Vesicles from Professional Antigen-Presenting Cells. *Annu. Rev. Immunol.* **36**, 435–459 (2018).

166. Tkach, M. *et al.* Qualitative differences in T-cell activation by dendritic cell-derived extracellular vesicle subtypes. *EMBO J.* **36**, 3012–3028 (2017).

167. Grange, C. & Camussi, G. Immunosuppressive role of extracellular vesicles: HLA-G, an important player. *Ann. Transl. Med.* **5**, 223 (2017).

168. Ma, J. *et al.* Mechanisms by Which Dendritic Cells Present Tumor Microparticle Antigens to CD8+ T Cells. *Cancer Immunology Research* **6**, 1057–1068 (2018).

169. Raimondo, S., Pucci, M., Alessandro, R. & Fontana, S. Extracellular Vesicles and Tumor-Immune Escape: Biological Functions and Clinical Perspectives. *Int. J. Mol. Sci.* **21**, 2286 (2020).

170. Robbins, P. D. & Morelli, A. E. Regulation of immune responses by extracellular vesicles. *Nat. Rev. Immunol.* **14**, 195–208 (2014).

171. Tang, K. *et al.* Microparticles mediate enzyme transfer from platelets to mast cells: A new pathway for lipoxin A4 biosynthesis. *Biochem. Biophys. Res. Commun.* **400**, 432–436 (2010).

172. Berchem, G. *et al.* Hypoxic tumor-derived microvesicles negatively regulate NK cell function by a mechanism involving TGF-β and miR23a transfer. *OncoImmunology* **5**, e1062968 (2016).

173. Kumar, V., Kiran, S., Kumar, S. & Singh, U. P. Extracellular vesicles in obesity and its associated inflammation. *International Reviews of Immunology* **41**, 30–44 (2022).

174. Turpin, D. *et al.* Role of extracellular vesicles in autoimmune diseases. *Autoimmunity reviews* **15**, 174–83 (2016).

175. Davidson, S. M. *et al.* Methods for the identification and characterization of extracellular vesicles in cardiovascular studies: from exosomes to microvesicles. *Cardiovasc. Res.* (2022). doi:10.1093/cvr/cvac031

176. Coumans, F. A. W. *et al.* Methodological guidelines to study extracellular vesicles. *Circ. Res.* **120**, 1632–1648 (2017).

177. Siwaponanan, P., Keawvichit, R., Lekmanee, K., Chomanee, N. & Pattanapanyasat, K. Enumeration and phenotyping of circulating microvesicles by flow cytometry and nanoparticle tracking analysis: Plasma versus serum. *Int. J. Lab. Hematol.* **43**, 506–514 (2021).

178. Witwer, K. W. *et al.* Standardization of sample collection, isolation and analysis methods in extracellular vesicle research. *J. Extracell. Vesicles* **2**, 20360 (2013).

179. Badimon, L., Suades, R., Crespo, J., Padró, T. & Chiva-Blanch, G. Diet, MVs and atherothrombosis. *Front. Biosci.* **23**, 432–457 (2018).

180. Madden, L. A. *et al.* Microparticle-associated vascular adhesion molecule-1 and tissue factor follow a circadian rhythm in healthy human subjects. *Thromb. Haemost.* **99**, 909–915 (2008).

181. De Sousa, K. P. *et al.* Isolation and characterization of extracellular vesicles and future directions in diagnosis and therapy. *WIREs Nanomedicine and Nanobiotechnology* **15**, e1835 (2023).

182. Van Der Pol, E., Böing, A. N., Gool, E. L. & Nieuwland, R. Recent developments in the nomenclature, presence, isolation, detection and clinical impact of extracellular vesicles. *J. Thromb. Haemost.* **14**, 48–56 (2016).

183. Momen-Heravi, F. *et al.* Current methods for the isolation of extracellular vesicles. *Biol. Chem.* **394**, 1253–1262 (2013).

184. Deb, P. K., Kokaz, S. F., Abed, S. N., Paradkar, A. & Tekade, R. K. Pharmaceutical and Biomedical Applications of Polymers. in *Basic Fundamentals of Drug Delivery* 203–267 (Elsevier, 2019). doi:10.1016/B978-0-12-817909-3.00006-6

185. Konoshenko, M. Y., Lekchnov, E. A., Vlassov, A. V. & Laktionov, P. P. Isolation of Extracellular Vesicles: General Methodologies and Latest Trends. *BioMed Res. Int.* **2018**, 8545347 (2018).

186. De Menezes-Neto, A. *et al.* Size-exclusion chromatography as a stand-alone methodology identifies novel markers in mass spectrometry analyses of plasma-derived vesicles from healthy individuals. *J. Extracell. Vesicles* **4**, 27378 (2015).

187. Taylor, D. D. & Shah, S. Methods of isolating extracellular vesicles impact down-stream analyses of their cargoes. *Methods* **87**, 3–10 (2015).

188. Hartjes, T. A., Mytnyk, S., Jenster, G. W., van Steijn, V. & van Royen, M. E. Extracellular vesicle quantification and characterization: Common methods and emerging approaches. *Bioengineering* **6**, 103390 (2019).

189. Bio-Rad. Flow Cytometry Flow Cytometry Basics Guide. Available at: https://www.bio-rad-antibodies.com/introduction-to-flow-cytometry.html. (Accessed: 6th August 2022)

190. van der Pol, E. *et al.* Standardization of extracellular vesicle measurements by flow cytometry through vesicle diameter approximation. *J. Thromb. Haemost.* **16**, 1236–1245 (2018).

191. Larson, M. C., Luthi, M. R., Hogg, N. & Hillery, C. A. Calcium-phosphate microprecipitates mimic microparticles when examined with flow cytometry. *Cytometry A* **83 A**, 242–250 (2013).

192. Théry, C. *et al.* Journal of Extracellular Vesicles Minimal information for studies of extracellular vesicles 2018 (MISEV2018): a position statement of the International Society for Extracellular Vesicles and update of the MISEV2014 guidelines. *J. Extracell. Vesicles* **7**, 1535750 (2018).

193. Welsh, J. A. *et al.* MIFlowCyt-EV: a framework for standardized reporting of extracellular vesicle flow cytometry experiments. *J. Extracell. Vesicles* **9**, 1713526 (2020).

194. Van Deun, J. *et al.* EV-TRACK: Transparent reporting and centralizing knowledge in extracellular vesicle research. *Nat. Methods.* **14**, 228–232 (2017).

195. Ha, M. & Kim, V. N. Regulation of microRNA biogenesis. *Nat. Rev. Mol. Cell Biol.* **15**, 509–524 (2014).

196. Vasudevan, S. Posttranscriptional Upregulation by MicroRNAs. *Wiley Interdiscip. Rev. RNA* **3**, 311–330 (2012).

197. Stavast, C. J. & Erkeland, S. J. The Non-Canonical Aspects of MicroRNAs: Many Roads to Gene Regulation. *Cells* **8**, 1465 (2019).

198. Finicelli, M., Squillaro, T., Galderisi, U. & Peluso, G. Micro-RNAs: Crossroads between the exposure to environmental particulate pollution and the obstructive pulmonary disease. *Int. J. Mol. Sci.* **21**, 7221 (2020).

199. De Rosa, R. *et al.* MicroRNAs and cardiovascular diseases: from bench to bedside. *Transl. Med. UniSa* **17**, 12–18 (2017).

200. Figueiredo, R., Adão, R., Leite-Moreira, A. F., Mâncio, J. & Brás-Silva, C. Candidate microRNAs as prognostic biomarkers in heart failure: A systematic review. *Revista Portuguesa de Cardiologia* **41**, 865–885 (2022).

201. Siasos, G. *et al.* MicroRNAs in cardiovascular disease. *Hellenic journal of cardiology : HJC = Hellenike kardiologike epitheorese* **61**, 165–173 (2020).

202. Kadir, R. R. A., Alwjwaj, M. & Bayraktutan, U. MicroRNA: An Emerging Predictive, Diagnostic, Prognostic and Therapeutic Strategy in Ischaemic Stroke. *Cell. Mol. Neurobiol.* **42**, 1301–1319 (2022).

203. Saenz-Pipaon, G. *et al.* The Role of Circulating Biomarkers in Peripheral Arterial Disease. *Int. J. Mol. Sci.* **22**, 3601 (2021).

204. Deng, J. & Zhong, Q. Advanced research on the microRNA mechanism in heart failure. *Int. J. Cardiol.* **220**, 61–64 (2016).

205. O'Brien, J., Hayder, H., Zayed, Y. & Peng, C. Overview of microRNA biogenesis, mechanisms of actions, and circulation. *Front. Endocrinol. (Lausanne)* **9**, 402 (2018).

206. Gebert, L. F. R. & MacRae, I. J. Regulation of microRNA function in animals. *Nat. Rev. Mol. Cell Biol.* **20**, 21–37 (2019).

207. Sygitowicz, G., Maciejak-Jastrzębska, A. & Sitkiewicz, D. MicroRNAs in the development of left ventricular remodeling and postmyocardial infarction heart failure. *Polish Arch. Intern. Med.* **130**, 59–65 (2020).

208. Bryzgunova, O., Konoshenko, M., Zaporozhchenko, I., Yakovlev, A. & Laktionov, P. Isolation of cell-free mirna from biological fluids: Influencing factors and methods. *Diagnostics* **11**, 865 (2021).

209. Wang, K. *et al.* Comparing the MicroRNA spectrum between serum and plasma. *PLoS ONE* **7**, e41561 (2012).

210. Boon, R. A. & Vickers, K. C. Intercellular Transport of MicroRNAs. *Arterioscler. Thromb. Vasc. Biol.* **33**, 186–192 (2013).

211. Wu, Q., Li, L., Jia, Y., Xu, T. & Zhou, X. Advances in studies of circulating microRNAs: origination, transportation, and distal target regulation. *Journal of cell communication and signaling* 1–11 (2022). doi:10.1007/s12079-022-00705-y

212. Chaput, N. & Théry, C. Exosomes: Immune properties and potential clinical implementations. *Semin. Immunopathol.* **33**, 419–440 (2011).

213. Kosaka, N. *et al.* Neutral sphingomyelinase 2 (nSMase2)-dependent exosomal transfer of angiogenic micrornas regulate cancer cell metastasis. *J. Biol. Chem.* **288**, 10849–10859 (2013).

214. Villarroya-Beltri, C. *et al.* Sumoylated hnRNPA2B1 controls the sorting of miRNAs into exosomes through binding to specific motifs. *Nat. Commun.* **4**, 2980 (2013).

215. Ben-Aicha, S., Badimon, L. & Vilahur, G. Advances in HDL: Much More than Lipid

Transporters. *Int. J. Mol. Sci.* **21**, 732 (2020).

216. Vickers, K. C., Palmisano, B. T., Shoucri, B. M., Shamburek, R. D. & Remaley, A. T. MicroRNAs are transported in plasma and delivered to recipient cells by high-density lipoproteins. *Nat. Cell Biol.* **13**, 423–435 (2011).

217. Wagner, J. *et al.* Characterization of levels and cellular transfer of circulating lipoprotein-bound microRNAs. *Arterioscler. Thromb. Vasc. Biol.* **33**, 1392–1400 (2013).

218. Mori, M. A., Ludwig, R. G., Garcia-Martin, R., Brandão, B. B. & Kahn, C. R. Extracellular miRNAs: From Biomarkers to Mediators of Physiology and Disease. *Cell Metab.* **30**, 656–673 (2019).

219. Arroyo, J. D. *et al.* Argonaute2 complexes carry a population of circulating microRNAs independent of vesicles in human plasma. *Proc. Natl. Acad. Sci. U. S. A.* **108**, 5003–5008 (2011).

220. Turchinovich, A., Weiz, L., Langheinz, A. & Burwinkel, B. Characterization of extracellular circulating microRNA. *Nucleic Acids Res.* **39**, 7223–7233 (2011).

221. Wang, K. *et al.* Circulating microRNAs, potential biomarkers for drug-induced liver injury. *Proc. Natl. Acad. Sci. U. S. A.* **106**, 4402–4407 (2009).

222. Ji, X. *et al.* Plasma miR-208 as a Biomarker of Myocardial Injury. *Clin. Chem.* **55**, 1944–1949 (2009).

223. Zhao, C., Sun, X. & Li, L. Biogenesis and function of extracellular miRNAs. *ExRNA* **1**, 38 (2019).

224. Jonas, S. & Izaurralde, E. Towards a molecular understanding of microRNA-mediated gene silencing. *Nat. Rev. Genet.* **16**, 421–433 (2015).

225. Dutka, M., Bobiński, R. & Korbecki, J. The relevance of microRNA in post-infarction left ventricular remodelling and heart failure. *Heart Fail. Rev.* **24**, 575–586 (2019).

226. Varzideh, F. *et al.* Cardiac Remodeling After Myocardial Infarction: Functional Contribution of microRNAs to Inflammation and Fibrosis. *Front. Cardiovasc. Med.* **9**, 863238 (2022).

227. Topkara, V. K. & Mann, D. L. Clinical applications of miRNAs in cardiac remodeling and heart failure. *Personalized medicine* **7**, 531–548 (2010).

228. Chen, C. *et al.* MicroRNA as a Therapeutic Target in Cardiac Remodeling. *BioMed Res. Int.* **2017**, 1278436 (2017).

229. Sansonetti, M. & De Windt, L. J. Non-coding RNAs in cardiac inflammation: key drivers in the pathophysiology of heart failure. *Cardiovasc. Res.* **118**, 2058–2073 (2022).

230. Pinti, M. V, Hathaway, Q. A. & Hollander, J. M. Role of microRNA in metabolic shift during heart failure. *Am. J. Physiol. Heart Circ. Physiol.* **312**, H33–H45 (2017).

231. Zhang, X. & Schulze, P. C. MicroRNAs in heart failure: Non-coding regulators of metabolic function. *Biochim. Biophys. Acta* **1862**, 2276–2287 (2016).

232. el Azzouzi, H. *et al.* The Hypoxia-Inducible MicroRNA Cluster miR-199a~214 Targets Myocardial PPARδ and Impairs Mitochondrial Fatty Acid Oxidation. *Cell Metab.* **18**, 341–354 (2013).

233. Wang, J., Liew, O., Richards, A. & Chen, Y.-T. Overview of MicroRNAs in Cardiac Hypertrophy, Fibrosis, and Apoptosis. *Int. J. Mol. Sci.* **17**, 749 (2016).

234. Luo, F., Liu, W. & Bu, H. MicroRNAs in hypertrophic cardiomyopathy: pathogenesis, diagnosis, treatment potential and roles as clinical biomarkers. *Heart Fail. Rev.* **27**, 2211–2221 (2022).

235. Dong, Y., Peng, N., Dong, L., Tan, S. & Zhang, X. Non-coding RNAs: Important participants in cardiac fibrosis. *Front. Cardiovasc. Med.* **9**, 937995 (2022).

236. Gargiulo, P. *et al.* MicroRNAs: diagnostic, prognostic and therapeutic role in heart failure—a review. *ESC Heart Fail.* (2022). doi:10.1002/ehf2.14153

237. Felekkis, K. & Papaneophytou, C. Challenges in using circulating micro-rnas as biomarkers for cardiovascular diseases. *Int. J. Mol. Sci.* **21**, 561 (2020).

238. Precazzini, F., Detassis, S., Imperatori, A. S., Denti, M. A. & Campomenosi, P. Measurements methods for the development of microRNA-based tests for cancer diagnosis. *Int. J. Mol. Sci.* **22**, 1176 (2021).

239. Panshin, D. D. & Kondratov, K. A. The Efficiency of Immunoprecipitation of microRNA/Ago2 Complexes from Human Blood Plasma Is Protocol Dependent. *Mol. Biol.* **54**, 213–219 (2020).

240. Siddika, T. & Heinemann, I. U. Bringing MicroRNAs to Light: Methods for MicroRNA Quantification and Visualization in Live Cells. *Front. Bioeng. Biotechnol.* **8**, 619583 (2021).

241. Saliminejad, K., Khorram Khorshid, H. R., Soleymani Fard, S. & Ghaffari, S. H. An overview of microRNAs: Biology, functions, therapeutics, and analysis methods. *J. Cell. Physiol.* **234**, 5451–5465 (2019).

242. Ye, J., Xu, M., Tian, X., Cai, S. & Zeng, S. Research advances in the detection of miRNA. *J. Pharm. Anal.* **9**, 217–226 (2019).

243. Moody, L., He, H., Pan, Y.-X. & Chen, H. Methods and novel technology for microRNA quantification in colorectal cancer screening. *Clin. Epigenetics* **9**, 119 (2017).

244. Rössig, L. *et al.* Congestive heart failure induces endothelial cell apoptosis: Protective role of carvedilol. *J. Am. Coll. Cardiol.* **36**, 2081–2089 (2000).

245. Garcia, S. *et al.* Phenotypic assessment of endothelial microparticles in patients with heart failure and after heart transplantation: Switch from cell activation to apoptosis. *J. Heart Lung Transplant.* **24**, 2184–2189 (2005).

246. Rössig, L. *et al.* Vitamin C Inhibits Endothelial Cell Apoptosis in Congestive Heart Failure. *Circulation* **104**, 2182–2187 (2001).

247. Bulut, D., Scheeler, M., Niedballa, L. M., Miebach, T. & Mügge, A. Effects of immunoadsorption on endothelial function, circulating endothelial progenitor cells and circulating microparticles in patients with inflammatory dilated cardiomyopathy. *Clin. Res. Cardiol.* **100**, 603–610 (2011).

248. Ivak, P. *et al.* Endothelial Dysfunction Expressed as Endothelial Microparticles in Patients With End-Stage Heart Failure. *Physiol. Res.* **63**, S369–S373 (2014).

249. Nascimbene, A. *et al.* Association between cell-derived microparticles and adverse events in patients with nonpulsatile left ventricular assist devices. *J. Heart Lung Transplant.* **33**, 470–477 (2014).

250. Sansone, R. *et al.* Macrovascular and microvascular function after implantation of left ventricular assist devices in end-stage heart failure: Role of microparticles. *J. Heart Lung Transplant.* **34**, 921–932 (2015).

251. Diehl, P. *et al.* Enhanced microparticles in ventricular assist device patients predict platelet, leukocyte and endothelial cell activation. *Interactive CardioVascular and Thoracic Surgery* **11**, 133–137 (2010).

252. Berezin, A. E., Kremzer, A. A., Martovitskaya, Y. V., Samura, T. A. & Berezina, T. A. The predictive role of circulating microparticles in patients with chronic heart failure. *BBA Clin.* **3**, 18–24 (2015).

253. Berezin, A. E., Kremzer, A. A., Martovitskaya, Y. V., Samura, T. A. & Berezina, T. A. The association of subclinical hypothyroidism and pattern of circulating endothelial-derived microparticles among chronic heart failure patients. *Res. Cardiovasc. Med.* **4**, 7 (2015).

254. Berezin, A. E., Kremzer, A. A., Martovitskaya, Y. V., Berezina, T. A. & Gromenko, E. A. Pattern of endothelial progenitor cells and apoptotic endothelial cell-derived microparticles in chronic heart failure patients with preserved and reduced left ventricular ejection fraction. *EBioMedicine* **4**, 86–94 (2016).

255. Kou, Y. *et al.* Intravascular cells and circulating microparticles induce procoagulant activity via phosphatidylserine exposure in heart failure. *J. Thromb. Thrombolysis* **48**, 187–194 (2019).

256. Schurgers, L. J. *et al.* Circulating annexin A5 predicts mortality in patients with heart failure. *J. Intern. Med.* **279**, 89–97 (2016).

257. Berezin, A. E. & Kremzer, A. A. Relationship between circulating endothelial progenitor cells and insulin resistance in non-diabetic patients with ischemic chronic heart failure. *Diabetes & metabolic syndrome* **8**, 138–144 (2014).

258. Berezin, A. E., Kremzer, A. A., Berezina, T. A. & Martovitskaya, Y. V. Pattern of circulating microparticles in chronic heart failure patients with metabolic syndrome: Relevance to neurohumoral and inflammatory activation. *BBA Clin.* **4**, 69–75 (2015).

259. Berezin, A. E., Kremzer, A. A., Samura, T. A. & Martovitskaya, Y. V. Circulating Endothelial-Derived Apoptotic Microparticles in the Patients with Ischemic Symptomatic Chronic Heart Failure: Relevance of Pro-Inflammatory Activation and Outcomes. *Int. Cardiovasc. Res. J.* **8**, 116–123 (2014).

260. Montoro-García, S. *et al.* Small-size Microparticles as Indicators of Acute Decompensated State in Ischemic Heart Failure. *Rev. Esp. Cardiol.* **68**, 951–958 (2015).

261. Berezin, A. E., Kremzer, A. A., Samura, T. A. & Berezina, T. A. Altered signature of apoptotic endothelial cell-derived microvesicles predicts chronic heart failure phenotypes. *Biomark. Med.* **13**, 737–750 (2019).

262. Berezin, A. E. *et al.* The utility of biomarker risk prediction score in patients with chronic heart failure. *Int. J. Clin. Exp. Med.* **8**, 18255–18264 (2015).

263. Bulut, D. *et al.* Circulating Endothelial Microparticles Correlate Inversely With Endothelial Function in Patients With Ischemic Left Ventricular Dysfunction. *J. Card. Fail.* **14**, 336–340 (2008).

264. Tijsen, A. J. *et al.* MiR423-5p as a circulating biomarker for heart failure. *Circ. Res.* **106**, 1035–1039 (2010).

265. Voellenkle, C. *et al.* MicroRNA signatures in peripheral blood mononuclear cells of chronic heart failure patients. *Physiol. Genomics* **42**, 420–426 (2010).

266. Fukushima, Y., Nakanishi, M., Nonogi, H., Goto, Y. & Iwai, N. Assessment of plasma miRNAs in congestive heart failure. *Circ. J.* **75**, 336–340 (2011).

267. Goren, Y. *et al.* Serum levels of microRNAs in patients with heart failure. *Eur. J. Heart Fail.* **14**, 147–154 (2012).

268. Ellis, K. L. *et al.* Circulating microRNAs as candidate markers to distinguish heart failure in breathless patients. *Eur. J. Heart Fail.* **15**, 1138–1147 (2013).

269. Fan, K. L., Zhang, H. F., Shen, J., Zhang, Q. & Li, X. L. Circulating microRNAs levels in Chinese heart failure patients caused by dilated cardiomyopathy. *Indian Heart J.* **65**, 12–16 (2013).

270. Gupta, M. K. *et al.* MiRNA-548c: A specific signature in circulating PBMCs from dilated cardiomyopathy patients. *J. Mol. Cell. Cardiol.* **62**, 131–141 (2013).

271. Nair, N., Kumar, S., Gongora, E. & Gupta, S. Circulating miRNA as novel markers for diastolic dysfunction. *Mol. Cell. Biochem.* **376**, 33–40 (2013).

272. Vogel, B. *et al.* Multivariate miRNA signatures as biomarkers for non-ischaemic systolic heart failure. *Eur. Heart J.* **34**, 2812–2822 (2013).

273. Goldraich, L. A. *et al.* Transcoronary gradient of plasma microRNA 423-5p in heart failure: Evidence of altered myocardial expression. *Biomarkers* **19**, 135–141 (2014).

274. Sygitowicz, G. *et al.* Circulating microribonucleic acids miR-1, miR-21 and miR-208a

in patients with symptomatic heart failure: Preliminary results. *Arch. Cardiovasc. Dis.* **108**, 634–642 (2015).

275. Marques, F. Z., Vizi, D., Khammy, O., Mariani, J. A. & Kaye, D. M. The transcardiac gradient of cardio-microRNAs in the failing heart. *Eur. J. Heart Fail.* **18**, 1000–1008 (2016).

276. Beaumont, J. *et al.* MicroRNA-19b is a potential biomarker of increased myocardial collagen cross-linking in patients with aortic stenosis and heart failure. *Sci. Rep* **7**, 40696 (2017).

277. Beg, F. *et al.* Inflammation-associated microRNA changes in circulating exosomes of heart failure patients. *BMC Res. Notes* **10**, 751 (2017).

278. Scrutinio, D. *et al.* Circulating microRNA-150-5p as a novel biomarker for advanced heart failure: A genome-wide prospective study. *J. Heart Lung Transplant.* **36**, 616–624 (2017).

279. Vegter, E. L. *et al.* Low circulating microRNA levels in heart failure patients are associated with atherosclerotic disease and cardiovascular-related rehospitalizations. *Clin. Res. Cardiol.* **106**, 598–609 (2017).

280. Zhang, J. *et al.* Circulating miRNA-21 is a promising biomarker for heart failure. *Mol. Med. Rep.* **16**, 7766–7774 (2017).

281. Zhao, Z. & Zhou, Y. Circulating miR-21 and miR-423-5p as biomarkers for heart failure in heart valve disease patients. *Int. J. Clin. Exp. Pathol.* **10**, 5703–5711 (2017).

282. Guo, M. *et al.* Combined use of circulating miR-133a and NT-proBNP improves heart failure diagnostic accuracy in elderly patients. *Med. Sci. Monit.* **24**, 8840–8848 (2018).

283. Chen, F., Yang, J., Li, Y. & Wang, H. Circulating microRNAs as novel biomarkers for heart failure. *Hellenic J. Cardiol.* **59**, 209–214 (2018).

284. Jiao, M. *et al.* Circulating microRNA signature for the diagnosis of childhood dilated cardiomyopathy. *Sci. Rep* **8**, 724 (2018).

285. Liu, W. *et al.* Association of miR-197-5p, a circulating biomarker for heart failure, with myocardial fibrosis and adverse cardiovascular events among patients with stage C or D heart failure. *Cardiology* **141**, 212–225 (2019).

286. MacIejak, A. *et al.* Circulating miR-30a-5p as a prognostic biomarker of left ventricular dysfunction after acute myocardial infarction. *Sci. Rep* **8**, 9883 (2018).

287. Tomaniak, M. *et al.* MiR-1, miR-21, and galectin-3 in hypertensive patients with symptomatic heart failure and left ventricular hypertrophy. *Kardiol. Pol.* **76**, 1009–1011 (2018).

288. Yao, Y. *et al.* Combination of peripheral blood mononuclear cell miR-19b-5p, miR-221, miR-25-5p, and hypertension correlates with an increased heart failure risk in

coronary heart disease patients. *Anatol. J. Cardiol.* **20**, 100–109 (2018).

289. Meiri, E. *et al.* Differential expression of microRNA in serum fractions and association of Argonaute 1 microRNAs with heart failure. *J. Cell. Mol. Med.* **24**, 6586–6595 (2020).

290. Zhang, B. *et al.* Expression of serum microRNA-155 and its clinical importance in patients with heart failure after myocardial infarction. *J. Int. Med. Res.* **47**, 6294–6302 (2019).

291. Han, R., Li, K., Li, L., Zhang, L. & Zheng, H. Expression of microRNA-214 and galectin-3 in peripheral blood of patients with chronic heart failure and its clinical significance. *Exp. Ther. Med.* **19**, 1322–1328 (2020).

292. Ishiguro, T. *et al.* Circulating miR-489 as a potential new biomarker for idiopathic dilated cardiomyopathy. *Fujita medical journal* **7**, 18–22 (2021).

293. Zhang, L. *et al.* Diagnostic value of circulating microRNA-19b in heart failure. *Eur. J. Clin. Investig.* **50**, e13308 (2020).

294. Ding, H. *et al.* Combined detection of miR-21-5p, miR-30a-3p, miR-30a-5p, miR-155-5p, miR-216a and miR-217 for screening of early heart failure diseases. *Biosci. Rep.* **40**, BSR20191653 (2020).

295. Wu, H. B. *et al.* MicroRNA-365 expression in the serum of patients with heart failure with reduced ejection fraction after myocardial infarction. *Am. J. Emerg. Med.* **S0735**-**6757**, 31026–31033 (2020).

296. Xu, Y. *et al.* Long non-coding RNA CASC7 is associated with the pathogenesis of heart failure via modulating the expression of miR-30c. *J. Cell. Mol. Med.* **24**, 11500–11511 (2020).

297. Yang, H. *et al.* MicroRNA-181b Serves as a Circulating Biomarker and Regulates Inflammation in Heart Failure. *Dis. Markers* **2021**, 4572282 (2021).

298. Brundin, M., Wågsäter, D., Alehagen, U. & Carlhäll, C. J. Circulating microRNA-29-5p can add to the discrimination between dilated cardiomyopathy and ischaemic heart disease. *ESC Heart Fail.* **8**, 3865–3874 (2021).

299. Jin, D., Yang, X.-Y. & Wang, J.-S. MicroRNA-126 Level Increases During Exercise Rehabilitation of Heart Failure with a Preserved Ejection Fraction. *Int. J. Gen. Med.* **Volume 14**, 3397–3404 (2021).

300. Li, D.-M. *et al.* Diagnostic value of circulating microRNA-208a in differentiation of preserved from reduced ejection fraction heart failure. *Heart Lung* **50**, 71–74 (2021).

301. Tu, J., Ma, L., Zhang, M. & Zhang, J. Long Non-Coding RNA SOX2 Overlapping Transcript Aggravates H9c2 Cell Injury via the miR-215-5p/ZEB2 Axis and Promotes Ischemic Heart Failure in a Rat Model. *Tohoku J. Exp. Med.* **254**, 221–231 (2021).

302. Zhu, Q. *et al.* Differentially expressed TUG1 and miR-145-5p indicate different

severity of chronic heart failure and predict 2-year survival prognosis. *Exp. Ther. Med.* **22**, 1362 (2021).

303. Fayez, A. G. *et al.* miR-454-3p and miR-194-5p targeting cardiac sarcolemma ion exchange transcripts are potential noninvasive diagnostic biomarkers for childhood dilated cardiomyopathy in Egyptian patients. *The Egyptian Heart Journal* **74**, 65 (2022).

304. Li, W., Li, Y., Jiang, F. & Liu, H. Correlation between serum levels of microRNA-21 and inflammatory factors in patients with chronic heart failure. *Medicine (Baltimore)* **101**, e30596 (2022).

305. Qian, L. *et al.* Diagnostic potential of a circulating miRNA model associated with therapeutic effect in heart failure. *J. Transl. Med.* **20**, 267 (2022).

306. Endo, K. *et al.* MicroRNA 210 as a Biomarker for Congestive Heart Failure. *Biol. Pharm. Bull.* **36**, 48–54 (2013).

307. D'alessandra, Y. *et al.* Differential role of circulating micrornas to track progression and pre-symptomatic stage of chronic heart failure: A pilot study. *Biomedicines* **8**, 597 (2020).

308. Seronde, M. F. *et al.* Circulating microRNAs and outcome in patients with acute heart failure. *PLoS ONE* **10**, e0142237 (2015).

309. Bayés-Genís, A. *et al.* Prognostic value of circulating microRNAs on heart failure-related morbidity and mortality in two large diverse cohorts of general heart failure patients. *Eur. J. Heart Fail.* **20**, 67–75 (2018).

310. Masson, S. *et al.* Circulating microRNA-132 levels improve risk prediction for heart failure hospitalization in patients with chronic heart failure. *Eur. J. Heart Fail.* **20**, 78–85 (2018).

311. Van Boven, N. *et al.* Serially measured circulating microRNAs and adverse clinical outcomes in patients with acute heart failure. *Eur. J. Heart Fail.* **20**, 89–96 (2018).

312. Stojkovic, S. *et al.* Liver-specific microRNA-122 as prognostic biomarker in patients with chronic systolic heart failure. *Int. J. Cardiol.* **303**, 80–85 (2020).

313. Rincón, L. M. *et al.* Serum microRNAs are key predictors of long-term heart failure and cardiovascular death after myocardial infarction. *ESC Heart Fail.* **9**, 3367–3379 (2022).

314. Galluzzo, A. *et al.* Identification of novel circulating microRNAs in advanced heart failure by next-generation sequencing. *ESC Heart Fail.* **8**, 2907–2919 (2021).

315. Wong, L. L. *et al.* Circulating microRNAs in heart failure with reduced and preserved left ventricular ejection fraction. *Eur. J. Heart Fail.* **17**, 393–404 (2015).

316. Watson, C. J. *et al.* MicroRNA signatures differentiate preserved from reduced ejection fraction heart failure. *Eur. J. Heart Fail.* **17**, 405–415 (2015).

317. Wong, L. L. *et al.* Combining Circulating MicroRNA and NT-proBNP to Detect and Categorize Heart Failure Subtypes. *J. Am. Coll. Cardiol.* **73**, 1300–1313 (2019).

318. Matsumoto, S. *et al.* Circulating p53-responsive MicroRNAs are predictive indicators of heart failure after acute myocardial infarction. *Circ. Res.* **113**, 322–326 (2013).

319. Liu, Q., Li, H., Wang, N., Chen, H. & Wang, J. Expression of miR-126 and miR-508-5p in endothelial progenitor cells is associated with the prognosis of chronic heart failure patients. *Int. J. Cardiol.* **168**, 2082–2088 (2013).

320. De Rosa, S. *et al.* Transcoronary concentration gradients of circulating microRNAs in heart failure. *Eur. J. Heart Fail.* **20**, 1000–1010 (2018).

321. Lin, X., Zhang, S. & Huo, Z. Serum circulating miR-150 is a predictor of post-acute myocardial infarction heart failure. *Int. Heart J.* **60**, 280–286 (2019).

322. Liang, J. *et al.* A subset of circulating microRNAs is expressed differently in patients with myocardial infarction. *Mol. Med. Rep.* **12**, 243–247 (2015).

323. Zhang, M. *et al.* Circulating MicroRNA-145 is Associated with Acute Myocardial Infarction and Heart Failure. *Chin. Med. J.* **130**, 51–56 (2017).

324. Bauters, C. *et al.* Circulating miR-133a and miR-423-5p fail as biomarkers for left ventricular remodeling after myocardial infarction. *Int. J. Cardiol.* **168**, 1837–1840 (2013).

325. Reid, V. L. & Webster, N. R. Role of microparticles in sepsis. *Br. J. Anaesth.* **109**, 503–513 (2012).

326. Hu, T., Wolfram, J. & Srivastava, S. Extracellular Vesicles in Cancer Detection: Hopes and Hypes. *Trends in cancer* **7**, 122–133 (2021).

327. Zhang, J., Li, H., Fan, B., Xu, W. & Zhang, X. Extracellular vesicles in normal pregnancy and pregnancy-related diseases. *J. Cell. Mol. Med.* **24**, 4377–4388 (2020).

328. Suades, R., Padró, T., Vilahur, G. & Badimon, L. Circulating and platelet-derived microparticles in human blood enhance thrombosis on atherosclerotic plaques. *Thromb. Haemost.* **108**, 1208–1219 (2012).

329. Suades, R., Padró, T., Alonso, R., Mata, P. & Badimon, L. Lipid-lowering therapy with statins reduces microparticle shedding from endothelium, platelets and inflammatory cells. *Thromb. Haemost.* **110**, 366–377 (2013).

330. Nieuwland, R. *et al.* Cellular origin and procoagulant properties of microparticles in meningococcal sepsis. *Blood* **95**, 930–935 (2000).

331. Agarwal, V., Bell, G. W., Nam, J.-W. & Bartel, D. P. Predicting effective microRNA target sites in mammalian mRNAs. *Elife* **4**, e05005 (2015).

332. Sticht, C., De La Torre, C., Parveen, A. & Gretz, N. miRWalk: An online resource for prediction of microRNA binding sites. *PLoS ONE* **13**, e0206239 (2018).

333. Chen, Y. & Wang, X. MiRDB: An online database for prediction of functional microRNA targets. *Nucleic Acids Res.* **48**, D127–D131 (2020).

334. Liu, W. & Wang, X. Prediction of functional microRNA targets by integrative modeling of microRNA binding and target expression data. *Genome Biol.* **20**, 18 (2019).

335. Vejnar, C. E. & Zdobnov, E. M. MiRmap: Comprehensive prediction of microRNA target repression strength. *Nucleic Acids Res.* **40**, 11673–11683 (2012).

336. Shannon, P. *et al.* Cytoscape: A software Environment for integrated models of biomolecular interaction networks. *Genome Res.* **13**, 2498–2504 (2003).

337. Szklarczyk, D. *et al.* The STRING database in 2021: Customizable protein-protein networks, and functional characterization of user-uploaded gene/measurement sets. *Nucleic Acids Res.* **49**, D605–D612 (2021).

338. Su, G., Kuchinsky, A., Morris, J. H., States, D. J. & Meng, F. GLay: Community structure analysis of biological networks. *Bioinformatics* **26**, 3135–3137 (2010).

339. Ge, S. X., Jung, D. & Yao, R. ShinyGO: a graphical gene-set enrichment tool for animals and plants. *Bioinformatics* **36**, 2628–2629 (2020).

340. Kanehisa, M. & Goto, S. KEGG: Kyoto Encyclopedia of Genes and Genomes. *Nucleic Acids Res.* **28**, 27–30 (2000).

341. Kanehisa, M., Furumichi, M., Sato, Y., Ishiguro-Watanabe, M. & Tanabe, M. KEGG: Integrating viruses and cellular organisms. *Nucleic Acids Res.* **49**, D545–D551 (2021).

342. Valadi, H. *et al.* Exosome-mediated transfer of mRNAs and microRNAs is a novel mechanism of genetic exchange between cells. *Nat. Cell Biol.* **9**, 654–659 (2007).

343. Suades, R. *et al.* Circulating microparticle signature in coronary and peripheral blood of ST elevation myocardial infarction patients in relation to pain-to-PCI elapsed time. *Int. J. Cardiol.* **202**, 378–387 (2016).

344. Suades, R. *et al.* Growing thrombi release increased levels of CD235a+ microparticles and decreased levels of activated platelet-derived microparticles. Validation in ST-elevation myocardial infarction patients. *J. Thromb. Haemost.* **13**, 1776–1786 (2015).

345. Chiva-Blanch, G. *et al.* Monocyte-derived circulating microparticles (CD14+, CD14+/CD11b+ and CD14+/CD142+) are related to long-term prognosis for cardiovascular mortality in STEMI patients. *Int. J. Cardiol.* **227**, 876–881 (2017).

346. Chiva-Blanch, G. *et al.* Platelet-, monocyte-derived & tissue factor-carrying circulating microparticles are related to acute myocardial infarction severity. *PLoS ONE* **12**, 0172558 (2017).

347. Sionis, A. *et al.* Circulating microparticles are associated with clinical severity of persistent ST-segment elevation myocardial infarction complicated with cardiogenic

shock. *Int. J. Cardiol.* **258**, 249–258 (2018).

348. Chiva-Blanch, G. *et al.* Microparticle shedding from neural progenitor cells and vascular compartment cells is increased in ischemic stroke. *PLoS ONE* **11**, e0148176 (2016).

349. Chiva-Blanch, G. *et al.* CD3+/CD45+ and SMA-α+ circulating microparticles are increased in individuals at high cardiovascular risk who will develop a major cardiovascular event. *Int. J. Cardiol.* **208**, 147–149 (2016).

350. Suades, R. *et al.* Circulating CD45+/CD3+ lymphocyte-derived microparticles map lipid-rich atherosclerotic plaques in familial hypercholesterolaemia patients. *Thromb. Haemost.* **111**, 111–121 (2014).

351. Chiva-Blanch, G. *et al.* Liquid Biopsy of Extracellular Microvesicles Maps Coronary Calcification and Atherosclerotic Plaque in Asymptomatic Patients with Familial Hypercholesterolemia: A Computed Tomographic Angiography Imaging Study. *Arterioscler. Thromb. Vasc. Biol.* **39**, 945–955 (2019).

352. Suades, R., Padró, T., Alonso, R., Mata, P. & Badimon, L. High levels of TSP1+/CD142+ platelet-derived microparticles characterise young patients with high cardiovascular risk and subclinical atherosclerosis. *Thromb. Haemost.* **114**, 1310–1321 (2015).

353. Steffens, S. *et al.* Stimulating pro-reparative immune responses to prevent adverse cardiac remodelling: consensus document from the joint 2019 meeting of the ESC Working Groups of cellular biology of the heart and myocardial function. *Cardiovasc. Res.* **116**, 1850–1862 (2020).

354. Carrillo-Salinas, F. J., Ngwenyama, N., Anastasiou, M., Kaur, K. & Alcaide, P. Heart Inflammation: Immune Cell Roles and Roads to the Heart. *Am. J. Pathol.* **189**, 1482–1494 (2019).

355. Ong, S. *et al.* Natural killer cells limit cardiac inflammation and fibrosis by halting eosinophil infiltration. *Am. J. Pathol.* **185**, 847–861 (2015).

356. Bozkurt, B., Mann, D. L. & Deswal, A. Biomarkers of inflammation in heart failure. *Heart Fail. Rev.* **15**, 331–341 (2010).

357. Dixon, D.-L., Griggs, K. M., Bersten, A. D. & De Pasquale, C. G. Systemic inflammation and cell activation reflects morbidity in chronic heart failure. *Cytokine* **56**, 593–599 (2011).

358. Chaikijurajai, T. & Tang, W. H. W. Reappraisal of Inflammatory Biomarkers in Heart Failure. *Curr. Heart Fail. Rep.* **17**, 9–19 (2020).

359. Kologrivova, I., Shtatolkina, M., Suslova, T. & Ryabov, V. Cells of the Immune System in Cardiac Remodeling: Main Players in Resolution of Inflammation and Repair After Myocardial Infarction. *Front. Immunol.* **12**, 664457 (2021).

360. Shirazi, L. F., Bissett, J., Romeo, F. & Mehta, J. L. Role of Inflammation in Heart Failure. *Curr. Atheroscler. Rep.* **19**, 27 (2017).

361. Escate, R. *et al.* High miR-133a levels in the circulation anticipates presentation of clinical events in familial hypercholesterolaemia patients. *Cardiovasc. Res.* **117**, 109–122 (2021).

362. Liu, Y., Song, J. W., Lin, J. Y., Miao, R. & Zhong, J. C. Roles of MicroRNA-122 in Cardiovascular Fibrosis and Related Diseases. *Cardiovasc. Toxicol.* **20**, 463–473 (2020).

363. Charrier, H. *et al.* Integrative system biology analyses identify seven microRNAs to predict heart failure. *Non-coding RNA* **5**, 22 (2019).

364. Essandoh, K., Li, Y., Huo, J. & Fan, G.-C. MiRNA-Mediated Macrophage Polarization and its Potential Role in the Regulation of Inflammatory Response. *Shock (Augusta, Ga.)* **46**, 122–131 (2016).

365. Wang, L., Xia, J., Ke, Z. & Zhang, B. Blockade of NEAT1 represses inflammation response and lipid uptake via modulating miR-342-3p in human macrophages THP-1 cells. *J. Cell. Physiol.* **234**, 5319–5326 (2019).

366. Ray, S. L. *et al.* The role of miR-342 in vascular health. Study in subclinical cardiovascular disease in mononuclear cells, plasma, inflammatory cytokines and PANX2. *Int. J. Mol. Sci.* **21**, 7217 (2020).

367. Liu, Y. *et al.* H2O2 down-regulates SIRT7's protective role of endothelial premature dysfunction via microRNA-335-5p. *Biosci. Rep.* **42**, BSR20211775 (2022).

368. Rech, M. *et al.* AntagomiR-103 and -107 Treatment Affects Cardiac Function and Metabolism. *Mol. Ther. Nucleic Acids* **14**, 424–437 (2019).

369. Cai, Z. *et al.* MiR-125a-5p ameliorates monocrotaline-induced pulmonary arterial hypertension by targeting the TGF-β1 and IL-6/STAT3 signaling pathways. *Experimental & Molecular Medicine* **50**, 45 (2018).

370. Song, L. *et al.* MiR-451 is decreased in hypertrophic cardiomyopathy and regulates autophagy by targeting TSC1. *J. Cell. Mol. Med.* **18**, 2266–2274 (2014).

371. He, J. *et al.* MicroRNA-30b-5p is Involved in the Regulation of Cardiac Hypertrophy by Targeting CaMKIIδ. *Journal of Investigative Medicine* **61**, 604–612 (2013).

372. Chen, Y.-H. *et al.* Integrated Analysis of circRNA-miRNA-mRNA ceRNA Network in Cardiac Hypertrophy. *Front. Genet.* **13**, 781676 (2022).

373. Matsuda, T. *et al.* H-Ras Isoform Mediates Protection Against Pressure Overload-Induced Cardiac Dysfunction in Part Through Activation of AKT. *Circ. Heart Fail.* **10**, e003658 (2017).

374. Qin, W., Cao, L. & Massey, I. Y. Role of PI3K/Akt signaling pathway in cardiac fibrosis. *Mol. Cell. Biochem.* **476**, 4045–4059 (2021).

375. Ghafouri-Fard, S. *et al.* Interplay between PI3K/AKT pathway and heart disorders. *Mol. Biol. Rep.* **49**, 9767–9781 (2022).

376. Shanbhag, S. M. *et al.* Prevalence and prognosis of ischaemic and non-ischaemic myocardial fibrosis in older adults. *Eur. Heart J.* **40**, 529–538 (2019).

377. Yousefi, F. *et al.* TGF-β and WNT signaling pathways in cardiac fibrosis: Non-coding RNAs come into focus. *Cell Commun. Signal.* **18**, 87 (2020).

378. Mehdizadeh, M., Aguilar, M., Thorin, E., Ferbeyre, G. & Nattel, S. The role of cellular senescence in cardiac disease: basic biology and clinical relevance. *Nat. Rev. Cardiol.* **19**, 250–264 (2022).

379. Kintscher, U., Foryst-Ludwig, A., Haemmerle, G. & Zechner, R. The Role of Adipose Triglyceride Lipase and Cytosolic Lipolysis in Cardiac Function and Heart Failure. *Cell Reports Med.* **1**, 100001 (2020).

380. Petersen, K. M., Bøgevig, S., Holst, J. J., Knop, F. K. & Christensen, M. B. Hemodynamic Effects of Glucagon: A Literature Review. *J. Clin. Endocrinol. Metab.* **103**, 1804–1812 (2018).

381. Lee, D. S. *et al.* Relation of disease pathogenesis and risk factors to heart failure with preserved or reduced ejection fraction: Insights from the framingham heart study of the national heart, lung, and blood institute. *Circulation* **119**, 3070–3077 (2009).

382. Wang, J. & Chen, X. Junctional Adhesion Molecules: Potential Proteins in Atherosclerosis. *Front. Cardiovasc. Med.* **9**, 888818 (2022).

'I didn't think it would end this way.'
'End? No, the journey doesn't end here. Death is just another path, one that we all must take. The grey rain-curtain of this world rolls back, and all turns to silver glass, and then you see it.'
'What? Gandalf? See what?'
'White shores, and beyond, a far green country under a swift sunrise.'
'Well, that isn't so bad.'
'No. No, it isn't.'
-Pippin and Gandalf,
The Lord of the Rings: The Return of the King, **J.R.R. Tolkien (1955)**

Annex

Table A1: List of EVs studies in chronic heart failure.

EVs	POPULATION	FINDINGS	REFERENCES
AV⁺	11 HS 15 HF	- EVs increased in CHF vs HS. - EVs correlated with NYHA.	244
AV⁺	34 CHF (NYHA II-IV): - 17 Vitamin C - 17 Placebo	- EVs reduced in CHF after vitamin C treatment. - No changes in CHF after placebo treatment.	246
CD31⁺ **CD62E⁺**	23 HS 23 CHF 23 CHF after HTx	- CD62E⁺ eEVs increased in CHF vs CHF after HTx. - CD62E⁺ eEVs increased in CHF vs HS. - CD31⁺ eEVs increased in CHF vs HS. - CD31⁺ eEVs remained elevated in CHF after HTx.	245
CD31⁺/AV⁺	Ischaemic CHF: - 18 HFrEF men - 17 HFpEF men	- CD31⁺/AV⁺ eEVs increased in HFrEF vs HFpEF. - CD31⁺/AV⁺ eEVs inversely correlated with endothelium-dependent vasodilation.	263
CD144⁺	31 HS 169 CHF: - 33 CVE - 22 All-cause mortality	- CD144⁺ eEVs increased in CHF vs HS. - CD144⁺ eEVs positively correlated with NYHA. - CD144⁺ eEVs associated with CVE or CV-death (CVE and CV-death were more frequent in patients with high CD144⁺ eEVs levels than in patients with lower levels). - Multivariate regression analysis: high CD144⁺ eEVs levels (above mean), NYHA, eGFR and high BNP levels were independent predictors of CVE. - Multivariate regression analysis: DM, HTN, eGFR, LVEF and beta-blocker treatment were independent predictors of CVE.	139
CD31⁺/CD61⁺ **CD11b⁺** **CD62E⁺**	16 Controls 12 CHF with LVAD	- CD31⁺/CD61⁺ pEVs increased in CHF vs controls. - CD11b⁺ LEVs increased in CHF vs controls. - CD62E⁺ eEVs increased in CHF vs controls.	251
AV⁺ **CD31⁺/CD42b⁻/AV⁺**	HFrEF due to inflammatory DCM (NYHA III-IV): - 7 Immunoadsorption	- AV⁺ EVs decreased after immunoadsorption treatment. - CD31⁺/CD41b⁻/AV⁺ eEVs decreased after immunoadsorption treatment.	247

EVs	POPULATION	FINDINGS	REFERENCES
	- 5 No immunoadsorption	- AV^+ and $CD31^+/CD41b^-/AV^+$ EVs negatively correlated with LVEF, which increased 6 months after immunoadsorption treatment.	
$CD31^+/AV^+$	154 Ischaemic CHF: - 21 Died during follow-up - 133 Survived follow-up	- $CD31^+/AV^+$ eEVs increased in dead vs surviving patients. - $CD31^+/AV^+$ eEVs positively correlated with TNFα, FAS, sFAS ligand and FAS/sFAS ligand ratio, NT-proBNP and NYHA. - $CD31^+/AV^+$ eEVs negatively correlated with LVEF and eGFR. - Multivariate analysis: $CD31^+/AV^+$ eEVs levels and NT-proBNP independently predicted long-term cumulative survival, CHF-related rehospitalisation and CHF-related death.	259
AV^+	10 HS 20 CHF	- AV^+ EVs increased in CHF vs HS at baseline. - AV^+ EVs increased after LVAD implantation and returned to baseline after 3 months. - AV^+ EVs increased in CHF that developed an adverse event during the 3-month follow-up.	249
AV^+	30 CHF with LVAD: - 18 Ischaemic CHF - 12 Non-ischaemic CHF	- AV^+ EVs levels decreased after LVAD implantation.	248
$CD31^+/AV^+$	300 ischaemic CHF: - 171 With insulin resistance - 129 Without insulin resistance	- $CD31^+/AV^+$ eEVs increased in CHF with insulin resistance vs CHF without insulin resistance. - $CD31^+/AV^+$ eEVs positively correlated NYHA, HOMA-IR, NT-proBNP, hsCRP, BMI. - Multivariate regression analysis: NYHA, NT-proBNP, hsCRP, LVEF were independent predictors of increased $CD31^+/AV^+$ in circulation.	257
AV^+ **$CD31^+$** **$CD41a^+$** **$CD64^+$** **$CD62E^+$** **$CD105^+$** **$CD144^+$** **$CD31^+/AV^+$** **$CD144^+/CD31^+$** **$CD144^+/CD31^+/AV^+$**	35 HS 101 Metabolic syndrome: - 54 With CHF - 47 Without CHF	- AV^+, $CD41a^+$, $CD64^+$, $CD144^+$ $CD144^+/AV^+$, $CD144^+/CD31^+$, $CD144^+/CD31^+/AV^+$ EVs and $CD105^+$ to $CD31^+/AV^+$ ratio were similar in metabolic syndrome patients (CHF and non-CHF) vs HS. - $CD62E^+$ and $CD105^+$ eEVs and $CD62E^+$ to $CD31^+/AV^+$ ratio decreased in metabolic syndrome patients (CHF and non-CHF) vs HS. - $CD31^+/AV^+$ eEVs increased in metabolic syndrome patients (CHF and non-CHF) vs HS. - AV^+, $CD41a^+$, $CD64^+$, $CD62E^+$, $CD105^+$, $CD144^+$ $CD144^+/AV^+$, $CD144^+/CD31^+$ and $CD144^+/CD31^+/AV^+$ EVs and $CD105^+$ to $CD31^+/AV^+$ ratio were similar in metabolic syndrome patients (CHF and non-CHF) vs HS. - $CD31^+/AV^+$ eEVs increased in patients with metabolic syndrome with CHF vs non-CHF. - $CD62E^+$ to $CD31^+/AV^+$ ratio decreased in metabolic syndrome patients with CHF vs non-CHF.	258

EVs	POPULATION	FINDINGS	REFERENCES
		- CD62E+ to CD31+/AV+ ratio correlated positively with eGFR, waist circumference, male gender. - CD62E+ to CD31+/AV+ ratio correlated negatively with NT-proBNP, BMI, osteoprotegerin, HOMA-IR, dyslipidaemia, creatinine, Framingham risk score, age, smoking. - Multivariate analysis: NT-proBNP, osteoprotegerin, and BMI were independent factors of CD62E+ to CD31+/AV+ ratio reduction.	
AV+ **CD31+/AV+** **CD144+** **CD62E+** **CD144+/CD31+** **CD144+/CD31+/AV+**	388 Ischaemic CHF (HFrEF): - 58 With subclinical hypothyroidism - 335 Without subclinical hypothyroidism	- CD31+/AV+ eEVs and CD31+/AV+ to CD62E+ ratio, increased in CHF with subclinical hypothyroidism vs CHF without clinical hypothyroidism. - CD144+, CD144+/CD31+, CD144+/CD31+/AV+, CD62E+ eEVs were similar between CHF with and without hypothyroidism. - CD31+/AV+ to CD62E+ ratio positively correlated with NT-proBNP, TSH, hsCRP, NYHA, dyslipidaemia, T2DM, creatinine, SUA, being male, age, smoking. - CD31+/AV+ to CD62E+ ratio negatively correlated with BMI, eGFR. - Multivariate analysis: NT-proBNP, TSH, NYHA, hsCRP, T2DM, dyslipidaemia, BMI, SUA and creatinine were independently associated with CD31+/AV+ to CD62E+ ratio.	253
AV+ **CD31+/AV+** **CD144+** **CD62E+** **CD144+/AV+** **CD144+/CD31+** **CD144+/CD31+/AV+**	388 Ischaemic CHF (HFrEF): - 110 CVE (47 deaths, 90 rehospitalisations [74 due to CHF]) - 278 no CVE	- CD144+/AV+ and CD62E+ eEVs were similar in CVE and non-CVE. - CD144+/CD31+, CD144+/CD31+/AV+, CD31+/AV+ eEVs increased in CVE vs non-CVE. - CD144+/AV+ eEVs correlated positively with NYHA and NT-proBNP, and negatively with LEVF. - CD144+/CD31+ and CD31+/AV+ eEVs correlated positively with NYHA, NT-proBNP, SUA, hsCRP and T2DM, and negatively with LVEF and HDL. CD31+/AV+ eEVs correlated negatively with eGFR. - CD62E+ eEVs correlated positively with hsCRP and SUA, and negatively with HDL. - CD144+/CD31+/AV+ and CD31+/AV+ eEVs added to a multivariate model including NYHA, HFrEF, NT-proBNP and hsCRP improved CVE prediction.	252
CD31+/AV+	388 Ischaemic CHF: - 285 CVE (43 deaths, 206 rehospitalisations due to CHF, 36 non-CHF related) - 103 No CVE	- Best discriminative value for CVE prediction obtained with CD31+/AV+ to CD14+/CD309+ mononuclear progenitor cells ratio and CD14+CD309+Tie2+ mononuclear progenitor cells. - Biomarker risk score for cumulative CVE, comprising NT-proBNP, galectin-3, hsCRP, osteoprotegerin, CD31+/AV+ to CD14+/CD309+ mononuclear progenitor cells ratio, is a reliable prediction for the probability of survival of patients with CHF, independently of age, sex, LEVF and number of comorbidities.	262

EVs	POPULATION	FINDINGS	REFERENCES
$CD31^+/CD41^+$ **$CD62E^+$** **$CD144^+$** **$CD31^+/CD41^-$** **$CD235^+$** **$CD45^+$**	10 HS 10 Stable CAD 10 CHF awaiting HTx 8 CHF after HTx 14 CHF with LVAD until HTx	- $CD235^+$ erEVs, $CD45^+$LEVs and $CD31^+/CD41^+$ pEVs increased in LVAD vs HS and CAD. - $CD144^+$, $CD31^+/CD41^-$ and $CD62E^+$ eEVs increased after LVAD implantation.	250
AV^+ **$CD42b^+$** **$CD144^+$**	25 CAD 88 Ischaemic HFrEF: - 49 ADHF - 39 CHF	- Baseline: $CD42b^+$ pEVs and $CD144^+$ eEVs were similar in ADHF vs CHF, but increased in CAD. - Baseline: AV^+ EVs increased in ADHF vs CHF and CAD. - 3 months follow-up: $CD42b^+$ pEVs and $CD144^+$ eEVs increased in ADHF. No changes in AV^+ EVs. - 3 months follow-up: $CD144^+$ eEVs were increased in ADHF vs CHF. - Baseline: AV^+ correlated with haemoglobin in ADHF. $CD42^+$ pEVs correlated with LVEF in ADHF. AV^+ EVs correlated with monocyte subsets (Mon1, Mon2, Mon3) in ADHF. - 3 months follow-up: AV^+ correlated with $CD42b^+$ pEVs and $CD144^+$ eEVs in ADHF - AV^+ correlated positively with NYHA. - Multivariate analysis: South Asian ethnicity and thienopyridine treatment influenced AV^+ EVs.	260
$CD31^+/AV^+$ **$CD105^+$** **$CD62E^+$**	35 HS 164 CHF: - 79 HFpEF - 85 HFrEF	- $CD31^+/AV^+$ eEVs increased in HFrEF vs HFpEF; HS had lower eEVs levels than all CHF, independently of LVEF. - $CD62E^+$ eEVs increased in CHF vs HS, independently of LVEF. - Multivariate logistic regression analysis: T2DM. obesity, previous myocardial infarction, NT-proBNP, galectin-3, $CD31^+/AV^+$ eEVs, and $CD14^+/CD309^+$ and $CD14^+/CD309^+/Tie2^+$ cells were independent predictors of HFpEF. - Multivariate Cox-regression analysis adjusted with aetiology and CV risk factors (obesity and T2DM) revealed that NT-proBNP and $CD31^+/AV^+$ eEVs and $CD14^+/CD309^+$ cells ratio were independent predictors for HFpEF. It had a better discriminative value than NT-proBNP and CV risk factors alone.	254
AV^+	20 HS 180 CHF (NYHA II–IV): - 30 Died during follow-up - 150 Survived follow-up	- AV^+ EVs increased in CHF vs HS at baseline. - Combination of AV^+ EVs and NT-proBNP predicted mortality better than NT-proBNP alone. - AV^+ EVs were better than the combination of NT-proBNP, eGFR and CRP in mortality prediction.	256

EVs	POPULATION	FINDINGS	REFERENCES
		- Combination of AV^+ EVs with NT-proBNP, eGFR and CRP, had the best prediction of 3-year mortality.	
$CD31^+/AV^+$ **$CD144^+/AV^+$**	388 CHF: - 85 HFrEF - 125 HFmrEF - 178 HFpEF	- $CD31^+/AV^+$ eEVs decreased in HFpEF vs HFrEF and HFmrEF; while similar in HFrEF vs HFmrEF. - $CD144^+/AV^+$ eEVs reduced in HFrEF vs HFpEF and HFmrEF, while similar in HFpEF vs HFmrEF. - $CD31^+/AV^+$ and $CD144^+/AV^+$ eEVs positively correlated with NT-proBNP, NYHA, galectin-3, T2DM, previous myocardial infarction, LVEF, hsCRP, sST2, SUA, low-density lipoprotein. - Multivariate analysis: $CD31^+/AV^+$ eEVs associated with HFpEF, galectin-3, NT-proBNP, GDF-15, while $CD144^+/AV^+$ eEVs associated with HFrEF, HFmrEF, galectin-3, NT-proBNP, GDF-15, sST2. - Adjusted multivariate Cox-regression analysis: previous myocardial infarction, DCM, T2DM, galectin-3, GDF-15 and $CD31^+/AV^+$ eEVs were predictors of HFpEF, while HFmrEF was predicted by sST2 and $CD31^+/AV^+$ eEVs. HFrEF was predicted by sST2, NT-proBNP, galectin-3, GDF-15 and $CD144^+/AV^+$ eEVs. - HFpEF best discrimination by ROC was the combination of $CD31^+/AV^+$ eEVs and galectin-3. - HFrEF best discrimination by ROC was the combination of $CD144^+/AV^+$ eEVs and galectin-3.	261
$CD41a^+$/Lactadherin$^+$ **$CD235a^+$/Lactadherin$^+$** **$CD31^+/CD41a^-$/Lactadherin$^+$** **$CD3^+$/Lactadherin$^+$** **$CD19^+$/Lactadherin$^+$** **$CD66b^+$/Lactadherin$^+$** **$CD142^+$/Lactadherin$^+$**	25 HS 90 CHF: - 30 NYHA II - 30 NYHA III - 30 NYHA III	- Lactadherin$^+$ (PS^+) EVs increased in CHF vs HS and correlated with NYHA. - $CD41a^+$/lactadherin$^+$ pEVs, $CD235a^+$/lactadherin$^+$ erEVs, $CD31^+/CD41a^-$/lactadherin$^+$ eEVs, $CD3^+$/lactadherin$^+$, $CD14^+$/lactadherin$^+$, $CD19^+$/lactadherin$^+$, $CD66b^+$/lactadherin$^+$ LEVs and $CD142^+$/lactadherin$^+$ EVs increased in CHF vs HS and correlated with NYHA. - PS^+ in blood cells and EVs shortens coagulation time in CHF by increasing thrombin and Factor Xa generation. They also facilitate prothrombinase assembly and fibrin formation.	255

ADHF: acute decompensated heart failure; **AV**: annexin V (PS); **BMI**: body mass index; **BNP**: Brain/B-type natriuretic peptide; **CAD**: coronary artery disease; **CHF**: chronic heart failure; **CRP**: C-reactive protein (*hsCRP*: high-sensitivity C-reactive protein); **CV**: cardiovascular; **CVE**: cardiovascular event; **DCM**: dilated cardiomyopathy; **DM**: diabetes mellitus (*T2DM*: DM type 2), **eEVs**: endothelial-derived EVs; **eGFR**: estimated glomerular filtration rate; **erEVs**: erythrocyte-derived EVs; **EVs**: extracellular vesicles; **GDF-15**: growth/differentiation factor 15; **HFmrEF**: heart failure with mildly reduced ejection fraction; **HFpEF**: heart failure with preserved ejection fraction (preserved LV function); **HFrEF**: heart failure with reduced ejection fraction (LV dysfunction); **HOMA-IR**: homeostasis model assessment of insulin resistance; **HS**: healthy subjects; **HTx**: heart transplantation; **LEVs**: leukocyte-derived EVs; **LV**: left ventricle; **LVAD**: LV assist device; **LVEF**: left ventricular ejection fraction; **NT-proBNP**: N-terminal pro-hormone of brain natriuretic peptide; **NYHA**: New York Heart Association; **pEVs**: platelet-derived EVs; **PS**: phosphatidylserine; **ROC**: receiver operating characteristic; **sFAS**: soluble FAS; **sST2**: soluble suppression of tumorigenesis 2; **SUA**: serum uric acid; **TNFα**: tumour necrosis factor α; **TSH**: thyroid stimulating hormone

Table A2: List of miRNA studies in chronic heart failure.

miRNA	POPULATION	FINDINGS	REFERENCES
miR-18b* ***miR-129-3p*** ***miR-432-5p*** ***miR-622*** ***miR-675*** ***miR-1254*** ***HS_202.1***	**Screening** - 12 HS - 12 Acute HF **Validation** - 39 HS - 20 no HF (with dyspnoea) - 30 HF (with dyspnoea): ○ 19 HFrEF ○ 11 HFpEF	- *miRNA-432-5p*, *129-3p*, *675*, *18b**, *HS_202.1*, *1254*, *622* upregulated in HF vs HS, confirmed in **validation**. - Multivariate logistic regression: *miR-423-5p* upregulated in HF vs non-HF and HS. - ROC: *miR-423-5p* discriminated between HF vs HS and HF vs non-HF. - *miR-423-5p* correlated positively with LVEF and negatively with NT-proBNP. - *miR-423-5p* and *miR-18b** correlated positively with NYHA. - *miR-423-5p* and *miR-675* were upregulated in atherosclerotic-HF vs non-atherosclerotic-HF.	264
miR-21 ***miR-29*** ***miR-34a*** ***miR-99a*** ***miR-107*** ***miR-125b*** ***miR-139*** ***miR-142-3p*** ***miR-142-5p*** ***miR-154*** ***miR-326*** ***miR-497*** ***miR-502***	**Screening** - 9 HS - 8 Ischaemic HFrEF - 7 Non-ischaemic HFrEF **Validation** - 19 HS - 15 Ischaemic HFrEF - 19 Non-ischaemic HFrEF	**Screening** - *miR-21*, *29*, *142-3p* upregulated in ischaemic HFrEF vs HS. - *miR-107*, *125b*, *139*, *497* downregulated in ischaemic HFrEF vs HS. - *miR-29b*, *34a*, *99a*, *154*, *326* upregulated in non-ischaemic HFrEF vs HS. - *miR-502* downregulated in non-ischaemic HFrEF vs HS. - No differences between ischaemic and non-ischaemic HFrEF. **Validation** - *miR-107*, *139*, *142-5p* downregulated in non-ischaemic HFrEF vs HS. - *miR-142-3p*, *29b* upregulated in non-ischaemic HFrEF vs HS. - *miR-107*, *125b*, *139*, *142-5p*, *497* downregulated in ischaemic HFrEF vs HS.	265
miR-122 ***miR-126-3p*** ***miR-423-5p*** ***miR-499***	17 HS 33 Ischaemic disease 10 HF	- *miR-126-3p* downregulated in CHF vs HS. - *miR-126-3p* associated negatively with NYHA (downregulated in more severe phenotypes). - *miR-126-3p* correlated negatively with age in HS, and with BNP in the NYHA II-IV groups. - *miR-126-3p* was increased in HF patients that improved NYHA stage (IV to III). - *miR-122* positively correlated with ALT in HS and NYHA II.	266

miRNA	POPULATION	FINDINGS	REFERENCES
miR-17 ***miR-21*** ***miR-22*** ***miR-30a*** ***miR-92a*** ***miR-92b*** ***miR-101*** ***miR-320a*** ***miR-423-5p*** ***miR-532-3p***	30 HS 30 HFrEF (ACC/AHA HF stage C)	- *miR-423-5p*, *320a*, *22*, *92b*, *17*, *532-3p*, *92a*, *30a*, *21*, *101* upregulated in HF vs HS. - Differences between miRNAs in HF and HS were similar in serum and exosomal fraction. - Chronic renal failure did not affect miRNA levels. - *miR-423-5p*, *320a*, *22*, *92b* were those miRNAs most upregulated in HF vs HS. - ROC: combination of *miR-423-5p*, *320a*, *22*, *92b*: best discrimination of HF vs HS.	267
miR-133a ***miR-423-5p***	246 with first anterior wall Q-wave MI: - LV remodelling after MI - Ischaemic HF due to MI with LV remodelling	- *miR-133a* upregulated 12 months after MI vs 3 months after MI. - *miR-423-5p* upregulated at 1, 3 and 12 months after MI vs baseline. - *miR-133a*, *423-5p* did not associate with infarct size indicators (creatinine kinase, LVEF). - *miR-133a*, *423-5p* similar in MI that developed HF and MI that did not during hospitalisation. - *miR-133a*, *423-5p* did not associate with LV remodelling. - *miR-423-5p*, *133a* do not work as biomarkers.	324
let-7b ***miR-23a*** ***miR-27b*** ***miR-29a*** ***miR-30b*** ***miR-103*** ***miR-142-3p*** ***miR-150*** ***miR-185*** ***miR-199a-3p*** ***miR-324-5p*** ***miR-342-3p*** ***miR-423-5p*** ***miR-598***	Patients with shortness of breath: **Screening** - 14 HS - 32 Breathlessness with HF (16 HFpEF, 16 HFrEF) - 15 COPD **Validation** - 15 HS - 44 Breathlessness with HF (22 HFpEF, 22 HFrEF) - 32 COPD - 59 Other breathless causes	**Screening** miRNA selection: - HF vs HS: *miR-185*, *29a*, *342-3p*, *1909*, *324-5p*, *150*, *let-7b.* - HF vs COPD: *miR-598*, *142-3p*, *103*, *342-3p*, *30b.* - COPD vs HS: *miR-324-5p*, *185*, *1909*, *150.* - HFpEF vs HFrEF: *miR-342-3p*, *199a-3p*, *150*, *29a*, *2110*, *27b*, *940*, *23a.* **Validation**: - *miR-103*, *142-3p*, *30b*, *342-3p* downregulated in HF vs HS, COPD, other breathless causes. - *miR-185* upregulated in HF vs HS. - *miR-150* downregulated in HF vs HS. - *miR-199a-3p*, *23a*, *27b* downregulated in HF vs COPD, other breathless causes. - No differences between HFpEF and HFrEF. - *miR-423-5p* no differences in HF vs HS, nor diagnostic predictor.	268

miRNA	POPULATION	FINDINGS	REFERENCES
miR-940 ***miR-1909*** ***miR-2110***		- No differences in miRNAs between COPD and non-HF-related breathlessness. - NT-proBNP correlated positively with *let-7b*, *miR-138*, *423-5p*, *miR-2110;* and negatively with *miR-30b*, *103*, *142-3p*, *150*, *199a-3p*, *27b*, *342-3p*. - Troponin T correlated positively with *let-7b*, *miR-185*, *423-5p* and negatively with *30b*, *103*, *142-3p*, *150*, *199a-3p*, *27b*, *342-3p*, *29a*. - *let-7b*, *miR-103*, *142-3p*, *199a-3p*, *23a*, *27b*, *324-5p*, *342-3p* associated with HF in breathlessness group (HF, COPD, other breathlessness causes). Associations of NT-proBNP and troponin T were better than that of miRNAs. - ROC: *miR-103*, *142-3p*, *199a-3p*, *23a*, *27b*, *30b*, *324-5p*, *342-3p*, *598* discriminated of HF in breathlessness cohort, but NT-proBNP and troponin T were better than miRNAs. - Best AUC: combination of NT-proBNP, miRNAs associated with HF and *miR-423-5p*.	
miR-210	6 HS 13 HF: - 8 NYHA II - 5 NYHA III-IV	- *miR-210* upregulated in NYHA III-IV vs NYHA II or HS. - *miR-210* upregulated in HF with less favourable outcomes.	306
miR-126 ***miR-146a*** ***miR-155*** ***miR-361-5p*** ***miR-423-5p***	39 HS 45 HFrEF due to DCM	- *miR-126*, *361-5p*, *146a*, *155* did not differ between HFrEF due to DCM and HS. - *miR-423-5p* upregulated in HFrEF due to DCM vs HS. - *miR-423-5p* positively correlated with NT-proBNP. - ROC: *miR-423-5p* discrimination of HFrEF due to DCM vs HS.	269
miR-548c	**Screening** - 7 DCM without HF - 7 HFrEF due to DCM **Validation** - 41 DCM without HF - 37 HFrEF due to DCM	- *miR-548c* downregulated in HF due to DCM vs HS. - ROC: *miR-548c* discriminated between DCM and HS.	270
miR-34a ***miR-192*** ***miR-194***	**Screening** - 7 MI non-HF - 7 Ischaemic HF **Validation**	- *miR-34a*, *192*, *194* upregulated in ischaemic HF. - *miR-34a*, *192*, *194* regulated p53 pathway. - *miR-34a*, *194* correlated with LVEDd 1 year after MI.	318

miRNA	POPULATION	FINDINGS	REFERENCES
	- 65 MI non-HF - 21 Ischaemic HF		
miR-124-5p ***miR-142-5p*** ***miR-454*** ***miR-500*** ***miR-1246***	8 HS 8 HFpEF 10 HFpEF with decompensated DCM 13 HFpEF with compensated DCM	- *miR-454*, *500* downregulated in HFpEF vs HS. - *miR-1246* upregulated in HFpEF vs HS. - *miR-142-5p* is downregulated in DCM with and without HF vs HS, but not in HFpEF vs HS. - *miR-124-5p* upregulated in DCM, but not in DCM with HF or in HFpEF vs HS.	271
let-7i* ***miR-34a*** ***miR-126-3p*** ***miR-186**** ***miR-200a**** ***miR-200b**** ***miR-210*** ***miR-220c*** ***miR-490-3p*** ***miR-508-5p*** ***miR-513-5p*** ***miR-517c*** ***miR-518e*** ***miR-595*** ***miR-589*** ***miR-662***	**Screening** - 10 HS - 10 Ischaemic CHF - 10 Non-ischaemic CHF **Validation** - 30 HS (1 died) - 55 Ischaemic CHF (14 died) - 51 Non-ischaemic CHF (12 died)	**Screening** - *miR-126*, *508-5p*, *34a*, *210*, *490-3p*, *513-5p*, *517c*, *518e*, *589*, *220c*, *200a**, *186**, *let-7i**, *200b**, *595*, *662* differential patterns between ischaemic and non-ischaemic CHF. **Validation** - *miR-126* downregulated in CHF. - *miR-508-5p* upregulated in CHF. - *miR-126*, *508-5p* independent prognostic factors for the outcome of ischaemic and non-ischaemic HF. - *miR-126*, *508-5p* most likely regulate angiogenesis.	319
miR-122* ***miR-200b*** ***miR-519e**** ***miR-520d-5p*** ***miR-558*** ***miR-622***	- 39 HS - 53 Non-ischaemic HFrEF	- Discrimination of HFrEF from HS: best single miRNAs: *miR-558*, *122**, *520d-5p*. - ROC: best discrimination of HFrEF vs HS: combination of *miR-520d-5p*, *558*, *122**, *200b**, *622*, *519e**, *1231*, *1228**. - *miR-622*, *520d-5p*, *519e**, *200b**, *122** correlated with LVEF. - Kaplan-Meier: *miR-519e** associated with disease severity and event presentation (hospitalisation due to HF, HTx, CV death).	272

miRNA	POPULATION	FINDINGS	REFERENCES
miR-1228* ***miR-1231***			
miR-29b ***miR-133a*** ***miR-423-5p***	10 HS 17 HFrEF	- *miR-29b*, *133a* upregulated in femoral vein vs femoral artery or coronary sinus in HF. - *miR-133a* upregulated in femoral artery vs other sites in HS. - *miR-423-5p* upregulated in HFrEF vs HS. - *miR-423-5p, 133a* correlated with BNP. - *miR-423-5p* seems to have a cardiac origin.	273
miR-19a-3p ***miR-24-2-5p*** ***miR-124-3p*** ***miR-130a-3p*** ***miR-214-3p*** ***miR-335-5p*** ***miR-338-5p*** ***miR-369-3p*** ***miR-433*** ***miR-493-5p*** ***miR-495*** ***miR-409-5p*** ***miR-596*** ***miR-657*** ***miR-877-3p*** ***miR-1249*** ***miR-1306-3p*** ***miR-1470*** ***miR-2110*** ***miR-3130-5p*** ***miR-3615*** ***miR-4258***	10 HS 10 MI (no HF) 15 Ischaemic HFrEF (new MI) 10 Ischaemic HFpEF (old MI)	- *miR-493-5p*, *369-3p*, *495*, *3615*, *433* upregulated in new ischaemic HF vs MI (no HF). - *miR-877-3p*, *1306-3p*, *3130-5p*, *hsvl-miR-H2*, *hcmv-miR-UL22A* downregulated in new ischaemic HF vs MI (no HF). - *miR-596*, *657*, *1306-3p*, *3130-5p*, *hsv1-miR-H2* upregulated in MI (no HF) vs HS. - *miR-409-5p*, *24-2-5p*, *335-5p*, *19a-3p*, *130a-3p* downregulated in MI (no HF) vs HS. - *miR-338-5p*, *124-3p*, *214-3p*, *433*, *19a-3p* upregulated in new ischaemic HF vs old ischaemic HF. - *miR-1249*, *4258*, *1470*, *2110*, *hsv2-miR-H24* downregulated in new ischaemic HF vs old ischaemic HF.	322

miRNA	POPULATION	FINDINGS	REFERENCES
hcmv-miR-UL22A ***hsv1-miR-H2*** ***hsv2-miR-H24***			
miR-1 ***miR-126*** ***miR-423-5p***	**Screening** - 44 Stable CHF - 58 Non-acute HF dyspnoea - 236 Acute HF dyspnoea **Validation** - 711 Acute HF	**Screening** - *miR-1* downregulated in acute HF and stable CHF vs non-acute HF. - *miR-126*, *423-5p* downregulated in acute and non-acute HF vs stable CHF. - *miR-423-5p* downregulated in patients readmitted to the hospital that those that weren't during follow-up. **Validation** - *miR-423-5p* predicted 1-year mortality. - Patients in the lowest *miR-423-5p* quartile were at high risk of long-term mortality.	308
miR-1 ***miR-21-5p*** ***miR-208a***	17 HS 61 ADHF or HFrEF: - 35 NYHA I-II - 26 NYHA IV	- *miR-1* downregulated in HF. - *miR-21-5p* upregulated in HF. - *miR-1, 21-5p* inversely correlated with NYHA. - *miR-1* negatively correlated with NT-proBNP and creatinine in NYHA II-III patients. - *miR-21-5p* correlated positively with galectin-3 in NYHA IV.	274
miR-30c ***miR-146a*** ***miR-221*** ***miR-328*** ***miR-375***	**Discovery** - 15 HS - 15 HFpEF - 15 HFrEF **Validation** - 75 HS - 75 HFpEF - 75 HFrEF	**Discovery**: *miR-30c*, *146a*, *221*, *328*, *375* were differential in HFpEF and HFrEF. **Validation**: - *miR-221*, *328*: discriminated HF vs HS (ROC). Downregulated in HF vs HS. Best AUC achieved combining each miRNA with BNP. - *miR-146a*, *221*, *328*, *375* independently discriminated HFpEF and HFrEF. AUC improved when combined with BNP.	316
miR-125a-5p ***miR-183-3p*** ***miR-190a*** ***miR-193b-3p***	**Screening** - 28 HS - 19 HFpEF - 39 HFrEF	**Screening**: selection of *miR-1225-3p*, *1233*, *125a-5p*, *1299*, *130a-5p*, *1322*, *145-3p*, *17-3p*, *1825*, *183-3p*, *186-5p*, *190a*, *193b-3p*, *193b-5p*, *204-5p*, *211-5p*, *301a-3p*, *320d*, *326*, *361-3p*, *423-3p*, *431-5p*, *485-3p*, *494*, *509-3p*, *545-5p*, *550a-5p*, *625-5p*, *629-3p*, *638*, *671-5p*, *82b-3p*.	315

miRNA	POPULATION	FINDINGS	REFERENCES
miR-193b-5p ***miR-211-5p*** ***miR-368*** ***miR-494*** ***miR-545-5p*** ***miR-550a-5p*** ***miR-671-5p*** ***miR-1233***	**Validation** - 30 HS - 30 HFpEF - 30 HFrEF	**Validation**: - HF vs HS: *miR-1233*, *671-5p* (upregulated in HF), *miR-183-3p*, *190a*, *193b-3p*, *193b-5p*, *211-5p*, *494* (downregulated in HF). - HFrEF vs HS: *miR-125a-5p*, *671-5p* (upregulated in HFrEF), *miR-183-3p*, *193b-3p*, *211-5p*, *494*, *638* (downregulated in HFrEF). - HFpEF vs HS: *miR-1233*, *545-5p* (upregulated in HFpEF), *miR-183-3p*, *190a*, *193b-3p*, *193b-5p* (downregulated in HFpEF). - HFpEF vs HFrEF: *miR-125a-5p*, *190a*, *550a-5p* (upregulated in HFrEF), *miR-638* (downregulated in HFrEF). - *miR-671-5p* best predictive value for HF vs HS, HFrEF vs HS. - *miR-1233*, *193b-3p* best predictive value for HFpEF vs HS. - *miR-190a* best predictive value for HFpEF vs HFrEF.	
let-7a-5p ***let-7c-5p*** ***let-7e-5p*** ***miR-16-5p*** ***miR-23b-3p*** ***miR-27a-3p*** ***miR-27b-3p*** ***miR-29b-3p*** ***miR-29c-3p*** ***miR-30e-5p*** ***miR-92a-3p*** ***miR-107*** ***miR-125b-5p*** ***miR-140-5p*** ***miR-155-5p*** ***miR-181a-5p*** ***miR-195-5p***	8 HS 9 Congestive HF	In coronary sinus: - *miR-16-5p*, *27a-3p*, *27b-3p*, *29b-3p*, *29c-3p, 30e-5p*, *92a-3p*, *125b-5p*, *140-5p*, *195-5p*, *424-5p*, *451a* downregulated in HF vs HS. - *let-7a-5p*, *let-7c-5p*, *let-7e-5p*, *23b-3p*, *miR*-107, *155-5p*, *181a-5p*, *181b-5p*, *320a* upregulated in HF vs HS.	275

miRNA	POPULATION	FINDINGS	REFERENCES
miR-320a ***miR-424-5p*** ***miR-541a***			
miR-1254 ***miR-1306-5p***	**Cohort 1** - 834 CHF **Cohort 2** - 1369 CHF	- High levels of *miR-1254, 1306-5p* associated with increased risk of combined endpoint (all-cause mortality and HF rehospitalisation). - ROC: adding these miRNAs to established predictors (age, sex, haemoglobin, renal function, NT-proBNP) did not improve discrimination.	309
miR-19b ***miR-21*** ***miR-133a***	28 aortic stenosis 13 HF due to aortic stenosis (HVD)	- Myocardial and serum samples of aortic stenosis: downregulated *miR-133a*, *19b* vs HS. No differences in *miR-21*. - *miR-21* downregulated in aortic stenosis with HF vs aortic stenosis without HF.	276
(in plasma and EVs) ***miR-146a*** ***miR-486***	20 HS 40 HFrEF (NYHA III-IV): - 19 Ischaemic HFrEF - 14 Non-ischaemic HFrEF - 7 Other aetiology	- Plasma: *miR-486*, *146a* upregulated trend in HFrEF vs HS (trend but non-significant). - EVs: *miR-146a* upregulated in HFrEF vs HS.	277
miR-26a-5p ***miR-145-3p*** ***miR-150-5p*** ***miR-485-3p*** ***miR-487b-3p***	**Screening** - 5 HS - 10 HF **Validation** - 15 HS - 54 HF ○ Mild-moderate HF ○ Advanced HF	**Screening**: - *miR-26a-5p, 150-5p*, *485-3p*, *487b-3p* downregulated in HF vs HS. - *miR-145-3p* upregulated in HF vs HS. **Validation***:* - *miR-26a*-5p downregulated in advanced HF vs HS. - *miR-150*-5p downregulated in HF (advanced and mild HF) vs HS. - *miR-150-5p* associated with upregulated risk of urgent LVAD implantation, HTx, death. - *miR-150-5p* correlated positively with LVEF, Na^+ and negatively NT-proBNP, LVEDv. - *miR-26a-5p* associated positively with NT-proBNP. - *miR-150-5p* associated negatively with NYHA stages. - COX: *miR-150-5p* associated with higher risk of composite endpoint for HF patients.	278

miRNA	POPULATION	FINDINGS	REFERENCES
let-7i-5p ***miR-16-5p*** ***miR-18a-5p*** ***miR-27a-3p*** ***miR-30e*** ***miR-106a-5p*** ***miR-199a*** ***miR-223-3p*** ***miR-423-5p*** ***miR-652-3p***	10 HS 114 HF: - 62 CAD - 15 TIA - 24 PAD	- *miR-18a-5p*, *27a-3p*, *30e*, *199a-3p*, *223-3p* downregulated in HF vs HS. - *miR-423-5p* upregulated in HF vs HS. - *miR-16-5p* no change in HF vs HS. - *miR-18a-5p*, *27a-3p*, *199a-3p*, *223-3p*¸*652-3p* levels negatively associated with an increase of atherosclerotic disease manifestations. - *miR-18a-5p*, *27a-3p*, *30e-5p*, *106a-5p*, *199a-3p*, *223-3p*, *652-3p* downregulated in HF with PAD vs HF without PAD. - *miR-423-5p* upregulated in HF with PAD vs HF without PAD. - COX: *miR-106a-5p*, *223-3p*, *27a-3p*, *16-5p*, *30e-5p*, *let-7i-5p* predictive of CV-related hospitalisation (low miRNA levels associated with upregulated risk of reaching endpoint). - ROC: best predictor power of CV-related hospitalisation: *let-7i-5p*.	279
miR-145	100 chest pain: - 30 No MI (CTLs) - 30 STEMI - 40 NSTEMI	- *miR-145* negatively correlated with the number of lesions on coronary arteries and the number of diseased vessels. - *miR-145* levels downregulated in STEMI vs NSTEMI and no MI. - *miR-145* levels in NSTEMI downregulated vs no MI. - *miR-145* correlated positively with infarct size (troponin T levels), and negatively with LVEF. - *miR-145* downregulated in patients that developed HF. - *miR-145* negatively correlated with BNP in HF.	323
miR-21	Serum from coronary and peripheral veins: 40 Non-HF 80 HFrEF (17 died, 23 hospitalised): - 41 Ischaemic HF - 33 DCM - 6 Other	- BNP and *miR-21* upregulated in serum from the coronary sinus vs peripheral vein in both HF and non-HF. - *miR-21* upregulated in HF vs non-HF. - *miR*-21 was similar in ischaemic and DCM-related HF. - *miR-21* correlated positively with NYHA, BNP; and negatively with LVEF. - ROC: *miR-21* discriminated between HF and non-HF, independently of localisation source. - COX regression model with: LVEF, BNP from peripheral blood, creatinine, cardiac resynchronisation therapy and *miR-21* (from both peripheral and sinus blood). Both *miR-21* correlated with endpoint. - Binary logistic analysis: no association of *miR-21* from peripheral blood and rehospitalisation, but *miR-21* from coronary blood associated with rehospitalisation.	280

miRNA	POPULATION	FINDINGS	REFERENCES
miR-21 ***miR-423-5p***	60 HS 60 CHF due to HVD	- *miR-21, 423-5p* upregulated in CHF vs HF. - *miR-21, 423-5p* correlated with hsCRP (in HVD). - ROC: *miR-21*, *423-5p* discriminated CHF vs HS. Best: *miR-423-5p* (better than NT-proBNP). - *miR-423-5p* was upregulated in HVD-CHF with PHTN than in those without PHTN.	281
miR-3135b ***miR-3908*** ***miR-5571-5p***	**Screening** - 3 HS - 13 HF **Validation** - 20 HS - 33 HF: o 18 HFrEF o 14 HFpEF	- *miR-3135b, 3908* and *5571-5p* upregulated in HF vs HS. - Best discrimination of HF vs HS (ROC): *miR-3135b*. - *miR-3135b*, *5571-5p* similar discrimination power than NT-proBNP. - *miR-3135b*, *3908* upregulated in HFpEF vs HFrEF (discriminative potential).	283
miR-21-3p ***miR-30a*** ***miR-34a*** ***miR-126*** ***miR-199*** ***miR-423***	11 HS 23 Non-ischaemic HF 41 Ischaemic HF	- *miR-423*, *34a* had a positive trans-coronary gradient in ischaemic HF. - *miR-21-3p*, *30a* had a positive trans-coronary gradient in non-ischaemic HF.	320
miR-133a ***miR-221***	31 HS 94 HF: - 32 NYHA II - 32 NYHA III - 30 NYHA IV	- *miR-133a*, *221* upregulated in HF vs HS (also after adjusting for age, sex, diabetes mellitus, HTN, BMI, creatinine, CRP, LVEF). - *miR-133a*, *221* upregulated in HF (NYHA II, III, IV) vs HS. - *miR-133a* correlated with NT-proBNP, CRP, LVEF, heart functional status. - *miR-221* correlated with heart functional status. - ROC: best discrimination of HF vs HS: combination of *miR-133a* with NT-proBNP. Addition of *miR-221* did not improve discrimination substantially.	282
let-7g ***miR-27b-3p*** ***miR-126-3p*** ***miR-142-5p***	**Screening**: - 12 HS - 16 Childhood DCM **Validation**:	- Signature of *miR-142-5p*, *143-3p*, *27b-3p*, *126-3p* differentiated childhood DCM vs HS. - *miR-126-3p*, *let-7g* correlated negatively with LVEF in childhood DCM. - *miR-126-3p* correlated negatively with heart systolic dysfunction.	284

miRNA	POPULATION	FINDINGS	REFERENCES
miR-143-3p	- 16 HS - 30 Childhood DCM with or without HF		
miR-197-5p	**Discovery** - 7 HS - 9 end-stage HF **Extension** - 30 HS - 80 end-stage HF	**Discovery** - *miR-494-3p, 1275*, *1268a*, *197-5p*, *150-3p*, *320a*, *939-5p* upregulated in HF vs HS. **Validation** - *miR-494-3p, 1275*, *1268a*, *197-5p*, *150-3p*, *320a*, *939-5p* upregulated in HF vs HS. - ROC: best discrimination of HF vs HS with *miR-320a*. - *miR-197-5p* correlated positively with myocardial fibrosis (markedly upregulated in end-stage HF <50 years). - Multivariate analysis for major adverse event prediction *miR-197-5p* independent prediction of major adverse event end-stage HF patients <50 years.	285
miR-30a-5p ***miR-99b-5p***	**Screening**: 14 STEMI - 7 HFrEF (LVEF ≤ 50%, NT-proBNP≥150pg/ml) - 7 No HF **Validation**: 85 STEMI - 22 HFrEF - 51 Mod-HF (either LVEF>50 or <150pg/ml NT-proBNP) - 12 No HF - 12 CAD (HS)	- *miRNA-30a-5p*, *99b-5p* upregulated in HF vs non-HF, in both serum and plasma. - *miR-30a-5p* validated in validation cohort. - *miR-30a-5p* in mod-HF presented intermediate levels compared to HF and non-HF and upregulated levels than HF (*miR-30a-5p* levels correlated positively with LV dysfunction). - *miR-30a-5p* correlated negatively with LVEF. - ROC: *miR-30a-5p* discriminated HF and non-HF.	286
miR-132	GISS-HF trial: 6975 patients In this study: 953 CHF - 225 Dead (190 CV death) - 530 Hospitalisations (301 due CHF)	- High levels of *miR-132* associated with young age, low serum creatinine, NYHA III-IV and ischaemic aetiology. - Multilinear regression analysis: hsCRP associated with *miR-132* - *miR-132* levels not affected by treatment with poly-unsaturated fatty acids, rosuvastatin or placebo.	310

miRNA	POPULATION	FINDINGS	REFERENCES
		- Kaplan-Meier: *miR-132* inversely associated with total and CV death, and first hospitalisation due to HF. - Cox-proportional hazard models: *miR-132* associated with all-cause and CV death, and HF hospitalisation. - *miR-132* correctly classified HF hospitalisation when added to 2 models including CV risk factors, with and without baseline NT-proBNP.	
miR-1 ***miR-21***	17 HS 59 Symptomatic HFrEF (ADHF or decompensated CHF): - 41 HTN and LV hypertrophy - 27 Severe LV hypertrophy	- *miR-1* was downregulated in HF with severe LV hypertrophy vs HS. - *miR-1* correlated negatively with interventricular septal thickness diameter and posterior wall diastolic thickness. - *miR-21* downregulated in all HF patients vs HS. - *miR-21* correlated positively with galectin-3.	287
miR-320a ***miR-378a-3p*** ***miR-423-5p*** ***miR-1254*** ***miR-1306-5p***	496 Acute HF - 188 Primary endpoint (all-cause mortality and rehospitalisation)	- Higher values of repeatedly measured *miR-1306-5p* positively associated with high risk of reaching primary endpoint. - ROC: *miR-1306-5p* did not improve discrimination achieved by NT-proBNP. - After adjustment with age and sex, *miR-320a*, *378a-3p*, *423-5p*, *1254* associated with primary endpoint.	311
miR-19a-5p ***miR-25-5p*** ***miR-133a*** ***miR-221*** ***miR-222*** ***miR-320c*** ***miR-455-3p*** ***miR-532-3p***	**Screening** - 6 CHD with HF - 6 CHD without HF **Validation** - 44 CHD with HF - 42 CHD without HF	**Screening** - *miR-222*, *221*, *25-5p* upregulated in CHD with HF vs without HF. - *miR-455-3p*, *133a*, *19b-5p*, *320c*, *532-3p* downregulated in CHD with HF vs without HF. **Validation** - *miR-221*, *25-5p* upregulated in CHD with HF vs without HF. - *miR-19b-5p* downregulated in CHF with HF vs without HF. - Univariate logistic regression model in PBMCs: upregulated *miR-221*, *25-5p* and downregulated *19b-5p* associated with upregulated HF risk. - CHF with HTN, BMI and upregulated low-density lipoprotein-cholesterol levels were upregulated for HF risk.	288

miRNA	POPULATION	FINDINGS	REFERENCES
		- Multiple logistic regression in PBMCs: upregulated *miR-221*, *25-5p* correlated with upregulated HF risk, while *miR-19b-5p* associated with downregulated HF risk in CHD. HTN independent predictive factor for HF risk in CHD. - ROC: combination of *miR-221*, *25-5p* and *miR-19b-5p* best discrimination of HF development. Improved with addition of HTN.	
miR-214	30 HS 50 CHF: - 19 Good efficacy - 31 Poor efficacy	- *miR-214* and galectin-3 upregulated in CHF vs HS. - ROC: *miR-214* was better than galectin-3 in discriminating CHF vs HS. - *miR-214* and galectin-3 downregulated in CHF after guideline-directed treatment. - *miR-214* and galectin-3 levels were lower in the good efficacy compared with bad efficacy. - ROC: *miR-214* and galectin-3 after treatment discriminated good and bad efficacy. - *miR-214* and galectin-3 positively correlated.	291
miR-29a ***miR-34a*** ***miR-133a*** ***miR-150*** ***miR-192*** ***miR-194*** ***miR-208b*** ***miR-499***	59 HS 113 STEMI: - 54 No HF after MI - 59 Ischaemic HF (due to MI)	- *miR-29a*, *133a*, *208b*, *499*, *194*, *34a* upregulated in MI vs HS, but similar in post-MI-HF and non-MI-HF. - *miR-150* downregulated in MI vs HS and in post-MI-HF vs non-MI-HF. - *miR-150* correlated with LVEF (1y after discharge). - ROC: *miR-150* predicted HF post-MI-HF better than BNP (but non-significant). Combination of *miR-150* and BNP was the best and significant. - *miR-150* was independently associated with post-MI-HF.	321
let-7a-5p ***miR-21-5p*** ***miR-222-3p*** ***miR-497-5p***	10 HS 8 HFrEF (NYHA I-III, ACC/AHA stage C)	- In AGO1 serum fractions, *miR-222-3p*, *497-5p, 21-5p* upregulated in HF vs HS. *Let-7a-5p* downregulated in CHF vs HS. - Combination of AGO1-carried *let-7a-5p*, *miR-222-3p*, *497-5p, 21-5p* discriminated HF vs HS better that the same miRNAs analysed in serum.	289
let-7a-5p ***miR-10b-5p*** ***miR-21-5p*** ***miR-22-3p*** ***miR-24-3p***	**Discovery** - 208 HS - 158 HFpEF - 180 HFrEF **Validation cohort 1**	**Discovery** - *miR-125a-5p*, *423-5p*, *30a-5p*, *21-5p*, *22-3p*, *30c-5p*, *103a-3p*, *30b-5p*, *191-5p*, *150-5p*, *454-3p*, *500a-5p* were downregulated in HF vs HS. - *let-7a-5p* and *miR-454-3p* discriminated HF vs HS (ROC).	317

miRNA	POPULATION	FINDINGS	REFERENCES
miR-30a-5p ***miR-30b-5p*** ***miR-30c-5p*** ***miR-103a-3p*** ***miR-106a5p*** ***miR-125a-5p*** ***miR-150-5p*** ***miR-181a-2-3p*** ***miR-185-5p*** ***miR-191-5p*** ***miR-193a-5p*** ***miR-199b-5p*** ***miR-223-5p*** ***miR-423-5p*** ***miR-454-3p*** ***miR-486-5p*** ***miR-500a-5p*** ***miR-503-5p*** ***miR-550a-5p*** ***miR-551b-3p*** ***miR-598-3p*** ***miR-660-5p*** ***miR-1280***	- 241 HS - 72 HFpEF - 116 HFrEF **Validation cohort 2** - 358 HS - 179 HFpEF - 145 HFrEF	- 41 miRNAs differed HFpEF and HFrEF. Best AUCs with *miR-223-5p*, *185-5p*. **Validation** - Best discrimination of HF and non-HF was achieved with a panel of the combination of 8 miRNAs (*miR-503-5p*, *454-3p*, *551b-3p*, *1280*, *24-3p*, *10b-5p*, *598-3p*, *193a-5p*) and NT-proBNP. - Best discrimination of HFpEF and HFrEF was achieved with a panel of the combination of 8 miRNA (*193a-5p*, *30a-5p*, *106a-5p*, *191-5p*, *486-5p*, *181a-2-3p*, *660-5p*, *199b-5p*) and NT-proBNP.	
miR-155	80 HS 90 Ischaemic HF (due to MI) 88 MI	- *miR-155* levels were upregulated in HF due to MI > MI > HS - ROC: *miR-155* discriminated HF vs HS. - *miR-155* correlated positively with NT-proBNP, LVEDd, NYHA, and negatively with LVEF.	290
miR-1 ***miR-21*** ***miR-154***	30 HS 61 CHF: - 14 NYHA I	- *miR-1*, *21*, *154*, *221*, *376a*, *379*, *382*, *409-5p*, *423-5p*, *499-5p*, *654-5p*, *744* upregulated in most CHF NYHA class vs HS. - *miR-21*, *154*, *221*, *299-5p*, *409-5p* positively correlated with NT-proBNP.	307

miRNA	POPULATION	FINDINGS	REFERENCES
miR-221 ***miR-376a*** ***miR-379*** ***miR-382*** ***miR-409-5p*** ***miR-423-5p*** ***miR-499-5p*** ***miR-654-5p*** ***miR-744***	- 17 NYHA II - 16 NYHA III - 14 NYHA IV	- *miR-451* negatively correlated with NT-proBNP. - *miR-423-5p* positively correlated with NT-proBNP and LVEF. - *miR-499-5p* negatively associated with VO_2 peak. - *miR-221* was the most informative to distinguish HS from CHF NYHA I. - ROC: combination of *miR-221*, *21*, *409-5p*, *376a*, *154* best discrimination potential.	
miR-21-5p ***miR-30a-3p*** ***miR-30a-5p*** ***miR-155-5p*** ***miR-216a*** ***miR-217***	60 HS 60 HF	- miRNA literature search and selection: *miR-217*, *216a*, *21-5p*, *30a-3p*, *30a-5p*, *155-5p*. - *miR-217*, *216a*, *21-5p*, *30a-3p*, *30a-5p*, *155-5p* upregulated in HF vs HS. - ROC: *miR-21-5p* best discrimination of HF from HS.	294
miR-1 ***miR-134*** ***miR-423-5p*** ***miR-489*** ***miR-496*** ***miR-3156*** ***miR-4721*** ***miR-4745*** ***miR-4781*** ***miR-5010*** ***miR-5088*** ***miR-8052***	**Screening** - 3 HS - 6 DCM **Validation** - 5 HS - 20 DCM	**Screening** - *miR-489, 5088* upregulated in DCM vs HS. - *miR-496*, *3156*, *4721*, *4745*, *4781*, *5010*, *8052* downregulated in DCM vs HS. **Validation** - *miR-489* upregulated in DCM vs HS. - *miR-489* correlated positively with LVEF.	292

miRNA	POPULATION	FINDINGS	REFERENCES
miR-122 ***miR-126*** ***miR-423***	**Screening** - 40 HFrEF that died - 36 HFrEF survivors (CTLs) **Validation** - 76 HFrEF that died - 158 HFrEF survivors (CTLs)	**Screening** - *miR-122*, *126*, *423* differentially expressed in survivors and dead HFrEF. **Validation** - *miR-122*, *423* upregulated in dead vs survivors HFrEF. - *miR-122*, *423* correlated positively with NT-proBNP in univariable and multivariable models. - *miR-122* associated with right ventricular dysfunction in multivariate models. - *miR-423* associated with previous MI. - COX hazard regression model: *miR-122*, *423* predicted all-cause mortality. - *miR-122*, *423* were independent predictors of all-cause and CV mortality in HFrEF. - *miR-122* provided prognostic information on clinical risk factors and NT-proBNP.	312
miR-365	48 HS 144 HF: - 45 NYHA II - 47 NYHA III - 52 NYHA IV	- *miR-365* upregulated in HF vs HS. - *miR-365* associated positively with NYHA.	295
miR-30c ***miR-146a*** ***miR-221*** ***miR-328*** ***miR-375*** ***lncRNA-CASC7*** ***lncRNA-CCAT1*** ***lncRNA-AK017368***	62 HS 62 HFpEF 62 HFrEF	- *miR-30c* downregulated in HF vs HS (plasma and PBMCs). - *miR-30c* downregulated in HFrEF vs HFpEF (plasma and PBMCs) - *miR-146a*, *miR-221*, *miR-328*, *miR-375* similar in HF vs HS; and in HFpEF and HFrEF. - ROC: *miR-30c* best discrimination of HF vs HS. - *lncRNA-CASC7* upregulated in HF vs HS; and in HFpEF and HFrEF (plasma and PBMCs). - *lncRNA-CCAT1* and *lncRNA-AK017368* similar in HF vs HS; and in HFpEF and HFrEF (plasma and PBMCs). - *LncRNA-CASC7* negatively correlated with *miR-30c* (plasma and PBMCs). - ROC: *lncRNA-CASC7* best discrimination of HF vs HS. - *miR-30c* inhibited *lncRNA-CASC7* and regulated IL-11 expression.	296
miR-19b	100 HS 200 Ischaemic CHF:	- *miR-19b* downregulated in HF vs HS. - *miR-19b* downregulated in HFrEF vs HFpEF. NT-proBNP was similar in HFrEF and HFpEF.	293

miRNA	POPULATION	FINDINGS	REFERENCES
	- 100 HFrEF - 100 HFpEF	- *miR-19b* negatively correlated with NT-proBNP. - ROC: *miR-19b* could discriminate HF vs HS. NT-proBNP alone or in combination with *miR-19b* had similar AUCs. *miR-19b* could not be linked to improved accuracy. - ROC: combination of *miR-19b* and NT-proBNP improved NT-proBNP discrimination of HFpEF and HFrEF.	
miR-16-5p ***miR-21-5p*** ***miR-29-5p*** ***miR-133a-3p*** ***miR-191-5p*** ***miR-320a*** ***miR-423-5p***	- 48 HS - 53 HF due to DCM - 34 Ischaemic HF	- *miR-29-5p*, *320a*, *423-5p* differed between HS, HF due to DCM or ischaemic-HF. - *miR-29-5p* upregulated in HF due to DCM vs ischaemic HF. - *miR-320a* upregulated in HF due to DCM vs HS. - ROC: *miR-29-5p* discriminated between HF due to DCM and ischaemic HF. - ROC: *miR-320a* discriminated between HF due to DCM and HS. ROC improved when BMI was combined with *miR-320a*.	298
miR-9-5p ***miR-10b-5p*** ***miR-21-3p*** ***miR-22-3p*** ***miR-22-5p*** ***miR-30d-5p*** ***miR-125a-5p*** ***miR-148a-3p*** ***miR-148a-5p*** ***miR-152-3p*** ***miR-181d-5p*** ***miR-210-3p*** ***miR-328-3p*** ***miR-330-5p*** ***miR-339-3p*** ***miR-340-3p*** ***miR-361-3p*** ***miR-423-3p***	36 HS 30 Advanced CHF (60% ischaemic HF, 21% HFrEF; 100% NYHA III): followed-up until endpoint: - 3 CV death - 5 HTx - 6 LVAD implantation - 22 Hospitalised for ADHF	**Screening**: - *miR-210-3p*, *1287-5p*, *148a-3p*, *148a-5p*, *629-5p*, *22-5p*, *339-3p*, *1285-5p*, *5480-3p*, *22-3p*, *550a-5p*, *6515-5p*, *152-3p*, *330-5p*, *3120-5p*, *503-5p*, *361-3p, 21-3p*, *765-5p*, *576-3p* upregulated in CHF vs HS. - *miR-340-3p*, *423-3p*, *628-3p*, *6721-5p*, *485-3p*, *125a-5p*, *664a-3p*, *505-5p*, *181d-5p*, *484*, *328-3p*, *30d-5p* downregulated in CHF vs HS. **Validation**: high fold change and good p-value in 15 CHF vs 15 HS in the same cohort: - *miR-210-3p*, *1287-5p*, *148a-5p*, *629-5p* upregulated in CHF vs HS. **MiRNAs and biomarkers**: - NT-proBNP correlated positively with *miR-210-3p*, *22-5p*, *22-3p*, *21-3p*, *339-3p* and negatively with *miR-125a-5p*. - sST2 correlated negatively with *miR-125a-5p.* - BCN BioHF score correlated positively with *miR-210-3p*, *21-3p*, *339-3p* and negatively with *miR-125a-5p*. - ROC discrimination using these miRNAs did not improve currently used biomarkers.	314

miRNA	POPULATION	FINDINGS	REFERENCES
miR-484 ***miR-485-3p*** ***miR-503-5p*** ***miR-505-5p*** ***miR-550a-5p*** ***miR-576-3p*** ***miR-628-3p*** ***miR-629-5p*** ***miR-664a-3p*** ***miR-765-5p*** ***miR-1285-5p*** ***miR-1287-5p*** ***miR-3120-5p*** ***miR-5480-3p*** ***miR-6515-5p*** ***miR-6721-5p***		**MiRNAs and clinical outcomes**: - *miR-125a-5p*, *10b-5p* downregulated in endpoint vs non-endpoint outcome. - *miR-9-5p* upregulated in endpoint vs non-endpoint. - *BCN BioHF score positively correlated with miR-125a-5p, 106-5p*, *9-5p* in HFrEF. - Prediction model with BCN BioHF, VO_2 max and transpulmonary pressure gradient, improved prognostic stratification after a*ddition of miR-125a-5p, 106-5p*, *9-5p*.	
miR-126	30 HS 60 HFpEF under exercise rehabilitation	- *miR-126* downregulated in HFpEF vs HS at baseline. - *miR-126* upregulated in HFpEF after training vs HFpEF levels at baseline but downregulated vs HS. - *miR-126* correlated positively with peak O_2, METs, VO_2AT, LVEF; and negatively with NT-proBNP, LAVI, E/e’, MLHF score and VE/VCO_2 slop. - Multiple regression analysis: *miR-126* associated positively with peak VO_2, MET; and negatively with MLHF score and NT-proBNP.	299
miR-208a	60 HS 60 HFrEF 60 HFpEF	- *miR-208a* was upregulated in HFrEF>HFpEF>HS. - *miR-208a* correlated negatively with NT-proBNP. - ROC: NT-proBNP best in discriminating HF vs HS. Combination of *miR-208a* and NT-proBNP discriminated HFpEF and HFrEF better than NT-proBNP.	300
miR-21 ***miR-155*** ***miR-181b***	31 HS 41 Non-ischaemic HFrEF due to DCM	- *miR-181b* downregulated in HF vs HS (both DCM and ischaemia-induced HF). - *miR-21* downregulated in DCM-induced HF and upregulated in ischaemia-induced HF.	297

miRNA	POPULATION	FINDINGS	REFERENCES
	31 Ischaemic HFrEF	- *miR-155* no changes between groups. - *miR-181b* correlated negatively with hsCRP. - ROC: *miR-181b* discriminated DCM-induced HF vs HS, and ischaemia-induced HF vs HS. - *miR-181b* is related to inflammation (anti-inflammatory) and is deregulated in initial HF stages (animal model experiments).	
miR-145-5p	86 HS 98 CHF (NYHA II-IV)	- *miR-145-5p* downregulated in CHF vs HS. - *TUG1* (lncRNA) expression negatively correlated with *miR-145-5p*. - *miR-145-5p* negatively correlated with NYHA, TUG1 positively correlated with NYHA. - ROC of combined probabilities of *miR-145-5p*, TUG1 and BNP best discriminative potential for CHF diagnosis. - *miR-145-5p* and *TUG1* high expression associated with survival and poor survival, respectively. - Multivariate analysis: BNP, NYHA, *TUG1*, *miR-145-5p* independently associated with CHF survival. - *TUG1* positively correlated while *miR-145-5p* negatively correlated with CRP, IL-6 and TNFα.	302
miR-194-5p ***miR-454-3p*** ***miR-518-3p*** ***miR-618*** ***miR-875-3p***	37 HS 37 Childhood DCM	- *miR-454-3p*, *194-5p* upregulated in childhood DCM vs HS. - *miR-875-3p* downregulated in childhood DCM vs HS. - ROC: *miR-194-5p*, *454-3p* discriminated childhood DCM vs HS. - Target genes associated with TGF-β pathway. - *miR-194-5p*, *454-3p* could cause childhood DCM impairing Ca^{2+}, Na^{+}, K^{+} homeostasis in sarcolemma.	303
miR-21	100 HS 120 CHF (NYHA I-IV)	- *miR-21* downregulated in CHF vs HS. - BNP, NT-proBNP, hsCRP, TNFα, IL-6, IL-17 upregulated in CHF vs HS. - *miR-21* negatively correlated with NYHA severity (prognostic value). - *miR-21* negatively correlated with LVEF, right ventricular ejection fraction, stroke volume and inflammation in CHF. - *miR-21* target genes were enriched in immune and inflammatory pathways.	304
miR-30a-5p ***miR-100***	**Discovery**	- **Discovery**: *miR-30a-5p*, *100*, *499b*, *320a*, *433* downregulated in HF after guideline-directed medical treatment.	305

miRNA	POPULATION	FINDINGS	REFERENCES
miR-320a ***miR-433*** ***miR-499b*** ***miR-654-5p***	- 40 HF before and after guideline-directed medical treatment **Training** - 15 HS - 30 HF **Validation** - 25 HS - 50 HF **Additional validation** - 27 HF without LVAD - 10 HF 3 months after LVAD implantation - 10 HF 6 months after LVAD implantation	- **Discovery**: *miR-654-5p* upregulated in HF after guideline-directed medical treatment. - **Discovery**: *miR-30a-5p*, *654-5p* most significantly changed with treatment → **validation**. - **Training and validation**: *miR-30a-5p* upregulated in HF vs HS, *miR-654-5p* downregulated in HF vs HS. - **Training and validation**: ROC: best discrimination of HF vs HS obtained with combination of *miR-30a-5p* and *miR-654-5p*. - Target genes: *miR-30c-5p*, *654-5p* related to apoptosis and p53 signalling, viral myocarditis, dilated cardiomyopathy, atherosclerosis and adrenergic signalling in cardiomyocytes. - **Additional validation**: after LVAD implantation (at 3 and 6 months), *miR-30c-5p* downregulated and *miR-654-5p* upregulated in HF. This associated with improvement of cardiac function.	
miR-20a-5p ***miR-21-5p*** ***miR-23a-3p*** ***miR-27b-3p*** ***miR-30b-5p*** ***miR-106b-5p*** ***miR-107*** ***miR-122-5p*** ***miR-148b-3p*** ***miR-210-3p*** ***miR-221-3p***	30 HS 311 MI: - 268 No event at follow-up - 43 Event at follow-up: ○ 24 HF hospitalisation ○ 25 CV death	- *miRNAs 20a-5p, 21-5p*, *23a-3p*, *27b-3p*, *30b-5p*, *106b-5p*, *107*, *184b-3p*, *210-3p* and *221-3p* upregulated in MI with highest Killip class, GRACE score, troponin I, NT-proBNP and poorer LVEF. - *miRNAs 21-5p*, *23a-3p*, *210-3p* and *221-3p* predicted primary endpoint. - *miRNAs 21-5p*, *23a-3p*, *27b-3p*, *106b-5p*, *107*, *122-3p*, *210-3p* and *221-3p* independently predicted CV death. - *miR-23a-3p*, *210-3p*, *221-3p* identified MI patients at high risk for HF hospitalisation. - *miR-21-5p*, *23a-3p*, *210-3p* and *221-3p* identified patients with NHYA II or higher.	313

ACC/AHA: American College of Cardiology/American Heart Association; **ADHF**: acute decompensated heart failure; **AUC**: area under the curve; **BMI**: body mass index; **BNP**: brain natriuretic peptide; **CAD**: coronary artery disease; **CHD**: coronary heart disease; **CHF**: chronic heart failure; **COPD**: chronic obstructive pulmonary disease; **CRP**: C-reactive protein (hsCRP: high-sensitivity C-reactive protein); **CTLs**: controls; **CV**: cardiovascular; **DCM**: dilated cardiomyopathy; **EVs**: extracellular vesicles; **HF**: heart failure; **HFpEF**: heart failure with preserved ejection fraction; **HFrEF**: heart failure with reduced ejection fraction; **HS**: healthy subjects; **HTN**: hypertension; **HTx**: heart transplantation; **HVD**: heart valve disease; **IL**: interleukin; **lncRNA**: long non-coding RNA; **LV**: left ventricle; **LVAD**: LV assist device; **LVEDd**: LV end-diastolic diameter; **LVEDv**: LV end-diastolic volume; **LVEF**: left ventricular ejection fraction; **LVESVI**: LV end-systolic volume index; **MI**: myocardial infarction; **mRNA**: messenger RNA;

miRNA	POPULATION	FINDINGS	REFERENCES

NSTEMI: non-ST elevation myocardial infarction; **NT-proBNP**: N-terminal prohormone of the brain natriuretic peptide; **NYHA**: New York Heart Association; **PAD**: peripheral artery disease; **PBMCs**: peripheral blood mononuclear cells; **PHTN**: pulmonary hypertension; **RNA**: ribonucleic acid; **ROC**: receiver operating characteristic; **sST2**: soluble suppressor of tumorigenicity-2; **STEMI**: ST-elevation myocardial infarction; **TGF**: transforming growth factor; **TIA**: transient ischaemic attack; **TNFα**: tumour necrosis factor α; **VO_2**: oxygen uptake